

20S PROTEASOME ACTIVATION AS AN INNOVATIVE THERAPEUTIC STRATEGY

By

Taylor Joseph Martinez-Fiolek

A DISSERTATION

Submitted to
Michigan State University
in partial fulfillment of the requirements
for the degree of

Chemistry – Doctor of Philosophy
Pharmacology and Toxicology – Dual Major

2023

ABSTRACT

Accumulation and aggregation of intrinsically disordered proteins (IDPs), such as α -synuclein, amyloid β , and tau, is associated with the pathogenesis of several neurodegenerative diseases, including Parkinson's disease and Alzheimer's disease. The 20S proteasome is the primary protease charged with regulating cellular levels of IDPs, but as humans age these proteins can become dysregulated resulting in their accumulation and aggregation seen in neurodegenerative diseases. Although the pathogenesis of these neurodegenerative diseases is still under intense investigation, it has been shown that the oligomeric forms of IDPs, including α -synuclein and amyloid β , are toxic to neurons and can impair proteasome function. This leads to additional accumulation of the IDPs, further promoting disease progression. Additionally, IDPs released by degenerating neurons activate the native immune cells of the brain, microglia, and induce their activation. These activated microglia release pro-inflammatory signaling molecules, which when coupled with continued IDP accumulation and release results in chronic neuroinflammation, contributing to further neuron degeneration.

The Tepe Lab aims to develop small molecule activators of the 20S proteasome that enhance its ability to degrade IDPs, thus assisting in the prevention of their further accumulation and aggregation. We propose that these small molecule 20S proteasome activators represent a novel therapeutic method by which we may impede neurodegenerative disease progression. Here, I report the identification of novel small molecule 20S proteasome activator scaffolds that selectively enhance 20S proteasome activity. These activators enhance 20S-mediated degradation of IDPs that are implicated in neurodegenerative disease development. The identification of these novel activator scaffolds will enhance the chance of success while developing this novel therapeutic strategy and permit development of additional analogues with promising activities and

drug-like properties.

With these activators in hand, several novel methods were developed that demonstrate the potential of small molecule 20S proteasome activation as an innovative therapeutic strategy for combating neurodegenerative diseases. It was demonstrated for the first time that small molecule activators can protect against inhibition of the 20S proteasome by IDP oligomers associated with neurodegenerative disease pathogenesis and that these oligomers can be reduced through 20S proteasome activation *in vitro*. These results suggest that small molecule 20S proteasome activation has the potential to assist in re-establishing proteostasis in diseased neurons. Additionally, it was found that small molecule 20S proteasome activators can counteract the accumulation of an overexpressed familial Parkinson's disease related IDP, A53T α -synuclein, in cells. This demonstrated that this method shows promise for translation into cellular systems. As such, additional cellular models were conceived, and their development initiated to generate more disease relevant models for further evaluating this method. Finally, small molecule 20S proteasome activators were found to reduce IDP-induced release of the pro-inflammatory cytokine TNF- α by microglia. Thus, this work begins to illuminate the great potential of small molecule 20S proteasome activators to counteract multiple IDP-driven aspects of neurodegenerative disease pathogenesis.

ACKNOWLEDGEMENTS

I am fortunate to have many people in my life who have supported me throughout my journey to get here, to the end of my PhD.

First, I would like to thank my advisor, Dr. Jetze Tepe. Your support, guidance and mentorship have helped to make me into the scientist that I am today. Thank you for encouraging me to make my project my own, explore my own ideas and to take on a leadership role in the lab. These things have allowed me to grow and mature as a scientist beyond my expectations.

To my committee, Dr. Huang, Dr. Draths, and Dr. Hong. Thank you for all your feedback and willingness to help me through this process. Whether it was to borrow equipment, problem solve, or simply to give me a drink to calm me down after my seminar, you were each always willing to help. Thank you to Dr. Dexheimer for your help with my high-throughput assays. Thank you to Dr. Sortwell and her lab for collaborating with me on the primary neuron studies. Thank you to Dr. Dorrance, Dr. Neubig, Dr. Liby and many others in the Pharmacology and Toxicology department. I learned a great deal in classes, workshops, and gatherings while in the IPSTP program and PharmTox department. I am so thankful that I was able to be a part of both during my time here. Thank you to Dr. Blanchard for helping me with fellowship applications. Thank you to all the people who make the Chemistry and PharmTox departments run and to make our lives easier in a multitude of ways, Anna, Mary, Dawn, Eric, Bob, Tiphani, Jake, and many others. I appreciate all that you do for these departments and for us.

Thank you to Dr. Adam Mosey and his lab at Lake Superior State University for collaborating with me on the Dihydroquinazoline project. Our collaboration was very enjoyable and rewarding.

Thank you to my previous mentors, Dr. Benjamin Swarts and Dr. Choon Lee. Your

mentorship and the things I learned while working with you were instrumental to my success.

Thank you to all my lab mates, both current and former. I have had the privilege of watching our lab grow from 5 to 15 people and during that time it evolved into a close-knit family. While some of the faces and personalities have changed with time, the feelings of support and togetherness have remained. I hope that carries on for all of you because it has been invaluable to me. To Evert and Corey, thank you for your mentorship and guidance. To Grace, we finally made it! Thank you for always being someone with whom I could share my struggles knowing that you understand and were often experiencing similar ones. To Katarina, Grace, Allison, Sophie, Charles, and Konika, thank you all for becoming great friends and for encouraging me to come out and have some fun. It was always a great time! To the biology subgroup, I am proud of what our group has become and how we have grown together as a team. I know you all will continue to do so. To all those mentioned above, Christi, Ayoob, Shafaat, Dare, Daniel, Evan, Kyra, Bahar, Sydney, Shannon, and Miracle, thank you all for your support, questions, and friendship.

To my friends, I cannot name you all here, but I appreciate all of you and thank you all for your support. To Ankush and Emmanuel, thank you for being there to chat and go to lunch on Fridays. It has been something to look forward to throughout our years together here. To Nate and Kaleb, thank you for always being there to get my mind away from work and have some fun. Kaleb, thank you for helping around the house while I've been busy and for doing some spelling and grammar checking for me. To Herbert, thank you for being a source of advice, both for science and life, and for being a friend who is ready to go out for a drink and food whenever life permits.

To my family, I cannot express in words how thankful I am for each of you and your undying support and encouragement. I would not have made it here without you. Thank you for always believing in me and helping me to follow whatever path I choose in life. Thank you to my

pets back at home and here with me, who have served as my emotional support animals. We have a long-standing joke in the Tepe lab about animal pictures in our slides and in zoom meetings, but they truly have been an important part of my support system and family. To my loved ones who are no longer with us. Thank you for helping to shape me into the man I am today. Finally, thank you to my loving wife, Mariah. I could not have done this without you at my side. I am forever grateful for you and your unyielding support, love, and encouragement through what has been one of the most difficult times in my life. We have been through a lot during my time here, but we have made it through together and will continue to do so. I love you all and I hope I have made you proud.

TABLE OF CONTENTS

LIST OF ABBREVIATIONS.....	viii
CHAPTER ONE Proteostasis, the Proteasome and a Novel Therapeutic Strategy for Neurodegenerative Diseases	1
1.1 Introduction.....	2
1.2 The ubiquitin proteasome system	5
1.3 Proteostasis disruption contributes to aging and neurodegenerative diseases	14
1.4 The 20S proteasome as a novel therapeutic target.....	24
1.5 Conclusions.....	30
REFERENCES	32
CHAPTER TWO Identification and Structure Activity Relationship of Dihydroquinazoline as a Novel 20S Proteasome Activator Scaffold	55
2.1 Introduction.....	56
2.2 Results and Discussion	61
2.3 Conclusions.....	72
REFERENCES	74
CHAPTER THREE Repurposed Neuroleptic Agents as Novel 20S Proteasome Activator Scaffolds	80
3.1 Introduction.....	81
3.2 Results and Discussion	86
3.3 Conclusions.....	108
3.4 Experimental.....	110
REFERENCES	123
APPENDIX.....	130
CHAPTER FOUR Development of Neurodegenerative Disease Model Systems for Evaluating 20S Proteasome Activation as an Innovative Therapeutic Strategy	142
4.1 Introduction.....	143
4.2 Results and Discussion	147
4.3 Conclusions.....	171
4.4 Experimental.....	173
REFERENCES	176
APPENDIX.....	184
CHAPTER FIVE Conclusions and Future Directions.....	187
5.1 Conclusions and Future Directions.....	188
REFERENCES	191
CHAPTER SIX Materials and Methods	195
6.1 Materials	196
6.2 Methods.....	198

LIST OF ABBREVIATIONS

3D	3-dimensional
ACN	Acetonitrile
AD	Alzheimer's disease
AFM	Atomic force microscopy
ALS	Amyotrophic lateral sclerosis
AMC	7-amino-4-methylcoumarin
APP	Amyloid precursor protein
Atm	Atmospheric pressure
ATP	Adenosine triphosphate
BBB	Blood-brain barrier
Boc-LRR-AMC	Tert-butoxyl-leucyl-arginyl-arginyl-7-amino-4-methylcoumarin
BTZ	Bortezomib
°C	Degrees Celsius
Casp-L	Caspase-like
CD	Circular dichroism
CP	Core particle
CT-L	Chymotrypsin-like
DCM	Dichloromethane
DMF	Dimethylformamide
DMSO	Dimethyl sulfoxide
EC ₂₀₀	200% effective concentration
Equiv.	Equivalents

ESI	Electrospray ionization
FBS	Fetal bovine serum
FTIR	Fourier transform infrared
HbYX	Hydrophobic-tyrosine-any amino acid
HD	Huntington's disease
HEK-293T	Human embryonic kidney 293 cells containing SV40 T-antigen
HFIP	Hexafluoroisopropanol
HRMS	High-resolution mass spectrometry
HT-22	Immortalized mouse hippocampal neurons
IDP	Intrinsically disordered protein
IDR	Intrinsically disordered region
IMG	Immortalized mouse microglial cells
LB	Lysogeny broth
MHC	Major histocompatibility complex
mp	Melting point
MS	Mass spectrometry
NMR	Nuclear magnetic resonance
PA200	Proteasome activator 200 kDa
PAGE	Poly acrylamide gel electrophoresis ^[L] _[SEP]
PBS	Phosphate-buffered saline
PD	Parkinson's disease
Ph	Phenyl-
RP	Regulatory particle

Rpn	Non-ATPase regulatory particle
Rpt	ATPase regulatory particle
SDS	Sodium dodecyl sulfate
SNpc	Substantia nigra pars compacta
Suc-LLVY-AMC	Succinyl-leucyl-leucyl-valyl-tyrosyl-7-amido-4-methylcoumarin
TBS	Tris-buffered saline
TEA	Triethylamine
THF	Tetrahydrofuran
TLC	Thin layer chromatography
ToF	Time of flight
Tryp-L	Trypsin-like
UCH37	Ubiquitin C-terminal hydrolase 37
UPS	Ubiquitin proteasome system
USP14	Ubiquitin specific peptidase 14
WT	Wild type
Z-LLE-AMC	Carboxylbenzyl-leucyl-leucyl-glutamyl-7-amido-4-methylcoumarin

CHAPTER ONE

Proteostasis, the Proteasome and a Novel Therapeutic Strategy for Neurodegenerative Diseases

1.1 Introduction

1.1.1 Proteostasis

The regulation of protein synthesis, folding, and degradation within a cell is collectively known as protein homeostasis (proteostasis).¹ Proteostasis is maintained by a wide array of cellular machinery (~2,000 proteins) that work in tandem to ensure that proteins are present in the proper locations, forms, and amounts to perform their required functions.²⁻⁶ These processes also serve to prevent the accumulation of redundant, misfolded or damaged proteins, which is necessary to avoid their cytotoxic aggregation.⁷ The maintenance of proteostasis in human cells is a monumental task, considering the presence of over 10,000 proteins in human cells and significant variations in proteome composition seen between cell types and tissues.⁸ This is further complicated by large protein-to-protein variations in terms of abundance, location, function and half-life.⁹⁻¹² Additionally, the cellular proteome is in constant flux over the lifetime of a cell, which is necessary to permit proper cellular functions. This includes the ability of a cell to progress through the cell cycle, differentiate, respond to extracellular signals, or signal to other cells. Each of these processes involve transient modifications to the cellular proteome.^{1, 12} Balance must be maintained through this constant flux in the proteome by the various components of the proteostasis network, including protein synthesis machinery (ribosomes), protein folding complexes (chaperones), and proteolytic systems, including the ubiquitin proteasome system (UPS) and lysosome-autophagy system (autophagy, **Fig. 1.1**).²⁻⁶

During protein synthesis, molecular chaperones participate in co-translational folding of peptides as they exit the ribosome to promote proper folding into their final 3-dimensional (3D) structure.^{13, 14} This is required for proper biological function for most proteins, apart from intrinsically disordered proteins (IDPs), which will be discussed in more detail in a later section.

Similar chaperone proteins also assist in refolding of misfolded proteins when possible. These activities help to prevent undesired interactions and aggregation of exposed hydrophobic regions resulting from improper protein folding.^{15, 16} When proteins cannot be properly refolded, are damaged beyond repair or simply become redundant, they are recycled through the proteolytic pathways (UPS and autophagy) to regenerate amino acids and avoid their accumulation.¹⁷⁻²⁰ If damaged, misfolded, or redundant proteins are not repaired or disposed of quickly they can accumulate, which leads to aggregation, undesired signaling events and toxicity.^{17, 21-23}

The three main branches of the proteostasis network (synthesis, folding and degradation) are functionally coupled to one another, allowing for constant crosstalk and rapid adaptation to preserve the balance of proteostasis through a variety of pathophysiological states.^{11, 23-27} Despite this, the proteostasis network is not infallible. The constant flux and complexity of the cellular proteome, coupled with the accumulation of various internal and external stresses, inevitably result in a decline of the capacity of the proteostasis network. The result of which, is loss of proteome integrity and dysregulation of proteostasis.^{2, 4, 5, 12, 28} This dysregulation of proteostasis is responsible for many non-infectious and age-related human diseases.

The common association between proteostasis disruption and disease development, especially in the context of age-related diseases, makes the various components of the proteostasis network promising targets for therapeutic intervention.^{1, 4, 10, 12, 28} As such, methods that allow for modulation of the activity of proteolytic machinery have garnered much attention.^{24, 29-34} Specifically, the Tepe lab has developed an interest in exploring modulation of proteasome activity as a novel route for addressing certain proteostasis-related diseases.

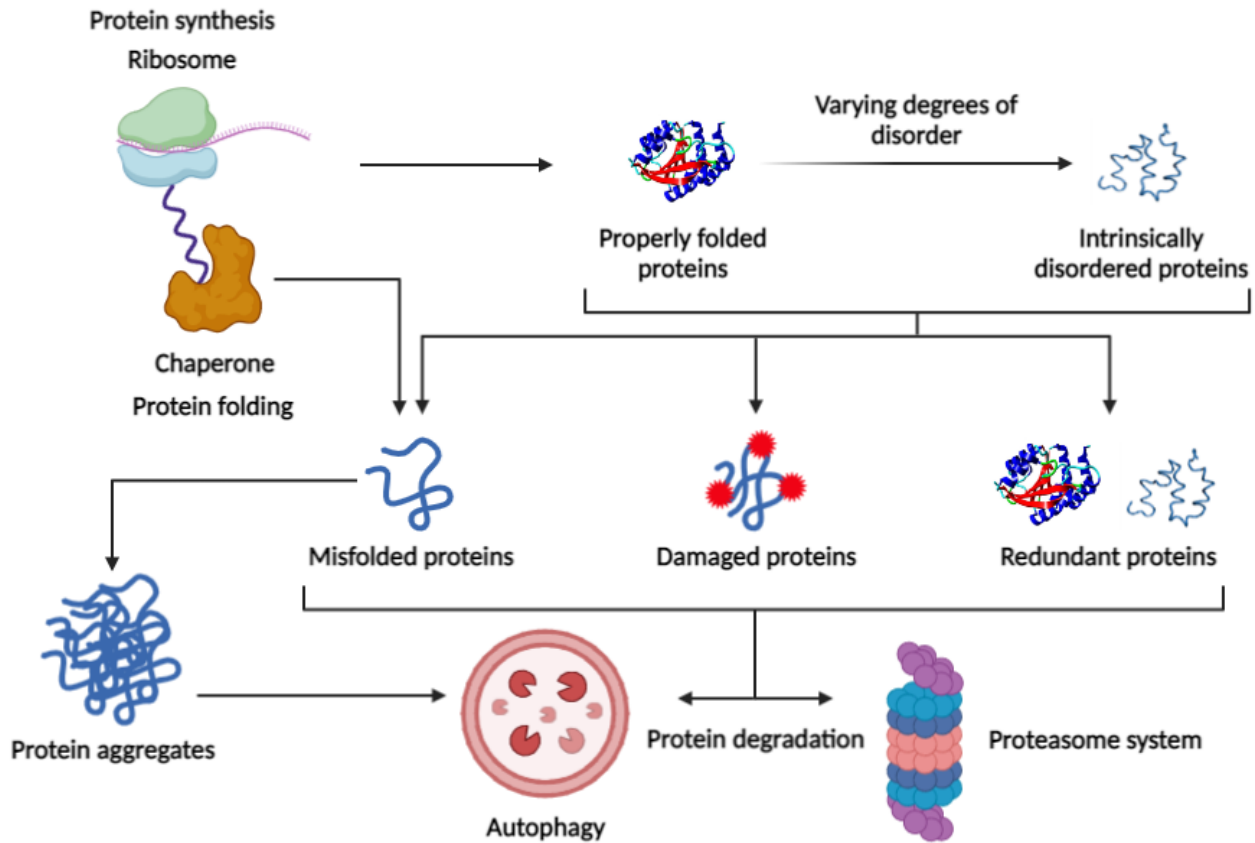


Figure 1.1: Proteostasis network breakdown. During protein synthesis by the ribosomes, nascent peptides are assisted with folding into their native conformations by molecular chaperones. This process can generate a range of proteins with varying degrees of disorder all of which perform key roles within a cell. Proteins that have become redundant, damaged, or misfolded, either during initial folding or sometime thereafter, must then be degraded via autophagy or the proteasome system. Failure to promptly remove these undesired proteins can lead to protein aggregation. Some of these protein aggregates can be degraded through the autophagy pathway, however their accumulation can become toxic and contribute to disease development. Created with BioRender.com.

1.2 The ubiquitin proteasome system

1.2.1 Proteasome structural features

The UPS is the primary system responsible for selective regulation of protein levels within a cell.³⁵⁻³⁸ The UPS plays a critical role in maintaining cellular health through regulation of cell cycle progression, genome integrity, transcriptional regulation, apoptosis, immune responses, overall maintenance of proteostasis and other cellular processes.^{30, 39, 40} As a result, decline or dysregulation of the UPS is associated with the pathogenesis of numerous human diseases.⁴¹⁻⁴⁷ The primary activity of the UPS centers around proteolytic cleavage of peptides by the massive (~2,000 kDa) multi-subunit enzyme complex known as the proteasome. The proteasome exists in multiple forms; however, the classical form is known as the 26S proteasome. The 26S proteasome is made up of one 20S core particle (CP), often referred to as the 20S proteasome, and one or two 19S regulatory particles (RP), or caps (**Fig. 1.2A**).^{35, 48-50} The 19S, 20S and 26S forms of the proteasome are so named due to their sedimentation coefficients, as determined by density-gradient centrifugation analysis. While a double capped proteasome (i.e., 19S-20S-19S) has a sedimentation coefficient of 30S and a single capped proteasome (i.e., 19S-20S) of 26S, these two forms are both commonly referred to as the 26S proteasome in the literature.⁵¹ For the sake of maintaining consistency with the literature and simplicity of discussions, the same naming scheme will be used herein.

The CP or 20S proteasome, is a 750 kDa enzyme complex made up 28 subunits organized into four concentric heptameric rings (**Fig. 1.2A**), two α -rings (subunits $\alpha 1$ – $\alpha 7$, **Fig. 1.2B**) and two β -rings (subunits $\beta 1$ – $\beta 7$, **Fig. 1.2C**).^{48-50, 52-54} The two β -rings of the 20S proteasome each contain three different catalytic sites, for a total of six catalytic sites within one 20S proteasome. These three sites provide three different threonine protease activities, one chymotrypsin-like (CT-L, $\beta 5$ -

subunit) that preferentially cleaves after hydrophobic residues, one trypsin-like (Tryp-L, β 2-subunit) that preferentially cleaves after basic residues, and one caspase-like (Casp-L, β 1-subunit) that preferentially cleaves after acidic residues (**Fig. 1.2C**).⁵⁵⁻⁵⁸ These catalytic sites work congruently to enable efficient proteolytic cleavage of a massive range of protein substrates at numerous and varied sites. The resulting small peptide fragments can be further processed by other proteases and recycled as amino acids. The two α -rings of the 20S proteasome act as docking sites for the 19S caps and as a gating-mechanism that can restrict substrate access to the catalytic sites of the 20S proteasome. The gating-mechanism is facilitated through the convergence of the N-terminal residues of the α -subunits over the pore leading into the core of the 20S proteasome.^{39, 59} In addition to the 19S cap, there exist other regulatory particles, like the 11S cap and PA200 (Proteasome activator 200 kDa), that also can associate with the α -rings of the 20S proteasome.⁶⁰⁻⁶³ The 20S proteasome has often been referred to as the latent state of the proteasome, because of the action of the α -ring gates and the lack of 19S caps, which promote ubiquitin-dependent proteolysis. However, as will be discussed in coming sections, this notion is not entirely accurate, as the 20S proteasome performs key roles in protein regulation without the need for binding of the 19S or other regulatory particles.^{25, 64-66}

Upon binding to the α -rings of the 20S proteasome and formation of the 26S proteasome, the 19S RPs are responsible for gate-opening, substrate detection, unfolding and movement into the catalytic core for proteolytic cleavage.^{54, 67-69} The 19S RP is another large complex (~700 kDa) that is composed of 19 subunits, that can be sub-divided into those associated with the base and lid portions of the 19S. The base is made up of four non-ATPase subunits (Rpn 1, 2, 10 and 13) and six ATPase subunits (Rpt1-6),⁴⁸⁻⁵⁰ the latter of which interact with the α -ring of the 20S proteasome via insertion of their C termini into hydrophobic inter-subunit pockets between the α -

ring subunits. The C termini of the Rpt1–6 subunits each have a hydrophobic-tyrosine-any residue (HbYX) motif that bind to conserved regions within the inter-subunit pockets and induce a conformational change that leads to gate-opening of the 20S proteasome.^{67, 68, 70} The exact mechanism of this gate-opening is still not clear, however. Binding of the last eight residues of Rpt5, including its HbYX-motif, is sufficient to allosterically induce conformational changes in the α -ring needed for gate opening. The ATPase activities of Rpt1–6 power the unfolding and translocation of substrates into the 20S catalytic core, through coupled ATP (adenosine triphosphate) hydrolysis.^{67, 68, 70} Rpn1, 10 and 13 act as substrate receptors that reversibly associate with ubiquitin. The presence of these multiple ubiquitin binding subunits allows the 26S proteasome to recognize and degrade a wide range of poly-ubiquitinated substrates. The lid of the 19S is made up of nine subunits (Rpn3, 5–9, 11, 12 and Sem1).⁷¹ Rpn11 functions as a deubiquitinase, allowing for recycling of the ubiquitin tags removed from 26S proteasome substrates as they enter the complex.⁷² The subunits of the lid also act as docking sites for other proteins, like other deubiquitinating enzymes (Ubiquitin specific peptidase 14 (USP14) and Ubiquitin C-terminal hydrolase 37 (UCH37)), that assist the 26S proteasome in substrate recognition and trafficking.^{48, 50, 71, 73}

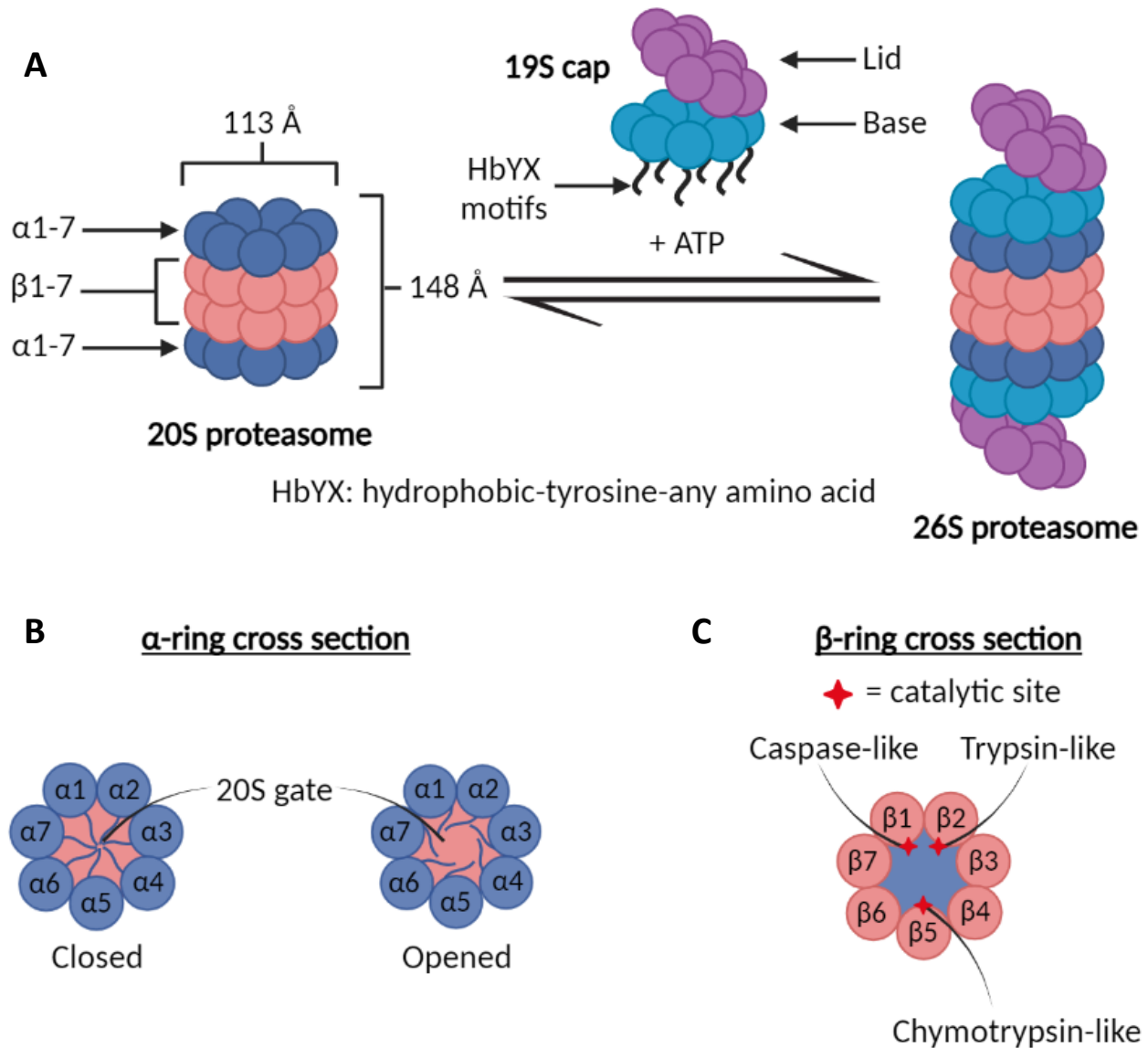


Figure 1.2: Proteasome structural overview. (A) The equilibrium between the 20S and 26S proteasome is dictated by the ATP-dependent binding of the 19S caps. Shown are measurements of the 20S proteasome (148 angstroms (Å) x 113 Å). (B) Cross sectional view of closed and opened α-rings of the 20S proteasome, dictated by the conformation of the N-terminal tails of the α-subunits (α1–α7). (C) Cross sectional view of a β-ring of the 20S proteasome with catalytic sites labeled with red diamonds. Created with BioRender.com.

1.2.2 Ubiquitin-dependent proteolysis by the 26S proteasome

The classical proteasome pathway for regulation of protein levels within the cell involves the 26S proteasome, a family of ubiquitin enzymes and occurs through ubiquitin-dependent proteolysis. Ubiquitin-dependent proteolysis, as the name suggests, requires, and is initiated by the polyubiquitination of proteins that are destined for degradation. The ubiquitin tags serve as a means for the 26S proteasome to selectively identify, via Rpn10 and Rpn13 binding, and degrade proteins that have become redundant or damaged. As the substrate protein is being unfolded by the ATPase subunits of the 19S base,^{54, 67-69} the ubiquitin tags are removed by deubiquitinases, such as the Rpn11, USP14 or UCH37, so that they may be recycled.⁷⁴

Ubiquitin itself is an 8 kDa protein with seven lysine residues, at positions 6, 11, 27, 29, 33, 48 and 63, that can be conjugated to other ubiquitin molecules to allow for polyubiquitination. The K48 residue is the primary binding site when conjugated to proteins that are destined for degradation by the 26S proteasome, whereas the other positions are used when ubiquitin is performing other roles.⁷⁵⁻⁷⁷ The process of ubiquitination starts with activation of ubiquitin by an E1 ubiquitin activating enzyme, which is an ATP-dependent process. Reaction between a cysteine residue in the active site of E1 and the C-terminal end of ubiquitin results in a thioester-linkage. Following this, the ubiquitin is passed to the E2 ubiquitin-conjugating enzyme, through formation of a similar thioester bond with E2. Finally, the E3 ubiquitin ligase binds to both the E2-ubiquitin complex and the protein substrate that requires ubiquitination. Together E2 and E3 catalyze the transfer of the ubiquitin to the substrate protein, where a lysine residue of the target protein will bind the C-terminal end of ubiquitin. Typically, for 26S proteasome degradation, several (4 or more) ubiquitin molecules are attached to the substrate protein, in a chain, prior to its recognition by the 26S (**Fig. 1.3**).^{75, 78-80}

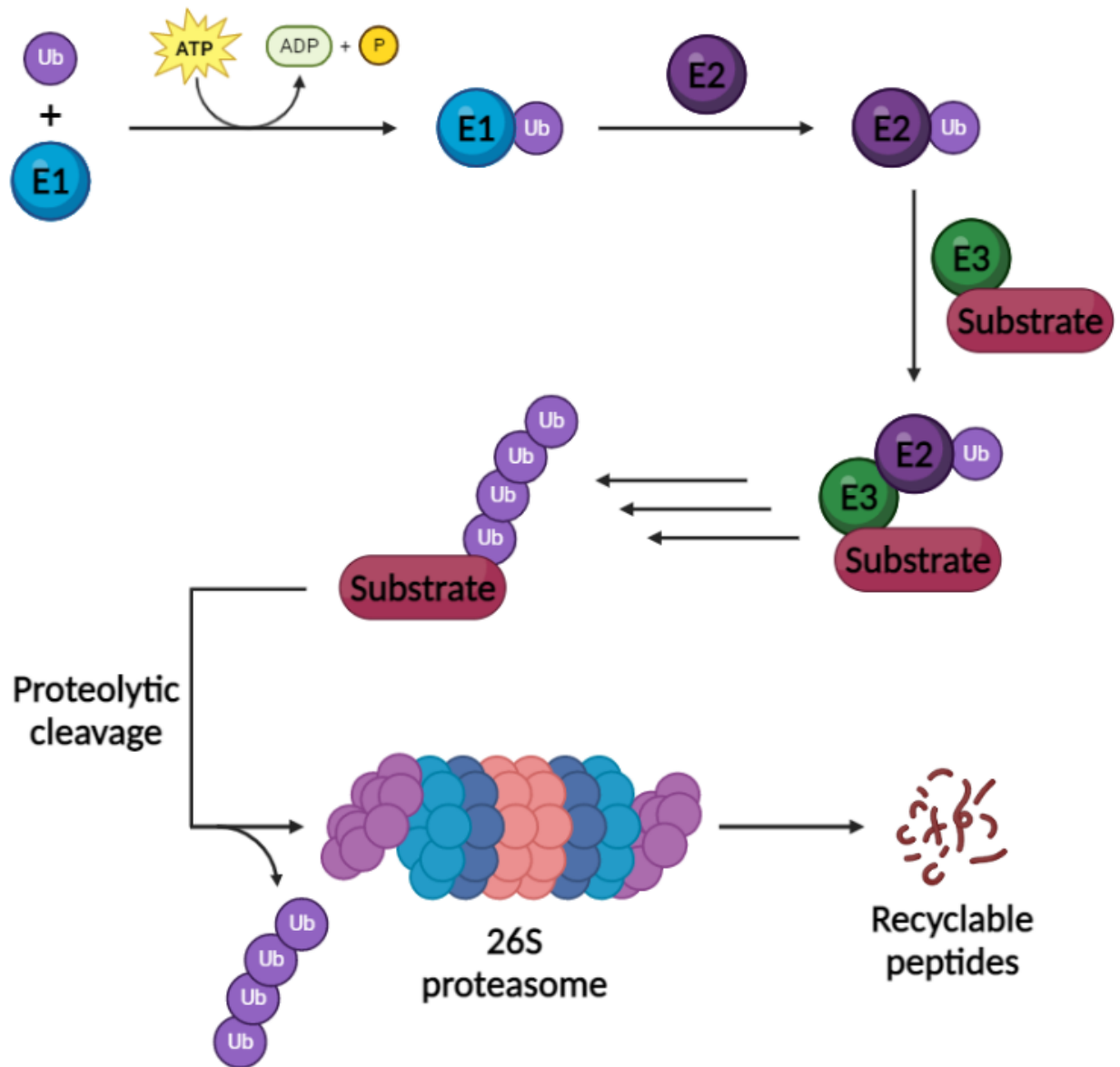


Figure 1.3: Ubiquitin-dependent proteolysis by the 26S proteasome. Ubiquitin is first activated by E1 in an ATP-dependent step. This is followed by transfer of the activated ubiquitin to E2, which then associates with the E3-substrate complex. E2 and E3 facilitate the transfer of ubiquitin to the substrate protein, which is repeated to achieve polyubiquitination of the substrate prior to its unfolding, removal of ubiquitin tags and degradation by the 26S proteasome. The resulting peptide fragments can be further processed by other proteases and recycled for use in protein synthesis. The ubiquitin tags are also recycled. Created with BioRender.com.

1.2.3 Intrinsically disordered proteins

The classical depiction of a protein involves a well-defined 3D structure, permitting for highly specific interactions and functions.⁸¹ While this is the case for many proteins, not all proteins fit this depiction. A more realistic view is that proteins exist on a continuum of order and disorder (**Fig. 1.4**). On this continuum, there are those classical highly structured proteins, but there are also proteins that lack any well-defined 3D structure, as well as everything in between.⁸²⁻⁸⁵ Many proteins possess regions, known as intrinsically disordered regions (IDRs), that are unable to fold into stable 3D structures. Other proteins, known as intrinsically disordered proteins (IDPs), are comprised primarily of disordered regions and may have little, if any, well-defined 3D structure or folded regions. A large portion of the proteome (~30%) is made up of IDPs or proteins with substantial IDRs.⁸⁶ IDPs and IDRs are such because of biased amino acid compositions and low sequence complexities. For instance, they tend to have low proportions of bulky hydrophobic amino acids and high proportions of charged and hydrophilic amino acids. This results in their inability to fold into stable 3D structures, since the driving force for formation of those structures is generally hydrophobic interactions between amino acids.⁸⁷⁻⁹⁰ These commonalities associated with specific amino acid proportions within IDPs and IDRs has allowed for the development of predictive software for protein disorder. PONDR,⁹¹ IUPred⁹² and SPOT-Disorder-Single⁹³ are examples of these types of software. Experimental confirmation of protein disorder can be achieved through the use of nuclear magnetic resonance (NMR) spectroscopy⁹⁴ and circular dichroism (CD).⁹⁵

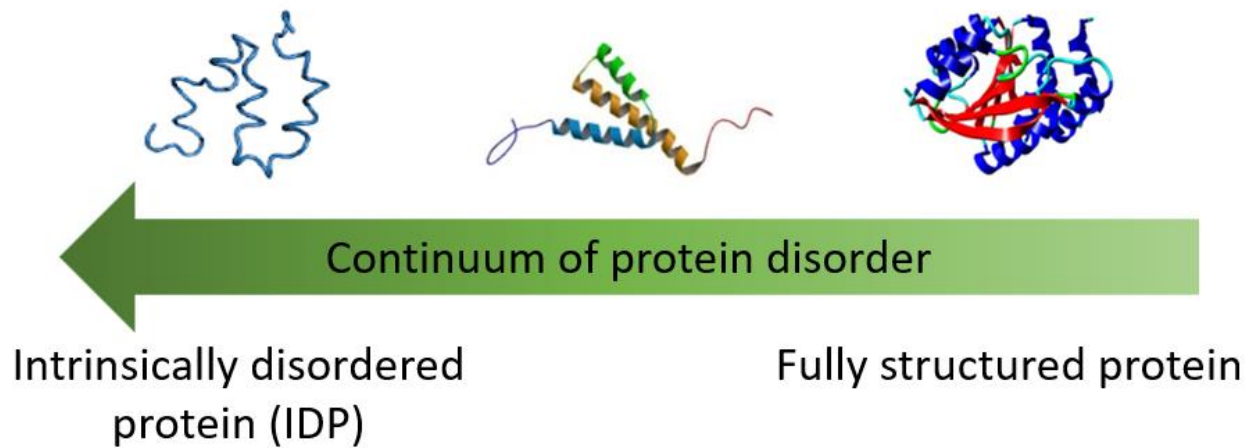


Figure 1.4: Continuum of protein disorder. Proteins exist in a variety of states of order and disorder, where some have stable and well-defined 3D structures and others have large regions that lack any defined 3D structure or stable folding. IDPs are proteins that have few if any stable 3D structured regions when free in solution.

Without substantial folding, IDPs and IDRs have very dynamic structures that can fluctuate rapidly through many conformations. This flexible nature permits IDPs and IDRs to interact with a range of binding partners and perform multiple roles within a cell or system. As such, IDPs are often involved in, or act as, hubs in protein-interaction networks.^{96, 97} They are often signaling molecules (about 75% of known IDPs) or participate in the regulation of signaling pathways. For this reason, their cellular abundance must be tightly regulated to ensure proper signaling occurs for important cellular processes, like in the regulation of cell cycle progression, transcription, or translation.⁹⁶⁻⁹⁸ Their critical involvement with these pathways is evident in that dysregulation of IDPs is associated with the development of a variety of human diseases.^{84, 85, 99, 100} Under healthy conditions, the abundance of IDPs is tightly regulated through proteolytic cleavage by the 20S proteasome.^{99, 101-103} However, in human diseases associated with IDPs, they often begin to accumulate as some aspect of their regulation breaks down. These accumulated IDPs can cause

toxic signaling and are prone to aggregation, as seen in neurodegenerative diseases.^{7, 100, 104-110} Due to their high degree of flexibility and lack of well-defined binding pockets, IDPs have often been thought of as “undruggable”. As such, activation of 20S proteasome-mediated degradation of IDPs seems like a promising target for therapeutic intervention in diseases associated with their dysregulation.

1.2.4 20S proteasome-mediated regulation of IDPs and other unfolded peptides through ubiquitin-independent proteolysis

As was alluded to above, the 20S proteasome, while often considered the latent state of the proteasome, plays a critical role in the regulation of cellular levels of IDPs, as well as some misfolded and oxidatively damaged proteins, through proteolytic cleavage. These processes do not require the unfolding activity of the 19S RP, nor the ubiquitination of the protein substrates as seen with the 26S proteasome.¹¹¹⁻¹¹³ As a result, the 20S proteasome can unremittingly degrade these substrates without the need for RPs, however some natural activators exist that can assist with this process.⁶¹⁻⁶³ The 20S proteasome exists primarily in a closed-gated conformation, by way of the α -ring gates, which restricts access to the catalytic core.¹¹⁴ However, it is believed that direct interaction of protein substrates with the α -ring can bring about a conformational change that permits gate-opening and substrate degradation.⁹⁹ Despite this, the activity of the 20S proteasome towards its substrates can be enhanced via methods that promote open-gate conformations. Native examples of this can be seen through the action of non-ATPase regulatory particles of the proteasome, such as the 11S cap and PA200. Their association with the 20S proteasome leads to open-gate conformations that can promote proteolysis of 20S proteasome substrates.⁶¹⁻⁶³ In light of these native activating factors, similar activation of the 20S proteasome, via small molecules that induce open-gate conformations, could allow for enhancement of its activity and therapeutic

intervention in diseases where accumulation of its substrates, like IDPs, contribute to disease progression.

1.3 Proteostasis disruption contributes to aging and neurodegenerative diseases

1.3.1 Aging and proteostasis decline

Age-related cellular dysfunction and degenerative diseases are thought to be the result of an age-dependent decline in a cell's ability to maintain proteostasis. This decline in the capacity of the proteostasis network is complex, but is likely rooted in changes in expression and activity of proteostasis machinery and an increasing burden of oxidatively damaged and misfolded proteins.^{2, 4, 12, 28} This results in an accumulation of these and other proteins, like IDPs, which are similarly regulated by the 20S proteasome. This accumulation eventually leads to their aggregation and further disruption of proteostasis through inhibition of the proteasome by some of these aggregate forms.¹¹⁵⁻¹²⁰ This initiates a cycle of continuing accumulation, aggregation, and disruption of proteostasis, which ultimately results in cellular toxicity and death. These effects are especially pronounced in nondividing, long-lived cells like neurons, where high levels of oxidative stress and an extended duration of accumulation exacerbate the problem.^{3, 121, 122} The disruption of proteostasis can spread from cell to cell, through seeding of aggregation, leading to widespread degeneration of neurons.¹²³⁻¹²⁹ The result of this spreading disruption of proteostasis and neuron death is the onset of neurodegenerative diseases, such as Parkinson's disease (PD), Alzheimer's disease (AD), and Huntington's disease (HD). The development of each of these diseases is thought to be associated with the accumulation and aggregation of IDPs, such as α -synuclein, amyloid β and huntingtin protein.^{104, 130-133}

To combat the declining proteostasis network seen in neurodegenerative diseases and to help re-establish normal levels of disease related IDPs, 20S proteasome activation has been

proposed as a therapeutic strategy to selectively target IDPs for degradation through the native mechanism for their disposal.^{25, 134-136} This proposed strategy is supported by studies done in animal models, where genetic manipulation of the proteasome system suggests that stimulation of its activity could aid in treatment of these diseases.^{41, 137} As humans age, the 20S proteasome becomes increasingly more prevalent than its 26S counterpart, so targeting of the 20S proteasome may prove to be more beneficial in these age-related diseases.^{47, 138-140} The strategy of targeting the 20S proteasome specifically, looks even more promising when it is considered that the proteins involved in the pathogenesis of neurodegenerative diseases, like α -synuclein and amyloid β , are IDPs and thus likely substrates of the 20S proteasome.^{100, 134, 141} Additionally, selective activation of the 20S proteasome should provide a degree of specificity towards its usual substrates, oxidatively damaged proteins and IDPs, whereas activation of all proteasomal degradation may result in undesired degradation of other proteins. Indeed, it has been recently demonstrated that activation of the 20S proteasome only enhances the degradation of its normal substrates, with highly disordered proteins being most quickly degraded.¹⁴² Furthermore, it has been demonstrated that desirable IDPs can be protected from ubiquitin-independent degradation by the 20S proteasome through what has come to be known as the “nanny model”.¹⁴³ In this model, it was hypothesized and later shown that protection of IDPs occurs through transient binding to nanny proteins that protect their disordered regions from being able to be degraded by the 20S proteasome so that they can perform necessary functions.¹⁴³ In the cases of neurodegenerative diseases, the capacity of the nanny proteins is likely quickly exceeded with the accumulating levels of pathogenic IDPs.

1.3.2 Parkinson’s disease

PD is the second most common neurodegenerative disease overall¹⁴⁴ and the most common neurodegenerative disease primarily associated with decline of motor functions.¹⁴⁵ Early

symptoms of PD are commonly tremors, loss of balance and rigidity. As the disease progresses, additional symptoms can arise that include cognitive changes, like mood disorders and depression, in addition to further degeneration of motor function, including difficulty swallowing, chewing, and speaking. These symptoms are a result of degeneration of dopaminergic neurons within the substantia nigra pars compacta (SNpc) and resulting loss of dopamine signaling in the striatum.^{146,}

147

There is currently no cure for PD, nor any treatments that can hinder disease progression. So, treatments are focused on relieving symptoms and improving quality of life. The most common treatments for PD are related to the restoration of dopamine levels to make up for loss of dopamine signaling, which is a major causative factor for the motor-related symptoms.¹⁴⁶ This is often done through treatment with a combination of Levodopa, also known as L-DOPA, and Carbidopa. Levodopa is a dopamine precursor, that once it has entered the brain can be metabolized into dopamine, by aromatic L-amino acid decarboxylase, and subsequently used for dopamine signaling. Carbidopa, on the other hand, is a Levodopa mimic that cannot pass the blood-brain barrier (BBB) and serves to boost the exposure of Levodopa to the brain and reduce side effects through inhibition of Levodopa's premature metabolism outside of the brain.¹⁴⁸⁻¹⁵⁰ In addition to Levodopa/Carbidopa, there are other methods that are used to increase dopamine signaling, like treatment with dopamine receptor agonists or dopamine metabolism inhibitors. In cases where methods to restore dopamine signaling are not as effective, or certain symptoms, like tremors, are persistent, other more invasive therapies can be applied. This includes things like deep brain stimulation and lesion surgery, which can in some cases help to alleviate these persistent symptoms. Regardless of which current treatment method is used, however, PD continues to progress, and treatment efficacy will decline. For this reason, novel treatments are desperately

needed to not only combat the devastating symptoms of this disease, but also to provide hope for disease-modifying treatments.¹⁴⁶

Although the pathogenesis of PD is not yet fully understood, it is widely accepted that proteostasis disruption in the afflicted neurons is closely linked to disease development.¹⁵¹ The initial disruption of proteostasis is thought to be due in part to the age-related decline in proteasome function in dopaminergic neurons of the SNpc, as a result of decreasing subunit levels and reduction in proteolytic activity.^{152, 153} This reduction in proteasome activity is thought to make these neurons susceptible to the disruption of proteostasis by the ever-present need for clearance of oxidatively damaged proteins and regulation of native proteins, such as the IDP α -synuclein.¹⁵⁴ When proteostasis falls out of balance, α -synuclein and other proteins begin to accumulate and aggregate, which is thought to lead to further disruption of proteasome activity and proteostasis in general. This results in a vicious cycle of proteasome impairment and proteotoxicity in PD.^{120, 155-159} As such, the maintenance of proteasome function, and thus proteostasis, is critical to preventing the constant accumulation and aggregation of unwanted proteins seen in PD progression.

One of the major hallmarks of PD is the accumulation and aggregation of the IDP α -synuclein. α -Synuclein is a 140 amino acid IDP that is predicted to be approximately 91% disordered, according to the PONDR software.^{91, 104, 130, 146, 147, 158, 160-162} The normal function of α -synuclein in non-diseased neurons is not well understood, despite substantial efforts to elucidate it.¹⁶³ What is known is that α -synuclein appears to play a role in membrane curvature, vesicle trafficking and vesicle budding. This would explain its relative abundance in neuron synapses and association with lipid membranes and SNARE complexes, but additional studies are required to fully understand its role in these processes and any other potential roles that it may play.¹⁶³⁻¹⁶⁸ Regardless of its normal function, in PD α -synuclein has been implicated as a likely contributor to

disease progression due to the association of duplication,¹⁶⁹ triplication^{170, 171} and mutations in the SNCA gene, encoding for α -synuclein,¹⁷²⁻¹⁷⁶ with early onset forms of PD. Additionally, α -synuclein accumulation, aggregation and presence as the primary protein within Lewy bodies, which are large protein aggregates seen in the cytoplasm of neurons in a PD afflicted brain, further implicate it in disease pathogenesis.^{130, 147, 158}

In PD, α -synuclein exists in multiple forms upon its accumulation, including monomers, various oligomers, aggregates, and fibrils.^{109, 177, 178} While early identification of Lewy bodies and large fibrils suggested they might be responsible for the neuron degeneration and toxicity, mounting evidence suggests that it is the smaller soluble oligomeric forms of α -synuclein that are the more toxic species. Whereas, the larger fibril and aggregate forms may serve a more neuroprotective role, by sequestering the small toxic oligomers.^{127, 179-181} However, their presence is still a hallmark of disease development and progression, considering in a healthy system they should not be present.^{130, 147} Furthermore, it has been recently shown that some of the soluble oligomeric forms of α -synuclein are also responsible for direct binding to and inhibition of the proteasome, leading to further proteostasis disruption.^{115, 116, 155, 156} Compounding the issue, α -synuclein is known to be a substrate of the 20S proteasome, so through proteasome inhibition additional α -synuclein accumulation and aggregation is promoted. This leads to the vicious cycle of proteasome inhibition and IDP accumulation, mentioned previously.¹⁵⁵⁻¹⁵⁷ The involvement of α -synuclein with PD pathogenesis, and its place as a natural substrate for the 20S proteasome make it a promising target for therapeutic intervention through the activation of its degradation by the 20S proteasome. Activation of the 20S proteasome could also assist in the clearance of other accumulating disordered or damaged proteins and help to re-establish proteostasis in PD. For these

reasons, the Tepe lab has begun exploring small molecule activation of the 20S proteasome as a novel therapeutic strategy for PD.

1.3.3 Alzheimer's disease

AD is the most common neurodegenerative disease, affecting approximately 45 million people worldwide. Early symptoms of AD are primarily cognitive, including progressive memory loss, difficulty multi-tasking and finding the right words, etc. Later in disease progression, these cognitive problems continue to worsen and additional symptoms, such as behavioral changes, impairment of mobility, hallucinations, and seizures, may develop.^{182, 183} Memory loss can become extreme, to the extent that a patient cannot recognize people that they have known their entire life. The devastating symptoms, poor prognosis, and lack of disease modifying treatments make AD an extremely difficult disease to cope with for the patient and their loved ones. This also means that development of novel therapeutic strategies that provide hope for disease modifying treatments is of great importance.

Similar to what is seen with PD, the major hallmark of AD is also IDP accumulation and aggregation. In the case of AD, the primary IDP involved with its pathogenesis is amyloid β , instead of α -synuclein. Amyloid plaques are extracellular aggregates that are primarily composed of amyloid β and represent the final large aggregate form of the IDP. Amyloid β is a peptide by-product of the metabolism of the amyloid precursor protein (APP) and commonly is either 40 or 42 amino acids, with the 42 amino acid form being the primary component of amyloid plaques, due to a faster rate of aggregation.¹⁸⁴⁻¹⁸⁶ The leading theory of AD pathogenesis is known as the amyloid hypothesis, which suggests that the accumulation of pathological forms of amyloid β , resulting from the cleavage of APP by β - and γ -secretase enzymes, is caused by an imbalance between its production and degradation.^{183, 184, 187} As was discussed above, a reduction in

proteasome activity during the aging process could be one factor that contributes to the eventual disruption of proteostasis in regard to amyloid β peptides. Upon their accumulation, amyloid β peptides can form a variety of aggregates, much like what is seen with α -synuclein.¹⁸⁸⁻¹⁹⁰ Also similar to α -synuclein in PD, it is thought that soluble oligomeric forms of amyloid β are likely the more toxic species, instead of the larger aggregates and fibrils.¹⁹¹⁻¹⁹⁵ Additionally, amyloid β oligomers have been shown to directly bind to and inhibit the 20S proteasome, further contributing to amyloid β accumulation and disease progression.^{115, 116} The similarities between PD and AD, in regard to IDPs and proteostasis disruption, make both promising targets for treatment through 20S proteasome activation.

1.3.4 Other neurodegenerative diseases associated with IDP accumulation and aggregation

Other neurodegenerative diseases, like Huntington's disease and amyotrophic lateral sclerosis (ALS), also share some similarities with PD and AD. They are also associated with accumulation and aggregation of IDPs and misfolded proteins, as well as proteostasis disruption.^{132, 196, 197} Oligomers of the Huntingtin protein have recently been shown to directly inhibit the 20S proteasome, similar to α -synuclein and amyloid β .¹¹⁵ In some familial forms of ALS, associated with mutations in the gene for C9orf72, disordered dipeptide repeat proteins accumulate, aggregate and can further disrupt proteasome function.¹⁹⁷⁻¹⁹⁹ The similarities in pathogenesis and the involvement of IDPs in these neurodegenerative diseases suggest that small molecule 20S proteasome activation may represent a promising therapeutic strategy for multiple neurodegenerative diseases. The studies herein will focus primarily on PD, however similar studies can be envisioned for the other neurodegenerative diseases mentioned above. Studies focused on other neurodegenerative diseases should be explored in the future to better understand the breadth of potential disease targets for this proposed therapeutic method.

1.3.5 Neuroinflammation in neurodegenerative disease pathogenesis

In recent years, growing evidence has been collected implicating neuroinflammation as another major factor in the pathogenesis of neurodegenerative diseases. This has been demonstrated in multiple neurodegenerative diseases, like PD, AD and ALS, and is thought to result from activation of the native immune system in the brain by IDPs released from degenerating neurons. While the degree to which neuroinflammation contributes to progression of these neurodegenerative diseases is not fully understood, it likely plays a deleterious role through causing further neuron degeneration via inflammatory signaling and further spreading of disease pathology.^{126, 200-211} As such, during the exploration of novel methods for treatment of neurodegenerative diseases the effects a novel treatment method has on this neuroinflammation should also be evaluated, to gain a better understanding of the breadth of effects and potential benefits. Treatments that can affect proteostasis disruption or IDP accumulation/aggregation, as well as neuroinflammation may show greater promise for successfully modifying disease progression, considering that each plays a part in the pathogenesis of these diseases.

In the brain, immune responses are primarily controlled by a cell type known as microglia. Microglia act as specialized macrophages, but differ in several ways, including but not limited to their origin, turnover rate, gene expression while in their resting state and that they are much more tightly regulated spatially and temporally.²¹² Microglial cells perform a variety of roles within the brain that are essential to healthy brain development and function. They are central to neurodevelopment and plasticity through extracellular signaling to neurons.²¹³⁻²¹⁶ They participate in numerous extracellular signaling events related to inflammatory responses, anti-inflammatory responses, antigen presentation, synaptic remodeling and cytotoxic signaling.^{212, 217} They also act similar to macrophages by probing and sensing their surroundings constantly and when activated

they can scavenge and phagocytose foreign material and cellular debris.^{212, 217, 218} Their overall role within the brain is to support neuron health and maintain brain homeostasis.^{212, 219-221}

Microglia can take on several forms associated with their degree of activation and location. Perivascular and Juxtavascular microglia associate closely with the vasculature of the brain, as their names suggest.^{222, 223} Standard microglia within the rest of the brain vary in form from their resting, otherwise known as ramified, state through a continuum of activated forms based on the degree of activation and type of activating stimuli.^{212, 224, 225} Microglia become activated following detection of pro-inflammatory stimuli, like cytokines, chemokines, necrosis factors, foreign materials, or potassium level changes.^{212, 223} During this progressive activation, which amplifies as signals are continually detected, microglia begin to proliferate rapidly and undergo morphological changes, becoming more ameboid-like and reducing processes used for detection.^{224, 225} They also begin to upregulate Major Histocompatibility Complex (MHC) class I/II proteins and secrete cytotoxic factors, recruitment molecules and inflammatory signaling molecules.^{212, 223, 226} Upon further activation, they can transition into phagocytic microglia, where they phagocytose foreign material, cellular debris and dead or dying cells.^{212, 222, 224}

Microglia can become significantly altered as humans age, resulting in what are called “primed” microglia. Microglia can become primed via stimulation with inflammatory stimuli throughout their lifespan. These primed microglia are associated with hyperactive inflammatory responses upon re-exposure to activating stimuli.^{227, 228} Additionally, microglia from elderly people tend to maintain an increased active state, relative to microglia found in younger individuals. This is a result of differences in gene expression and increased basal release of pro-inflammatory signaling molecules by the microglia.^{227, 229, 230} The changes seen in these aged microglia also result in a reduced propensity to enter their phagocytotic form, instead favoring

continued secretion of inflammatory signaling molecules.^{227, 229, 230} These effects together lead to an overall weakening of the ability of microglia to maintain homeostasis and a propensity to cause more severe inflammation in response to perturbations in the brain.²¹⁹

Neuroinflammation seen in neurodegenerative diseases, like PD and AD, involves activation of microglia by IDPs released from degenerating neurons. Multiple cell surface receptors, such as toll-like receptors (TLR2 and TLR4) and CD36, have been implicated in the detection of IDPs in the extracellular space by microglia.^{126, 200-211} Following IDP detection, a pro-inflammatory response is initiated through pro-inflammatory pathways, like the NF- κ B pathway, resulting in release of pro-inflammatory signaling molecules, like cytokines (i.e. TNF- α , IL-1 β) and chemokines (i.e. IFN- γ) and reactive oxygen species (ROS).^{201, 204, 219, 231} These signaling molecules and ROS promote further neuron degeneration, which in turn leads to more release of IDPs. This results in a vicious cycle of increasing neuron degeneration and neuroinflammation (**Fig. 1.5**).^{126, 200-211} Under normal circumstances neuroinflammation would be resolved following clearance of the perturbing species that activated the microglia and re-establishment of brain homeostasis.²¹² However, aged and primed microglia are less capable of removal of these aberrant proteins and cellular debris through phagocytosis and in neurodegenerative diseases neuron degeneration and IDP release lead to persistent activation of microglia.^{219, 227-230} The result is chronic neuroinflammation, which is a hallmark of and a contributor to neurodegenerative disease pathogenesis.^{126, 200-211} As such, treatments aimed at modifying progression of these diseases should be evaluated for their effects on microglia and neuroinflammation, in addition to neurons and the other pathological aspects of these diseases.

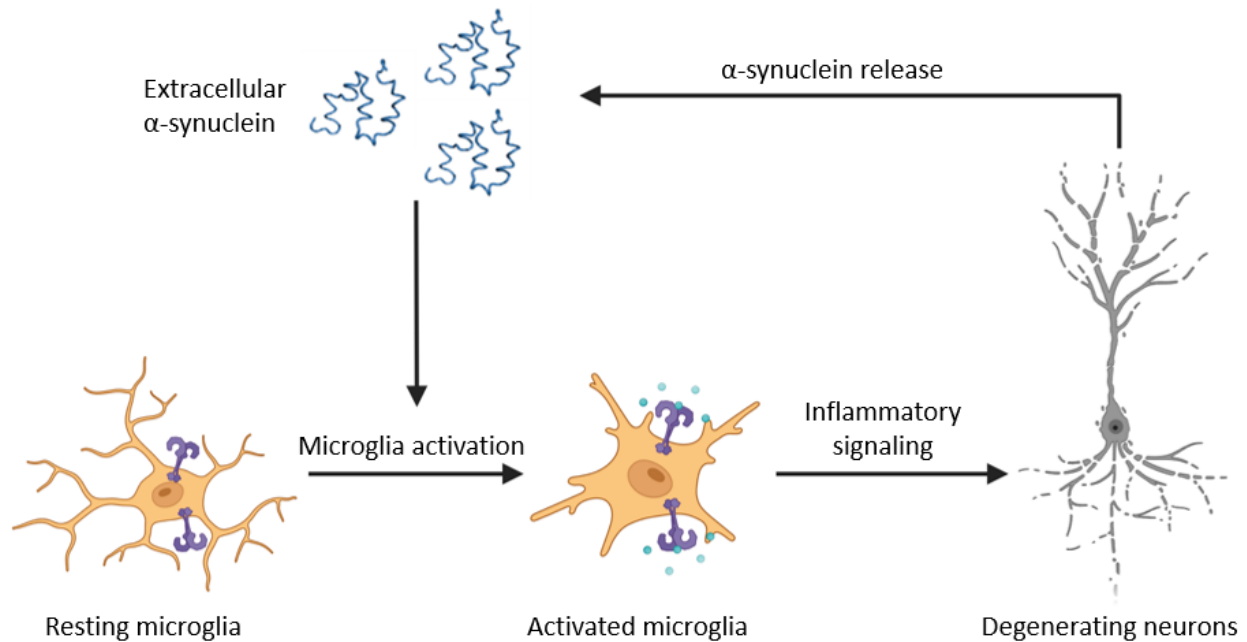


Figure 1.5: Vicious cycle of increasing neuron degeneration and neuroinflammation seen in Parkinson's disease pathogenesis. Degeneration of dopaminergic neurons in PD leads to release of accumulated α -synuclein into the extracellular space. Resting microglia detect this aberrant protein and become activated. Activated microglia secrete various inflammatory factors, which contribute to further neuron degeneration, thus initiating a cycle of increasing neuron degeneration and inflammation. Created with BioRender.com.

1.4 The 20S proteasome as a novel therapeutic target

The key involvement of the proteasome in the maintenance of proteostasis and in numerous essential biological pathways has long garnered attention to it as a promising therapeutic target for treatment of a variety of diseases.^{30, 39, 40, 134, 232-234} Specific targeting of the 20S proteasome has been proposed as a novel strategy to counteract the accumulation of IDPs associated with neurodegenerative disease development.^{25, 134-136} By targeting the 20S proteasome, IDPs and oxidatively damaged proteins that accumulate in these diseases can be selectively targeted,

considering the 20S proteasome's limited substrate scope of unfolded proteins.¹¹¹⁻¹¹³ 20S proteasome activation could assist in re-establishing proteostasis via clearing of accumulated IDPs and maintain its activity in neurodegenerative diseases, where proteasome activity is known to be reduced^{24, 153} and even inhibited.^{115, 116} Additionally, the 20S proteasome becomes more prevalent as humans age, relative to the 26S proteasome, so it may represent the more promising target in these systems.^{47, 138-140} The studies outlined herein will focus on the development of small molecule 20S proteasome activators as a novel therapeutic strategy for neurodegenerative diseases. As such, a brief summarization of the history of this technology is required to set the stage for the upcoming chapters.

1.4.1 Small molecule 20S proteasome activators

It was first demonstrated that the 20S proteasome could be activated using low concentrations (0.04-0.08%) of sodium dodecyl sulfate (SDS), which proved to be a useful tool for *in vitro* studies of the 20S proteasome. However, at higher concentrations SDS inhibits the proteasome, suggesting that it is acting as a partial denaturant, allowing for easier access to the catalytic core of the proteasome at low concentrations.^{55, 114} Other SDS-like activators of the proteasome have since been identified, but due to their inability to be used in physiologically relevant systems they are reserved for use as *in vitro* tools.²³⁵⁻²³⁷

Some years following the discovery of SDS as a means to activate the 20S proteasome, researchers have begun focusing on the identification and development of more drug-like small molecule activators of the 20S proteasome. Perhaps the next small molecule 20S proteasome activator identified was betulinic acid (**Fig. 1.6A**).²³⁸ Betulinic acid, a triterpenoid, was found to enhance the CT-L activity of the 20S proteasome *in vitro*. However, the development of analogues of betulinic acid and investigation of its structure activity relationships (SAR) proved to be

complicated due to changes in its structure resulting in inhibitors, as opposed to the desired activators.²³⁸ Additionally, it was later found that this apparent activity did not translate to the degradation of IDPs.²³⁹

Following the discovery of betulinic acid as a 20S activator,²³⁸ researchers began trying to identify novel activators that have more drug-like properties and lack the issues seen with betulinic acid. Among the first, was a study done by Kodadek *et al.*²³⁹ where they developed a series of assays designed to allow for screening of small molecules for 20S proteasome activation. Two novel 20S proteasome activators, MK-866 (**Fig. 1.6B**) and AM-404 (**Fig. 1.6C**), were identified in their screening. These small molecules were able to enhance the degradation of the IDP α -synuclein in cell culture.²³⁹ Extending upon this work, Coleman and Trader²⁴⁰ identified additional 20S proteasome activators, including ursolic acid (**Fig. 1.6D**), a derivative of betulinic acid, and a cytosine derivative (**Fig. 1.6E**).²⁴⁰

Concurrently, the Tepe lab identified their first small molecule 20S proteasome activator and were working to identify additional novel 20S activator scaffolds using a combination of biochemical assays and *in vitro* experiments.^{135, 136} The first 20S proteasome activators published by the Tepe lab were identified in a high-throughput screen of the NIH clinical collection and Prestwick library, where the neuroleptic agent Chlorpromazine (**Fig. 1.6F**) and other phenothiazine derivatives were identified as novel 20S proteasome activators.¹³⁵ Several analogues of Chlorpromazine were synthesized to diminish its dopamine D2 receptor activity and enhance/maintain its 20S proteasome activity. These phenothiazine analogues were found to enhance the rate of degradation of 20S proteasome substrates in biochemical and cellular assays, and due to their drug-likeness, they represented some of the most promising candidates for drug development at that time.¹³⁵

Prior to the discovery of the Chlorpromazine analogues as 20S proteasome activators, but published thereafter, Njomen *et al.*¹³⁶ discovered TCH-165 (**Fig. 1.6G**), to be a potent 20S proteasome activator. TCH-165 was found to promote an open-gate conformation of the 20S proteasome using atomic force microscopy (AFM) to visualize the gate-opening.¹³⁶ This represents the first and only biophysical data supporting this mechanism of small molecule 20S proteasome activation. TCH-165 remains one of the most potent 20S proteasome activators identified and has become a benchmark compound to which newly developed activators have been compared.¹³⁶

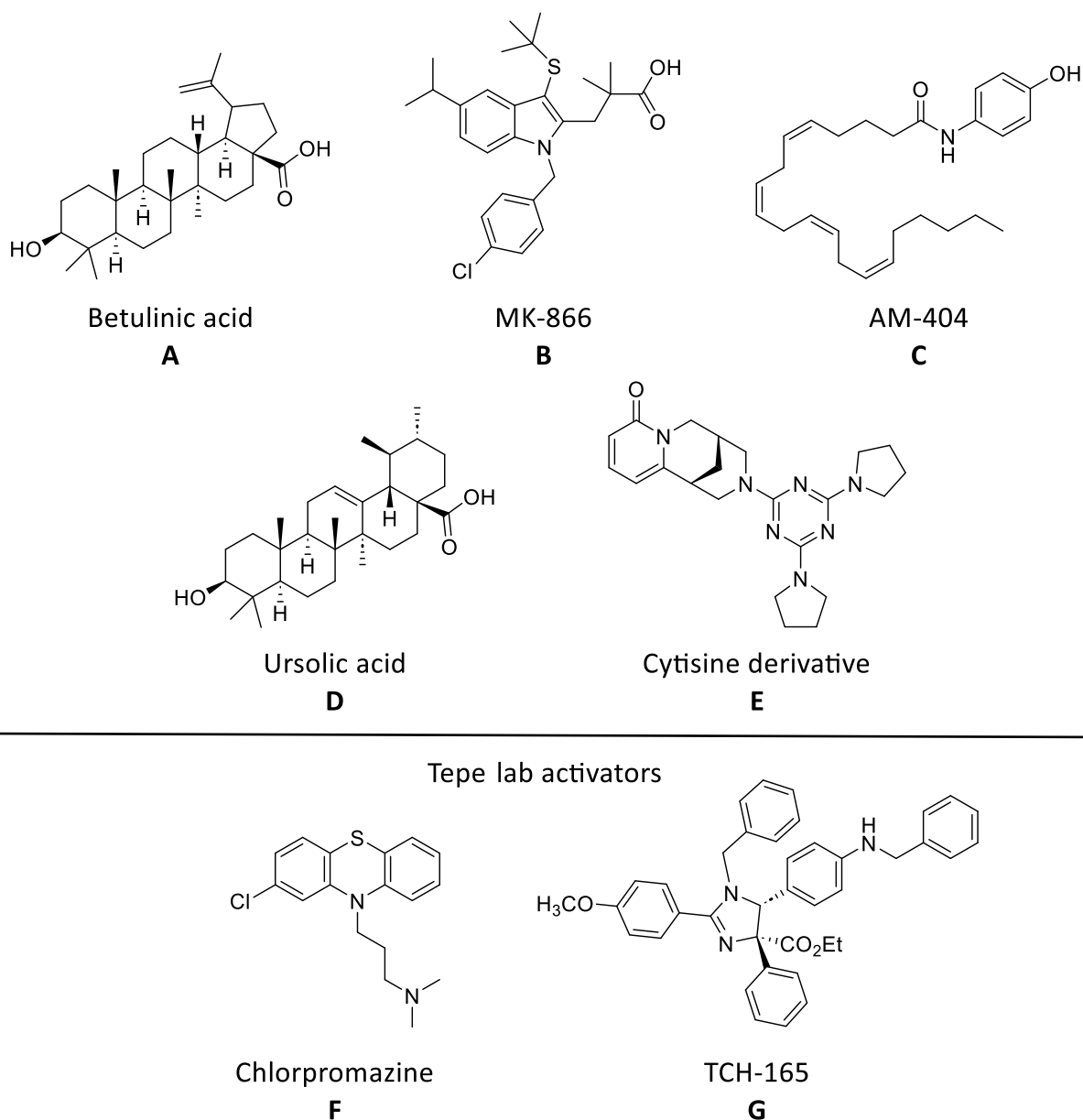


Figure 1.6: Selection of known small molecule 20S proteasome activators.^{135, 136, 238-240}

1.4.2 Continuing the investigation of small molecule 20S proteasome activation as a therapeutic strategy

Despite the recent advances in the field of small molecule 20S proteasome activation, there remains a great need for the identification of novel molecular classes of 20S activators, due to a variety of limitations seen with previously identified activators. BBB permeability, low potency,

non-translatable activity to physiologically relevant substrates or systems and target promiscuity, represent some of the current limitations of previously identified activators. To overcome these limitations, the Tepe lab continues to investigate novel analogues of Chlorpromazine,¹³⁵ TCH-165¹³⁶ and other molecular scaffolds, discovered during the high-throughput screen that show 20S proteasome activity.

Due to the field of small molecule 20S proteasome activation being relatively young, there is still much to be discovered in terms of the utility and effects of 20S proteasome activators in more disease relevant systems. For example, although it has been shown that these activators can enhance the rate of degradation of IDPs in purified protein and cellular assays, it is not known what effect these activators may have on the toxic oligomeric forms of IDPs that are associated with many neurodegenerative diseases.^{83, 107, 108, 133, 186, 241-246} It is thought that these oligomeric IDPs exist in an equilibrium with the monomeric form.^{188-190, 247} So, if 20S proteasome activators can enhance clearance of monomeric IDPs in systems with various IDP forms, then they may also reduce the toxic oligomeric forms. However, this has not yet been explored. Further complicating this, it was recently found by Smith *et al.*¹¹⁵ that the 20S proteasome can be inhibited by some oligomeric forms of IDPs. A study examining if 20S proteasome activators can influence IDP oligomer concentrations and maintain 20S proteasome activity in the presence of inhibitory oligomers may provide invaluable support for 20S proteasome activators as a potential therapeutic strategy for the treatment of neurodegenerative diseases.

The studies outlined herein were aimed at furthering the development of 20S proteasome activators as a novel therapeutic strategy for treatment of neurodegenerative diseases. Chapters 2 and 3 focus on the identification of novel 20S proteasome activator scaffolds through collaboration with Dr. Adam Mosey's lab (**Chapter 2**) and from the high-throughput screen run by our lab

previously (**Chapter 3**).¹³⁵ Evaluation of these scaffolds sought to ensure that they show promising levels of activity, activate all catalytic sites of the 20S proteasome and that their activity translates to degradation of disease relevant substrates. Furthermore, these studies sought to begin to explore these novel scaffolds in terms of their structure activity relationship (SAR) towards 20S proteasome activation and pave the way for the development of future analogues, with promising drug-like properties and potent activity. **Chapter 4** will focus on the development of novel methods for evaluating the activity and utility of 20S proteasome activators in more disease relevant model systems. Additionally, these studies sought to further our understanding of the potential effects that small molecule 20S proteasome activators may have in diseased systems, where IDP oligomers, 20S proteasome inhibition and neuroinflammation all play a role.

1.5 Conclusions

The capability of a cell to maintain proteostasis is critical for it to properly perform its functions and to its overall health.²⁻⁶ The disruption of cellular proteostasis is associated with the development of numerous human diseases, with neurodegenerative diseases as a prime example.^{1, 4, 10, 12, 28, 151, 197, 248} As such, there is great interest in the development of therapeutics that can assist in re-establishing proteostasis in cells and diseases where it has been disrupted.^{1, 4, 10, 12, 28} One of the critical components of the proteostasis network that shows potential as a therapeutic target is the proteasome.^{25, 34, 134, 233, 234, 249, 250}

The proteasome is one of the major protein degradation machineries within a cell. It is responsible for helping to regulate protein levels to preserve proteostasis and allow for adaptation of the proteome to the needs of a cell.^{30, 39, 40} It has been demonstrated that enhancing the activity of the proteasome can alleviate the burden of proteotoxic protein accumulation and can delay aging²⁵¹⁻²⁵⁴ and extend lifespan,²⁵⁵⁻²⁵⁷ in cells,^{251, 258-263} rodents²⁶⁴⁻²⁶⁶ and humans.^{267, 268}

Furthermore, enhancement of proteasome activity has great therapeutic potential for treatment of proteotoxic diseases, like neurodegenerative diseases, where accumulation and aggregation of aberrant proteins leads to toxicity.^{104, 130-133} Specific targeting of the 20S proteasome should provide an added level of selectivity, considering its activity is restricted to the degradation of oxidatively damaged proteins and IDPs, relative to activation of all proteasomes or the 26S proteasome.^{99, 103, 269} The pathogenesis of neurodegenerative diseases, like PD and AD, are associated with the accumulation and aggregation of IDPs, which are natural substrates of the 20S proteasome, so it is an especially promising target for these diseases.^{100, 134, 141}

The field of small molecule 20S proteasome activation is relatively new and only a handful of *bona fide* activator scaffolds have been identified.^{25, 135, 136, 239, 270-272} As such, the identification of novel small molecule 20S proteasome activator scaffolds would greatly enhance the likelihood of success during the development of this novel strategy and assist in overcoming some of the limitations associated with previous scaffolds. Additionally, much remains unexplored regarding the potential of this therapeutic strategy and the effects that it may have on a neurodegenerative disease afflicted brain. These diseases are complex, involving multiple cell types, various forms of IDPs oligomers and neuroinflammation, in addition to widespread proteostasis disruption. Novel methods to evaluate the effects of small molecule 20S proteasome activators on these various aspects of neurodegenerative disease pathogenesis will be essential to their further development as a therapeutic strategy.

REFERENCES

- (1) Balch, W. E.; Morimoto, R. I.; Dillin, A.; Kelly, J. W. Adapting proteostasis for disease intervention. 2008; Vol. 319, pp 916-919.
- (2) Klaipts, C. L.; Jayaraj, G.; Hartl, F. Pathways of cellular proteostasis in aging and disease. *The Journal of cell biology* **2018**, *217* (1), 51-63. DOI: 10.1083/jcb.201709072.
- (3) Powers, E. T.; Morimoto, R. I.; Dillin, A.; Kelly, J. W.; Balch, W. E. Biological and Chemical Approaches to Diseases of Proteostasis Deficiency. *Annual Review of Biochemistry* **2009**, *78* (1), 959-991. DOI: 10.1146/annurev.biochem.052308.114844.
- (4) Labbadia, J.; Morimoto, R. I. The biology of proteostasis in aging and disease. *Annual review of biochemistry* **2015**, *84*, 435-464. DOI: 10.1146/annurev-biochem-060614-033955.
- (5) Hartl, F. U. Cellular Homeostasis and Aging. *Annual Review of Biochemistry* **2016**, *85* (1), 1-4. DOI: 10.1146/annurev-biochem-011116-110806.
- (6) Hetz, C.; Glimcher, L. H. Protein homeostasis networks in physiology and disease. *Current opinion in cell biology* **2011**, *23* (2), 123-125. DOI: 10.1016/j.ceb.2011.01.004.
- (7) Chiti, F.; Dobson, C. M. Protein Misfolding, Amyloid Formation, and Human Disease: A Summary of Progress Over the Last Decade. *Annual review of biochemistry* **2017**, *86*, 27-68. DOI: 10.1146/annurev-biochem-061516-045115.
- (8) Kulak, N. A.; Geyer, P. E.; Mann, M. Loss-less Nano-fractionator for High Sensitivity, High Coverage Proteomics. *Molecular & cellular proteomics : MCP* **2017**, *16* (4), 694-705. DOI: 10.1074/mcp.O116.065136.
- (9) Geiger, T.; Wehner, A.; Schaab, C.; Cox, J.; Mann, M. Comparative proteomic analysis of eleven common cell lines reveals ubiquitous but varying expression of most proteins. *Molecular & cellular proteomics : MCP* **2012**, *11* (3). DOI: 10.1074/mcp.M111.014050.
- (10) Korovila, I.; Hugo, M.; Castro, J. P.; Weber, D.; Höhn, A.; Grune, T.; Jung, T. Proteostasis, oxidative stress and aging. *Redox biology* **2017**, *13*, 550-567. DOI: 10.1016/j.redox.2017.07.008.
- (11) Tanaka, K.; Matsuda, N. Proteostasis and neurodegeneration: the roles of proteasomal degradation and autophagy. *Biochimica et biophysica acta* **2014**, *1843* (1), 197-204. DOI: 10.1016/j.bbamcr.2013.03.012.
- (12) Hipp, M. S.; Kasturi, P.; Hartl, F. U. The proteostasis network and its decline in ageing. *Nature reviews. Molecular cell biology* **2019**, *20* (7), 421-435. DOI: 10.1038/s41580-019-0101-y.
- (13) Frydman, J. Folding of newly translated proteins in vivo: the role of molecular chaperones. *Annual review of biochemistry* **2001**, *70*, 603-647. DOI: 10.1146/annurev.biochem.70.1.603.

- (14) Hartl, F. U. Molecular chaperones in cellular protein folding. *Nature* **1996**, *381* (6583), 571-579. DOI: 10.1038/381571a0.
- (15) Kim, Y. E.; Hipp, M. S.; Bracher, A.; Hayer-Hartl, M.; Ulrich Hartl, F. Molecular Chaperone Functions in Protein Folding and Proteostasis. *Annual Review of Biochemistry* **2013**, *82* (1), 323-355. DOI: 10.1146/annurev-biochem-060208-092442.
- (16) Balchin, D.; Hayer-Hartl, M.; Hartl, F. U. In vivo aspects of protein folding and quality control. *Science (New York, N.Y.)* **2016**, *353* (6294). DOI: 10.1126/science.aac4354.
- (17) Cohen-Kaplan, V.; Livneh, I.; Avni, N.; Cohen-Rosenzweig, C.; Ciechanover, A. The ubiquitin-proteasome system and autophagy: Coordinated and independent activities. *The international journal of biochemistry & cell biology* **2016**, *79*, 403-418. DOI: 10.1016/j.biocel.2016.07.019.
- (18) Ciechanover, A. Intracellular protein degradation: From a vague idea thru the lysosome and the ubiquitin-proteasome system and onto human diseases and drug targeting. *Best practice & research. Clinical haematology* **2017**, *30* (4), 341-355. DOI: 10.1016/j.beha.2017.09.001.
- (19) Dikic, I. Proteasomal and Autophagic Degradation Systems. *Annual review of biochemistry* **2017**, *86*, 193-224. DOI: 10.1146/annurev-biochem-061516-044908.
- (20) Varshavsky, A. The ubiquitin system, an immense realm. *Annual review of biochemistry* **2012**, *81*, 167-176. DOI: 10.1146/annurev-biochem-051910-094049.
- (21) Niforou, K.; Cheimonidou, C.; Trougakos, I. P. Molecular chaperones and proteostasis regulation during redox imbalance. *Redox biology* **2014**, *2*, 323-332. DOI: 10.1016/j.redox.2014.01.017.
- (22) Douglas, P. M.; Summers, D. W.; Cyr, D. M. Molecular chaperones antagonize proteotoxicity by differentially modulating protein aggregation pathways. *Prion* **2009**, *3* (2), 51-58. DOI: 10.4161/pri.3.2.8587.
- (23) Ji, C. H.; Kwon, Y. T. Crosstalk and Interplay between the Ubiquitin-Proteasome System and Autophagy. *Molecules and cells* **2017**, *40* (7), 441-449. DOI: 10.14348/molcells.2017.0115.
- (24) McNaught, K.; Olanow, C. W.; Halliwell, B.; Isacson, O.; Jenner, P. Failure of the ubiquitin-proteasome system in Parkinson's disease. *Nature Reviews Neuroscience* **2001**, *2* (8), 589-594. DOI: 10.1038/35086067.
- (25) Njomen, E.; Tepe, J. J. Proteasome Activation as a New Therapeutic Approach to Target Proteotoxic Disorders. *Journal of Medicinal Chemistry* **2019**, *62* (14), 6469-6481. DOI: 10.1021/acs.jmedchem.9b00101.
- (26) Korolchuk, V. I.; Mansilla, A.; Menzies, F. M.; Rubinsztein, D. C. Autophagy inhibition compromises degradation of ubiquitin-proteasome pathway substrates. *Molecular cell* **2009**, *33* (4), 517-527. DOI: 10.1016/j.molcel.2009.01.021.

- (27) Zheng, Q.; Su, H.; Tian, Z.; Wang, X. Proteasome malfunction activates macroautophagy in the heart. *American journal of cardiovascular disease* **2011**, *1* (3), 214-226.
- (28) Taylor, R. C.; Dillin, A. Aging as an Event of Proteostasis Collapse. *Cold Spring Harbor Perspectives in Biology* **2011**, *3*, a004440. DOI: 10.1101/cshperspect.a004440.
- (29) Calamini, B.; Morimoto, R. Protein homeostasis as a therapeutic target for diseases of protein conformation. *Current Topics in Medicinal Chemistry* **2012**, *12* (22), 2623-2640. DOI: 10.2174/1568026611212220014.
- (30) Voges, D.; Zwickl, P.; Baumeister, W. The 26S Proteasome: A Molecular Machine Designed for Controlled Proteolysis. *Annual Review of Biochemistry* **1999**, *68*, 1015-1068, review-article. DOI: 10.1146/annurev.biochem.68.1.1015.
- (31) Voorhees, P.; Dees, E.; O'Neil, B.; Orlowski, R. The proteasome as a target for cancer therapy. *Clinical cancer research* **2003**, *9* (17), 6316-6325.
- (32) Ostrowska, H. The ubiquitin-proteasome system: a novel target for anticancer and anti-inflammatory drug research. *Cellular & Molecular Biology Letters* **2008**, *13* (3), 353-365. DOI: 10.2478/s11658-008-0008-7.
- (33) Demasi, M.; Faria, B. F. Activation of the ubiquitin-proteasome system: implications for neurodegeneration, aging, and tumorigenesis. *Journal of Neurology & Neuromedicine* **2017**, *2* (8), 1-4.
- (34) Opattova, A.; Cente, M.; Novak, M.; Filipcik, P. The ubiquitin proteasome system as a potential therapeutic target for treatment of neurodegenerative diseases. *General physiology and biophysics* **2015**, *34* (4), 337-352. DOI: 10.4149/gpb_2015024.
- (35) Tanaka, K.; Mizushima, T.; Saeki, Y. The proteasome: Molecular machinery and pathophysiological roles. 2012/03//, Vol. 393, pp 217-234. DOI: 10.1515/hsz-2011-0285.
- (36) Hochstrasser, M. UBIQUITIN-DEPENDENT PROTEIN DEGRADATION. *Annual Review of Genetics* **2003**, *30*, 405-439, review-article. DOI: 10.1146/annurev.genet.30.1.405.
- (37) Tomko, R. J.; Hochstrasser, M. Molecular architecture and assembly of the eukaryotic proteasome. *Annual review of biochemistry* **2013**, *82*, 415-445. DOI: 10.1146/annurev-biochem-060410-150257.
- (38) Wehmer, M.; Sakata, E. Recent advances in the structural biology of the 26S proteasome. *The international journal of biochemistry & cell biology* **2016**, *79*, 437-442. DOI: 10.1016/j.biocel.2016.08.008.
- (39) Thibaudeau, T. A.; Smith, D. M. A Practical Review of Proteasome Pharmacology. *Pharmacological reviews* **2019**, *71* (2), 170-197. DOI: 10.1124/pr.117.015370.

- (40) Shang, F.; Taylor, A. Ubiquitin-proteasome pathway and cellular responses to oxidative stress. *Free radical biology & medicine* **2011**, *51* (1), 5-16. DOI: 10.1016/j.freeradbiomed.2011.03.031.
- (41) Bedford, L.; Hay, D.; Devoy, A.; Paine, S.; Powe, D. G.; Seth, R.; Gray, T.; Topham, I.; Fone, K.; Rezvani, N.; et al. Depletion of 26S Proteasomes in Mouse Brain Neurons Causes Neurodegeneration and Lewy-Like Inclusions Resembling Human Pale Bodies. *Journal of Neuroscience* **2008**, *28* (33), 8189-8198. DOI: 10.1523/JNEUROSCI.2218-08.2008.
- (42) Bonet-Costa, V.; Pomatto, L. C.-D.; Davies, K. J. A. The Proteasome and Oxidative Stress in Alzheimer's Disease. *Antioxidants & Redox Signaling* **2016**, *25* (16), 886-901. DOI: 10.1089/ars.2016.6802.
- (43) Bulteau, A.-L.; Szwedda, L. I.; Friguet, B. Age-Dependent Declines in Proteasome Activity in the Heart. *Archives of Biochemistry and Biophysics* **2002**, *397* (2), 298-304. DOI: 10.1006/abbi.2001.2663.
- (44) Carrard, G.; Bulteau, A.-L.; Petropoulos, I.; Friguet, B. Impairment of proteasome structure and function in aging. *The international journal of biochemistry & cell biology* **2002**, *34* (11), 1461-1474. DOI: 10.1016/s1357-2725(02)00085-7.
- (45) Cekarini, V.; Ding, Q.; Keller, J. N. Oxidative inactivation of the proteasome in Alzheimer's disease. *Free Radical Research* **2007**, *41* (6), 673-680. DOI: 10.1080/10715760701286159.
- (46) Zheng, Q.; Huang, T.; Zhang, L.; Zhou, Y.; Luo, H.; Xu, H.; Wang, X. Dysregulation of Ubiquitin-Proteasome System in Neurodegenerative Diseases. *Frontiers in Aging Neuroscience* **2016**, *8*, 303-303. DOI: 10.3389/fnagi.2016.00303.
- (47) Tomaru, U.; Takahashi, S.; Ishizu, A.; Miyatake, Y.; Gohda, A.; Suzuki, S.; Ono, A.; Ohara, J.; Baba, T.; Murata, S.; et al. Decreased Proteasomal Activity Causes Age-Related Phenotypes and Promotes the Development of Metabolic Abnormalities. *The American Journal of Pathology* **2012**, *180* (3), 963-972. DOI: 10.1016/j.ajpath.2011.11.012.
- (48) Budenholzer, L.; Cheng, C. L.; Li, Y.; Hochstrasser, M. Proteasome Structure and Assembly. Academic Press: 2017; Vol. 429, pp 3500-3524.
- (49) Saeki, Y.; Tanaka, K. Assembly and function of the proteasome. *Methods in molecular biology (Clifton, N.J.)* **2012**, *832*, 315-337. DOI: 10.1007/978-1-61779-474-2_22.
- (50) Bard, J.; Goodall, E.; Greene, E.; Jonsson, E.; Dong, K.; Martin, A. Structure and Function of the 26S Proteasome. *Annual review of biochemistry* **2018**, *87*, 697-724. DOI: 10.1146/annurev-biochem-062917-011931.
- (51) Yoshimura, T.; Kameyama, K.; Takagi, T.; Ikai, A.; Tokunaga, F.; Koide, T.; Tanahashi, N.; Tamura, T.; Cejka, Z.; Baumeister, W. Molecular characterization of the "26S" proteasome complex from rat liver. *Journal of structural biology* **1993**, *111* (3), 200-211. DOI: 10.1006/jsbi.1993.1050.

- (52) Xie, Y. Structure, assembly and homeostatic regulation of the 26S proteasome. *Journal of molecular cell biology* **2010**, 2 (6), 308-317. DOI: 10.1093/jmcb/mjq030.
- (53) Huang, X.; Luan, B.; Wu, J.; Shi, Y. An atomic structure of the human 26S proteasome. *Nature structural & molecular biology* **2016**, 23 (9), 778-785. DOI: 10.1038/nsmb.3273.
- (54) da Fonseca, P. C. A.; Morris, E. P. Structure of the human 26S proteasome: subunit radial displacements open the gate into the proteolytic core. *The Journal of Biological Chemistry* **2008**, 283 (34), 23305-23314. DOI: 10.1074/jbc.m802716200.
- (55) Tanaka, K.; Yoshimura, T.; Kumatori, A.; Ichihara, A.; Ikai, A.; Nishigai, M.; Kameyama, K.; Takagi, T. Proteasomes (multi-protease complexes) as 20 S ring-shaped particles in a variety of eukaryotic cells. *The Journal of biological chemistry* **1988**, 263 (31), 16209-16217.
- (56) Groll, M.; Heinemeyer, W.; Jäger, S.; Ullrich, T.; Bochtler, M.; Wolf, D. H.; Huber, R. The catalytic sites of 20S proteasomes and their role in subunit maturation: A mutational and crystallographic study. *PNAS* **1999**, 20, 10976-10983, research-article. DOI: doi.org/10.1073/pnas.96.20.10976.
- (57) Groll, M.; Bochtler, M.; Brandstetter, H.; Clausen, T.; Huber, R. Molecular machines for protein degradation. *Chembiochem : a European journal of chemical biology* **2005**, 6 (2), 222-256. DOI: 10.1002/cbic.200400313.
- (58) Unno, M.; Mizushima, T.; Morimoto, Y.; Tomisugi, Y.; Tanaka, K.; et al. The Structure of the Mammalian 20S Proteasome at 2.75 Å Resolution. *Structure* **2002**, 10 (5), 609-618. DOI: 10.1016/S0969-2126(02)00748-7.
- (59) Groll, M.; Bajorek, M.; Köhler, A.; Moroder, L.; Rubin, D. M.; Huber, R.; Glickman, M. H.; Finley, D. A gated channel into the proteasome core particle. *Nature Structural Biology* **2000**, 7 (11), 1062-1067. DOI: 10.1038/80992.
- (60) Ustrell, V.; Hoffman, L.; Pratt, G.; Rechsteiner, M. PA200, a nuclear proteasome activator involved in DNA repair. *European Molecular Biology Organization Journal* **2002**, 21 (13), 3515-3525. DOI: 10.1093/emboj/cdf333.
- (61) Stadtmueller, B.; Hill, C. Proteasome activators. *Molecular cell* **2011**, 41 (1), 8-19. DOI: 10.1016/j.molcel.2010.12.020.
- (62) Sadre-Bazzaz, K.; Whitby, F. G.; Robinson, H.; Formosa, T.; Hill, C. P. Structure of a Blm10 complex reveals common mechanisms for proteasome binding and gate opening. *Molecular Cell* **2010**, 37 (5), 728-735. DOI: 10.1016/j.molcel.2010.02.002.
- (63) Whitby, F. G.; Masters, E. I.; Kramer, L.; Knowlton, J. R.; Yao, Y.; Wang, C. C.; Hill, C. P. Structural basis for the activation of 20S proteasomes by 11S regulators. *Nature* **2000**, 408 (6808), 115-120, OriginalPaper. DOI: doi:10.1038/35040607.

- (64) Deshmukh, F. K.; Yaffe, D.; Olshina, M. A.; Ben-Nissan, G.; Sharon, M. The Contribution of the 20S Proteasome to Proteostasis. *Biomolecules* **2019**, *9* (5), 190, Review. DOI: 10.3390/biom9050190.
- (65) Ben-Nissan, G.; Sharon, M. Regulating the 20S proteasome ubiquitin-independent degradation pathway. *Biomolecules* **2014**, *4* (3), 862-884. DOI: 10.3390/biom4030862.
- (66) Ding, Q.; Dimayuga, E.; Keller, J. N. Proteasome Regulation of Oxidative Stress in Aging and Age-Related Diseases of the CNS. *Antioxidants & Redox Signaling* **2006**, *8* (1-2), 163-172. DOI: 10.1089/ars.2006.8.163.
- (67) Smith, D. M.; Chang, S. C.; Park, S.; Finley, D.; Cheng, Y.; Goldberg, A. L. Docking of the proteasomal ATPases' carboxyl termini in the 20S proteasome's alpha ring opens the gate for substrate entry. *Molecular cell* **2007**, *27* (5), 731-744. DOI: 10.1016/j.molcel.2007.06.033.
- (68) Rabl, J.; Smith, D. M.; Yu, Y.; Chang, S. C.; Goldberg, A. L.; Cheng, Y. Mechanism of Gate Opening in the 20S Proteasome by the Proteasomal ATPases. *Molecular Cell* **2008**, *30* (3), 360-368. DOI: 10.1016/j.molcel.2008.03.004.
- (69) Chu-Ping, M.; Vu, J. H.; Proske, R. J.; Slaughter, C. A.; DeMartino, G. N. Identification, purification, and characterization of a high molecular weight, ATP-dependent activator (PA700) of the 20 S proteasome. *The Journal of biological chemistry* **1994**, *269* (5), 3539-3547.
- (70) Ehlinger, A.; Walters, K. J. Structural insights into proteasome activation by the 19S regulatory particle. *Biochemistry* **2013**, *52* (21), 3618-3628. DOI: 10.1021/bi400417a.
- (71) Sharon, M.; Taverner, T.; Ambroggio, X. I.; Deshaies, R. J.; Robinson, C. V. Structural organization of the 19S proteasome lid: insights from MS of intact complexes. *Plos Biology* **2006**, *4* (8), e267. DOI: 10.1371/journal.pbio.0040267.
- (72) Verma, R.; Aravind, L.; Oania, R.; McDonald, W. H.; John R. Yates, I.; Koonin, E. V.; Deshaies, R. J. Role of Rpn11 Metalloprotease in Deubiquitination and Degradation by the 26S Proteasome. *Science* **2002**, *298* (5593), 611-615, research-article. DOI: 10.1126/science.1075898.
- (73) Schweitzer, A.; Aufderheide, A.; Rudack, T.; Beck, F.; Pfeifer, G.; Plitzko, J. M.; Sakata, E.; Schulten, K.; Förster, F.; Baumeister, W. Structure of the human 26S proteasome at a resolution of 3.9 Å. *PNAS* **2016**, *113* (28), 7816-7821, research-article. DOI: 10.1073/pnas.1608050113.
- (74) Lee, M. J.; Lee, B. H.; Hanna, J.; King, R. W.; Finley, D. Trimming of ubiquitin chains by proteasome-associated deubiquitinating enzymes. *Molecular & cellular proteomics : MCP* **2011**, *10* (5). DOI: 10.1074/mcp.R110.003871.
- (75) Komander, D.; Rape, M. The ubiquitin code. *Annual review of biochemistry* **2012**, *81*, 203-229. DOI: 10.1146/annurev-biochem-060310-170328.

- (76) Vijay-Kumar, S.; Bugg, C. E.; Cook, W. J. Structure of ubiquitin refined at 1.8 Å resolution. *Journal of molecular biology* **1987**, *194* (3), 531-544. DOI: 10.1016/0022-2836(87)90679-6.
- (77) Saeki, Y. Ubiquitin recognition by the proteasome. *Journal of biochemistry* **2017**, *161* (2), 113-124. DOI: 10.1093/jb/mvw091.
- (78) Hershko, A.; Ciechanover, A. The ubiquitin system. *Annual review of biochemistry* **1998**, *67*, 425-479. DOI: 10.1146/annurev.biochem.67.1.425.
- (79) Pickart, C. M. Mechanisms underlying ubiquitination. *Annual review of biochemistry* **2001**, *70* (1), 503-533. DOI: 10.1146/annurev.biochem.70.1.503.
- (80) Weissman, A. M. Themes and variations on ubiquitylation. *Nature Reviews Molecular Cell Biology* **2001**, *2* (3), 169-178, ReviewPaper. DOI: doi:10.1038/35056563.
- (81) Uversky, V. N. A decade and a half of protein intrinsic disorder: biology still waits for physics. *Protein science : a publication of the Protein Society* **2013**, *22* (6), 693-724. DOI: 10.1002/pro.2261.
- (82) Dunker, A. K.; Brown, C. J.; Lawson, J. D.; Iakoucheva, L. M.; Obradović, Z. Intrinsic disorder and protein function. *Biochemistry* **2002**, *41* (21), 6573-6582. DOI: 10.1021/bi012159+.
- (83) Uversky, V. N.; Oldfield, C. J.; Dunker, A. K. Intrinsically Disordered Proteins in Human Diseases: Introducing the D² Concept. *Annual Review of Biophysics* **2008**, *37* (1), 215-246. DOI: 10.1146/annurev.biophys.37.032807.125924.
- (84) Cheng, Y.; LeGall, T.; Oldfield, C.; Dunker, K.; Uversky, V. Abundance of Intrinsic Disorder in Protein Associated with Cardiovascular Disease. *Biochemistry* **2006**, *45* (35), 10448-10460, research-article. DOI: 10.1021/bi060981d.
- (85) Du, Z.; Uversky, V. N. A Comprehensive Survey of the Roles of Highly Disordered Proteins in Type 2 Diabetes. *International journal of molecular sciences* **2017**, *18* (10), 2010. DOI: 10.3390/ijms18102010.
- (86) Na, J. H.; Lee, W. K.; Yu, Y. G. How Do We Study the Dynamic Structure of Unstructured Proteins: A Case Study on Nopp140 as an Example of a Large, Intrinsically Disordered Protein. *International journal of molecular sciences* **2018**, *19* (2), 381. DOI: 10.3390/ijms19020381.
- (87) Williams, R. M.; Obradović, Z.; Mathura, V.; Braun, W.; Garner, E. C.; Young, J.; Takayama, S.; Brown, C. J.; Dunker, A. K. The protein non-folding problem: amino acid determinants of intrinsic order and disorder. *Pacific Symposium on Biocomputing* **2001**, 89-100. DOI: 10.1142/9789814447362_0010.
- (88) Romero, P.; Obradović, Z.; Li, X.; Garner, E. C.; Brown, C. J.; Dunker, A. K. Sequence complexity of disordered protein. *Proteins* **2001**, *42* (1), 38-48. DOI: 10.1002/1097-0134(20010101)42:1<38::aid-prot50>3.0.co;2-3.

- (89) Garner, E.; Cannon, P.; Romero, P.; Obradovic, Z.; Dunker, A. K. Predicting Disordered Regions from Amino Acid Sequence: Common Themes Despite Differing Structural Characterization. *Genome informatics. Workshop on Genome Informatics* **1998**, *9*, 201-213.
- (90) Dunker, A. K.; Garner, E.; Guillot, S.; Romero, P.; Albrecht, K.; Hart, J.; Obradovic, Z.; Kissinger, C.; Villafranca, J. E. Protein disorder and the evolution of molecular recognition: theory, predictions and observations. *Pacific Symposium on Biocomputing. Pacific Symposium on Biocomputing* **1998**, 473-484.
- (91) Xue, B.; Dunbrack, R. L.; Williams, R. W.; Dunker, A. K.; Uversky, V. N. PONDR-FIT: a meta-predictor of intrinsically disordered amino acids. *Biochimica et biophysica acta* **2010**, *1804* (4), 996-1010. DOI: 10.1016/j.bbapap.2010.01.011.
- (92) Mészáros, B.; Erdos, G.; Dosztányi, Z. IUPred2A: context-dependent prediction of protein disorder as a function of redox state and protein binding. *Nucleic acids research* **2018**, *46* (W1), 329-337. DOI: 10.1093/nar/gky384.
- (93) Hanson, J.; Paliwal, K.; Zhou, Y. Accurate Single-Sequence Prediction of Protein Intrinsic Disorder by an Ensemble of Deep Recurrent and Convolutional Architectures. *Journal of chemical information and modeling* **2018**, *58* (11), 2369-2376. DOI: 10.1021/acs.jcim.8b00636.
- (94) Goda, N.; Shimizu, K.; Kuwahara, Y.; Tenno, T.; Noguchi, T.; Ikegami, T.; Ota, M.; Hiroaki, H. A Method for Systematic Assessment of Intrinsically Disordered Protein Regions by NMR. *International journal of molecular sciences* **2015**, *16* (7), 15743-15760. DOI: 10.3390/ijms160715743.
- (95) Kumagai, P.; Araujo, A.; Lopes, J. Going deep into protein secondary structure with synchrotron radiation circular dichroism spectroscopy. *Biophysical reviews* **2017**, *9* (5), 517-527. DOI: 10.1007/s12551-017-0314-2.
- (96) Haynes, C.; Oldfield, J.; Ji, F.; Klitgord, N.; Cusick, E.; Radivojac, P.; Uversky, V.; Vidal, M.; Iakoucheva, L. Intrinsic Disorder Is a Common Feature of Hub Proteins from Four Eukaryotic Interactomes. *PLoS Comput Biol* **2006**, *2* (8). DOI: 10.1371/journal.pcbi.0020100.
- (97) Singh, G.; Ganapathi, M.; Dash, D. Role of intrinsic disorder in transient interactions of hub proteins. *Proteins* **2007**, *66* (4), 761-765. DOI: 10.1002/prot.21281.
- (98) Wright, P. E.; Dyson, H. J. Intrinsically disordered proteins in cellular signalling and regulation. *Nature reviews. Molecular cell biology* **2015**, *16* (1), 18-29. DOI: 10.1038/nrm3920.
- (99) Biran, A.; Myers, N.; Adler, J.; Broennimann, K.; Reuven, N.; Shaul, Y. A 20S proteasome receptor for degradation of intrinsically disordered proteins. *bioRxiv* **2017**, 210898. DOI: 10.1101/210898.
- (100) Uversky, V. N. Intrinsically disordered proteins and their (disordered) proteomes in neurodegenerative disorders. *Frontiers in aging neuroscience* **2015**, *7*, 18-18. DOI: 10.3389/fnagi.2015.00018.

- (101) Alvarez-Castelao, B.; Goethals, M.; Vandekerckhove, J.; Castaño, J. G. Mechanism of cleavage of alpha-synuclein by the 20S proteasome and modulation of its degradation by the RedOx state of the N-terminal methionines. *Biochimica et biophysica acta* **2014**, *1843* (2), 352-365. DOI: 10.1016/j.bbamcr.2013.11.018.
- (102) Asher, G.; Bercovich, Z.; Tsvetkov, P.; Shaul, Y.; Kahana, C. 20S Proteasomal Degradation of Ornithine Decarboxylase Is Regulated by NQO1. *Molecular Cell* **2005**, *17* (5), 645-655. DOI: 10.1016/j.molcel.2005.01.020.
- (103) Asher, G.; Reuven, N.; Shaul, Y. 20S proteasomes and protein degradation “by default”. *BioEssays* **2006**, *28* (8), 844-849. DOI: 10.1002/bies.20447.
- (104) Choi, M. L.; Gandhi, S. Crucial role of protein oligomerization in the pathogenesis of Alzheimer's and Parkinson's diseases. *The FEBS Journal* **2018**, *285* (19), 3631-3644. DOI: 10.1111/febs.14587.
- (105) Raychaudhuri, S.; Dey, S.; Bhattacharyya, N. P.; Mukhopadhyay, D. The Role of Intrinsically Unstructured Proteins in Neurodegenerative Diseases. *PLoS ONE* **2009**, *4* (5), e5566-e5566. DOI: 10.1371/journal.pone.0005566.
- (106) Babu, M. M.; van der Lee, R.; de Groot, N. S.; Gsponer, J. Intrinsically disordered proteins: Regulation and disease. Elsevier Current Trends: 2011; Vol. 21, pp 432-440.
- (107) Midic, U.; Oldfield, C. J.; Dunker, A. K.; Obradovic, Z.; Uversky, V. N. Protein disorder in the human diseasome: unfoldomics of human genetic diseases. *BMC Genomics* **2009**, *10* (Suppl 1), S12-S12. DOI: 10.1186/1471-2164-10-S1-S12.
- (108) Uversky, V. N. Wrecked regulation of intrinsically disordered proteins in diseases: pathogenicity of deregulated regulators. *Frontiers in Molecular Biosciences* **2014**, *1*, 6-6. DOI: 10.3389/fmolb.2014.00006.
- (109) Alam, P.; Bousset, L.; Melki, R.; Otzen, D. E. α -synuclein oligomers and fibrils: a spectrum of species, a spectrum of toxicities. *Journal of neurochemistry* **2019**, *150* (5). DOI: 10.1111/jnc.14808.
- (110) Cheng, B.; Gong, H.; Xiao, H.; Petersen, R. B.; Zheng, L.; Huang, K. Inhibiting toxic aggregation of amyloidogenic proteins: a therapeutic strategy for protein misfolding diseases. *Biochimica et biophysica acta* **2013**, *1830* (10), 4860-4871. DOI: 10.1016/j.bbagen.2013.06.029.
- (111) Baugh, J.; Viktorova, E.; Pilipenko, E. Proteasomes Can Degrade a Significant Proportion of Cellular Proteins Independent of Ubiquitination. *Journal of Molecular Biology* **2009**, *386* (3), 814-827. DOI: doi.org/10.1016/j.jmb.2008.12.081.
- (112) Pickering, A. M.; Davies, K. J. Degradation of damaged proteins: the main function of the 20S proteasome. *Progress in molecular biology and translational science* **2012**, *109*, 227-248. DOI: 10.1016/B978-0-12-397863-9.00006-7.

- (113) Eralles, J.; Coffino, P. Ubiquitin-independent proteasomal degradation. *Biochimica et biophysica acta* **2014**, *1843* (1), 216-221. DOI: 10.1016/j.bbamcr.2013.05.008.
- (114) Tanaka, K.; Yoshimura, T.; Ichihara, A. Role of substrate in reversible activation of proteasomes (multi-protease complexes) by sodium dodecyl sulfate. *Journal of biochemistry* **1989**, *106* (3), 495-500.
- (115) Thibaudeau, T. A.; Anderson, R. T.; Smith, D. M. A common mechanism of proteasome impairment by neurodegenerative disease-associated oligomers. *Nature Communications* **2018**, *9* (1), 1097-1097. DOI: 10.1038/s41467-018-03509-0.
- (116) Smith, D. M. Could a Common Mechanism of Protein Degradation Impairment Underlie Many Neurodegenerative Diseases? *Journal of experimental neuroscience* **2018**, *12*, 1179069518794675-1179069518794675. DOI: 10.1177/1179069518794675.
- (117) Bence, N.; Sampat, R.; Kopito, R. Impairment of the ubiquitin-proteasome system by protein aggregation. *Science (New York, N.Y.)* **2001**, *292* (5521). DOI: 10.1126/science.292.5521.1552.
- (118) Deger, J. M.; Gerson, J. E.; Kaye, R. The interrelationship of proteasome impairment and oligomeric intermediates in neurodegeneration. *Aging cell* **2015**, *14* (5), 715-724. DOI: 10.1111/accel.12359.
- (119) Tseng, B. P.; Green, K. N.; Chan, J. L.; Blurton-Jones, M.; LaFerla, F. M. Aβ inhibits the proteasome and enhances amyloid and tau accumulation. *Neurobiology of aging* **2008**, *29* (11), 1607-1618. DOI: 10.1016/j.neurobiolaging.2007.04.014.
- (120) Zondler, L.; Kostka, M.; Garidel, P.; Heinzlmann, U.; Hengerer, B.; Mayer, B.; Weishaupt, J. H.; Gillardon, F.; Danzer, K. M. Proteasome impairment by α-synuclein. *PLOS ONE* **2017**, *12* (9), e0184040-e0184040. DOI: 10.1371/journal.pone.0184040.
- (121) Kundra, R.; Ciryam, P.; Morimoto, R. I.; Dobson, C. M.; Vendruscolo, M. Protein homeostasis of a metastable subproteome associated with Alzheimer's disease. *Proceedings of the National Academy of Sciences of the United States of America* **2017**, *114* (28), E5703-E5711. DOI: 10.1073/pnas.1618417114.
- (122) Sala, A. J.; Bott, L. C.; Morimoto, R. I. Shaping proteostasis at the cellular, tissue, and organismal level. *The Journal of cell biology* **2017**, *216* (5), 1231-1241. DOI: 10.1083/jcb.201612111.
- (123) Danzer, K. M.; Haasen, D.; Karow, A. R.; Moussaïd, S.; Habeck, M.; Giese, A.; Kretschmar, H.; Hengerer, B.; Kostka, M. Different Species of α-Synuclein Oligomers Induce Calcium Influx and Seeding. *Journal of Neuroscience* **2007**, *27* (34), 9220-9232. DOI: 10.1523/JNEUROSCI.2617-07.2007.
- (124) Pinotsi, D.; Michel, C. H.; Buell, A. K.; Laine, R. F.; Mahou, P.; Dobson, C. M.; Kaminski, C. F.; Kaminski Schierle, G. S. Nanoscopic insights into seeding mechanisms and

toxicity of α -synuclein species in neurons. *Proceedings of the National Academy of Sciences* **2016**, *113* (14), 3815-3819. DOI: 10.1073/pnas.1516546113.

(125) Gerson, J. E.; Sengupta, U.; Kaye, R. Tau Oligomers as Pathogenic Seeds: Preparation and Propagation In Vitro and In Vivo. Vol. 1523; 2017; pp 141-157.

(126) Garcia, P.; Jürgens-Wemheuer, W.; Huarte, O.; Michelucci, A.; Masuch, A.; Brioschi, S.; Weihofen, A.; Koncina, E.; Coowar, D.; Heurtaux, T.; et al. Neurodegeneration and neuroinflammation are linked, but independent of alpha-synuclein inclusions, in a seeding/spreading mouse model of Parkinson's disease. *Glia* **2022**, *70* (5), 935-960. DOI: 10.1002/glia.24149.

(127) Kaye, R.; Dettmer, U.; Lesné, S. E. Soluble endogenous oligomeric α -synuclein species in neurodegenerative diseases: Expression, spreading, and cross-talk. *Journal of Parkinson's disease* **2020**, *10* (3), 791-818. DOI: 10.3233/JPD-201965.

(128) Lopes da Fonseca, T.; Villar-Piqué, A.; Outeiro, T. The Interplay between Alpha-Synuclein Clearance and Spreading. *Biomolecules* **2015**, *5* (2), 435-471. DOI: 10.3390/biom5020435.

(129) Thakur, P.; Breger, L. S.; Lundblad, M.; Wan, O. W.; Mattsson, B.; Luk, K. C.; Lee, V. M. Y.; Trojanowski, J. Q.; Björklund, A. Modeling Parkinson's disease pathology by combination of fibril seeds and α -synuclein overexpression in the rat brain. *Proceedings of the National Academy of Sciences of the United States of America* **2017**, *114* (39), E8284-E8293. DOI: 10.1073/pnas.1710442114.

(130) Alafuzoff, I.; Hartikainen, P. Alpha-synucleinopathies. *Handbook of clinical neurology* **2017**, *145*, 339-353. DOI: 10.1016/B978-0-12-802395-2.00024-9.

(131) Gammon, K. Neurodegenerative disease: brain windfall. *Nature* **2014**, *515* (7526), 299-300. DOI: 10.1038/nj7526-299a.

(132) Koyuncu, S.; Fatima, A.; Gutierrez-Garcia, R.; Vilchez, D. Proteostasis of Huntingtin in Health and Disease. *International journal of molecular sciences* **2017**, *18* (7). DOI: 10.3390/ijms18071568.

(133) Uversky, V. N.; Oldfield, C. J.; Midic, U.; Xie, H.; Xue, B.; Vucetic, S.; Iakoucheva, L. M.; Obradovic, Z.; Dunker, A. K. Unfoldomics of human diseases: linking protein intrinsic disorder with diseases. *BMC genomics* **2009**, *10 Suppl 1* (Suppl 1), S7-S7. DOI: 10.1186/1471-2164-10-S1-S7.

(134) Opoku-Nsiah, K. A.; Gestwicki, J. E. Aim for the core: suitability of the ubiquitin-independent 20S proteasome as a drug target in neurodegeneration. Mosby Inc.: 2018; Vol. 198, pp 48-57.

(135) Jones, C. L.; Njomen, E.; Sjögren, B.; Dexheimer, T. S.; Tepe, J. J. Small Molecule Enhancement of 20S Proteasome Activity Targets Intrinsically Disordered Proteins. *ACS Chemical Biology* **2017**, *12* (9), 2240-2247. DOI: 10.1021/acscchembio.7b00489.

- (136) Njomen, E.; Osmulski, P. A.; Jones, C. L.; Gaczynska, M.; Tepe, J. J. Small Molecule Modulation of Proteasome Assembly. *Biochemistry* **2018**, *57* (28), 4214-4224. DOI: 10.1021/acs.biochem.8b00579.
- (137) Liu, Y.; Hettinger, C. L.; Zhang, D.; Rezvani, K.; Wang, X.; Wang, H. The proteasome function reporter GFPu accumulates in young brains of the APP^{swe}/PS1^{dE9} Alzheimer's disease mouse model. *Cellular and molecular neurobiology* **2014**, *34* (3), 315-322. DOI: 10.1007/s10571-013-0022-9.
- (138) Grune, T. Oxidative stress, aging and the proteasomal system. *Biogerontology* **2000**, *1* (1), 31-40. DOI: 10.1023/a:1010037908060.
- (139) Zabel, C.; Nguyen, H. P.; Hin, S. C.; Hartl, D.; Mao, L.; Klose, J. Proteasome and oxidative phosphorylation changes may explain why aging is a risk factor for neurodegenerative disorders. *Journal of Proteomics* **2010**, *73* (11), 2230-2238. DOI: 10.1016/j.jprot.2010.08.008.
- (140) Vigouroux, S.; Briand, M.; Briand, Y. Linkage between the proteasome pathway and neurodegenerative diseases and aging. *Molecular neurobiology* **2004**, *30* (2), 201-221. DOI: 10.1385/MN:30:2:201.
- (141) Coleman, R. A.; Trader, D. J. All About the Core: A Therapeutic Strategy to Prevent Protein Accumulation with Proteasome Core Particle Stimulators. *ACS Pharmacology & Translational Science* **2018**, *1* (2), 140-142. DOI: 10.1021/acsptsci.8b00042.
- (142) Coleman, R.; Mohallem, R.; Aryal, U.; Trader, D. Protein degradation profile reveals dynamic nature of 20S proteasome small molecule stimulation. *RSC Chemical Biology* **2021**, *2*, 636-644. DOI: 10.1039/D0CB00191K.
- (143) Tsvetkov, P.; Reuven, N.; Shaul, Y. The nanny model for IDPs. *Nature Chemical Biology* **2009**, *5* (11), 778-781, BriefCommunication. DOI: doi:10.1038/nchembio.233.
- (144) Kulkarni, A.; Preeti, K.; Tryphena, K. P.; Srivastava, S.; Singh, S. B.; Khatri, D. K. Proteostasis in Parkinson's disease: Recent development and possible implication in diagnosis and therapeutics. *Ageing research reviews* **2023**, *84*, 101816. DOI: 10.1016/j.arr.2022.101816.
- (145) (WHO), W. H. O. *Parkinson disease*. 2022. (accessed 2023 April 15th).
- (146) Aging, N. N. I. o. *Parkinson's Disease: Causes, Symptoms, and Treatments*. @NIHAging, 2022. <https://www.ncbi.nlm.nih.gov/pubmed/> (accessed 2023 April 9th).
- (147) Bloem, B.; Okun, M.; Klein, C. Parkinson's disease. *The Lancet* **2021**, *397* (10291), 12-18. DOI: doi.org/10.1016/S0140-6736(21)00218-X.
- (148) Hornykiewicz, O. A brief history of levodopa. *Journal of Neurology* **2010**, *257* (2), 249-252, OriginalPaper. DOI: doi:10.1007/s00415-010-5741-y.
- (149) Gandhi, K. R.; Saadabadi, A. *Levodopa (L-Dopa)*; StatPearls Publishing, 2022. DOI: <https://www.ncbi.nlm.nih.gov/books/NBK482140/>.

- (150) Muller, T. Pharmacokinetics and pharmacodynamics of levodopa/carbidopa cotherapies for Parkinson's disease. *Expert Opinion on Drug Metabolism & Toxicology* **2020**, *16* (5), 403-414, review. DOI: doi.org/10.1080/17425255.2020.1750596.
- (151) Lehtonen, Š.; Sonninen, T. M.; Wojciechowski, S.; Goldsteins, G.; Koistinaho, J. Dysfunction of Cellular Proteostasis in Parkinson's Disease. *Frontiers in neuroscience* **2019**, *13* (10), 457. DOI: 10.3389/fnins.2019.00457.
- (152) McNaught, K. S. P.; Olanow, C. W.; Halliwell, B.; Isacson, O.; Jenner, P. Failure of the ubiquitin–proteasome system in Parkinson's disease. *Nature Reviews Neuroscience* **2001**, *2* (8), 589-594. DOI: 10.1038/35086067.
- (153) McNaught, K. S.; Belizaire, R.; Isacson, O.; Jenner, P.; Olanow, C. W. Altered proteasomal function in sporadic Parkinson's disease. *Experimental neurology* **2003**, *179* (1), 38-46. DOI: 10.1006/exnr.2002.8050.
- (154) Kurtishi, A.; Rosen, B.; Patil, K. S.; Alves, G. W.; G., M. S. Cellular Proteostasis in Neurodegeneration. *Molecular neurobiology* **2019**, *56* (5), 3676-3689. DOI: 10.1007/s12035-018-1334-z.
- (155) Emmanouilidou, E.; Stefanis, L.; Vekrellis, K. Cell-produced alpha-synuclein oligomers are targeted to, and impair, the 26S proteasome. *Neurobiology of aging* **2010**, *31* (6), 953-968. DOI: 10.1016/j.neurobiolaging.2008.07.008.
- (156) Lindersson, E.; Beedholm, R.; Højrup, P.; Moos, T.; Gai, W.; Hendil, K. B.; Jensen, P. H. Proteasomal inhibition by alpha-synuclein filaments and oligomers. *The Journal of biological chemistry* **2004**, *279* (13), 12924-12934. DOI: 10.1074/jbc.M306390200.
- (157) Snyder, H.; Mensah, K.; Theisler, C.; Lee, J.; Matouschek, A.; Wolozin, B. Aggregated and monomeric alpha-synuclein bind to the S6' proteasomal protein and inhibit proteasomal function. *The Journal of biological chemistry* **2003**, *278* (14), 11753-11759. DOI: 10.1074/jbc.M208641200.
- (158) Ingelsson, M. Alpha-Synuclein Oligomers-Neurotoxic Molecules in Parkinson's Disease and Other Lewy Body Disorders. *Frontiers in neuroscience* **2016**, *10*, 408-408. DOI: 10.3389/fnins.2016.00408.
- (159) Winner, B.; Jappelli, R.; Maji, S. K.; Desplats, P. A.; Boyer, L.; Aigner, S.; Hetzer, C.; Loher, T.; Vilar, M.; Campioni, S.; et al. In vivo demonstration that -synuclein oligomers are toxic. *Proceedings of the National Academy of Sciences* **2011**, *108* (10), 4194-4199. DOI: 10.1073/pnas.1100976108.
- (160) Bengoa-Vergniory, N.; Roberts, R. F.; Wade-Martins, R.; Alegre-Abarrategui, J. Alpha-synuclein oligomers: a new hope. *Acta neuropathologica* **2017**, *134* (6), 819-838. DOI: 10.1007/s00401-017-1755-1.

- (161) Conway, K. A.; Harper, J. D.; Lansbury, P. T. Accelerated in vitro fibril formation by a mutant α -synuclein linked to early-onset Parkinson disease. *Nature Medicine* **1998**, *4* (11), 1318-1320. DOI: 10.1038/3311.
- (162) Ibáñez, P.; Bonnet, A. M.; Débarges, B.; Lohmann, E.; Tison, F.; Agid, Y.; Dürr, A.; Brice, A.; Pollak, P. Causal relation between α -synuclein locus duplication as a cause of familial Parkinson's disease. *The Lancet* **2004**, *364* (9440), 1169-1171. DOI: 10.1016/S0140-6736(04)17104-3.
- (163) Liu, C.; Zhao, Y.; Xi, H.; Jiang, J.; Yu, Y.; Dong, W. The Membrane Interaction of Alpha-Synuclein. *Frontiers in cellular neuroscience* **2021**, *15*, 633727. DOI: 10.3389/fncel.2021.633727.
- (164) Iwai, A.; Masliah, E.; Yoshimoto, M.; Ge, N.; Flanagan, L.; de Silva, H. A.; Kittel, A.; Saitoh, T. The precursor protein of non-A beta component of Alzheimer's disease amyloid is a presynaptic protein of the central nervous system. *Neuron* **1995**, *14* (2), 467-475. DOI: 10.1016/0896-6273(95)90302-x.
- (165) Jakes, R.; Spillantini, M. G.; Goedert, M. Identification of two distinct synucleins from human brain. *FEBS letters* **1994**, *345* (1), 27-32. DOI: 10.1016/0014-5793(94)00395-5.
- (166) Withers, G. S.; George, J. M.; Banker, G. A.; Clayton, D. F. Delayed localization of synelfin (synuclein, NACP) to presynaptic terminals in cultured rat hippocampal neurons. *Brain research. Developmental brain research* **1997**, *99* (1), 87-94. DOI: 10.1016/s0165-3806(96)00210-6.
- (167) Kahle, P. J.; Neumann, M.; Ozmen, L.; Muller, V.; Jacobsen, H.; Schindzielorz, A.; Okochi, M.; Leimer, U.; van Der Putten, H.; Probst, A.; et al. Subcellular localization of wild-type and Parkinson's disease-associated mutant alpha -synuclein in human and transgenic mouse brain. *The Journal of neuroscience : the official journal of the Society for Neuroscience* **2000**, *20* (17), 6365-6373. DOI: 10.1523/JNEUROSCI.20-17-06365.2000.
- (168) Zhang, L.; Zhang, C.; Zhu, Y.; Cai, Q.; Chan, P.; Uéda, K.; Yu, S.; Yang, H. Semi-quantitative analysis of alpha-synuclein in subcellular pools of rat brain neurons: an immunogold electron microscopic study using a C-terminal specific monoclonal antibody. *Brain research* **2008**, *1244*, 40-52. DOI: 10.1016/j.brainres.2008.08.067.
- (169) Chartier-Harlin, M. C.; Kachergus, J.; Roumier, C.; Mouroux, V.; Douay, X.; Lincoln, S.; Levecque, C.; Larvor, L.; Andrieux, J.; Hulihan, M.; et al. Alpha-synuclein locus duplication as a cause of familial Parkinson's disease. *Lancet (London, England)* **2004**, *364* (9440), 1167-1169. DOI: 10.1016/S0140-6736(04)17103-1.
- (170) Miller, D. W.; Hague, S. M.; Clarimon, J.; Baptista, M.; Gwinn-Hardy, K.; Cookson, M. R.; Singleton, A. B. α -Synuclein in blood and brain from familial Parkinson disease with SNCA locus triplication. *Neurology* **2004**, *62* (10). DOI: 10.1212/01.WNL.0000127517.33208.F4.

- (171) Singleton, A. B.; Farrer, M.; Johnson, J.; Singleton, A.; Hague, S.; Kachergus, J.; Hulihan, M.; Peuralinna, T.; Dutra, A.; Nussbaum, R.; et al. -Synuclein Locus Triplication Causes Parkinson's Disease. *Science* **2003**, *302* (5646), 841-841. DOI: 10.1126/science.1090278.
- (172) Krüger, R.; Kuhn, W.; Müller, T.; Woitalla, D.; Graeber, M.; Kösel, S.; Przuntek, H.; Epplen, T.; Schöls, L.; Riess, O. Ala30Pro mutation in the gene encoding alpha-synuclein in Parkinson's disease. *Nature genetics* **1998**, *18* (2), 106-108. DOI: 10.1038/ng0298-106.
- (173) Simón-Sánchez, J.; Schulte, C.; Bras, M.; Sharma, M.; Gibbs, R.; Berg, D.; Paisan-Ruiz, C.; Lichtner, P.; Scholz, W.; Hernandez, G.; et al. Genome-wide association study reveals genetic risk underlying Parkinson's disease. *Nature genetics* **2009**, *41* (12), 1308-1312. DOI: 10.1038/ng.487.
- (174) Polymeropoulos, M. H.; Lavedan, C.; Leroy, E.; Ide, S. E.; Dehejia, A.; Dutra, A.; Pike, B.; Root, H.; Rubenstein, J.; Boyer, R.; et al. Mutation in the -Synuclein Gene Identified in Families with Parkinson's Disease. *Science* **1997**, *276* (5321), 2045-2047. DOI: 10.1126/science.276.5321.2045.
- (175) Zarranz, J.; Alegre, J.; Gómez-Esteban, C.; Lezcano, E.; Ros, R.; Ampuero, I.; Vidal, L.; Hoenicka, J.; Rodriguez, O.; Atarés, B.; et al. The new mutation, E46K, of alpha-synuclein causes Parkinson and Lewy body dementia. *Annals of neurology* **2004**, *55* (2), 164-173. DOI: 10.1002/ana.10795.
- (176) Conway, K. A.; Harper, J. D.; Lansbury, P. T. Accelerated in vitro fibril formation by a mutant alpha-synuclein linked to early-onset Parkinson disease. *Nature medicine* **1998**, *4* (11), 1318-1320. DOI: 10.1038/3311.
- (177) Lashuel, H. A.; Overk, C. R.; Oueslati, A.; Masliah, E. The many faces of α -synuclein: from structure and toxicity to therapeutic target. *Nat Rev Neurosci* **2013**, *14* (1), 38-48. DOI: 10.1038/nrn3406.
- (178) Cremades, N.; Cohen, S. I. A.; Deas, E.; Abramov, A. Y.; Chen, A. Y.; Orte, A.; Sandal, M.; Clarke, R. W.; Dunne, P.; Aprile, F. A.; et al. Direct observation of the interconversion of normal and toxic forms of α -synuclein. *Cell* **2012**, *149* (5), 1048-1059. DOI: 10.1016/j.cell.2012.03.037.
- (179) Brettschneider, J.; Del Tredici, K.; Lee, V. M.; Trojanowski, J. Q. Spreading of pathology in neurodegenerative diseases: a focus on human studies. *Nature reviews. Neuroscience* **2015**, *16* (2), 109-120. DOI: 10.1038/nrn3887.
- (180) Rubinsztein, D. C. The roles of intracellular protein-degradation pathways in neurodegeneration. *Nature* **2006**, *443* (7113), 780-786. DOI: 10.1038/nature05291.
- (181) Selkoe, D. J. Folding proteins in fatal ways. *Nature* **2003**, *426* (6968), 900-904, ReviewPaper. DOI: doi:10.1038/nature02264.
- (182) Aging, N. N. I. o. *What Is Alzheimer's Disease?* NIH, 2021. <https://www.ncbi.nlm.nih.gov/pubmed/> (accessed 2023 April 9th).

- (183) Lane, C.; Hardy, J.; Schott, J. Alzheimer's disease. *European Journal of Neurology* **2018**, *15* (1), 59-70. DOI: 10.1111/ene.13439.
- (184) Hampel, H.; Hardy, J.; Blennow, K.; Chen, C.; Perry, G.; Kim, S. H.; Villemagne, V. L.; Aisen, P.; Vendruscolo, M.; Iwatsubo, T.; et al. The Amyloid- β Pathway in Alzheimer's Disease. *Molecular Psychiatry* **2021**, *26* (10), 5481-5503, ReviewPaper. DOI: doi:10.1038/s41380-021-01249-0.
- (185) Jeong, S. Molecular and Cellular Basis of Neurodegeneration in Alzheimer's Disease. *Molecules and cells* **2017**, *40* (9), 613-620. DOI: 10.14348/molcells.2017.0096.
- (186) Korsak, M.; Kozyreva, T. Beta Amyloid Hallmarks: From Intrinsically Disordered Proteins to Alzheimer's Disease. Springer, Cham, 2015; pp 401-421.
- (187) Selkoe, D. J.; Hardy, J. The amyloid hypothesis of Alzheimer's disease at 25 years. *EMBO molecular medicine* **2016**, *8* (6), 595-608. DOI: 10.15252/emmm.201606210.
- (188) Michaels, T. C. T.; Šarić, A.; Curk, S.; Bernfur, K.; Arosio, P.; Meisl, G.; Dear, A. J.; Cohen, S. I. A.; Dobson, C. M.; Vendruscolo, M.; et al. Dynamics of oligomer populations formed during the aggregation of Alzheimer's A β 42 peptide. *Nature Chemistry* **2020**, *12* (5), 445-451, OriginalPaper. DOI: doi:10.1038/s41557-020-0452-1.
- (189) Gruning, C.; Klinker, S.; Wolff, M.; Schneider, M.; Toksoz, K.; Klein, A.; Nagel-Steger, L.; Willbold, D.; Hoyer, W. The Off-rate of Monomers Dissociating from Amyloid- β Protofibrils. *Journal of Biological Chemistry* **2013**, *288* (52), 37104-37111. DOI: 10.1074/jbc.M113.513432.
- (190) Carulla, N.; Caddy, G. L.; Hall, D. R.; Zurdo, J.; Gairí, M.; Feliz, M.; Giralt, E.; Robinson, C. V.; Dobson, C. M. Molecular recycling within amyloid fibrils. *Nature* **2023**, *436* (7050), 554-558, OriginalPaper. DOI: doi:10.1038/nature03986.
- (191) Haass, C.; Selkoe, D. J. Soluble protein oligomers in neurodegeneration: lessons from the Alzheimer's amyloid beta-peptide. *Nature reviews. Molecular cell biology* **2007**, *8* (2), 101-112. DOI: 10.1038/nrm2101.
- (192) Shankar, M.; Li, S.; Mehta, H.; Garcia-Munoz, A.; Shepardson, E.; Smith, I.; Brett, M.; Farrell, A.; Rowan, J.; Lemere, A.; et al. Amyloid-beta protein dimers isolated directly from Alzheimer's brains impair synaptic plasticity and memory. *Nature medicine* **2008**, *14* (8), 837-842. DOI: 10.1038/nm1782.
- (193) Brinkmalm, G.; Hong, W.; Wang, Z.; Liu, W.; O'Malley, T.; Sun, X.; Frosch, P.; Selkoe, J.; Portelius, E.; Zetterberg, H.; et al. Identification of neurotoxic cross-linked amyloid- β dimers in the Alzheimer's brain. *Brain : a journal of neurology* **2019**, *142* (5), 1441-1457. DOI: 10.1093/brain/awz066.
- (194) Walsh, M.; Klyubin, I.; Fadeeva, V.; Cullen, K.; Anwyl, R.; Wolfe, S.; Rowan, J.; Selkoe, J. Naturally secreted oligomers of amyloid beta protein potently inhibit hippocampal long-term potentiation in vivo. *Nature* **2002**, *416* (6880), 535-539. DOI: 10.1038/416535a.

- (195) Selkoe, J. Soluble oligomers of the amyloid beta-protein impair synaptic plasticity and behavior. *Behavioural brain research* **2008**, *192* (1), 106-113. DOI: 10.1016/j.bbr.2008.02.016.
- (196) Hardiman, O.; Al-Chalabi, A.; Chio, A.; Corr, E. M.; Logroscino, G.; Robberecht, W.; Shaw, P. J.; Simmons, Z.; van den Berg, L. H. Amyotrophic lateral sclerosis. *Nature Reviews Disease Primers* **2017**, *3* (1), 1-19, ReviewPaper. DOI: doi:10.1038/nrdp.2017.71.
- (197) Medinas, D.; Vicente, V.; Claudio, H. Proteostasis disturbance in amyotrophic lateral sclerosis. *Human Molecular Genetics* **2017**, *26* (R2). DOI: 10.1093/hmg/ddx274.
- (198) Mori, K.; Weng, S.-M.; Arzberger, T.; May, S.; Rentzsch, K.; Kremmer, E.; Schmid, B.; Kretzschmar, H. A.; Cruts, M.; Broeckhoven, C. V.; et al. The C9orf72 GGGGCC Repeat Is Translated into Aggregating Dipeptide-Repeat Proteins in FTL/ALS. *Science* **2013**, *339* (6125), 1335-1338, research-article. DOI: 10.1126/science.1232927.
- (199) Ruegsegger, C.; Saxena, S. Proteostasis impairment in ALS. *Brain research* **2016**, *1648*, 571-579. DOI: 10.1016/j.brainres.2016.03.032.
- (200) Su, X.; Maguire-Zeiss, K.; Giuliano, R.; Prifti, L.; Venkatesh, K.; Federoff, H. Synuclein activates microglia in a model of Parkinson's disease. *Neurobiology of Aging* **2007**, *29* (11), 1690-1701. DOI: 10.1016/j.neurobiolaging.2007.04.006.
- (201) Hoenen, C.; Gustin, A.; Birck, C.; Kirchmeyer, M.; Beaume, N.; Felten, P.; Grandbarbe, L.; Heuschling, P.; Heurtaux, T. Alpha-Synuclein Proteins Promote Pro-Inflammatory Cascades in Microglia: Stronger Effects of the A53T Mutant. *PloS one* **2016**, *11* (9), e0162717. DOI: 10.1371/journal.pone.0162717.
- (202) Cao, S.; Standaert, D.; Harms, A. The gamma chain subunit of Fc receptors is required for alpha-synuclein-induced pro-inflammatory signaling in microglia. *Journal of neuroinflammation* **2012**, *9*, 259. DOI: 10.1186/1742-2094-9-259.
- (203) Song, N.; Chen, L.; Xie, J. Alpha-Synuclein Handling by Microglia: Activating, Combating, and Worsening. *Neuroscience Bulletin* **2021**, *37* (5), 751-753, OriginalPaper. DOI: doi:10.1007/s12264-021-00651-6.
- (204) Xia, Y.; Zhang, G.; Kou, L.; Yin, S.; Han, C.; Hu, J.; Wan, F.; Sun, Y.; Wu, J.; Li, Y.; et al. Reactive microglia enhance the transmission of exosomal α -synuclein via toll-like receptor 2. *Brain : a journal of neurology* **2021**, *144* (7), 2024-2037. DOI: 10.1093/brain/awab122.
- (205) Heneka, M.; Carson, M.; El Khoury, J.; Landreth, G.; Brosseron, F.; Feinstein, D.; Jacobs, A.; Wyss-Coray, T.; Vitorica, J.; Ransohoff, R.; et al. Neuroinflammation in Alzheimer's disease. *The Lancet. Neurology* **2015**, *14* (4), 388-405. DOI: 10.1016/S1474-4422(15)70016-5.
- (206) Calsolaro, V.; Edison, P. Neuroinflammation in Alzheimer's disease: Current evidence and future directions. *Alzheimer's & dementia : the journal of the Alzheimer's Association* **2016**, *12* (6), 719-732. DOI: 10.1016/j.jalz.2016.02.010.

- (207) Nilson, A. N.; English, K. C.; Gerson, J. E.; Barton Whittle, T.; Nicolas Crain, C.; Xue, J.; Sengupta, U.; Castillo-Carranza, D. L.; Zhang, W.; Gupta, P.; et al. Tau Oligomers Associate with Inflammation in the Brain and Retina of Tauopathy Mice and in Neurodegenerative Diseases. *Journal of Alzheimer's disease : JAD* **2017**, *55* (3), 1083-1099. DOI: 10.3233/JAD-160912.
- (208) Onyango, I.; Jauregui, G.; Čarná, M.; Bennett, J.; Stokin, G. Neuroinflammation in Alzheimer's Disease. *Biomedicines* **2021**, *9* (5), 524. DOI: 10.3390/biomedicines9050524.
- (209) Lall, D.; Baloh, R. Microglia and C9orf72 in neuroinflammation and ALS and frontotemporal dementia. *The Journal of clinical investigation* **2017**, *127* (9), 3250-3258. DOI: 10.1172/JCI90607.
- (210) Liu, J.; Wang, F. Role of Neuroinflammation in Amyotrophic Lateral Sclerosis: Cellular Mechanisms and Therapeutic Implications. *Frontiers in immunology* **2017**, *8*, 1005. DOI: 10.3389/fimmu.2017.01005.
- (211) Chiot, A.; Lobsiger, C.; Boillée, S. New insights on the disease contribution of neuroinflammation in amyotrophic lateral sclerosis. *Current opinion in neurology* **2019**, *32* (5), 764-770. DOI: 10.1097/WCO.0000000000000729.
- (212) Aloisi, F. Immune function of microglia. *Glia* **2001**, *36* (2), 165-179. DOI: 10.1002/glia.1106.
- (213) Ueno, M.; Fujita, Y.; Tanaka, T.; Nakamura, Y.; Kikuta, J.; Ishii, M.; Yamashita, T. Layer V cortical neurons require microglial support for survival during postnatal development. *Nature neuroscience* **2013**, *16* (5), 543-551. DOI: 10.1038/nn.3358.
- (214) Cunningham, C.; Martínez-Cerdeño, V.; Noctor, S. Microglia regulate the number of neural precursor cells in the developing cerebral cortex. *The Journal of neuroscience : the official journal of the Society for Neuroscience* **2013**, *33* (10), 4216-4233. DOI: 10.1523/JNEUROSCI.3441-12.2013.
- (215) Frost, J.; Schafer, D. Microglia: Architects of the Developing Nervous System. *Trends in cell biology* **2016**, *26* (8), 587-597. DOI: 10.1016/j.tcb.2016.02.006.
- (216) Soteros, B.; Sia, G. Complement and microglia dependent synapse elimination in brain development. *WIREs mechanisms of disease* **2022**, *14* (3), e1545. DOI: 10.1002/wsbm.1545.
- (217) Orihuela, R.; McPherson, C.; Harry, G. Microglial M1/M2 polarization and metabolic states. *British Journal of Pharmacology* **2015**, *173* (4), 649-665. DOI: 10.1111/bph.13139.
- (218) Hickman, S. E.; Kingery, N. D.; Ohsumi, T. K.; Borowsky, M. L.; Wang, L.-c.; Means, T. K.; El Khoury, J. The microglial sensome revealed by direct RNA sequencing. *Nature Neuroscience* **2013**, *16* (12), 1896-1905, OriginalPaper. DOI: doi:10.1038/nn.3554.
- (219) Yang, Q.; Zhou, J. Neuroinflammation in the central nervous system: Symphony of glial cells. *Glia* **2019**, *67* (6), 1017-1035. DOI: 10.1002/glia.23571.

- (220) Davis, E.; Foster, T.; Thomas, W. Cellular forms and functions of brain microglia. *Brain research bulletin* **1994**, *34* (1), 73-78. DOI: 10.1016/0361-9230(94)90189-9.
- (221) Li, Q.; Barres, B. A. Microglia and macrophages in brain homeostasis and disease. *Nature Reviews Immunology* **2017**, *18* (4), 225-242, ReviewPaper. DOI: doi:10.1038/nri.2017.125.
- (222) Crews, F.; Newsom, H.; Gerber, M.; Sumners, C.; Chandler, L.; Freund, G. Molecular Mechanisms of Alcohol Neurotoxicity. In *Alcohol, Cell Membranes, and Signal Transduction in Brain*, Springer, 1993.
- (223) Gehrman, J.; Matsumoto, Y.; Kreutzberg, G. Microglia: intrinsic immune effector cell of the brain. *Brain research. Brain research reviews* **1995**, *20* (3), 269-287. DOI: 10.1016/0165-0173(94)00015-h.
- (224) Rawlinson, C.; Jenkins, S.; Thei, L.; Dallas, M.; Chen, R. Post-Ischaemic Immunological Response in the Brain: Targeting Microglia in Ischaemic Stroke Therapy. *Brain sciences* **2020**, *10* (3), 159. DOI: 10.3390/brainsci10030159.
- (225) Town, T.; Nikolic, V.; Tan, J. The microglial "activation" continuum: from innate to adaptive responses. *Journal of neuroinflammation* **2005**, *2*, 24. DOI: 10.1186/1742-2094-2-24.
- (226) Walker, D.; Lue, L. Immune phenotypes of microglia in human neurodegenerative disease: challenges to detecting microglial polarization in human brains. *Alzheimer's research & therapy* **2015**, *7* (1), 56. DOI: 10.1186/s13195-015-0139-9.
- (227) Sparkman, N.; Johnson, R. Neuroinflammation associated with aging sensitizes the brain to the effects of infection or stress. *Neuroimmunomodulation* **2008**, *15* (4-6), 323-330. DOI: 10.1159/000156474.
- (228) Block, M. L.; Zecca, L.; Hong, J.-S. Microglia-mediated neurotoxicity: uncovering the molecular mechanisms. *Nature Reviews Neuroscience* **2007**, *8* (1), 57-69, ReviewPaper. DOI: doi:10.1038/nrn2038.
- (229) Grabert, K.; Michoel, T.; Karavolos, M.; Clohisey, S.; Baillie, J.; Stevens, M.; Freeman, T.; Summers, K.; McColl, B. Microglial brain region-dependent diversity and selective regional sensitivities to aging. *Nature neuroscience* **2016**, *19* (3), 504-516. DOI: 10.1038/nn.4222.
- (230) Deczkowska, A.; Amit, I.; Schwartz, M. Microglial immune checkpoint mechanisms. *Nature neuroscience* **2018**, *21* (6), 779-786. DOI: 10.1038/s41593-018-0145-x.
- (231) Wu, X.; Schauss, A. Mitigation of inflammation with foods. *Journal of agricultural and food chemistry* **2012**, *60* (27), 6703-6717. DOI: 10.1021/jf3007008.
- (232) Rastogi, N.; Mishra, D. P. Therapeutic targeting of cancer cell cycle using proteasome inhibitors. *Cell Division* **2012**, *7* (1), 1-10, ReviewPaper. DOI: doi:10.1186/1747-1028-7-26.
- (233) Tundo, G.; Sbardella, D.; Santoro, A.; Coletta, A.; Oddone, F.; Grasso, G.; Milardi, D.; Lacal, P.; Marini, S.; Purrello, R.; et al. The proteasome as a druggable target with multiple

therapeutic potentialities: Cutting and non-cutting edges. *Pharmacology & therapeutics* **2020**, *213*, 107579. DOI: 10.1016/j.pharmthera.2020.107579.

(234) Huang, X.; Dixit, V. M. Drugging the undruggables: exploring the ubiquitin system for drug development. *Cell Research* **2016**, *26* (4), 484-498, ReviewPaper. DOI: doi:10.1038/cr.2016.31.

(235) Ruiz de Mena, I.; Mahillo, E.; Arribas, J.; Castaño, J. G. Kinetic mechanism of activation by cardiolipin (diphosphatidylglycerol) of the rat liver multicatalytic proteinase. *The Biochemical journal* **1993**, *296* (Pt 1) (Pt 1), 93-97.

(236) Watanabe, N.; Yamada, S. Activation of 20S proteasomes from spinach leaves by fatty acids. *Plant & cell physiology* **1996**, *37* (2), 147-151.

(237) Katsiki, M.; Chondrogianni, N.; Chinou, I.; Rivett, A. J.; Gonos, E. S. The Olive Constituent Oleuropein Exhibits Proteasome Stimulatory Properties *In Vitro* and Confers Life Span Extension of Human Embryonic Fibroblasts. *Rejuvenation Research* **2007**, *10* (2), 157-172. DOI: 10.1089/rej.2006.0513.

(238) Huang, L.; Ho, P.; Chen, C.-H. Activation and inhibition of the proteasome by betulinic acid and its derivatives. *FEBS Letters* **2007**, *581* (25), 4955-4959. DOI: 10.1016/j.febslet.2007.09.031.

(239) Trader, D. J.; Simanski, S.; Dickson, P.; Kodadek, T. Establishment of a suite of assays that support the discovery of proteasome stimulators. *Biochimica et Biophysica Acta (BBA) - General Subjects* **2017**, *1861* (4), 892-899. DOI: 10.1016/J.BBAGEN.2017.01.003.

(240) Coleman, R. A.; Trader, D. J. Development and Application of a Sensitive Peptide Reporter to Discover 20S Proteasome Stimulators. *ACS Combinatorial Science* **2018**, *20* (5), 269-276. DOI: 10.1021/acscmbosci.7b00193.

(241) Uversky, V. N. Targeting intrinsically disordered proteins in neurodegenerative and protein dysfunction diseases: another illustration of the D(2) concept. *Expert review of proteomics* **2010**, *7* (4), 543-564. DOI: 10.1586/epr.10.36.

(242) Uversky, V. N. *Synuclein Misfolding and Neurodegenerative Diseases*; 2008. <https://pdfs.semanticscholar.org/c720/c58ef79ccea1ceba137bb5208f5ba0df28d.pdf>.

(243) Levine, Z. A.; Larini, L.; LaPointe, N. E.; Feinstein, S. C.; Shea, J.-E. Regulation and aggregation of intrinsically disordered peptides. *Proceedings of the National Academy of Sciences of the United States of America* **2015**, *112* (9), 2758-2763. DOI: 10.1073/pnas.1418155112.

(244) Raychaudhuri, S.; Majumder, P.; Sarkar, S.; Giri, K.; Mukhopadhyay, D.; Bhattacharyya, N. P. Huntingtin interacting protein HYPK is intrinsically unstructured. *Proteins: Structure, Function, and Bioinformatics* **2007**, *71* (4), 1686-1698. DOI: 10.1002/prot.21856.

- (245) Uversky, V. N. Intrinsic Disorder in Proteins Associated with Neurodegenerative Diseases. Springer Netherlands, 2009; pp 21-75.
- (246) Longhena, F.; Spano, P.; Bellucci, A. Targeting of Disordered Proteins by Small Molecules in Neurodegenerative Diseases. Springer, Cham, 2017; pp 85-110.
- (247) Cremades, N.; Cohen, S. I. A.; Deas, E.; Abramov, A. Y.; Chen, A. Y.; Orte, A.; Sandal, M.; Clarke, R. W.; Dunne, P.; Aprile, F. A.; et al. Direct observation of the interconversion of normal and toxic forms of α -synuclein. *Cell* **2012**, *149* (5), 1048-1059. DOI: 10.1016/j.cell.2012.03.037.
- (248) Cozachenco, D.; Ribeiro, F.; Ferreira, S. Defective proteostasis in Alzheimer's disease. *Ageing research reviews* **2023**, *85*, 101862. DOI: 10.1016/j.arr.2023.101862.
- (249) Leestemaker, Y.; de Jong, A.; Witting, K. F.; Penning, R.; Schuurman, K.; Rodenko, B.; Zaal, E. A.; van de Kooij, B.; Laufer, S.; Heck, A. J. R.; et al. Proteasome Activation by Small Molecules. *Cell Chemical Biology* **2017**, *24* (6), 725-736.e727. DOI: 10.1016/j.chembiol.2017.05.010.
- (250) Trippier, P. C.; Zhao, K. T.; Fox, S. G.; Schiefer, I. T.; Benmohamed, R.; Moran, J.; Kirsch, D. R.; Morimoto, R. I.; Silverman, R. B. Proteasome activation is a mechanism for pyrazolone small molecules displaying therapeutic potential in amyotrophic lateral sclerosis. *ACS Chemical Neuroscience* **2014**, *5* (9), 823-829. DOI: 10.1021/cn500147v.
- (251) Chondrogianni, N.; Sakellari, M.; Lefaki, M.; Papaevgeniou, N.; Gonos, E. S. Proteasome activation delays aging in vitro and in vivo. *Free Radical Biology and Medicine* **2014**, *71*, 303-320. DOI: 10.1016/j.freeradbiomed.2014.03.031.
- (252) Gonos, E. Proteasome Activation Delays Aging and Protects Against Proteotoxicity in Neurodegenerative Disease. Vol. 821; 2015; pp 7-7.
- (253) Chondrogianni, N.; Voutetakis, K.; Kapetanou, M.; Delitsikou, V.; Papaevgeniou, N.; Sakellari, M.; Lefaki, M.; Filippopoulou, K.; Gonos, E. S. Proteasome activation: An innovative promising approach for delaying aging and retarding age-related diseases. *Ageing Research Reviews* **2015**, *23* (Pt A), 37-55. DOI: 10.1016/j.arr.2014.12.003.
- (254) Chondrogianni, N.; Gonos, E. S. Proteasome activation as a novel antiaging strategy. *IUBMB Life* **2008**, *60* (10), 651-655. DOI: 10.1002/iub.99.
- (255) Vilchez, D.; Morante, I.; Liu, Z.; Douglas, P. M.; Merkwirth, C.; Rodrigues, A. P. C.; Manning, G.; Dillin, A. RPN-6 determines *C. elegans* longevity under proteotoxic stress conditions. *Nature* **2012**, *489* (7415), 263-268. DOI: 10.1038/nature11315.
- (256) Kruegel, U.; Robison, B.; Dange, T.; Kahlert, G.; Delaney, J. R.; Kotireddy, S.; Tsuchiya, M.; Tsuchiyama, S.; Murakami, C. J.; Schleit, J.; et al. Elevated Proteasome Capacity Extends Replicative Lifespan in *Saccharomyces cerevisiae*. *PLoS Genetics* **2011**, *7* (9), e1002253-e1002253. DOI: 10.1371/journal.pgen.1002253.

- (257) Mayor, T.; Sharon, M.; Glickman, M. H. Tuning the proteasome to brighten the end of the journey. *American Journal of Physiology-Cell Physiology* **2016**, *311* (5), C793-C804. DOI: 10.1152/ajpcell.00198.2016.
- (258) Chondrogianni, N.; Gonos, E. S. Proteasome Function Determines Cellular Homeostasis and the Rate of Aging. 2010; pp 38-46.
- (259) Kapeta, S.; Chondrogianni, N.; Gonos, E. S. Nuclear Erythroid Factor 2-mediated Proteasome Activation Delays Senescence in Human Fibroblasts. *Journal of Biological Chemistry* **2010**, *285* (11), 8171-8184. DOI: 10.1074/jbc.M109.031575.
- (260) Kapetanou, M.; Chondrogianni, N.; Petrakis, S.; Koliakos, G.; Gonos, E. S. Proteasome activation enhances stemness and lifespan of human mesenchymal stem cells. *Free Radical Biology and Medicine* **2017**, *103*, 226-235. DOI: 10.1016/j.freeradbiomed.2016.12.035.
- (261) Chondrogianni, N.; Georgila, K.; Kourtis, N.; Tavernarakis, N.; Gonos Efstathios, S. Enhanced proteasome degradation extends *Caenorhabditis elegans* lifespan and alleviates aggregation-related pathologies. *Free Radical Biology and Medicine* **2014**, *75*, S18-S18. DOI: 10.1016/j.freeradbiomed.2014.10.632.
- (262) Chondrogianni, N.; Gonos, E. S. Overexpression of hUMP1/POMP proteasome accessory protein enhances proteasome-mediated antioxidant defence. *Experimental Gerontology* **2007**, *42* (9), 899-903. DOI: 10.1016/j.exger.2007.01.012.
- (263) Voutetakis, K.; Delitsikou, V.; Magouritsas, M. G.; Gonos, E. S. Anti-ageing properties of Khelma Longevity™: treatment of human fibroblasts increases proteasome levels and decreases the levels of oxidized proteins. *New Biotechnology* **2017**, *38* (Pt A), 36-39. DOI: 10.1016/j.nbt.2017.03.002.
- (264) Rodriguez, K. A.; Edrey, Y. H.; Osmulski, P.; Gaczynska, M.; Buffenstein, R. Altered Composition of Liver Proteasome Assemblies Contributes to Enhanced Proteasome Activity in the Exceptionally Long-Lived Naked Mole-Rat. *PLoS ONE* **2012**, *7* (5), e35890-e35890. DOI: 10.1371/journal.pone.0035890.
- (265) Rodriguez, K. A.; Osmulski, P. A.; Pierce, A.; Weintraub, S. T.; Gaczynska, M.; Buffenstein, R. A cytosolic protein factor from the naked mole-rat activates proteasomes of other species and protects these from inhibition. *Biochimica et Biophysica Acta (BBA) - Molecular Basis of Disease* **2014**, *1842* (11), 2060-2072. DOI: 10.1016/j.bbadis.2014.07.005.
- (266) Medina, D. X.; Caccamo, A.; Oddo, S. Methylene Blue Reduces A β Levels and Rescues Early Cognitive Deficit by Increasing Proteasome Activity. *Brain Pathology* **2011**, *21* (2), 140-149. DOI: 10.1111/j.1750-3639.2010.00430.x.
- (267) Chondrogianni, N.; Petropoulos, I.; Franceschi, C.; Friguet, B.; Gonos, E. S. Fibroblast cultures from healthy centenarians have an active proteasome. *Experimental gerontology* **2000**, *35* (6-7), 721-728. DOI: 10.1016/s0531-5565(00)00137-6.

- (268) Cabreiro, F.; Perichon, M.; Jatje, J.; Malavolta, M.; Mocchegiani, E.; Friguet, B.; Petropoulos, I. Zinc supplementation in the elderly subjects: Effect on oxidized protein degradation and repair systems in peripheral blood lymphocytes. *Experimental Gerontology* **2008**, *43* (5), 483-487. DOI: 10.1016/j.exger.2007.10.007.
- (269) Tsvetkov, P.; Asher, G.; Paz, A.; Reuven, N.; Sussman, J.; Silman, I.; Shaul, Y. Operational definition of intrinsically unstructured protein sequences based on susceptibility to the 20S proteasome. *Proteins* **2008**, *70* (4), 1357-1366. DOI: 10.1002/prot.21614.
- (270) Jones, C. L.; Tepe, J. J. Proteasome Activation to Combat Proteotoxicity. *Molecules* **2019**, *24* (15), 2841, Review. DOI: 10.3390/molecules24152841.
- (271) Coleman, R. A.; Muli, C. S.; Zhao, Y.; Bhardwaj, A.; Newhouse, T. R.; Trader, D. J. Analysis of chain length, substitution patterns, and unsaturation of AM-404 derivatives as 20S proteasome stimulators. *Bioorganic & Medicinal Chemistry Letters* **2019**, *29* (3), 420-423. DOI: 10.1016/J.BMCL.2018.12.030.
- (272) George, D.; Tepe, J. Advances in Proteasome Enhancement by Small Molecules. *Biomolecules* **2021**, *11* (12), 1789. DOI: 10.3390/biom11121789.

CHAPTER TWO

Identification and Structure Activity Relationship of Dihydroquinazoline as a Novel 20S Proteasome Activator Scaffold

Reproduced in part with permission from **Fiolek, T.**; Magyar, C.; Wall, T.; Davies, S.; Campbell, M.; Savich, C.; Tepe, J.; Mosey, R. Dihydroquinazolines enhance 20S proteasome activity and induce degradation of α -synuclein, an intrinsically disordered protein associated with neurodegeneration. *Bioorganic & Medicinal Chemistry Letters* **2021**, *36*, 127821. Copyright 2021 Elsevier Ltd.

2.1 Introduction

2.1.1 Background

The proteasome has long been considered a promising target for drug intervention in a variety of disease states involving disruptions of normal protein expression and regulation. This is due to the proteasomes deep involvement in maintaining protein homeostasis (proteostasis) and in numerous essential biological pathways.¹⁻⁸ The proteasome has been theorized as a potential drug target for the treatment of cancer,⁹⁻¹¹ neurodegenerative diseases,¹²⁻¹⁴ and age-related diseases.¹⁵⁻¹⁷ Modulation of proteasome activity with small molecule drugs was first approached via the use of proteasome inhibitors.^{9, 18-20}

Proteasome inhibition has been proven as an effective therapeutic method for the treatment of certain cancers, specifically multiple myeloma (MM).^{9, 18-20} The treatment of MM, a malignant tumor of differentiated B-cells,^{21, 22} via proteasome inhibition is made possible due to the production of large quantities of immature immunoglobulin by these cells.¹⁸ This makes them highly reliant upon the proteasome to clear these non-functional proteins and allow for the recycling of the amino acids. Partial inhibition of the proteasome leads to build up of these redundant proteins and disruption of proteostasis in these cancer cells.^{18, 19, 23} This disruption of proteostasis induces cell cycle arrest, inhibition of angiogenesis, and eventual apoptosis of the MM cells preferentially over healthy cells.¹¹

Several competitive small molecule inhibitors of the proteasome have been approved by the FDA, the first of which was bortezomib (BTZ) in 2003 (**Fig. 2.1A**).²⁴⁻²⁶ BTZ is a boronate peptide-based competitive proteasome inhibitor that covalently binds to the active site threonine of the proteasome to prevent substrate binding.²⁰ These drugs, while effective in many cases at treating MM and related cancers, suffer from problems associated with resistance and off-target toxicity.²⁷⁻

³⁰ These shortcomings led to efforts to develop non-competitive inhibitors of the proteasome, which would hopefully avoid the development of resistance due to active site mutations or the over-expression of the β -5 catalytic subunit.³¹⁻³³

During the Tepe lab's exploration of non-competitive inhibitors of the proteasome, it was discovered that imidazolines, like TCH-165 (**Fig. 2.1B**),^{34, 35} were actually able to enhance 20S proteasome-mediated degradation of fluorogenic peptide substrates *in vitro* (**Fig. 2.1C**).³⁶ These finding, while unexpected, were very exciting and warranted a detailed study to elucidate the mechanism of TCH-165 mediated 20S proteasome activation.

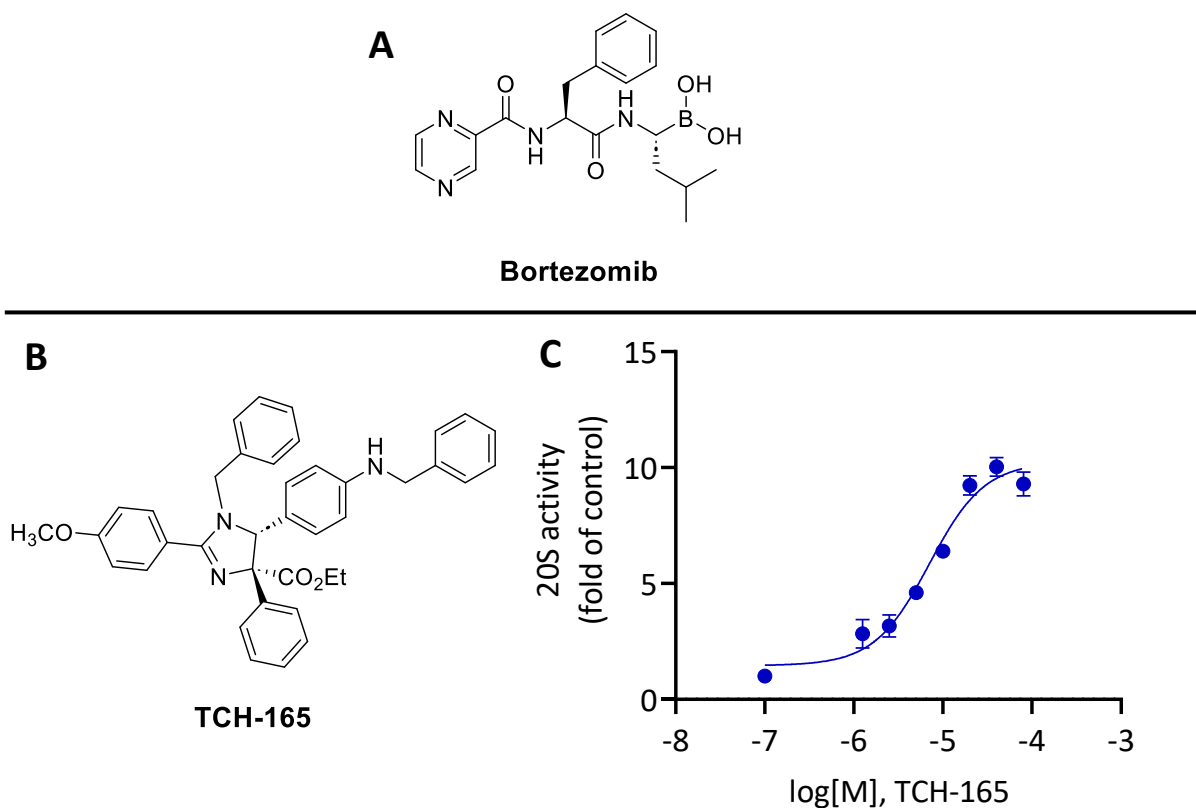


Figure 2.1: (A) Structure of Bortezomib. (B) Structure of TCH-165. (C) Concentration-dependent induction of the proteolytic activity of the 20S proteasome by TCH-165. These data were collected in triplicate (n=3). Error bars denote standard deviation.³⁶

Several experiments were conducted to explore TCH-165's mechanism of action on the 20S proteasome.³⁶ Firstly, the Tepe lab collaborated with Prof. Maria Gaczynska to perform atomic force microscopy (AFM) imaging experiments of the 20S proteasome. In these experiments, 20S proteasome particles were repeatedly scanned and imaged by oscillating (tapping) mode AFM in liquid. Under these conditions the proteasomes constantly change between open and closed forms, with a ratio of about 3:1 favoring the more stable close-gate conformation.^{37, 38} Interestingly, it was found that TCH-165 treatment resulted in a concentration-dependent increase in open-gate 20S proteasomes (**Fig. 2.2A/B**).³⁶

To begin exploring how this increase in open-gated conformations might be taking place, *in silico* molecular docking models were employed by Dr. Corey Jones in the Tepe lab. The resulting preferred docking poses suggested that TCH-165 is binding in the α 1-2 inter-subunit pocket within the α -rings of the 20S proteasome (**Fig. 2.2C**).³⁶ These pockets are typically occupied by the Hb-Y-X motifs of the C-terminal peptide tails, referred to as the Rpt peptides, of the 19S caps when assembled into the 26S form of the proteasome.^{39, 40} These peptide tails allow for docking of the 19S caps and contribute to their ability to induce an open gate conformation of the 20S core particle upon binding.⁴⁰ The α 1-2 inter-subunit pocket is typically occupied by the Rpt3 peptide of the 19S cap.

It was hypothesized that TCH-165 binds in a similar manner to that of the Rpt3 peptide in the α 1-2 inter-subunit pocket and induces a conformational change that promotes α -ring gate-opening or stabilization of the open-gate conformation. To further test this hypothesis, a competition experiment was performed by Prof. Maria Gaczynska with TCH-165 and the Rpt3 peptide. Treatment of the 20S with Rpt3 on its own does not lead to an increase in activity.⁴⁰ This study supported the hypothesis that TCH-165 is binding in the inter-subunit pocket when it was found

that activation of the 20S proteasome by TCH-165 could be partially inhibited through the addition of the Rpt-3 peptide (**Fig. 2.2D**).³⁶

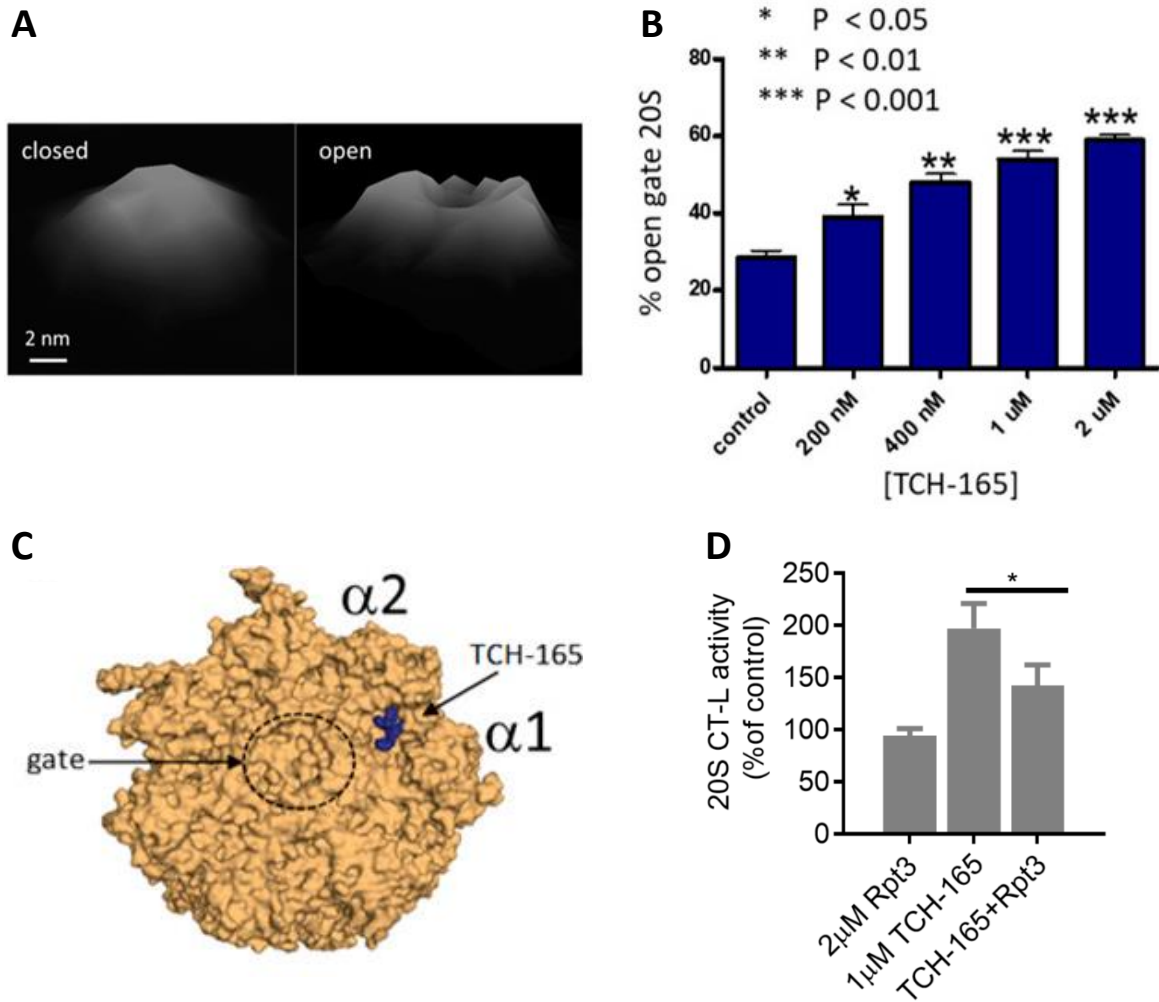


Figure 2.2: TCH-165 stabilizes the open-gate conformation of the 20S proteasome, presumably through interaction with the α 1-2 inter-subunit pocket. (A) Tilted top-view AFM images of standing 20S particles with closed- and open-gate conformations. (B) Percent of open-gate 20S particles in populations of the 20S proteasome treated with TCH-165. Data are mean \pm standard deviation of at least four fields with 120–260 particles per field (one-way ANOVA; * p < 0.05, ** p < 0.01, * p < 0.001). (C) Top view of the 20S α -ring showing the preferred docking**

site of TCH-165 utilizing Autodock Vina. (D) TCH-165 competition experiment with the Rpt3 peptide (which normally binds in the α 1-2 pocket) for 20S proteolysis (n = 3, *p<0.05).³⁶

The discovery and subsequent mechanistic studies of TCH-165 as a 20S proteasome activator by the Tepe lab³⁶ initiated an expanded investigation by our group to identify additional small molecular activators. Despite the several literature reports demonstrating the clinical relevance of 20S proteasome activation for treatment of a variety of diseases,⁹⁻¹⁷ there are very few molecules that had been identified as direct or indirect activators of the 20S proteasome. Additionally, many of these activators suffer from limitations, such as low potency, off-target effects, and poor drug-like properties.^{36, 41-47} The continued exploration of 20S proteasome activation as a therapeutic method will require additional molecular scaffolds to be explored to identify new lead molecules for testing in disease model systems.

As part of this effort to identify novel scaffolds of 20S proteasome activators, I began a collaboration with Prof. Adam Mosey and his lab at Lake Superior State University. The novel chemistry developed by Prof. Mosey's lab allowed for rapid generation of a small library of compounds with analogous structures to that seen in **Fig. 2.3**.⁴⁸ I screened the library of dihydroquinazoline analogues for 20S proteasome activity using a fluorogenic peptide degradation assay and evaluated the structure activity relationship (SAR) of the dihydroquinazoline scaffold.⁴⁹⁻

51

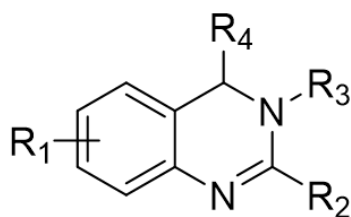


Figure 2.3: General structure of compounds synthesized by the Mosey group.

2.1.2 Objective

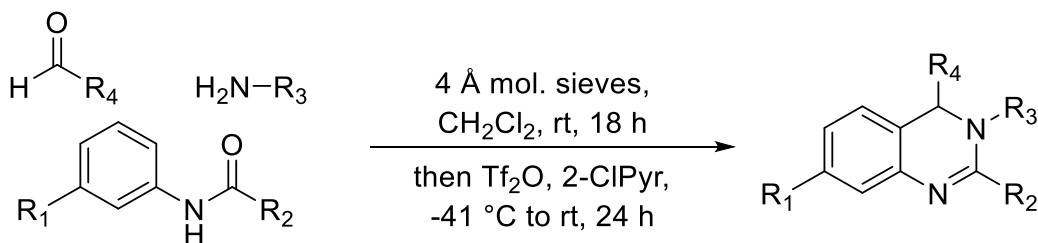
The goals of this project were (1) to further explore the robustness of allosteric small molecule 20S proteasome activation by evaluating a novel 20S activator scaffold, (2) to explore the SAR of the dihydroquinazoline 20S activator scaffold and (3) demonstrate the translation of 20S activity seen by dihydroquinazoline analogues to the enhancement of intrinsically disordered protein (IDP) digestion.

2.2 Results and Discussion

2.2.1 Synthesis of a small library of dihydroquinazoline analogues for exploration as 20S proteasome activators

Synthesis of the dihydroquinazoline analogues was accomplished via Prof. Adam Mosey's recently reported one-pot multicomponent reaction of amides, amines and aldehydes (**Scheme 2.1**).⁴⁸ This method involves *in situ* imine formation from an amine and an aldehyde in the presence of molecular sieves, followed by tandem assembly of the heterocyclic ring through successive Tf₂O-mediated amide dehydration, imine insertion, and Pictet-Spengler-like cyclization. The multicomponent nature of the method permits the construction of highly diverse dihydroquinazolines due to the compatibility of a wide range of simple starting materials.

Scheme 2.1: Multicomponent synthesis of dihydroquinazoline analogues.



A small library of dihydroquinazolines (**Fig. 2.4**) was generated using this multicomponent method to begin probing the ability of members of this class of compounds to activate the 20S

proteasome. Compounds synthesized to populate the library used for this study differed in their structural features at the 7-, 2- and 3-positions (R^1 , R^2 and R^3 , respectively) of the heterocyclic scaffold (**Fig. 2.3**). Variation at the 7- and 2-positions was accomplished using select amides (e.g. **1 – 9**), while the substituents at the 3-position were introduced using chosen amines (e.g. **10 – 24**). R^1 and R^2 groups introduced from the starting amides provided preliminary SAR information which was utilized for the construction of the remaining members of the compound library in which the R^3 group was varied. Simple alkyl and alkoxy substituents were explored at R^1 , along with the absence of any additional group at this location (e.g. **1 – 4**), and the investigated R^2 substituents included alkyl and cycloalkyl groups to compare them to the aromatic counterpart (e.g. **5 – 9** vs **2**). A range of R^3 substituents were installed to include aryl and heteroaryl groups (e.g. **10 – 13**), tethered heteroaryl groups (e.g. **14 – 15**), and alkyl groups with varying ring and heteroatom placement (e.g. **16 – 24**).

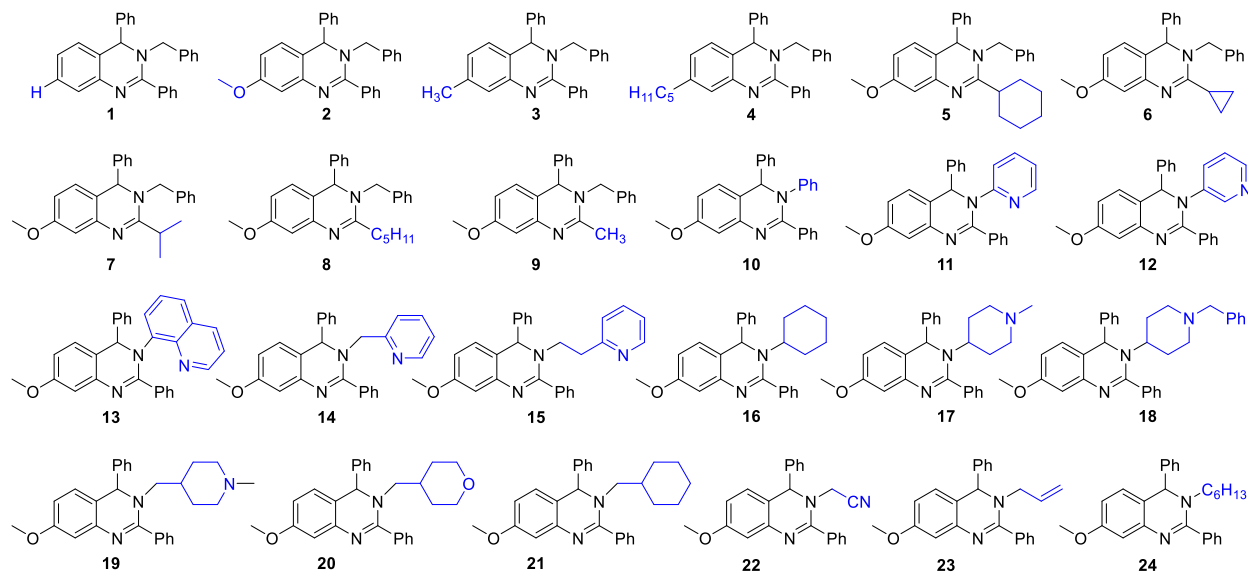


Figure 2.4: Structurally related dihydroquinazoline analogues analyzed in this SAR study.

A set of dihydroquinazoline analogues were synthesized with a variety of functionalities on their periphery to decipher a SAR for the activation of the 20S proteasome by this scaffold.

2.2.2 Screening and SAR of related dihydroquinazoline analogues as 20S proteasome activators

Screening of this small library of dihydroquinazolines (**Fig 2.4**) was performed in two stages. In the first stage, each compound was screened at 3 concentrations (3, 10 and 30 μM) to select lead agents. Secondly, lead agents were further analysed using full concentration responses (6-point titration ranging from 1.25 μM -40 μM) for each of the three proteolytic activities of the 20S proteasome and a combination thereof.

The proteolytic activity of the 20S proteasome can be monitored *in vitro* by measuring the increase in 7-amino-4-methylcoumarin (AMC) fluorescence over time, following the cleavage of fluorogenic peptide substrates for each of the different catalytic sites of the proteasome.^{49, 51} Proteolysis of the peptide substrates is enhanced if an open-gate conformation of the 20S proteasome is stabilized.³⁶ A combination of chymotrypsin-like (CT-L, Suc-LLVY-AMC), trypsin-like (Tryp-L, Boc-LRR-AMC) and caspase-like (Casp-L, Z-LLE-AMC) peptide substrates, one for each of the three different catalytic sites of the 20S, were used in equal amounts to provide a comprehensive look at the activation potential of each compound. In the initial screen, pure human 20S proteasome was pre-treated with 3, 10 or 30 μM of the analogues or DMSO (vehicle control) in 96-well plates for 15 minutes at 37 °C. To each sample was then added a mixture of the three substrates (each at a concentration of 13.3 μM). The release of AMC was measured every 5 minutes, over the course of 1 hour, and the resulting 20S activity changes were determined by comparing to the DMSO treated 20S. Relative changes in activity were quantified by calculating the fold-increase in activity over the vehicle control for each analogue at a given concentration (**Table 2.1**).

Table 2.1: 20S proteasome activity analysis of structurally related dihydroquinazoline analogues (compounds 1–24).

Compound	30 μ M	10 μ M	3 μ M
	(fold of control)		
1	4	1.9	1.5
2	7.9	3.5	2.2
3	8.1	2.8	1.6
4	2.8	2.8	2.6
5	6.5	3.8	1.8
6	2.7	1.5	1.3
7	2.3	1.5	1.4
8	1.8	2.8	1.8
9	1.8	1.1	0.7
10	9.5	4.8	2.1
11	6.9	3.5	1.3
12	5.9	2.4	1.2
13	5.3	4.2	2.8
14	2	1.4	1.3
15	2.8	1.7	1.3
16	6.7	3.2	1.6
17	1	1	0.9
18	7	4.1	2.9
19	1.1	0.9	0.8
20	1.6	1.4	1.2
21	8.2	3	1.6
22	2.7	1.3	0.6
23	2.3	1.3	0.9
24	1.3	1.5	1.6

The resulting data (**Table 2.1**) show a few insightful trends in the SAR of the dihydroquinazolines. Small changes in substitution at the 7-position appear to have a significant effect on activity of the dihydroquinazolines. Compound **1**, which displays 4-fold (i.e. 400%) increase over background 20S activity, lacks a substituent at the 7-position but is otherwise identical to compounds **2** (7.9-fold increase) and **3** (8.1-fold increase). This small change results in a reduction in 20S activity from 8-fold enhancement down to a 4-fold enhancement at 30 μ M. Similarly, the addition of a longer alkyl chain on compound **4** resulted in a steep drop in 20S activity to 2.8-fold at 30 μ M. Changes at the 2-position show similar effects to that of the 7-

position, where most substitutions other than a phenyl group (compounds **5–9**) caused marked decreases in 20S activity. All have less than 3-fold activation at 30 μ M, apart from compound **5** (6.5-fold increase).

Substitutions at the 3-position showed more flexibility to changes than either the 7- or 2-positions, while still having a significant effect on the relative 20S activities of the analogues. Many of the most active analogues, like compounds **2**, **3**, **5** and **10** (7.9, 8.1, 6.5 and 9.5-fold increase of 20S activity, respectively), contain a phenyl or benzyl functionality at the 3-position. Other similarly sized and shaped substituents like cyclohexane (compound **16** (6.7-fold)) and pyridine compounds **11** (6.9-fold) and **12** (5.9-fold)) also provided some of the most active analogues. Interestingly, larger substituents at the 3-position as seen in compounds **18** (7-fold) and **13** (5.3-fold) also yielded highly active analogues, suggesting that additional functionalities may be incorporated here for further optimization if necessary. The substitution of the phenyl or benzyl groups for some other heterocycles such as N-methyl piperidine (compounds **17** (1-fold) and **19** (1.2-fold)), tetrahydropyran (compound **20** (1.6-fold)) or even a pyridine linked by a methyl group in compound **14** (2-fold) lead to significant decreases in 20S activity. This suggests that placement of heteroatoms at the 3-position may have the potential to disrupt hydrophobic interactions in that region. The difference in activity shown between **17** and **18** could be caused by a disruption of hydrophobic interactions with the addition of the piperidine nitrogen, which could then be reinstated or replaced by new interactions made by the phenyl group in **18**. The addition of non-cyclic substituents at the 3-position (compounds **22**, **23** and **24**) resulted in very little 20S activity (2.7, 2.3 and 1.6-fold increase in 20S activity, respectively) in all cases suggesting that larger hydrophobic groups at the 3-position are likely required for 20S activity.

2.2.3 Select dihydroquinazoline analogues activate all catalytic sites of the 20S proteasome in a concentration-dependent manner

After analysing the results in **Table 2.1**, three of the most promising analogues were selected for further studies into their 20S activity. Compounds **2**, **10**, and **18** were selected to be carried forward due to their relatively high max-fold increases and more promising concentration-response at lower concentrations. Compound **17** was also carried forward to use as an inactive control since it had no discernible activity towards the 20S and was structurally similar to compound **18**.

Compounds **2**, **10**, **18** and **17** were further evaluated to obtain a full concentration-response (**Fig. 2.5**) of their activities towards the 20S proteasome using each of the three substrates for the three catalytic sites individually and the combination of the three substrates. This was done to ensure that each of the selected compounds activate the 20S proteasome at all three catalytic sites, which is critical for effective IDP degradation, as these proteins are likely to contain multiple cleavage sites for each. Previously identified 20S proteasome activators that were only able to activate a single catalytic site showed relatively poor enhancement of IDP degradation *in vitro* when compared to those that activated all three catalytic sites.⁴⁴ By fitting the relative fluorescent units and concentrations into a four-parameter dose-response curve the resulting data were analysed. Through this more thorough testing of the selected dihydroquinazoline analogue leads (compounds **2**, **10** and **18**), it was found that each was able to effectively enhance the degradation of all three different peptide substrates of the 20S proteasome in a concentration-dependent manner (**Fig. 2.5**). Whereas the inactive control (compound **17**) was unable to enhance the degradation of any of the peptide substrates in these experiments.

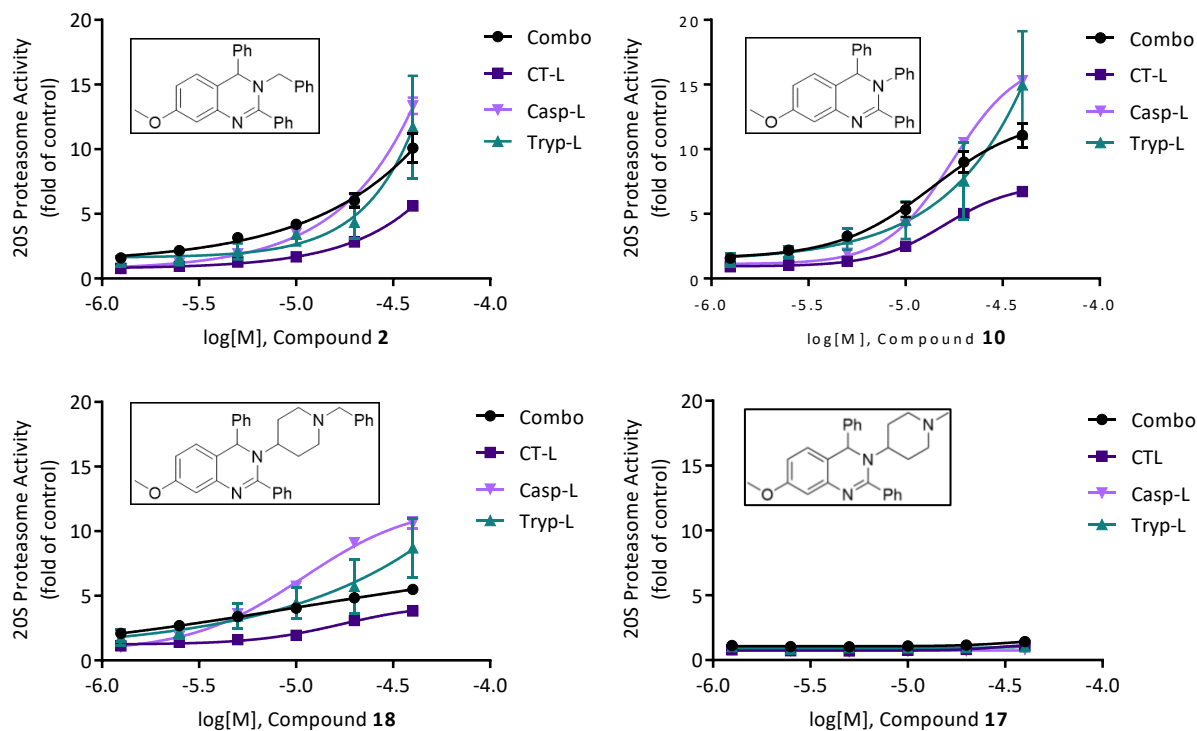


Figure 2.5: Select dihydroquinazoline analogues activate all catalytic sites of the 20S proteasome in a dose dependent manner. Concentration–response curves of compounds **2**, **10**, **18** and **17** for CT-L, Casp-L, Tryp -L, and the combination of the three sites of the 20S. These data were collected in triplicate (n=3). Error bars denote standard deviation.

From the data in **Fig. 2.5**, the concentration at which 20S activity was doubled (EC_{200}) was calculated for each compound using each substrate and the combination of the three substrates (**Table 2.2**). Because of variations in the maximum fold enhancement achieved by different 20S enhancers, EC_{200} values allow for easy comparisons to be made between activators. Additionally, these EC_{200} values may provide better insight into the potency of the activators, relative to their maximum achieved activity. Through these calculations, it was found that each of the active compounds (**2**, **10** and **18**) achieved high maximum fold increases in 20S activity towards each of the peptide substrates, as well as the combination of the three substrates (**Table 2.2**). This

demonstrates that these activators and this scaffold show potential to enhance the degradation of full length IDPs, for the reasons mentioned above. Additionally, it was found that each of the active analogues (compounds **2**, **10** and **18**) had EC₂₀₀'s for 20S enhancement in the low μM range (1 – 2.5 μM) when using the combination of the 3 peptide substrates (**Table 2.2**). This level of potency is on par with some of the most potent small activators discovered by the Tepe lab to date.^{36, 44}

Table 2.2: Detailed analysis of 20S activation by select dihydroquinazoline analogues.

Compound	Combo		CT-L		Casp-L		Tryp-L	
	EC ₂₀₀ (μM)	Max Fold	EC ₂₀₀ (μM)	Max Fold	EC ₂₀₀ (μM)	Max Fold	EC ₂₀₀ (μM)	Max Fold
2	2.0	10.1	12.9	5.6	5.6	13.4	5.0	11.7
10	2.3	11.1	8.1	6.7	5.8	15.3	2.5	15.0
18	1.3	5.5	10.5	3.8	2.8	10.6	1.7	8.7
17	N/A	1.4	N/A	1.1	N/A	0.8	N/A	1.0

2.2.4 Compound 18 enhances the degradation of the IDP α -synuclein *in vitro*

Although these three analogues showed near equipotent activities, compound **18** was selected as the lead molecule to move forward with due to its lowest overall EC₂₀₀ value (**Table 2.2**: combo, EC₂₀₀ 1.3 μM) and relatively low individual site activities for the 20S. The activity of compound **18** was further evaluated by observing its ability to enhance 20S mediated degradation of the intrinsically disordered protein (IDP) α -synuclein (**Fig. 2.6A**). This was done to determine if the activity seen by dihydroquinazoline analogues translates to more relevant full length protein targets of the 20S.⁵²⁻⁵⁴ The IDP α -synuclein was selected for these studies due to its predicted highly disordered nature (**Fig. 2.6A**) and its known association with the development of Parkinson's disease, as well as other synucleinopathies.⁵⁵⁻⁵⁹

Briefly, the 20S proteasome was incubated with compound **18**, followed by addition of pure human α -synuclein. This mixture was then incubated for 4 hours. The digestions were

analysed using silver stain (**Fig. 2.6C**) and densitometry was performed using image J software (**Fig. 2.6B**) to explore the ability of compound **18** to enhance α -synuclein degradation by the 20S. It was found that compound **18** effectively enhanced the rate of degradation of α -synuclein by the 20S *in vitro* in a concentration-dependant manner (**Fig. 2.6B and C**). As a control, the proteasome inhibitor, bortezomib, which prevented α -synuclein degradation, was used to confirm that the clearance of α -synuclein is a proteasome mediated event. The resulting data show that the prior fluorogenic peptide substrate-based results for the dihydroquinazoline scaffold are translatable to the degradation of IDPs.

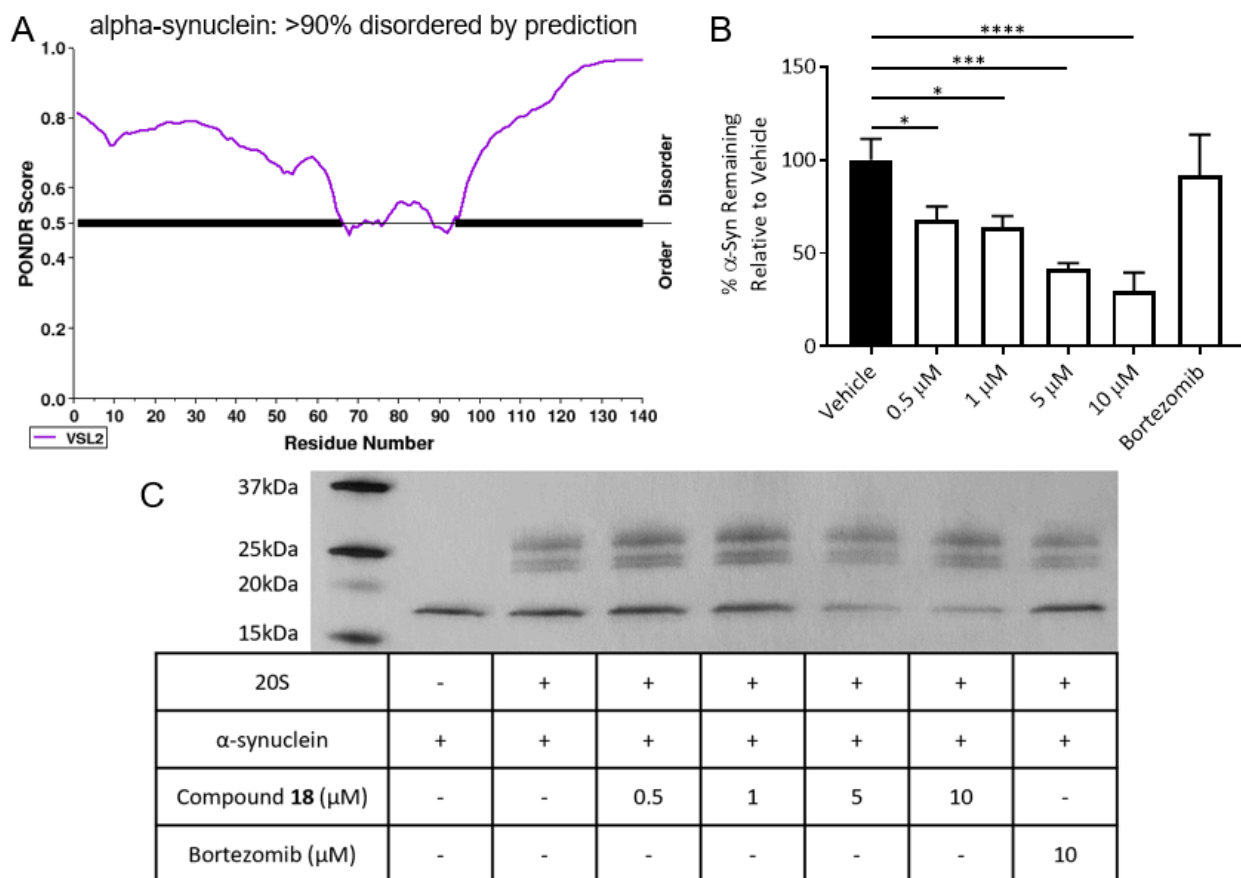


Figure 2.6: The most potent dihydroquinazoline analogue (compound 18) enhances 20S-mediated degradation of the IDP α -synuclein *in vitro*. (A) Intrinsic disorder in α -synuclein as predicted with PONDNR VSL2 software. (B) Densitometry of C using image J software. (C) Silver

stain of α -synuclein digestion with the 20S proteasome pretreated with dihydroquinazoline analogue (compound **18**) or the proteasome inhibitor bortezomib. These data were collected in triplicate (n=3). Error bars denote standard deviation. Ordinary one-way ANOVA statistical analysis was used to determine statistical significance (*p<0.05, ***p<0.001, ****p<0.0001).

These data demonstrate that dihydroquinazolines represent a promising scaffold from which potent 20S activators that enhance IDP degradation can be developed. Additionally, recently developed synthetic methods allow for access to a broad scope of dihydroquinazoline analogues, permitting the exploration of a variety of different substituents and substitution patterns. Among the analogues tested, several active compounds were identified, as well as a few of the most potent 20S activators identified to date. Further optimization and testing of dihydroquinazoline analogues may yield even more potent and drug-like leads, which can assist in the continued exploration of 20S activation as a novel therapeutic method.

2.2.5 Screening of an extended dihydroquinazoline library shows numerous 20S proteasome active analogues, but did not yield improved leads

In an effort to explore a larger library of dihydroquinazoline analogues and to identify even more potent lead molecules, the Mosey lab provided nearly 80 dihydroquinazoline analogues synthesized using their methodology.⁴⁸ To screen this larger library of dihydroquinazoline analogues economically and more rapidly, our standard 3-substrate combination fluorogenic peptide assay was modified slightly by using reduced volumes required for running the assay and fit it in 384-well plates. This was done following protocols used by our lab previously in a high throughput screen to identify 20S activators, that will be discussed in more detail in **Chapter 3**.⁴⁴ This study was done with assistance from Dr. Tomas Dexheimer and MSU's assay development and drug repurposing core (ADDRC). Human 20S proteasome was pretreated with various

concentrations of each analogue followed by addition of the 3-substrate combination. Proteasome activity was quantified by measuring fluorescence intensity associated with AMC release at time = 0 min and then again at time = 60 min. The level of activity for each treatment was determined by subtracting signal from time = 0 from that found at time = 60 min. The resulting difference in AMC fluorescence was compared to that of the DMSO vehicle control. This was done at 8- concentrations for each analogue to obtain concentration response curves. From these data, the maximum fold increase in activity over the vehicle control, as well as an EC₂₀₀ for each compound was determined, as described above. The resulting data is summarized in a graph showing the maximum fold increase over the vehicle (y-axis) and EC₂₀₀ (x-axis) of each compound (**Figure 2.7**).

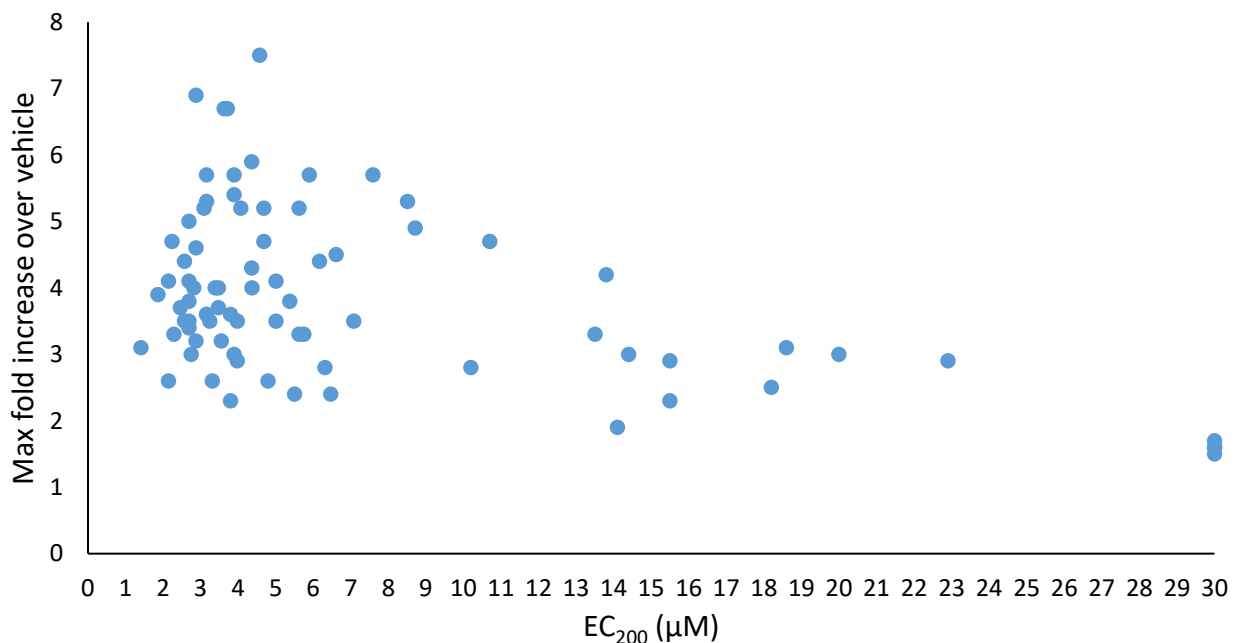


Figure 2.7: Screening of an extended library of dihydroquinazoline analogues using fluorogenic peptide substrates shows numerous active compounds. Graph summarizing EC₂₀₀ values (x-axis) and maximum fold increase over vehicle (30 µM). The top performing compounds

were those with the highest maximum fold increases, as well as those with the lowest EC₂₀₀ values. A combination of high max fold increase and low EC₂₀₀ value represents the ideal lead compounds.

Through the screening of this larger library, it was found that many of these dihydroquinazoline analogues activated the 20S proteasome to various degrees. However, none of the additional dihydroquinazoline analogues tested in this high throughput manner showed improvement relative to the most active analogues explored in the initial SAR study. After analysis of this data and discussions with Prof. Mosey, he and his lab have begun synthesizing additional dihydroquinazoline analogues to explore different substitutions at the 4-position to further diversify the scaffold.

2.3 Conclusions

In summary, a small library of dihydroquinazoline analogues were screened for 20S proteasome activity. It was found that several of these analogues effectively enhanced the activity of the 20S proteasome towards the degradation of fluorogenic peptide substrates for each of the catalytic sites of the proteasome. Comparison of the SAR of these dihydroquinazoline analogues identified structural motifs that, when used in combination, yielded some of the most potent 20S proteasome activators to date. Detailed evaluation of top dihydroquinazoline analogues (compounds **2**, **10** and **18**) from this library demonstrated that each was capable of activating all 3 catalytic sites of the 20S proteasome in a concentration-dependent manner. It was also demonstrated that the activity of compound **18** translates well to enhance the 20S mediated degradation of a natural IDP substrate of the 20S proteasome, α -synuclein. Continued screening of dihydroquinazoline analogues has yet to yield substantial improvements in activity relative to the top compounds identified in the aforementioned SAR study. However, ongoing efforts are being made to diversify this scaffold further and identify more potent leads, by making use of

recently developed synthetic methods that allow for rapid generation of dihydroquinazolines with varied substitutions and substitution patterns.

This work:

- (1) Further demonstrated the robustness of allosteric small molecule 20S proteasome activators through the identification of dihydroquinazolines as a novel 20S activator scaffold.
- (2) Explored the SAR of the dihydroquinazoline scaffolds 20S proteasome activity, and identified analogues with potencies on par with the most potent activators established thus far.
- (3) Demonstrated that the activity of the dihydroquinazoline scaffold translates to enhance 20S proteasome-mediated degradation of the natural IDP substrate α -synuclein *in vitro*.

REFERENCES

- (1) Voges, D.; Zwickl, P.; Baumeister, W. The 26S Proteasome: A Molecular Machine Designed for Controlled Proteolysis. *Annual Review of Biochemistry* **1999**, *68*, 1015-1068, review-article. DOI: 10.1146/annurev.biochem.68.1.1015.
- (2) McNaught, K. S. P.; Olanow, C. W.; Halliwell, B.; Isacson, O.; Jenner, P. Failure of the ubiquitin–proteasome system in Parkinson's disease. *Nature Reviews Neuroscience* **2001**, *2* (8), 589-594. DOI: 10.1038/35086067.
- (3) Voorhees, P.; Dees, E.; O'Neil, B.; Orłowski, R. The proteasome as a target for cancer therapy. *Clinical cancer research* **2003**, *9* (17), 6316-6325.
- (4) Ostrowska, H. The ubiquitin-proteasome system: a novel target for anticancer and anti-inflammatory drug research. *Cellular & Molecular Biology Letters* **2008**, *13* (3), 353-365. DOI: 10.2478/s11658-008-0008-7.
- (5) Calamini, B.; Morimoto, R. Protein homeostasis as a therapeutic target for diseases of protein conformation. *Current Topics in Medicinal Chemistry* **2012**, *12* (22), 2623-2640. DOI: 10.2174/1568026611212220014.
- (6) Huang, X.; Dixit, V. M. Drugging the undruggables: exploring the ubiquitin system for drug development. *Cell Research* **2016**, *26* (4), 484-498, ReviewPaper. DOI: doi:10.1038/cr.2016.31.
- (7) Njomen, E.; Tepe, J. J. Proteasome Activation as a New Therapeutic Approach to Target Proteotoxic Disorders. *Journal of Medicinal Chemistry* **2019**, *62* (14), 6469-6481. DOI: 10.1021/acs.jmedchem.9b00101.
- (8) Tundo, G.; Sbardella, D.; Santoro, A.; Coletta, A.; Oddone, F.; Grasso, G.; Milardi, D.; Lacal, P.; Marini, S.; Purrello, R.; et al. The proteasome as a druggable target with multiple therapeutic potentialities: Cutting and non-cutting edges. *Pharmacology & therapeutics* **2020**, *213*, 107579. DOI: 10.1016/j.pharmthera.2020.107579.
- (9) Mitsiades, N.; Mitsiades, C. S.; Poulaki, V.; Chauhan, D.; Fanourakis, G.; Gu, X.; Bailey, C.; Joseph, M.; Libermann, T. A.; Treon, S. P.; et al. Molecular sequelae of proteasome inhibition in human multiple myeloma cells. *PNAS* **2002**, *99* (22), 14374-14379, research-article. DOI: 10.1073/pnas.202445099.
- (10) D'Arcy, P.; Brnjic, S.; Olofsson, M. H.; Fryknäs, M.; Lindsten, K.; De Cesare, M.; Perego, P.; Sadeghi, B.; Hassan, M.; Larsson, R.; et al. Inhibition of proteasome deubiquitinating activity as a new cancer therapy. *Nature Medicine* **2011**, *17* (12), 1636-1640, OriginalPaper. DOI: doi:10.1038/nm.2536.
- (11) Rastogi, N.; Mishra, D. P. Therapeutic targeting of cancer cell cycle using proteasome inhibitors. *Cell Division* **2012**, *7* (1), 1-10, ReviewPaper. DOI: doi:10.1186/1747-1028-7-26.
- (12) Bedford, L.; Hay, D.; Devoy, A.; Paine, S.; Powe, D. G.; Seth, R.; Gray, T.; Topham, I.; Fone, K.; Rezvani, N.; et al. Depletion of 26S Proteasomes in Mouse Brain Neurons Causes

Neurodegeneration and Lewy-Like Inclusions Resembling Human Pale Bodies. *Journal of Neuroscience* **2008**, 28 (33), 8189-8198. DOI: 10.1523/JNEUROSCI.2218-08.2008.

(13) Demasi, M.; Faria, B. F. Activation of the ubiquitin-proteasome system: implications for neurodegeneration, aging, and tumorigenesis. *Journal of Neurology & Neuromedicine* **2017**, 2 (8), 1-4.

(14) Boland, B.; Yu, W. H.; Corti, O.; Mollereau, B.; Henriques, A.; Bezard, E.; Pastores, G. M.; Rubinsztein, D. C.; Nixon, R. A.; Duchen, M. R.; et al. Promoting the clearance of neurotoxic proteins in neurodegenerative disorders of ageing. *Nature Reviews Drug Discovery* **2018**, 17 (9), 660-688. DOI: 10.1038/nrd.2018.109.

(15) Chondrogianni, N.; Gonos, E. S. Proteasome activation as a novel antiaging strategy. *IUBMB Life* **2008**, 60 (10), 651-655. DOI: 10.1002/iub.99.

(16) Chondrogianni, N.; Sakellari, M.; Lefaki, M.; Papaevgeniou, N.; Gonos, E. S. Proteasome activation delays aging in vitro and in vivo. *Free Radical Biology and Medicine* **2014**, 71, 303-320. DOI: 10.1016/j.freeradbiomed.2014.03.031.

(17) Chondrogianni, N.; Voutetakis, K.; Kapetanou, M.; Delitsikou, V.; Papaevgeniou, N.; Sakellari, M.; Lefaki, M.; Filippopoulou, K.; Gonos, E. S. Proteasome activation: An innovative promising approach for delaying aging and retarding age-related diseases. *Ageing Research Reviews* **2015**, 23 (Pt A), 37-55. DOI: 10.1016/j.arr.2014.12.003.

(18) Meister, S.; Schubert, U.; Neubert, K.; Herrmann, K.; Burger, R.; Gramatzki, M.; Hahn, S. S. C.; Schreiber, S.; Wilhelm, S.; Herrmann, M.; et al. Extensive immunoglobulin production sensitizes myeloma cells for proteasome inhibition. *Cancer Research* **2007**, 67 (4), 1783-1792. DOI: 10.1158/0008-5472.CAN-06-2258.

(19) Bianchi, G.; Oliva, L.; Cascio, P.; Pengo, N.; Fontana, F.; Cerruti, F.; Orsi, A.; Pasqualetto, E.; Mezghrani, A.; Calbi, V.; et al. The proteasome load versus capacity balance determines apoptotic sensitivity of multiple myeloma cells to proteasome inhibition | Blood | American Society of Hematology. *Blood* **2009**, 113 (13), 3040-3049. DOI: 10.1182/blood-2008-08-172734.

(20) Kisselev, A.; Linden, W.; Overkleeft, H. Proteasome Inhibitors: An Expanding Army Attacking a Unique Target. *Chemistry & Biology* **2012**, 19 (1), 99-115. DOI: 10.1016/j.chembiol.2012.01.003.

(21) Chiang, M.; Stadtmauer, E. NF-kappaB, IL-6 and myeloma cell growth: making the connection. *Cancer biology & therapy* **2004**, 3 (10), 1018-1020. DOI: 10.4161/cbt.3.10.1326.

(22) Anderson, K.; Alsina, M.; Bensinger, W.; Biermann, J.; Chanan-Khan, A.; Cohen, A.; Devine, S.; Djulbegovic, B.; Faber, E.; Gasparetto, C.; et al. Multiple myeloma. *Journal of the National Comprehensive Cancer Network : JNCCN* **2011**, 9 (10), 1146-1183. DOI: 10.6004/jnccn.2011.0095.

- (23) Cenci, S.; Mezghrani, A.; Cascio, P.; Bianchi, G.; Cerruti, F.; Fra, A.; Lelouard, H.; Masciarelli, S.; Mattioli, L.; Oliva, L.; et al. Progressively impaired proteasomal capacity during terminal plasma cell differentiation. *The EMBO Journal* **2006**, *25* (5), 1104-1113. DOI: 10.1038/sj.emboj.7601009.
- (24) Kane, R.; Bross, P.; Farrell, A.; Pazdur, R. Velcade®: U.S. FDA Approval for the Treatment of Multiple Myeloma Progressing on Prior Therapy. *The Oncologist* **2003**, *8* (6), 508-513. DOI: 10.1634/theoncologist.8-6-508.
- (25) Kirk, C. Discovery and Development of Second-Generation Proteasome Inhibitors. *Seminars in Hematology* **2012**, *49* (3), 207-214. DOI: 10.1053/j.seminhematol.2012.04.007.
- (26) Kuhn, D.; Orłowski, R.; Bjorklund, C. Second generation proteasome inhibitors: carfilzomib and immunoproteasome-specific inhibitors (IPSI). *Current cancer drug targets* **2011**, *11* (3), 285-295. DOI: 10.2174/156800911794519725.
- (27) Murray, M.; Auger, M.; Bowles, K. Overcoming bortezomib resistance in multiple myeloma. *Biochemical Society transactions* **2014**, *42* (4), 804-808. DOI: 10.1042/BST20140126.
- (28) Lü, S.; Wang, J. The resistance mechanisms of proteasome inhibitor bortezomib. *Biomarker research* **2013**, *1*, 13. DOI: 10.1186/2050-7771-1-13.
- (29) Wu, Y.; Yang, J.; Saito, H. Bortezomib-resistance is associated with increased levels of proteasome subunits and apoptosis-avoidance. *Oncotarget* **2016**, *7* (47), 77622-77634. DOI: 10.18632/oncotarget.12731.
- (30) Carozzi, V.; Renn, C.; Bardini, M.; Fazio, G.; Chiorazzi, A.; Meregalli, C.; Oggioni, N.; Shanks, K.; Quartu, M.; Serra, M.; et al. Bortezomib-Induced Painful Peripheral Neuropathy: An Electrophysiological, Behavioral, Morphological and Mechanistic Study in the Mouse. *PLoS One* **2013**, *8* (9). DOI: 10.1371/journal.pone.0072995.
- (31) Anbanandam, A.; Albarado, D.; Tirziu, D.; Simons, M.; Veeraraghavan, S. Molecular basis for proline- and arginine-rich peptide inhibition of proteasome. *Journal of Molecular Biology* **2008**, *384* (1), 219-227. DOI: 10.1016/j.jmb.2008.09.021.
- (32) Ruschak, A.; Slassi, M.; Kay, L.; Schimmer, A. Novel proteasome inhibitors to overcome bortezomib resistance. *Journal of the National Cancer Institute* **2011**, *103* (13). DOI: 10.1093/jnci/djr160.
- (33) Gaczynska, M.; Osmulski, P.; Gao, Y.; Post, M.; Simons, M. Proline- and Arginine-Rich Peptides Constitute a Novel Class of Allosteric Inhibitors of Proteasome Activity†. *Biochemistry* **2003**, *42* (29), 8663-8670, rapid-communication. DOI: 10.1021/bi034784f.
- (34) Lansdell, T. A.; Hurchla, M. A.; Xiang, J.; Hovde, S.; Weilbaecher, K. N.; Henry, R. W.; Tepe, J. J. Noncompetitive Modulation of the Proteasome by Imidazoline Scaffolds Overcomes Bortezomib Resistance and Delays MM Tumor Growth in Vivo. *ACS Chemical Biology* **2012**, *8* (3), 578-587, research-article. DOI: 10.1021/cb300568r.

- (35) Azevedo, L. M.; Lansdell, T. A.; Ludwig, J. R.; Mosey, R. A.; Woloch, D. K.; Cogan, D. P.; Patten, G. P.; Kuszpit, M. R.; Fisk, J. S.; Tepe, J. J. Inhibition of the Human Proteasome by Imidazoline Scaffolds. *Journal of Medicinal Chemistry* **2013**, *56* (14), 5974-5978. DOI: 10.1021/jm400235r.
- (36) Njomen, E.; Osmulski, P. A.; Jones, C. L.; Gaczynska, M.; Tepe, J. J. Small Molecule Modulation of Proteasome Assembly. *Biochemistry* **2018**, *57* (28), 4214-4224. DOI: 10.1021/acs.biochem.8b00579.
- (37) Gaczynska, M.; Osmulski, P. A. Atomic Force Microscopy of Proteasome Assemblies. Vol. 736; 2011; pp 117-132.
- (38) Osmulski, P. A.; Hochstrasser, M.; Gaczynska, M. A Tetrahedral Transition State at the Active Sites of the 20S Proteasome Is Coupled to Opening of the α -Ring Channel. *Structure* **2009**, *17* (8), 1137-1147. DOI: 10.1016/j.str.2009.06.011.
- (39) Schweitzer, A.; Aufderheide, A.; Rudack, T.; Beck, F.; Pfeifer, G.; Plitzko, J. M.; Sakata, E.; Schulten, K.; Förster, F.; Baumeister, W. Structure of the human 26S proteasome at a resolution of 3.9 Å. *PNAS* **2016**, *113* (28), 7816-7821, research-article. DOI: 10.1073/pnas.1608050113.
- (40) Smith, D. M.; Chang, S. C.; Park, S.; Finley, D.; Cheng, Y.; Goldberg, A. L. Docking of the proteasomal ATPases' carboxyl termini in the 20S proteasome's alpha ring opens the gate for substrate entry. *Molecular cell* **2007**, *27* (5), 731-744. DOI: 10.1016/j.molcel.2007.06.033.
- (41) Huang, L.; Ho, P.; Chen, C.-H. Activation and inhibition of the proteasome by betulinic acid and its derivatives. *FEBS Letters* **2007**, *581* (25), 4955-4959. DOI: 10.1016/j.febslet.2007.09.031.
- (42) Lee, B.-H.; Lee, M. J.; Park, S.; Oh, D.-C.; Elsasser, S.; Chen, P.-C.; Gartner, C.; Dimova, N.; Hanna, J.; Gygi, S. P.; et al. Enhancement of proteasome activity by a small-molecule inhibitor of USP14. *Nature* **2010**, *467* (7312), 179-184. DOI: 10.1038/nature09299.
- (43) Trippier, P. C.; Zhao, K. T.; Fox, S. G.; Schiefer, I. T.; Benmohamed, R.; Moran, J.; Kirsch, D. R.; Morimoto, R. I.; Silverman, R. B. Proteasome activation is a mechanism for pyrazolone small molecules displaying therapeutic potential in amyotrophic lateral sclerosis. *ACS Chemical Neuroscience* **2014**, *5* (9), 823-829. DOI: 10.1021/cn500147v.
- (44) Jones, C. L.; Njomen, E.; Sjögren, B.; Dexheimer, T. S.; Tepe, J. J. Small Molecule Enhancement of 20S Proteasome Activity Targets Intrinsically Disordered Proteins. *ACS Chemical Biology* **2017**, *12* (9), 2240-2247. DOI: 10.1021/acscchembio.7b00489.
- (45) Leestemaker, Y.; de Jong, A.; Witting, K. F.; Penning, R.; Schuurman, K.; Rodenko, B.; Zaal, E. A.; van de Kooij, B.; Laufer, S.; Heck, A. J. R.; et al. Proteasome Activation by Small Molecules. *Cell Chemical Biology* **2017**, *24* (6), 725-736.e727. DOI: 10.1016/j.chembiol.2017.05.010.

- (46) Trader, D. J.; Simanski, S.; Dickson, P.; Kodadek, T. Establishment of a suite of assays that support the discovery of proteasome stimulators. *Biochimica et Biophysica Acta (BBA) - General Subjects* **2017**, *1861* (4), 892-899. DOI: 10.1016/J.BBAGEN.2017.01.003.
- (47) Coleman, R. A.; Muli, C. S.; Zhao, Y.; Bhardwaj, A.; Newhouse, T. R.; Trader, D. J. Analysis of chain length, substitution patterns, and unsaturation of AM-404 derivatives as 20S proteasome stimulators. *Bioorganic and Medicinal Chemistry Letters* **2019**, *29* (3), 420-423. DOI: 10.1016/j.bmcl.2018.12.030.
- (48) Magyar, C. L.; Wall, T. J.; Davies, S. B.; Campbell, M. V.; Barna, H. A.; Smith, S. R.; Savich, C. J.; Mosey, R. A. Triflic anhydride mediated synthesis of 3,4-dihydroquinazolines: A three-component one-pot tandem procedure. *Organic and Biomolecular Chemistry* **2019**, *17* (34), 7995-8000. DOI: 10.1039/c9ob01596e.
- (49) Kisselev, A. F.; Akopian, T. N.; Castillo, V.; Goldberg, A. L. Proteasome active sites allosterically regulate each other, suggesting a cyclical bite-chew mechanism for protein breakdown. *Molecular Cell* **1999**, *4* (3), 395-402. DOI: 10.1016/S1097-2765(00)80341-X.
- (50) Gaczynska, M.; Osmulski, P. A. Characterization of noncompetitive regulators of proteasome activity. Academic Press Inc.: 2005; Vol. 398, pp 425-438.
- (51) Kisselev, A.; Goldberg, A. Monitoring Activity and Inhibition of 26S Proteasomes with Fluorogenic Peptide Substrates. *Methods in Enzymology* **2005**, *398*, 364-378. DOI: 10.1016/S0076-6879(05)98030-0.
- (52) Bennett, M.; Bishop, J.; Leng, Y.; Chock, P.; Chase, T.; Mouradian, M. Degradation of α -Synuclein by Proteasome. *Journal of Biological Chemistry* **1999**, *274* (48), 33855-33858. DOI: 10.1074/jbc.274.48.33855.
- (53) Webb, J.; Ravikumar, B.; Atkins, J.; Skepper, J.; Rubinsztein, D. Alpha-Synuclein is degraded by both autophagy and the proteasome. *The Journal of biological chemistry* **2003**, *278* (27), 25009-25013. DOI: 10.1074/jbc.M300227200.
- (54) Alvarez-Castelao, B.; Goethals, M.; Vandekerckhove, J.; Castaño, J. G. Mechanism of cleavage of alpha-synuclein by the 20S proteasome and modulation of its degradation by the RedOx state of the N-terminal methionines. *Biochimica et Biophysica Acta (BBA) - Molecular Cell Research* **2014**, *1843* (2), 352-365. DOI: 10.1016/j.bbamcr.2013.11.018.
- (55) Wills, J.; Jones, J.; Haggerty, T.; Duka, V.; Joyce, J. N.; Sidhu, A. Elevated tauopathy and alpha-synuclein pathology in postmortem Parkinson's disease brains with and without dementia. *Experimental Neurology* **2010**, *225* (1), 210-218. DOI: 10.1016/j.expneurol.2010.06.017.
- (56) Alafuzoff, I.; Hartikainen, P. Alpha-synucleinopathies. *Handbook of clinical neurology* **2017**, *145*, 339-353. DOI: 10.1016/B978-0-12-802395-2.00024-9.
- (57) Berrocal, R.; Vasquez, V.; Krs, S. R.; Gadad, B. S.; Ks, R. α -Synuclein Misfolding Versus Aggregation Relevance to Parkinson's Disease: Critical Assessment and Modeling. Humana Press Inc.: 2015; Vol. 51, pp 1417-1431.

(58) Martí, M.; Tolosa, E.; Campdelacreu, J. Clinical overview of the synucleinopathies. *Movement disorders : official journal of the Movement Disorder Society* **2003**, *18* (6). DOI: 10.1002/mds.10559.

(59) Lehtonen, Š.; Sonninen, T. M.; Wojciechowski, S.; Goldsteins, G.; Koistinaho, J. Dysfunction of Cellular Proteostasis in Parkinson's Disease. *Frontiers in neuroscience* **2019**, *13* (10), 457. DOI: 10.3389/fnins.2019.00457.

CHAPTER THREE

Repurposed Neuroleptic Agents as novel 20S Proteasome Activator Scaffolds

Reproduced in part with permission from **Fiolek J. Taylor**, Keel L. Katarina and Tepe J. Jetze. Fluspirilene Analogs Activate the 20S Proteasome and Overcome Proteasome Impairment by Intrinsically Disordered Protein Oligomers. *ACS Chem. Neurosci.* **2021**. Copyright 2021 American Chemical Society

3.1 Introduction

3.1.1 Background

The regulation of protein synthesis, degradation and folding within a cell is collectively known as proteostasis. Proteostasis is maintained by a wide array of cellular machinery that works to ensure that proteins are present in the proper location and amounts to perform their required functions.¹⁻⁶ However, as humans age, dysregulation of the proteostasis network is inevitable. When this dysregulation of proteostasis occurs, there can be disastrous effects on the cell and even on neighboring cells due to interference with critical signaling pathways. These effects are associated with a variety of human diseases. One increasingly prevalent example of this is seen in neurodegenerative diseases, such as Parkinson's disease, Alzheimer's disease, Huntington's disease, and amyotrophic lateral sclerosis.⁷⁻¹⁹ In these neurodegenerative diseases, accumulation of specific IDPs leads to toxic signaling and disruption of proteostasis caused by their uncontrolled aggregation and oligomerization.²⁰⁻²⁷ As a result, novel therapeutic methods that have the potential to assist in reestablishing proper levels of these IDPs are of great interest.

Recently, it has been recognized that the 20S proteasome plays a critical role in maintaining proteostasis through the direct degradation of oxidatively damaged and intrinsically disordered proteins.^{6, 28-35} The 20S proteasome may therefore serve as the default protease to unremittently maintain low levels of IDPs, without the need for post-translational modifications, including protein ubiquitination.^{6, 28} Especially highly disordered proteins appear to be the main target of the 20S proteasome.³⁶ Unfortunately, when dysregulation of IDPs leads to production that outpaces their proteasomal clearance, the IDPs accumulate, and subsequently oligomerize and aggregate. The oligomeric forms of the IDPs in turn can inhibit the 20S proteasome, resulting in a downward spiral of IDP accumulation, oligomerization and disease progression.³⁷⁻⁴¹

These findings have sparked the search for small molecules capable of enhancing the proteolytic activity of the 20S proteasome.⁴²⁻⁴⁸ Small molecule proteasome enhancers are still relatively scarce, with only a few *bona fide* examples reported in the literature.⁴⁹⁻⁵⁵ The Tepe lab developed an interest in this field of 20S proteasome activation following their discovery of the small molecule 20S activator TCH-165 and related imidazoline analogues.⁵⁰ Since then, the Tepe lab has pursued novel 20S proteasome activator scaffolds through a variety of strategies, including design and synthesis of novel scaffolds, through collaborations (**Chapter 2**)⁴⁹ and through the repurposing and modification of established drugs (this Chapter).⁵¹

Repurposing of existing drugs was considered a promising strategy for the discovery of novel 20S proteasome activators, because it should allow for the identification of small molecule activator scaffolds with good drug-like properties. Our hypothesized strategy for targeting neurodegenerative diseases through 20S proteasome activation would require activators that can effectively cross the blood-brain barrier (BBB). So, by identifying 20S activator scaffolds amongst preexisting drugs, we could greatly increase our chances of success by starting with molecules that can cross the BBB.⁵⁶ This would allow for a much more streamlined drug development process and help to avoid issues with bioavailability in *in vivo* models, should this technology progress to that point.^{57, 58} This was also important because of the relatively few previously identified activators in the literature,⁴⁹⁻⁵⁵ several are not considered to be *bona fide* activators due to poor drug-like properties, detergent-like behavior, and a lack of translation of activity to physiologically relevant substrates and systems. This includes detergents, such as sodium dodecyl sulfate (SDS) and natural products, like oleuropein,⁵⁹ and betulinic acid.⁶⁰ These, as well as others, are questionable as true 20S agonists, since their activity does not translate under more physiologically

relevant conditions and may result in disruption of proteasome subunits.⁵⁴ This drug repurposing strategy should help to avoid future issues with other similar nondrug-like molecules.

To begin identifying 20S proteasome activator scaffolds amongst known drugs, the Tepe lab performed a high-throughput screen (HTPS) of the NIH Clinical Collection and Prestwick libraries.⁵¹ For this screen, purified 20S proteasome was exposed to the compounds (10 μ M) in the presence of the fluorogenic chymotrypsin-like (CT-L) peptide substrate (Suc-LLVY-AMC). In this activity assay, proteolysis of the peptide substrate is enhanced if a compound induces an open-gate conformation of the α -ring, or through other allosteric interactions, to allow for more rapid proteolytic cleavage inside the core particle. This enhanced proteolysis of the substrates is indicated by the release of AMC from the peptide substrate (as discussed in **Chapter 2**).⁶¹ The compounds were deemed inactive if the CT-L activity was <2 fold (at 10 μ M) over the DMSO vehicle control. From this screen, several novel small molecule activators of the 20S proteasome were identified. This included several neuroleptic agents, such as Chlorpromazine,⁶² other phenothiazines (**Fig. 3.1A**), Aripiprazole⁶³ and Fluspirilene^{64, 65} (**Fig. 3.2**), which could represent promising starting points for the development of BBB permeable 20S activators as therapeutics for neurodegenerative diseases.⁵¹

Chlorpromazine and related phenothiazine analogues were the first of these neuroleptic agents to be explored more thoroughly by the Tepe lab (**Fig. 3.1A**).⁵¹ It was found that Chlorpromazine could effectively enhance the proteolytic cleavage of the CT-L fluorogenic peptide (**Fig. 3.1B**) and IDP substrates (**Fig. 3.1C**) of the 20S proteasome *in vitro*.⁵¹ *In silico* docking done on Chlorpromazine suggests that it, similar to TCH-165, may be acting on the 20S proteasome by binding in an inter-subunit pocket of the α -ring (**Fig. 3.1D**).⁵⁰ Thus, promoting an

open-gate conformation of the 20S proteasome and allowing for easier substrate access to the catalytic core, where proteolytic cleavage can occur.⁴⁹⁻⁵¹

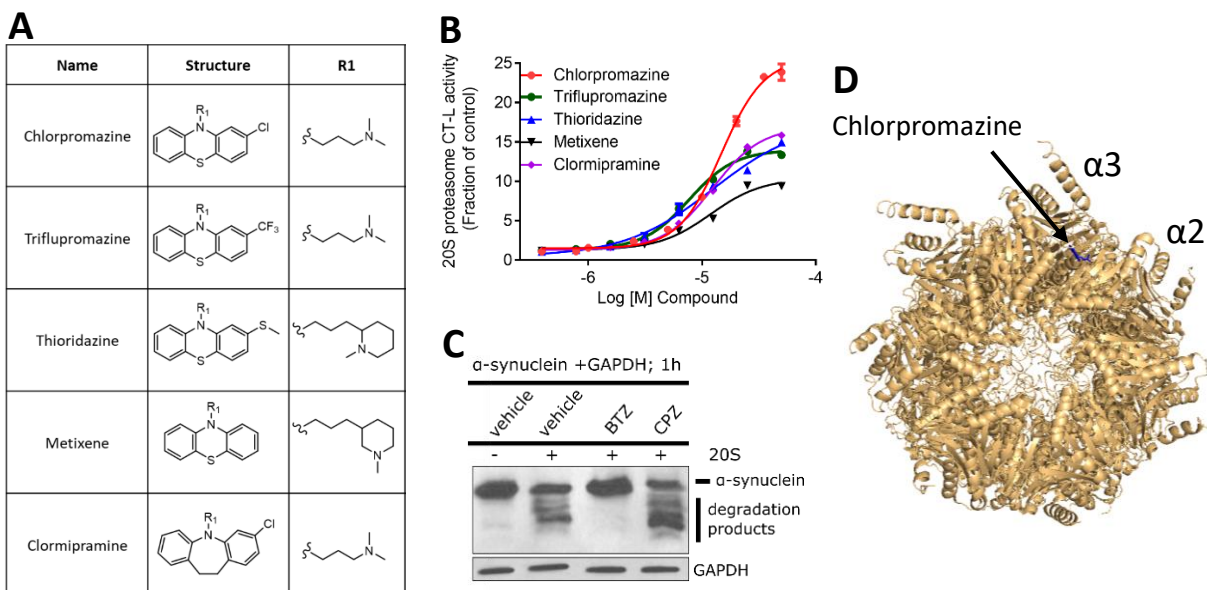


Figure 3.1: Phenothiazines, like Chlorpromazine, enhance 20S mediated degradation of peptide and IDP substrates, presumably through allosteric interactions with the α -ring. (A) Structures of phenothiazine analogues identified in a HTPS as 20S activators. **(B)** Concentration response (0–80 μ M) of phenothiazine analogues in fluorogenic peptide (CT-L) digestions with purified human 20S proteasome. Error bars denote standard deviation. **(C)** *In vitro* enhancement of purified human 20S proteasome-mediated α -synuclein degradation by Chlorpromazine, visualized using western blot.⁵¹ **(D)** *In silico* docking model suggests Chlorpromazine likely binds in the α -2-3 pocket of the α -ring of the 20S proteasome.

The exciting results obtained with Chlorpromazine encouraged additional studies,⁵¹ wherein I sought to validate the activation of the 20S proteasome by other neuroleptic agents identified in our HTPS, like Aripiprazole⁶³ and Fluspirilene^{64, 65} (**Fig. 3.2**), so that they may be repurposed. This would allow for the identification of other novel 20S activator scaffolds with promising drug-like

properties for use in studying the effects of 20S proteasome activation in neurodegenerative disease models. With a larger pool of drug-like small molecule scaffolds that activate the 20S proteasome, we increase our chances of success when developing them as therapeutics, learn more about what motifs can be used to generate novel activators, and can address some of the limitations of previously discovered activators. These limitations include poor drug-like properties, lack of BBB permeability, non-translatable activity to native IDP substrates, detergent-like behavior, troublesome synthesis, and off-target effects.^{51, 54, 59, 60}

In these studies, I explored the neuroleptic agents Aripiprazole⁶³ and Fluspirilene^{64, 65} (**Fig. 3.2**), and analogues thereof, as 20S proteasome activators. I evaluated their activity in detail using fluorogenic peptide and IDP substrates. Then, I employed *in silico* docking to assist in analogue design. In the case of Aripiprazole, I synthesized and evaluated the analogues. Whereas, in the case of Fluspirilene, I collaborated with Dr. Katarina Keel, who performed the synthesis of Fluspirilene and its analogues, and with whom I worked together on the docking and analogue design.

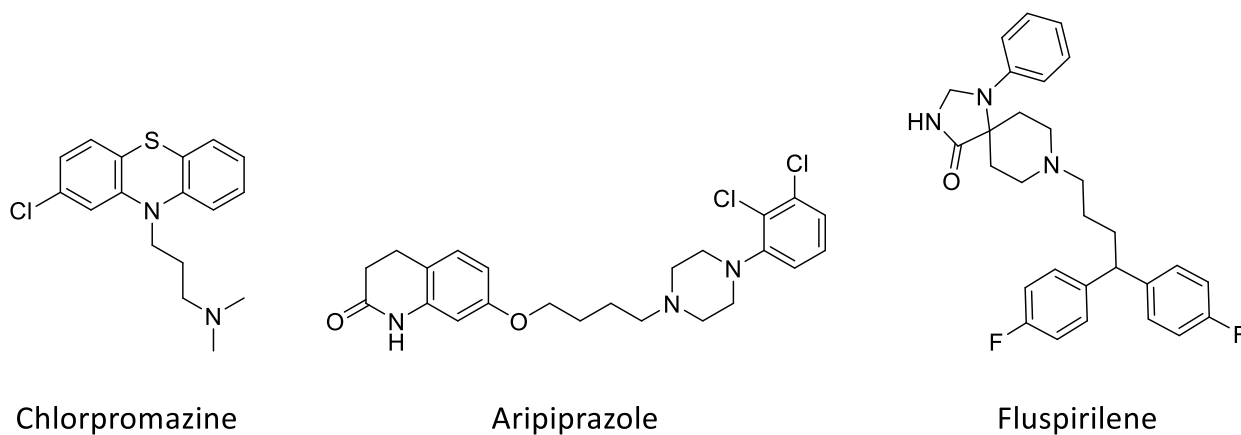


Figure 3.2: The neuroleptic agents Chlorpromazine, Aripiprazole and Fluspirilene were identified as potential 20S activator scaffolds in a HTPS.

3.1.2 Objective

The goals of these studies were (1) to validate the neuroleptic agents Aripiprazole and Fluspirilene as *bona fide* 20S activator scaffolds, (2) design, synthesize and evaluate novel analogues of these scaffolds to diminish their neuroleptic activity and maintain/enhance 20S activity, and (3) identify promising lead molecules for use in the development of novel assays exploring the potential of this strategy for targeting neurodegenerative diseases.

3.2 Results and Discussion

3.2.1 The neuroleptic agent Aripiprazole is a small molecule activator of the 20S proteasome

Aripiprazole (**Fig. 3.2**) was identified as a novel 20S activator in the HTPS performed by our lab previously, in which Chlorpromazine was also identified.⁵¹ Aripiprazole is a FDA approved neuroleptic agent with dopamine D2 receptor partial agonist activity used for the treatment of schizophrenia.⁶³ The studies outlined here were undertaken to verify Aripiprazole's 20S proteasome activity, develop analogues of Aripiprazole and to assess whether its activity translates to a more relevant IDP substrate. This was done as part of an effort to identify a promising activator for use in the development of novel methods for exploring the potential of this 20S activation strategy for combating neurodegenerative diseases.

First, I set out to evaluate Aripiprazole's activity utilizing fluorogenic peptide substrates for the 20S proteasome that are conjugated to AMC, as discussed in **Chapter 2**. This assay was similar to what was utilized in the HTPS that originally identified Aripiprazole among other compounds as 20S activators.⁵¹ Here, this assay was used to further evaluate Aripiprazole's activity at each of the 3 catalytic sites (CT-L, Tryp-L and Casp-L) of the proteasome, determine if this activity occurs in a concentration-dependent manner and to determine its relative potency. It should be noted that at the time that Aripiprazole was being tested, we did not yet utilize a

combination of the 3 fluorogenic peptide substrates to obtain a more comprehensive look at the activity of activators and to compare them. That practice began with my testing of Fluspirilene (**Fig. 3.6**) and the dihydroquinazoline analogues (**Chapter 2**).⁴⁹ From these data, it was found that Aripiprazole effectively activates each of the 3 catalytic sites in a concentration-dependent manner (**Fig. 3.3A**). It was able to achieve an EC₂₀₀ for each catalytic site at low μM concentrations and led to high maximum fold increases over the DMSO vehicle control at higher concentrations (**Fig. 3.3B**). These initial results suggested that Aripiprazole may represent a good scaffold from which other analogues may be developed and used to develop novel methods for exploring the potential of this therapeutic method.

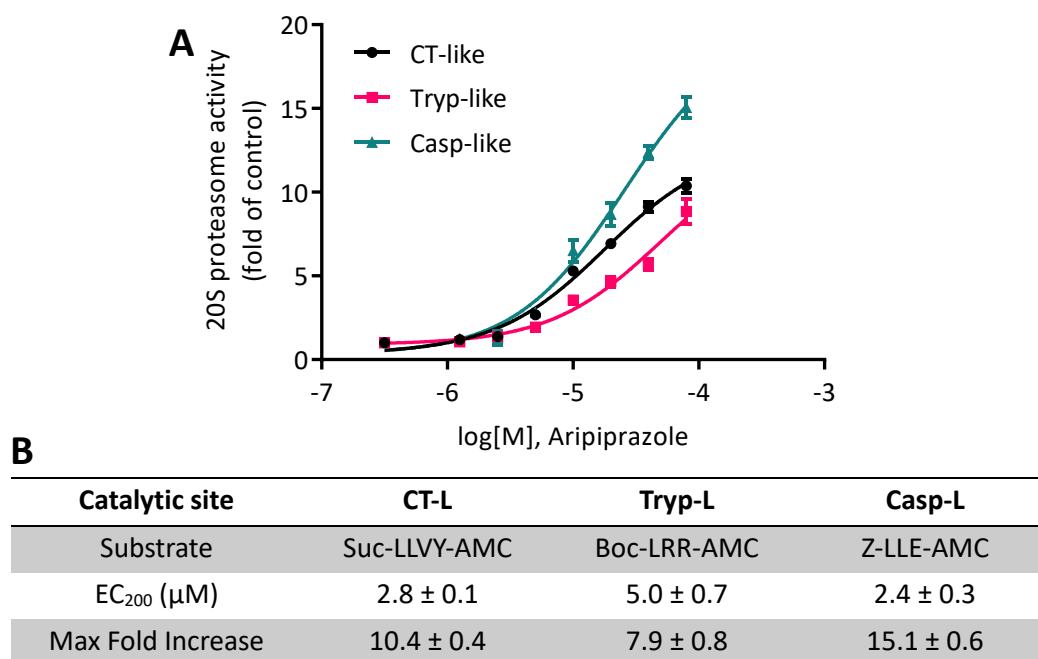


Figure 3.3: Aripiprazole enhances 20S mediated degradation of peptide substrates. (A) Concentration response (0–80 μM) from fluorogenic peptide digestions with Aripiprazole. These data were collected in triplicate. Error bars denote standard deviation. (B) Calculated EC₂₀₀ and max fold increases in activity over the vehicle control. Shown with calculated standard deviations.

3.2.2 Aripiprazole enhances the degradation of the IDP α -synuclein *in vitro*, but lacks translation in terms of potency

After confirming that Aripiprazole has promising activity on the 20S proteasome in fluorogenic peptide assays, relative to other activators that our lab has studied,^{50, 51} I then utilized α -synuclein, an IDP associated with Parkinson's disease, as a substrate.^{7, 10, 17-19, 22, 26} This was done to determine whether the activity of Aripiprazole translates well to the degradation of natural substrates for the 20S, not just small peptides.⁶⁶ For these experiments pure human 20S proteasome was incubated together with Aripiprazole (3, 10, 30 or 100 μ M), TCH-165 (10 μ M), the proteasome inhibitor Epoxomicin (1 μ M),⁶⁷ or DMSO (Vehicle, **Fig. 3.4**). Then, pure human α -synuclein substrate was introduced and the resulting mixture was incubated for 4 hours. The remaining α -synuclein, as well as 20S proteasome subunits, were subjected to denaturing conditions and sodium dodecyl sulfate-polyacrylamide gel electrophoresis (SDS-PAGE) was used to resolve the proteins. The resulting bands were stained using a Coomassie stain for visualization of remaining α -synuclein.

While these data showed that Aripiprazole was able to enhance the degradation of α -synuclein by the 20S *in vitro*, this effect is not very potent when compared to other previously identified activators, like TCH-165 (**Fig. 3.4**). The relatively poor potency and lack of translatable activity of Aripiprazole when using α -synuclein as a substrate may cause difficulty in obtaining clear 20S proteasome enhancement in more disease relevant systems. Despite this, analogue development was underway to explore whether this activity could be improved upon, while also making changes that may reduce the neuroleptic activity of Aripiprazole.

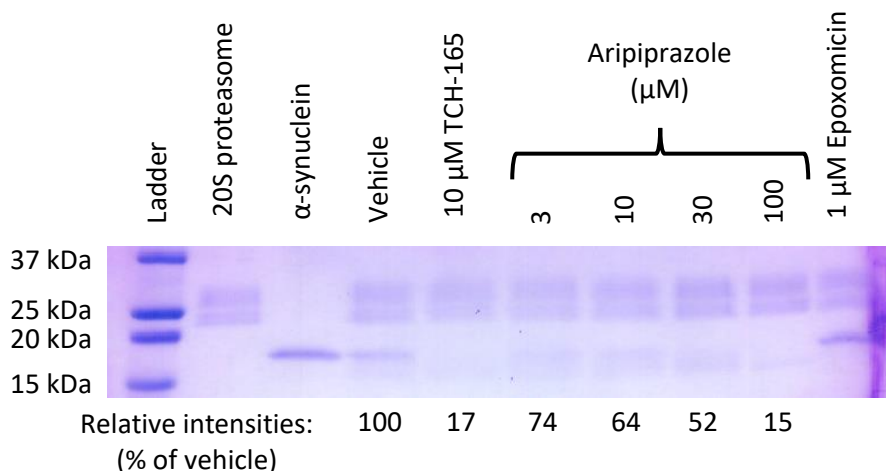


Figure 3.4: Aripiprazole enhances 20S proteasome mediated degradation of the IDP α -synuclein. Coomassie stain illustrating Aripiprazole’s enhancement of α -synuclein digestion by the 20S at 3, 10, 30 and 100 μ M. DMSO (vehicle), TCH-165 (10 μ M) and proteasome inhibitor (Epoxomicin, 1 μ M) treatments were included as controls. Relative intensities, shown as percent of vehicle, were obtained by densitometry of α -synuclein bands done using image J. Each lane was normalized using densitometry of total 20S proteasome subunits to control for loading differences.

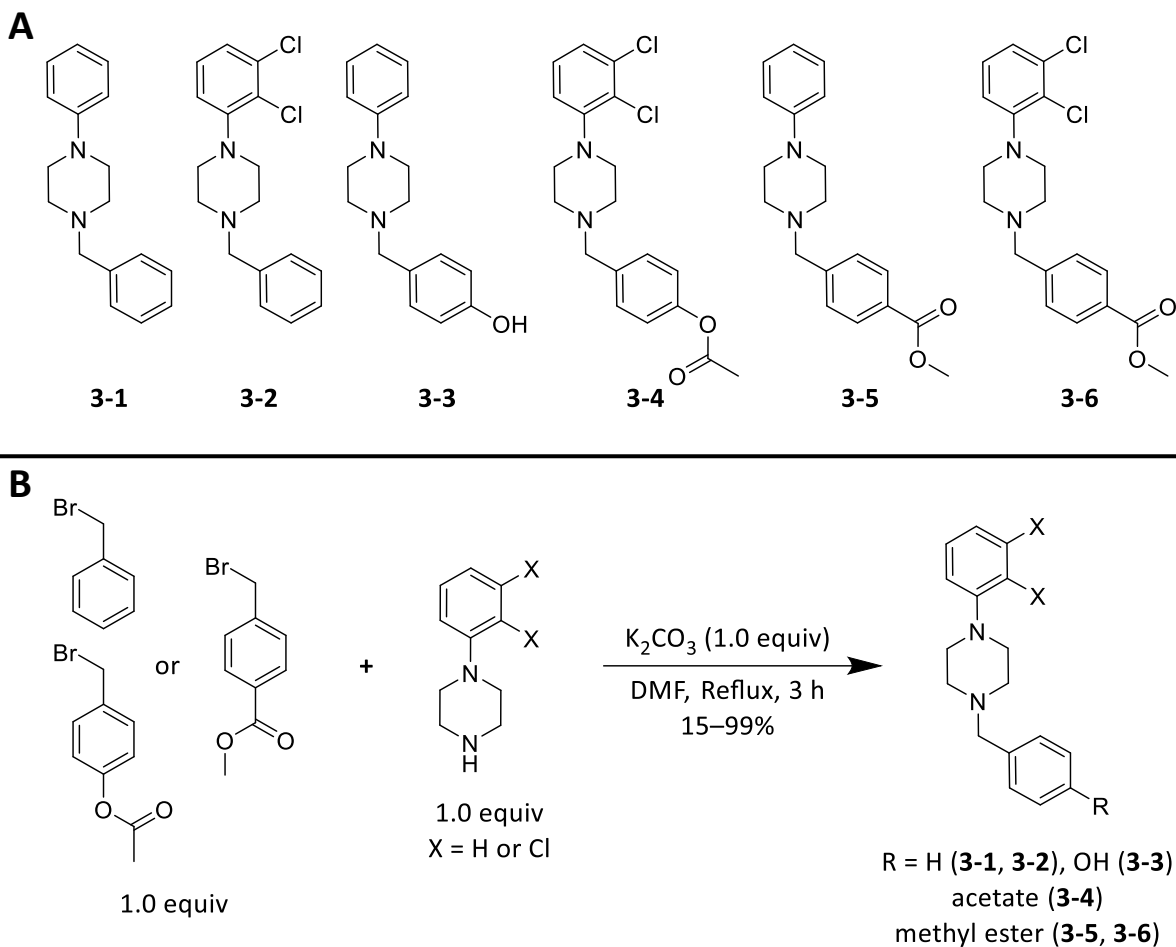
3.2.3 Synthesis and evaluation of Aripiprazole analogues did not yield any promising lead molecules

Despite the 20S activity seen for Aripiprazole in the fluorogenic peptide assays, analogue development is necessary due to its dopamine D2 receptor activity.⁶³ Additionally, Aripiprazole’s potency for enhancing the rate of degradation of IDPs *in vitro* is notably worse than that of TCH-165 (**Fig. 3.4**). Analogue development was undertaken to try to overcome these limitations and grant a better understanding of Aripiprazole’s activity toward the 20S proteasome. This was done by focusing on the two halves of the molecule, the quinolinone “head” and phenylpiperazine “tail”, and functionalizing them with groups that were shown to be active with previously discovered activators.⁵¹

The first series of analogues (compounds **3-1** through **3-6** (**Scheme 3.1**)) focused on the phenylpiperazine-tail of Aripiprazole and incorporated functionalities that were explored during analogue development of the phenothiazines.⁵¹ Compounds **3-1** through **3-6** retain the piperazine and N-linked phenyl or dichlorophenyl functionalities of Aripiprazole and replaced the quinolinone-head and linking alkyl chain with various benzyl-groups. This included, either an unsubstituted benzyl, methyl 4-methylbenzoate, or *p*-tolyl acetate functionality. These analogues were meant to explore whether the quinolinone functionality is necessary for 20S activation and how substitution for a variety of other functionalities seen in previously synthesized Chlorpromazine analogues would affect activity.⁵¹

Compounds **3-1** through **3-6** were synthesized following a similar procedure to that of Mohammadi et al.⁶⁸ Briefly, the piperazines were dissolved with potassium carbonate in dimethylformamide (DMF) and to this was added the corresponding benzyl bromide. The resulting mixtures were stirred and refluxed in DMF for 3 hours to produce the desired products (compounds **3-1** through **3-6**). The methyl ester analogue lacking the 2 chlorines on the phenyl piperazine was originally targeted for synthesis through this method, but it was found that the phenol analogue (compound **3-3**) was isolated in its place. This was likely due to partial hydrolysis of the methyl ester to the phenol, followed by isolation of the incorrect product. As will be discussed in the next paragraph, evaluation of the 20S activities of these analogues showed no activation by any of the analogues. So, considering compound **3-3** is further removed from the parent molecule than compound **3-4**, which showed no activity, the other methyl ester analogue was not pursued further.

Scheme 3.1: (A) Structures and (B) synthesis of Aripiprazole analogues 3-1 through 3-6.



Following the synthesis of this first set of analogues (compounds **3-1** through **3-6**), they were evaluated for 20S activity using the fluorogenic peptide substrates, but none of these analogues showed significant activity above the DMSO treated vehicle control (data not shown). Despite their inability to activate the 20S, these results still provided information about the activity of Aripiprazole and demonstrated that the functionalities explored here are not sufficient to maintain that activity.

Analogue development was continued by exploring the quinolinone-head group. Molecular docking studies were performed using Autodock VinaTM, supported through computational resources and services provided by the Institute for Cyber-Enabled Research at Michigan State

University. The entirety of the 20S proteasome was used to perform unbiased blind docking, allowing for true conformational preference. From the resulting docking models, it was determined that Aripiprazole is likely binding in the same α 2-3 pocket as Chlorpromazine (**Fig. 3.5A**). Additionally, both molecules seemed to orient similarly within the pocket. This resulted in the tail portions of each molecule roughly overlapping in these overlaid images. Following these docking studies, I hypothesized that analogues with Aripiprazole- and Chlorpromazine-like functionalities could help to elucidate what functionalities of Aripiprazole are important for binding and potentially yield active analogues. To this end, five new target molecules (**Fig. 3.5B**, compounds **3-7** through **3-11**) were designed.

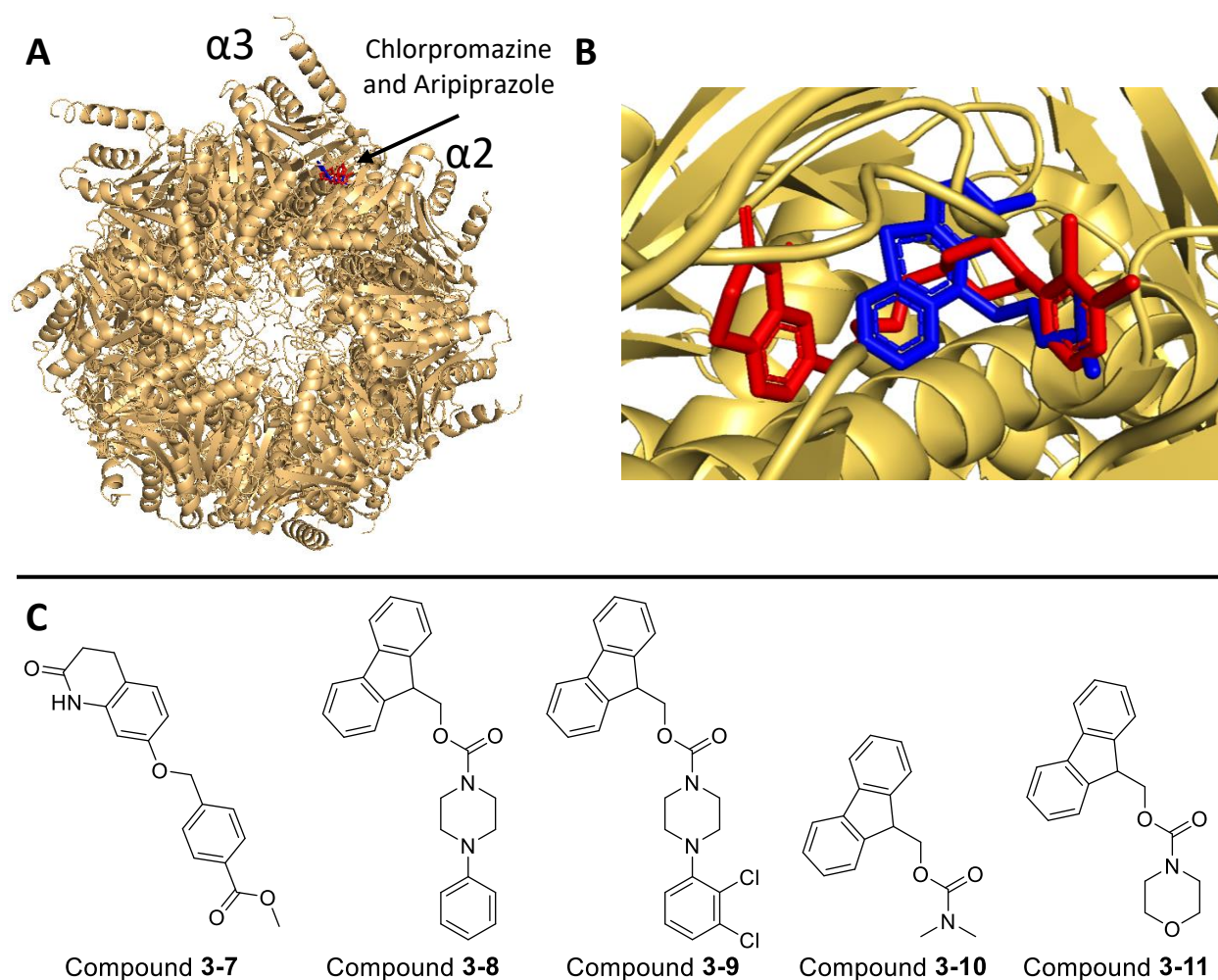


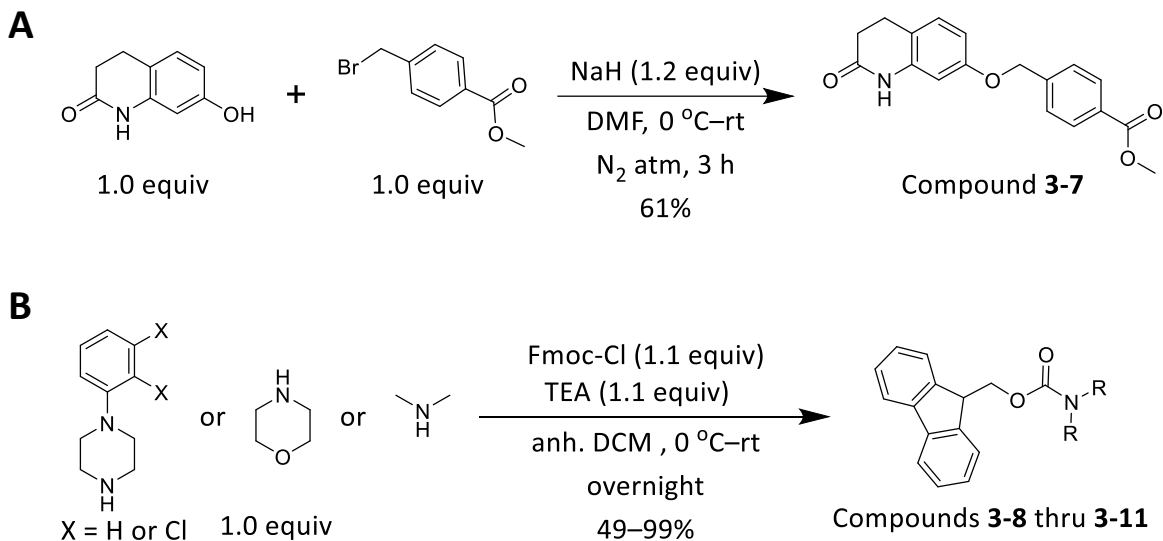
Figure 3.5: Molecular docking led design of Aripiprazole and Chlorpromazine-like analogues. (A) Preferred docking site of Chlorpromazine (blue) and Aripiprazole (red), utilizing Autodock Vina, in the $\alpha 2$ -3 inter-subunit binding pocket of the 20S proteasome's α -ring. (B) Proposed Aripiprazole and Chlorpromazine-like analogues (compounds **3-7** through **3-11**).

Compound **3-7** was designed to determine if the quinolinone functionality of Aripiprazole mimics the phenothiazine portion of Chlorpromazine. The benzoate that was chosen as the tail-portion of compound **3-7** was previously shown to enhance Chlorpromazine's activity when substituted in place of dimethylpropylamine.⁵¹ Compounds **3-8** and **3-9** represent hybrid molecules with parts mimicking both the phenothiazine of Chlorpromazine, in the form of an Fmoc protecting

group, and Aripiprazole, in the phenyl piperazine-tail. Compounds **3-10** and **3-11** sought to expand upon this and potentially provide further support for Fmoc as a potential mimic for phenothiazine when binding to the 20S. These analogues sought to explore the possibility of a new functional group, in Fmoc, that can be easily conjugated to a variety of tails and used in place of the phenothiazine, seen with Chlorpromazine. Additionally, the substitution of the phenothiazine with another similar functionality, like the Fmoc group seen here, would provide another route through which to potentially eliminate the dopamine receptor activity seen with Chlorpromazine.⁵¹ Previous efforts to discover active substitutes for the phenothiazine functionality yielded few promising results, so any progress that could be made to this end would be greatly beneficial for development of future 20S activators.

Compound **3-7** was synthesized by first adding sodium hydride to a solution of the quinolinone-head group of Aripiprazole in DMF at 0°C for 15 minutes. This was followed by addition of benzyl bromide, warming to room temperature, and stirring for an additional 3 hours to form compound **3-7**, in 61% yield (**Scheme 3.2**). Compound **3-8** through **3-11** were synthesized by addition of Fmoc-Cl to a stirring solution of the corresponding amine and triethylamine (TEA) at 0°C. The resulting mixtures were allowed to warm to room temperature and stirred overnight to give compounds **3-8** through **3-11** (**Scheme 3.2**).

Scheme 3.2: Synthesis of (A) compound **3-7** and (B) compounds **3-8** through **3-11**.

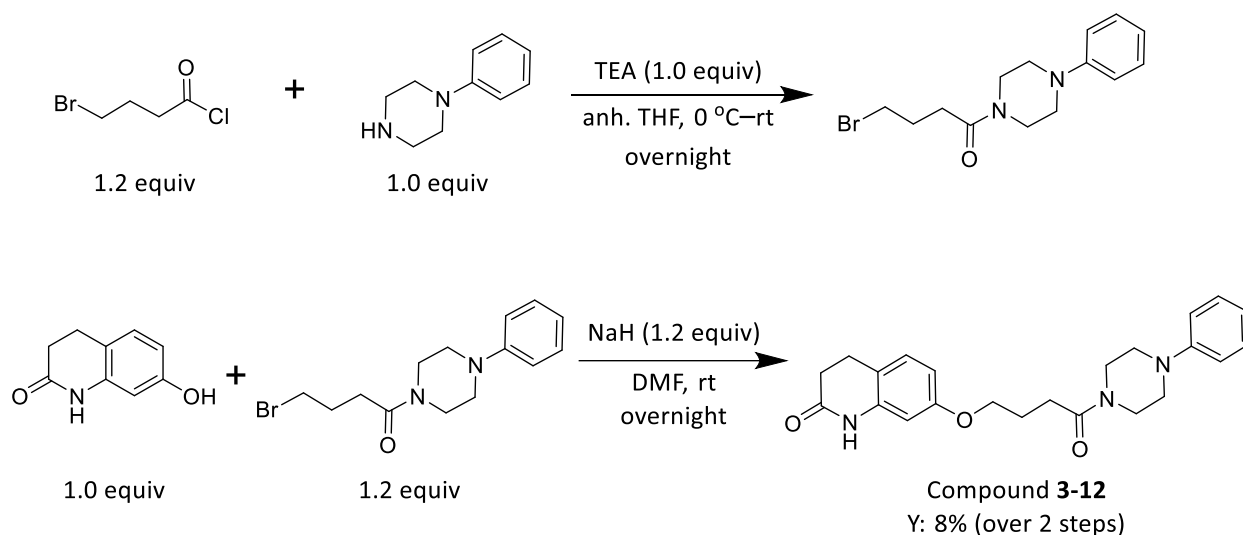


Following the synthesis of compound **3-7** through **3-11** (**Scheme 3.2**), they were evaluated for 20S proteasome activity using the fluorogenic peptide substrates. It was found that none of these analogues showed any activation of the 20S proteasome in this assay (data not shown). The lack of activity seen from compounds **3-8** through **3-11** suggest that the Fmoc functional group is not a suitable substitute for the phenothiazine of Chlorpromazine. Compound **3-7** being inactive suggested that the quinolinone functionality of Aripiprazole does not directly mimic the phenothiazine group of Chlorpromazine. This is clear, because the phenothiazine was shown to have enhanced activity when conjugated to the same benzoate functionality, in place of the dimethylamine.⁵¹ Additionally, it appears that the quinolinone group is not sufficient for maintaining any of Aripiprazole's prior activity on the 20S.

All Aripiprazole analogues up until this point had undergone significant modification when compared to Aripiprazole itself and it was thought that the truncated linker seen in compound **3-7** may not allow for enough flexibility in the molecule for it to properly bind to the 20S. To address this possibility, compound **3-12** was designed and synthesized (**Scheme 3.3**) with the goal of mimicking the overall structure and length of Aripiprazole more closely. Briefly, a solution of 1-

phenylpiperazine and TEA in THF was slowly added to a solution of 4-bromobutanoyl chloride at 0 °C in THF with molecular sieves. The mixture was allowed to gradually warm to room temperature overnight. Following workup, the crude material was carried forward due to an unidentified contaminant that was not separated via column chromatography. The quinolinone-head group of Aripiprazole was then dissolved in DMF and stirred in the presence of sodium hydride for 10 minutes. To this was then added the crude intermediate, produced in the previous reaction, and this mixture was stirred at room temperature overnight to yield compound **3-12**, in 8% yield over 2 steps.

Scheme 3.3: Synthesis of compound **3-12**.



Following the synthesis of compound **3-12**, it was tested in the fluorogenic peptide assay and was found to be inactive (data not shown). This suggested that Aripiprazole may not be an ideal scaffold from which to build novel 20S activators due to its activity apparently being highly sensitive to structural modifications. Modifications, such as those undergone in compound **3-12**, would likely be required to effectively diminish its neuroleptic activity or to improve its potency. This sensitivity to modification, coupled with Aripiprazole's relatively poor potency when translating activity to *in vitro* 20S proteasome mediated IDP digestions led me to explore other

neuroleptic agent scaffolds for their potential as 20S proteasome activators. For this, I revisited the HTPS run by our lab previously and further evaluated the activity of other 20S proteasome activator hits.

3.2.4 The neuroleptic agent Fluspirilene activates all 3 catalytic sites of the 20S proteasome but does not activate the 26S proteasome

Upon returning to the HTPS run by our lab previously, I retested several other hit molecules using fresh stocks of each compound. From these data (not shown), the small molecule antipsychotic drug Fluspirilene^{64,65} was identified as a promising new scaffold for the development of 20S activators, due to its enhancement of 20S proteasome-mediated proteolysis of fluorogenic peptide substrates. To further assess Fluspirilene's 20S proteasome activity, a series of assays were performed using the three previously mentioned fluorogenic peptide substrates. These substrates were a CT-L, a Tryp-L and a Casp-L substrate, one for each of the catalytic sites of the proteasome. It has also been shown that the proteasome's active sites allosterically regulate each other in the presence of their individual substrates.⁶⁹ Therefore, a combination of the three fluorogenic peptides, in equal amounts, was also used to represent the overall activity of a 20S activator more accurately in a system in which all catalytic sites are interacting.⁶⁹ This was the first time that this combination of peptide substrates was utilized by our lab, and has since become a common practice to obtain generalized levels of activity for a given compound, that can then be compared to other identified activators. The continued testing of the individual catalytic sites remains important because all of these catalytic sites will likely be required for the degradation of IDPs and other native substrates of the 20S that have many cleavage sites. So, while the combination of the three substrates provides a good overall view of activity, the individual substrate screenings each ensure that all catalytic sites are contributing to these results.

It was found that Fluspirilene activates all three catalytic sites of the 20S proteasome in a concentration-dependent manner (**Fig. 3.6A**) and achieved an EC₂₀₀ of 2.2 μM using the combination of substrates, with a maximum fold enhancement of nearly 10-fold (i.e. 1000%) relative to the DMSO treated vehicle control (**Fig. 3.6B**). The level of activity found for Fluspirilene in these studies is on par with some of the most active and potent small molecule 20S proteasome activators identified to date. This, coupled with Fluspirilene's good drug-like properties and BBB permeability,^{64,65} suggested that it may represent an ideal scaffold from which additional 20S proteasome activators can be developed.

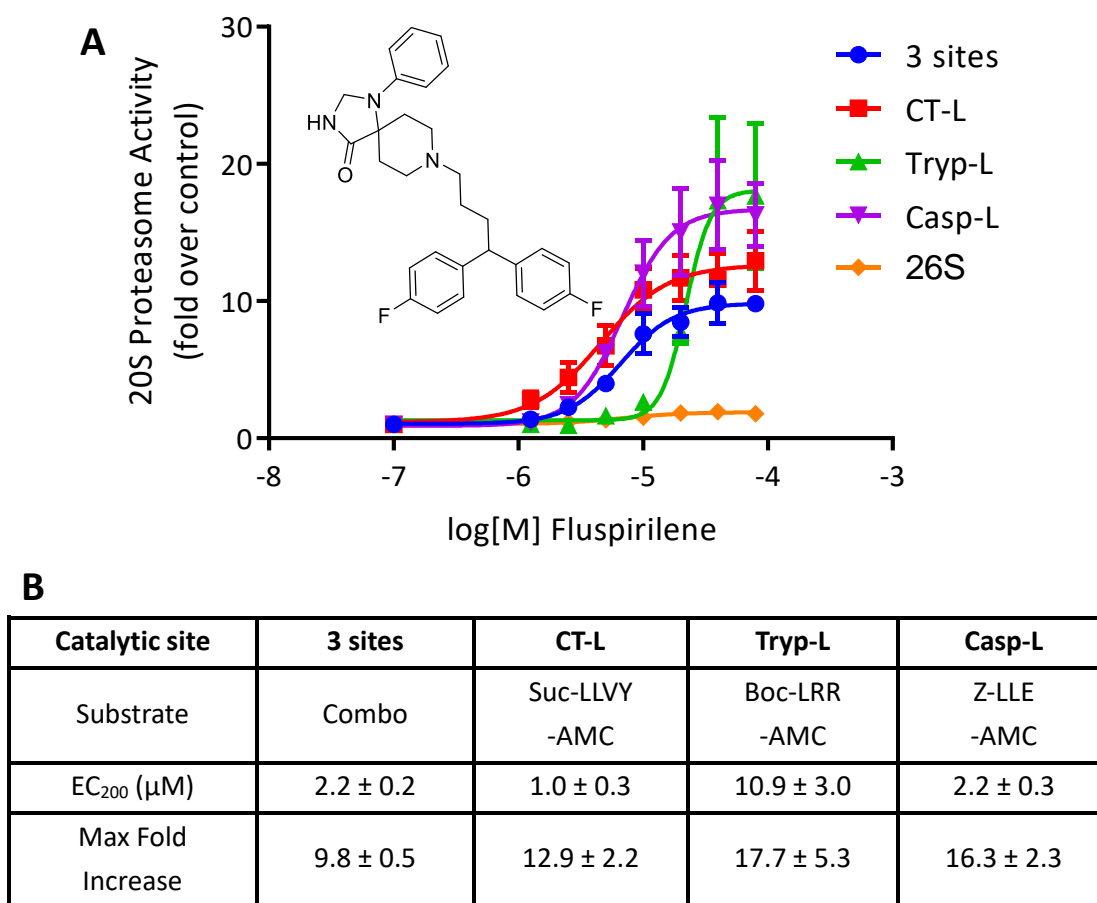


Figure 3.6: The neuroleptic agent Fluspirilene activates all 3 catalytic sites of the 20S proteasome but does not activate the 26S proteasome. (A) Concentration response (0–80 μM) from fluorogenic peptide digestions with Fluspirilene. These data were collected in triplicate. Error bars denote standard deviation. (B) Calculated EC₂₀₀ and max fold increases in activity over the vehicle control. Shown with calculated standard deviations.

3.2.5 Fluspirilene analogues designed using *in silico* docking models as a guide

Fluspirilene is a potent dopamine D2 receptor antagonist that has been used for the treatment of schizophrenia.^{64, 65} As such, it has good drug-like properties and penetrates the BBB effectively, which makes it a promising scaffold for development of novel 20S activators and for use in evaluating the potential of this therapeutic strategy. On the other hand, due to its potent D2

receptor activity it cannot be repurposed therapeutically without modification. Therefore, we next sought to explore whether Fluspirilene's 20S proteasome activity is amenable to structural modifications known to reduce the dopamine D2 receptor activity. For example, previous studies by our group showed that eliminating or disrupting the interaction of the critical basic amine with the D2 receptor abrogates this activity.^{51, 70}

Using molecular docking as a guide (this work was done collaboratively with Dr. Katarina Keel), *N*-acylated Fluspirilene (**Fig. 3.7A**), was designed to eliminate Fluspirilene's D2 receptor activity. In this scaffold, the basicity of the piperidine's amine has been reduced through conversion to an amide. Additionally, Fluspirilene and *N*-acylated Fluspirilene dock similarly within the proteasome. Molecular docking studies were performed using Autodock VinaTM, supported through computational resources and services provided by the Institute for Cyber-Enabled Research at Michigan State University. The entirety of the 20S proteasome was used to perform unbiased blind docking, allowing for true conformational preference. Fluspirilene and *N*-acylated Fluspirilene were found to preferentially bind to the α 2-3 inter-subunit pocket (**Fig. 3.7B and C**). This mode of binding is different from our previously reported 20S proteasome activator TCH-165 which, when docked, preferentially binds to the α 1-2 inter-subunit pocket.⁵⁰ To test the importance of the α 2-3 inter-subunit pocket, two other analogues of Fluspirilene were devised as negative controls. Compounds **3-13** and **3-14** (**Fig. 3.7A**) were designed to be less active towards the proteasome, based on assumptions regarding the diphenyl tail's optimal 3D conformation and the importance of the difluoro substituents, respectively. Molecular docking of these analogues showed less preference for the α 2-3 inter-subunit pocket, supporting these assumptions. Through these three analogues of Fluspirilene, we aimed to further understand the in-pocket binding interactions of our newly discovered 20S proteasome activator scaffold.

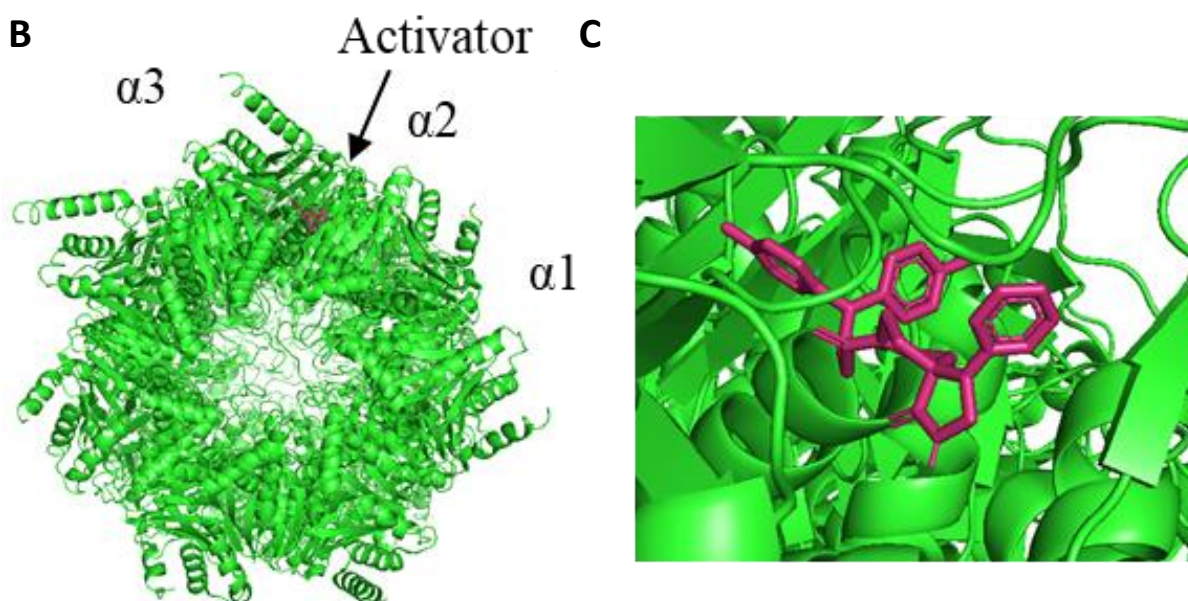
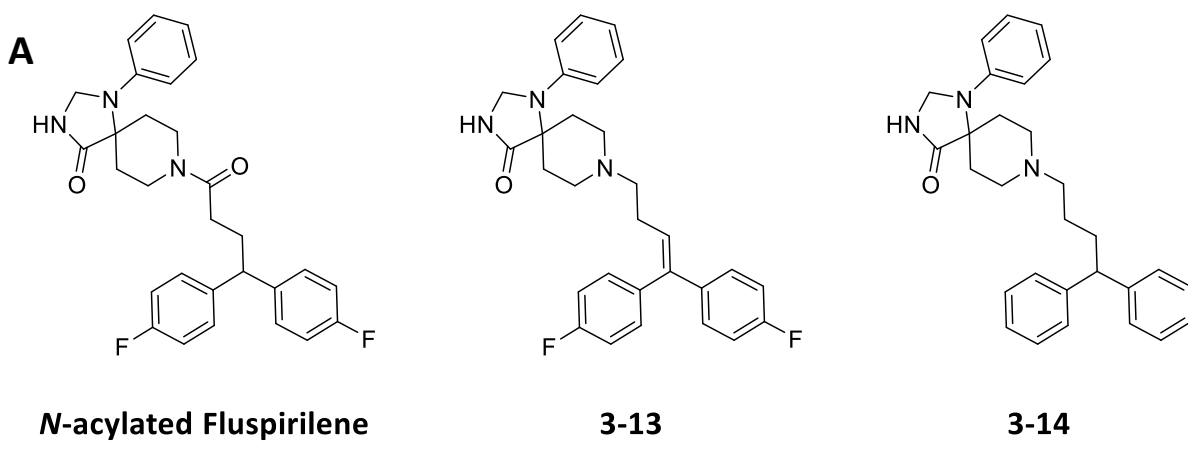


Figure 3.7: Fluspirilene and N-acylated Fluspirilene preferentially dock in the $\alpha 2$ -3 inter-subunit binding pocket of the 20S proteasome. (A) Structures of N-acylated Fluspirilene, compound 3-13 and compound 3-14. (B) Preferred docking site of N-acylated Fluspirilene, utilizing Autodock Vina™, in the $\alpha 2$ -3 inter-subunit pocket of the 20S proteasome's α -ring. (C) Zoomed in image of N-acylated Fluspirilene docked in the $\alpha 2$ -3 inter-subunit pocket.

3.2.6 Activity differences between Fluspirilene analogues support what was predicted with docking models

Fluspirilene and its analogues were synthesized by Dr. Katarina Keel according to literature.⁷¹ Each of the synthesized Fluspirilene analogues (Fluspirilene, *N*-acylated Fluspirilene, compound **3-13** and compound **3-14**) were tested for 20S proteasome activity (**Fig. 3.8**). To do this, the previously described fluorogenic peptide assay was employed to assess their activity using a combination of the three catalytic site substrates. The results obtained from the screening showed that the Fluspirilene analogues (*N*-acylated Fluspirilene, compound **3-13** and compound **3-14**) all showed some degree of activity and clear concentration-responses (**Fig. 3.8**). Excitingly, *N*-acylated Fluspirilene appeared to have comparable potency and greater maximum activity in this assay (**Fig. 3.8**) when compared to that of Fluspirilene (**Fig. 3.6B**). *N*-acylated Fluspirilene represents a promising scaffold from which to develop additional analogues due to its potent activation of the 20S. Additionally, *N*-acylated Fluspirilene lacks a basic nitrogen, which is known to be critical for D2 receptor activity.^{51, 70} While compounds **3-13** and **3-14** both showed some activity towards the 20S proteasome in this assay, their activity relative to Fluspirilene was greatly reduced, supporting what was predicted with the molecular docking models.

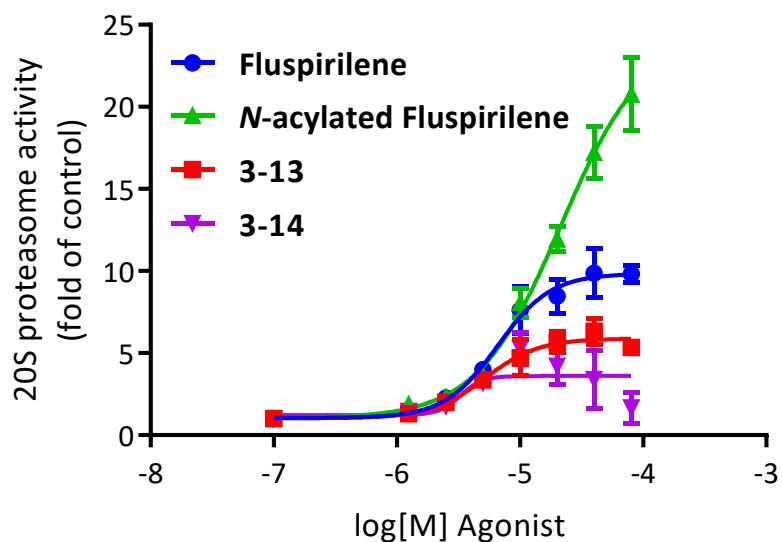


Figure 3.8: Fluspirilene analogues activate the 20S proteasome with varying effectiveness.

Concentration response (0–80 μM) from fluorogenic peptide digestions using the combination of three fluorogenic peptide substrates with Fluspirilene analogues. These data were collected in triplicate. Error bars denote standard deviation.

3.2.7 Detailed analysis of molecular docking yields insights into potential key interactions for Fluspirilene analogue activity

To further analyze why Fluspirilene and *N*-acylated Fluspirilene show such promising 20S proteasomal activity while compounds **3-13** and **3-14** display lessened activity, BIOVA Discovery Studio 2020 was used to observe interactions of the analogues within the α 2-3 inter-subunit pocket (**Fig. 3.9**).⁷² In multiple binding modes obtained for both Fluspirilene and *N*-acylated Fluspirilene, hydrogen bond interactions are observed between the imidazol-4-one's amide N-H and a variety of amino acid residues such as LYS77, ILE65, ASN84, TYR75, and GLN111 (**Fig. 3.9A and B**). Comparatively, while compounds **3-13** and **3-14** show hydrogen bonding with the amide's carbonyl, they display no interactions between the amide's N-H and any of the above-mentioned amino acid residues (**Fig. 3.9C and D**). Furthermore, compounds **3-13** and **3-14** display less

preference for the α 2-3 inter-subunit pocket, suggesting a strong N-H hydrogen bond interaction is necessary to support preferential binding. Fluspirilene, *N*-acylated Fluspirilene, and compound **3-14** also display pi-pi interactions with the diphenyl tail, specifically interacting with PHE60, PHE61, and TYR154, while compound **3-13** shows no pi-pi interactions between the amino acid residues and diphenyl tail. This suggests that restricting the conformational flexibility of the diphenyl tail with a double bond interferes with the binding of this scaffold. Further exploration is necessary to explain the importance of the difluoro substituents for proteasomal activity.

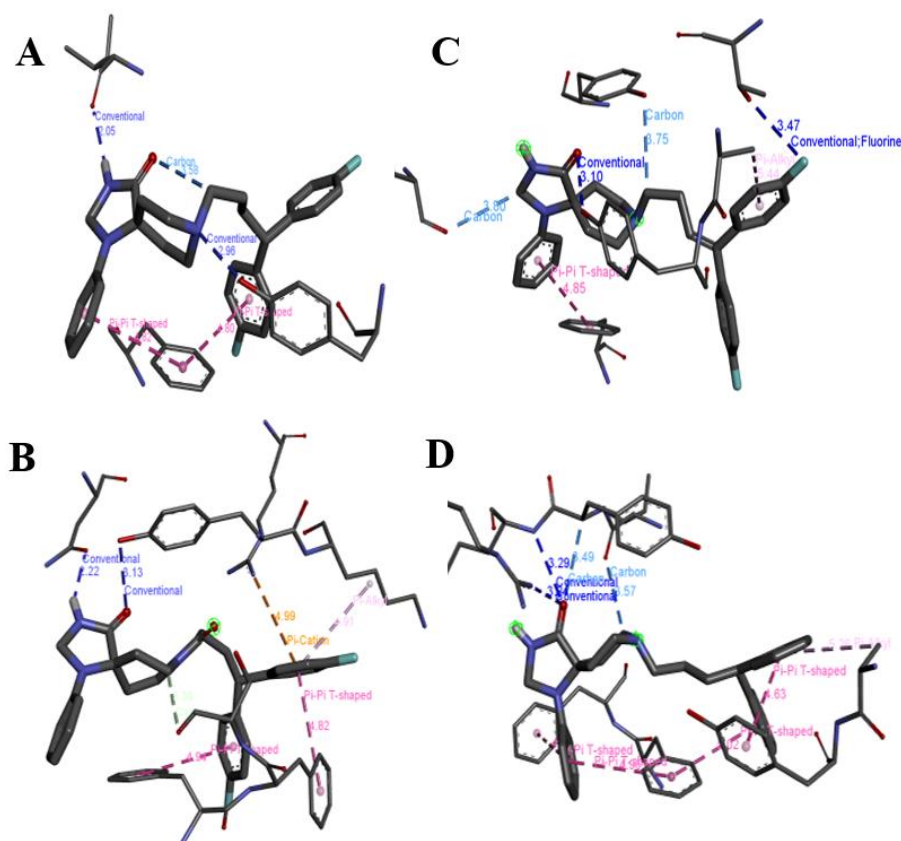
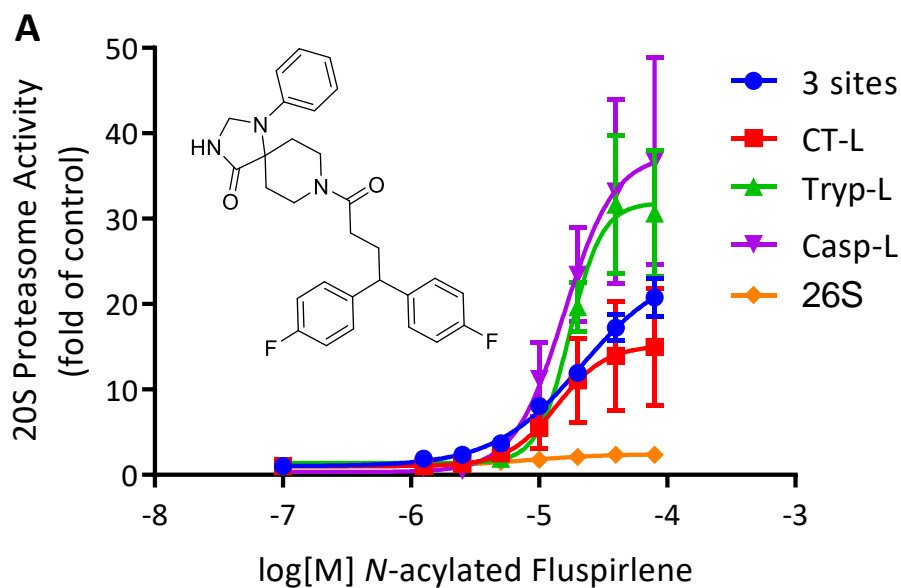


Figure 3.9: Fluspirilene analogues binding models show varied interactions supporting differences in activity. Binding models of Fluspirilene and the three analogues, viewed utilizing BIOVIA Discovery Studio 2020 (A) Fluspirilene (B) *N*-acylated Fluspirilene (C) compound **3-13** (D) compound **3-14**.

3.2.8 *N*-acylated Fluspirilene activates all three catalytic sites of the 20S proteasome but not the 26S proteasome

The 20S activity of *N*-acylated Fluspirilene was further assessed in the fluorogenic peptide assay, using each of the individual substrates (CT-L, Tryp-L and Casp-L) as well as the combination of the three (**Fig. 3.10**). *N*-Acylated Fluspirilene displayed a clear concentration-dependent enhancement of 20S proteasome-mediated degradation of each of the three fluorogenic peptide substrates. When compared to Fluspirilene, *N*-acylated Fluspirilene performs similarly using the combination of the three fluorogenic peptide substrates, with an EC₂₀₀ of 1.9 μM (**Fig. 3.10B**). Additionally, the *N*-acylated analogue achieved better activation of the Tryp-L site, but reduced activation of the CT-L site relative to Fluspirilene itself, when tested with the individual fluorogenic peptide substrates. The *N*-acylated analogue achieved higher max fold increases for each substrate/combination (>1500% increase over vehicle) but required slightly higher concentrations to reach doubling of activity at the CT-L (EC₂₀₀ = 4.7 μM) and Casp-L (EC₂₀₀ = 4.1 μM) sites (**Fig. 3.10B**). These results led to the decision to carry both Fluspirilene and *N*-acylated Fluspirilene forward into more physiologically relevant assays.



B

Catalytic site	3 sites	CT-L	Tryp-L	Casp-L
Substrate	Combo	Suc-LLVY -AMC	Boc-LRR -AMC	Z-LLE -AMC
EC ₂₀₀ (μM)	1.9 ± 0.5	4.7 ± 1.6	5.6 ± 0.8	4.1 ± 0.6
Max Fold Increase	20.8 ± 2.3	15.0 ± 6.9	30.6 ± 7.4	36.8 ± 12.2

Figure 3.10: *N*-acylated Fluspirilene is comparable to Fluspirilene in its ability to activate all 3 sites of the 20S proteasome, but not the 26S proteasome. (A) Extended fluorogenic peptide analysis of *N*-acylated Fluspirilene. These data were collected in triplicate. Error bars denote standard deviation. (B) Calculated EC₂₀₀ and max fold increases in activity over the vehicle control. Shown with calculated standard deviations.

3.2.9 Fluspirilene and *N*-acylated Fluspirilene enhance the rate of 20S mediated proteolysis of the Parkinson's disease related IDP α -synuclein *in vitro*

IDP accumulation and aggregation are commonly associated with the progression of neurodegenerative diseases. It is believed that these IDPs represent a promising therapeutic target that may allow for the development of the first disease altering treatment for many

neurodegenerative diseases.^{17, 22, 73-77} Parkinson's disease is currently the second most prevalent neurodegenerative disease and is characterized by accumulation and aggregation of the IDP α -synuclein.^{19, 78-83} Fluspirilene and *N*-acylated Fluspirilene were tested for their ability to enhance degradation of α -synuclein, to demonstrate their potential to prevent the toxic IDP accumulation and the translation of the activity towards the degradation of more relevant substrates, than the fluorogenic peptides.

Briefly, purified human 20S proteasome was incubated with DMSO (vehicle), Fluspirilene or *N*-acylated Fluspirilene at various concentrations (1, 3 or 10 μ M). Pure human α -synuclein substrate was subsequently added to the mixtures and incubated for 4-hours at 37 °C. Following this incubation, the remaining α -synuclein and 20S proteasome were subjected to denaturing conditions and resolved using SDS-PAGE. The resulting bands were visualized using silver stain. Enhanced 20S activity was measured as a reduction of remaining α -synuclein when compared to the vehicle (DMSO) control. As shown in **Fig. 3.11**, both Fluspirilene and *N*-acylated Fluspirilene were able to effectively enhance the degradation of α -synuclein by the 20S proteasome *in vitro*. Both compounds displayed a significant (**Fig. 3.11B-C**, >50%, $p < 0.001$) concentration-dependent decrease in α -synuclein at values near their EC₂₀₀. These results grant confidence in this novel 20S activator scaffold to induce the degradation of IDPs and prevent their accumulation. As such, Fluspirilene and *N*-acylated Fluspirilene were selected as the ideal compounds with which to begin developing novel methods to further evaluate the potential of 20S proteasome activation as a therapeutic strategy for combating neurodegenerative diseases.

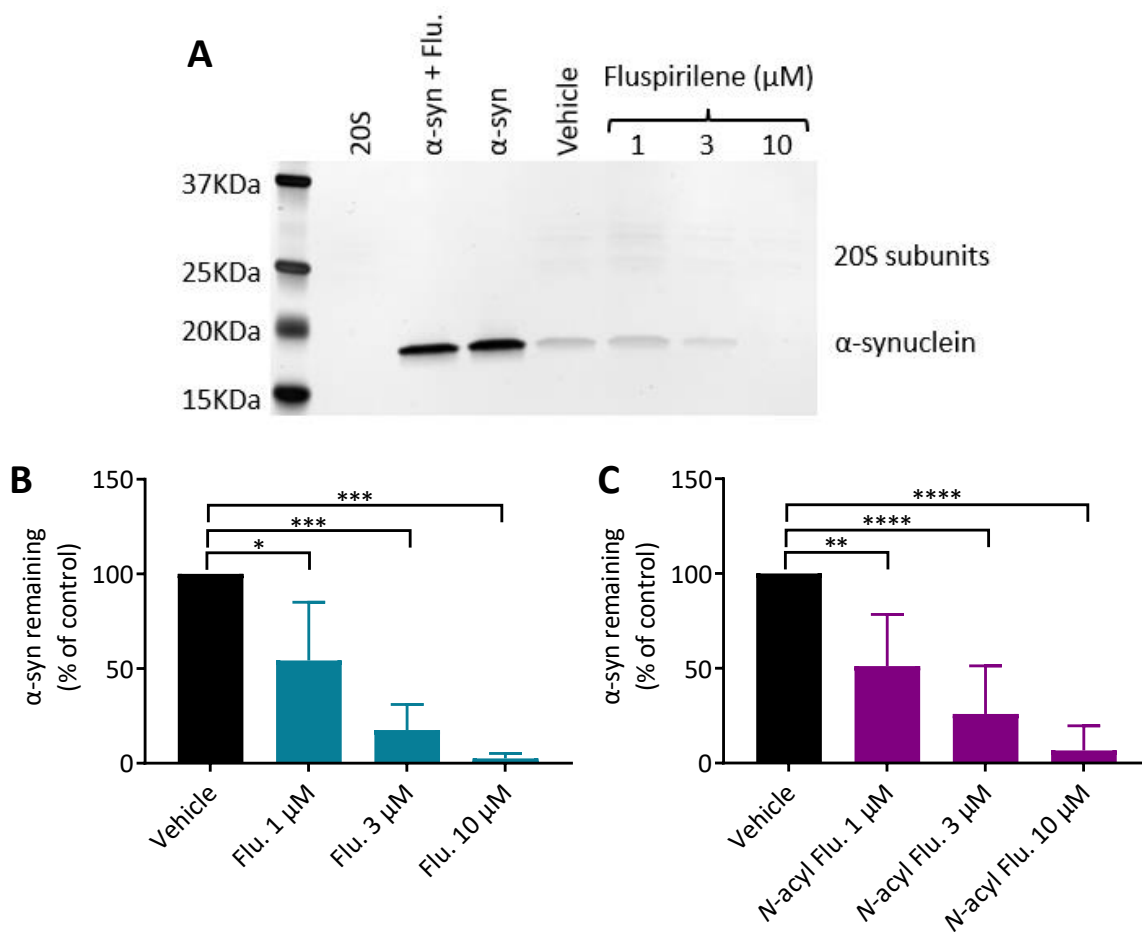


Figure 3.11: Fluspirilene and *N*-acylated Fluspirilene enhance the rate of 20S mediated proteolysis of the Parkinson’s disease related IDP α -synuclein *in vitro*. (A) Representative silver stain illustrating Fluspirilene’s enhancement of α -synuclein digestion by the 20S at 1, 3 and 10 μ M. (B) Densitometry of Fluspirilene α -synuclein digestions done using image J (n=3). (C) Densitometry of *N*-acylated Fluspirilene α -synuclein digestions done using image J (n=5). Error bars denote standard deviation. Ordinary one-way ANOVA statistical analysis was used to determine statistical significance (* p <0.05, ** p <0.01, *** p <0.001, **** p <0.0001).

3.3 Conclusions

In summary, these studies demonstrated that the previously FDA approved neuroleptic agents, Aripiprazole and Fluspirilene both represent novel 20S proteasome activator scaffolds. It

was found that Aripiprazole, while being a 20S proteasome activator, does not show great translation of activity to the enhancement of 20S-mediated degradation of IDP substrates, relative to other activators discussed here. Additionally, the analogues of Aripiprazole that were synthesized as part of these studies were all found to be inactive towards the 20S proteasome. For these reasons, Aripiprazole is not an ideal scaffold from which to develop additional 20S proteasome activators, nor for developing novel methods to further explore the potential of 20S activation as a therapeutic method.

However, the subsequent studies focused on Fluspirilene and analogues thereof, yielded much more promising results. Fluspirilene and *N*-acylated Fluspirilene were both found to effectively enhance 20S proteasome-mediated degradation of fluorogenic peptide substrates and the IDP α -synuclein *in vitro*. Neither of these activators showed substantial activity towards the 26S proteasome, which is desirable for specific targeting of IDPs associated with neurodegenerative diseases. Molecular docking analyses of the Fluspirilene analogues, synthesized by Dr. Katarina Keel, provided insight into potential key binding interactions, and suggest that these molecules act through a similar gate-opening mechanism as previously identified 20S activators. The relatively good potency, translatable activity to disease relevant substrates, BBB permeability and potential for docking-led analogue design seen with Fluspirilene and *N*-acylated Fluspirilene led to the conclusion that it represents an ideal scaffold from which novel activators can be developed. Additionally, Fluspirilene and *N*-acylated Fluspirilene were selected as lead molecules for use in developing novel methods to further explore the potential of 20S activation as an innovative therapeutic strategy.

1. The neuroleptic agents Aripiprazole and Fluspirilene were validated as 20S proteasome activators.

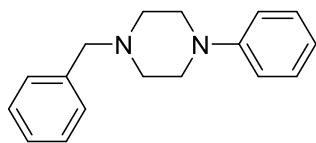
2. Analogues of Aripiprazole and Fluspirilene were synthesized by me or Dr. Katarina Keel (Fluspirilenes) and evaluated for 20S activity.
3. Fluspirilene and *N*-acylated Fluspirilene were determined to be ideal candidates for repurposing as 20S activators for further studies, based on a variety of advantages over other activators.

3.4 Experimental

General information

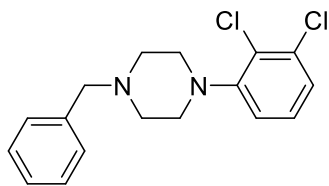
Reactions were carried out under a nitrogen atmosphere in flame-dried glassware. Solvents and reagents were purchased from commercial suppliers and used without further purification. Anhydrous tetrahydrofuran (THF) was distilled over sodium (dryness was monitored by the color of the solution, as indicated by benzophenone's ketyl radical), triethylamine (TEA) was distilled over calcium hydride, and dichloromethane (DCM) was dried over molecular sieves directly before use. Magnetic stirring was used for all reactions. Yields refer to chromatographically and spectroscopically pure compounds unless otherwise noted. Infrared spectra were recorded on a Jasco Series 6600 FTIR spectrometer. ^1H and ^{13}C NMR spectra were recorded on a Varian Unity Plus-500 spectrometer. Chemical shifts are reported relative to the residue peaks of the solvent (CDCl_3 : 7.26 ppm for ^1H and 77.0 ppm for ^{13}C) ($\text{DMSO-}d_6$: 2.50 ppm for ^1H and 39.5 ppm for ^{13}C). The following abbreviations are used to denote the multiplicities: s = singlet, d = doublet, dd = doublet of doublets, t = triplet, and m = multiplet. The following abbreviation is used to denote a broad signal: br. = broad. HRMS were obtained at the Mass Spectrometry Facility of Michigan State University with a Micromass Q-ToF Ultima API LC-MS/MS mass spectrometer. Column chromatography was performed using a Teledyne ISCO CombiFlash® NextGen system with prepacked columns (RediSep® Normal-phase silica, 20-40 microns). TLCs were performed on

pre-coated 0.25 mm thick silica gel 60 F254 plates and visualized using UV light and iodine staining.



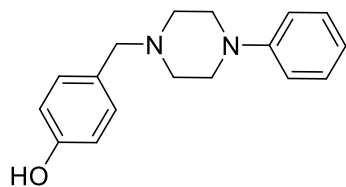
1-benzyl-4-phenylpiperazine (3-1). 1-phenylpiperazine (189 μ L, 1.23 mmol) and K_2CO_3 (170 mg, 1.23 mmol) were dissolved in DMF (10 mL) at room temperature. To this mixture, benzyl bromide (210.4 mg, 1.23 mmol) was added in DMF (5 mL). This solution was brought to reflux and allowed to stir for 3 hours before being allowed to cool back to room temperature. The reaction was then analyzed with TLC (3:1 hexanes/ethyl acetate) and it was determined that the reaction had gone to completion. The reaction mixture was then cooled to 0°C in an ice bath. Once cooled, the solution was acidified using 0.5 M HCl in water. This did not yield a precipitate that was expected based on the literature reference for the procedure. The solution was then neutralized with NaOH pellets. Then, ethyl acetate (40 mL) was added to the solution and the mixture was transferred to a separatory funnel. The water layer was removed, and the leftover organic layer was then washed three times with 10% LiBr solution to remove DMF and water-soluble byproducts. The remaining ethyl acetate layer was dried with Na_2SO_4 and concentrated affording **1** (brown solid, 307.5 mg, 99% yield).

1H NMR (500 MHz, $CDCl_3$) δ 7.54 – 7.45 (m, 4H), 7.42 – 7.37 (m, 3H), 7.07 – 7.03 (m, 2H), 6.99 (m, 1H), 3.69 (s, 2H), 3.32 (t, $J = 5.0$ Hz, 4H), 2.73 (t, $J = 5.0$ Hz, 4H). ^{13}C NMR (126 MHz, $CDCl_3$) δ 151.17, 137.86, 128.98, 128.88, 128.09, 126.94, 119.35, 115.78, 62.87, 52.91, 48.88. IR (neat): 3052, 2967, 1599, 1503 cm^{-1} . HRMS (ESI-TOF) m/z : $[(M+H)^+]$ calcd for $(C_{17}H_{21}N_2^+)$: 253.1705. Found: 253.1750. m.p.: 39 – 40 °C.



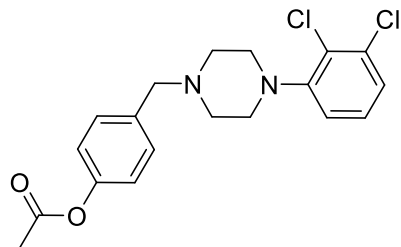
1-benzyl-4-(2,3-dichlorophenyl)piperazine (3-2). 1-(2,3-dichlorophenyl)piperazine (200 mg, 0.747 mmol) and K_2CO_3 (103.2 mg, 0.747 mmol) were dissolved in DMF (10 mL) at room temperature. To this solution, benzyl bromide (127.8 mg, 0.747 mmol) was added with more DMF (5 mL). This mixture was then brought to reflux and allowed to stir for three hours. After three hours, the reaction was allowed to cool to room temperature and TLC (3:1 hexanes/ethyl acetate) was used to determine that the reaction had gone to completion. To the reaction mixture ethyl acetate (40 mL) was added and the solution was transferred to a separatory funnel. The reaction mixture was then washed four times with 10% LiBr solution to remove the DMF and water-soluble byproducts. Next, the remaining ethyl acetate solution was dried with Na_2SO_4 and concentrated under vacuum. The resulting crude product was then purified by column chromatography (silica, 2:1 ethyl acetate/hexanes) affording **2** (brown solid, 101.1 mg, 42% yield).

1H NMR (500 MHz, $CDCl_3$) δ 7.41 – 7.27 (m, 5H), 7.17 – 7.12 (m, 2H), 6.96 (dd, $J = 7.2, 2.4$ Hz, 1H), 3.66 (s, 2H), 3.12 (s, 4H), 2.71 (s, 4H). ^{13}C NMR (126 MHz, $CDCl_3$) δ 151.01, 133.89, 129.41, 128.31, 127.40, 124.55, 118.58, 62.80, 53.00, 50.88. IR (neat): 3045, 2817, 1577 cm^{-1} . HRMS (ESI-TOF) m/z : $[(M+H)^+]$ calcd for $(C_{17}H_{19}Cl_2N_2^+)$: 321.0925. Found: 321.0929. m.p.: 59 – 60 $^{\circ}C$.



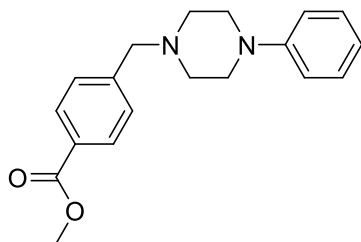
4-((4-phenylpiperazin-1-yl)methyl)phenol (3-3). 1-phenylpiperazine (189 μL , 1.23 mmol) and K_2CO_3 (170 mg, 1.23 mmol) were dissolved in DMF (10 mL) at room temperature. To this solution, 4-(bromomethyl)phenyl acetate (281.76 mg, 1.23 mmol) was added with more DMF (5 mL). This mixture was then brought to reflux and allowed to stir for three hours. After three hours, the reaction was allowed to cool to room temperature and TLC (3:1 hexanes/ethyl acetate) was used to determine that the reaction had gone to completion. To the reaction mixture ethyl acetate (40 mL) was added and the solution was transferred to a separatory funnel. The reaction mixture was then washed four times with 10% LiBr solution to remove the DMF and water-soluble byproducts. Next, the remaining ethyl acetate solution was dried with Na_2SO_4 and concentrated under vacuum. The resulting crude product was then purified by flash column chromatography (silica, ethyl acetate/hexanes) affording **3** (yellow powder, 50.4 mg, 15% yield).

^1H NMR (500 MHz, $\text{DMSO}-d_6$) δ 9.31 (s, 1H), 7.20 – 7.17 (m, 2H), 7.11 (d, $J = 8.4$ Hz, 2H), 6.91 (d, $J = 8.2$ Hz, 2H), 6.75 (t, $J = 7.3$ Hz, 1H), 6.72 (d, $J = 8.4$ Hz, 2H), 3.38 (s, 2H), 3.09 (t, $J = 4.8$ Hz, 4H), 2.46 (t, $J = 4.8$ Hz, 4H). ^{13}C NMR (126 MHz, $\text{DMSO}-d_6$) δ 156.36, 151.07, 130.18, 128.91, 128.01, 118.74, 115.35, 114.91, 61.69, 52.46, 48.20. IR (neat): 3098 (br.), 3006, 2814, 1598 cm^{-1} . HRMS (ESI-TOF) m/z : $[(\text{M}+\text{H})^+]$ calcd for ($\text{C}_{17}\text{H}_{21}\text{N}_2\text{O}^+$): 269.1654. Found: 269.1659. m.p.: 177 – 178 $^\circ\text{C}$.

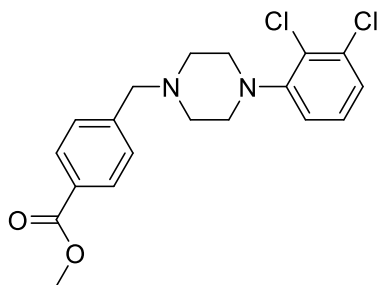


4-((4-(2,3-dichlorophenyl)piperazin-1-yl)methyl)phenyl acetate (3-4). 1-(2,3-dichlorophenyl)piperazine (200 mg, 0.747 mmol) and K_2CO_3 (103.2 mg, 0.747 mmol) were dissolved in DMF (10 mL) at room temperature. To this solution, 4-(bromomethyl)phenyl acetate (171.1 mg, 0.747 mmol) was added with more DMF (5 mL). This mixture was then brought to reflux and allowed to stir for three hours. After three hours, the reaction was allowed to cool to room temperature and TLC (3:1 hexanes/ethyl acetate) was used to determine that the reaction had gone to completion. To the reaction mixture ethyl acetate (40 mL) was added and the solution was transferred to a separatory funnel. The reaction mixture was then washed four times with 10% LiBr solution to remove the DMF and water-soluble byproducts. Next, the remaining ethyl acetate solution was dried with Na_2SO_4 and concentrated under vacuum. The resulting crude product was then purified by flash column chromatography (silica, ethyl acetate/hexanes) affording **4** (yellow powder, 163.1 mg, 58% yield).

1H NMR (500 MHz, $CDCl_3$) δ 7.38 (d, $J = 8.4$ Hz, 2H), 7.16 – 7.12 (m, 2H), 7.06 (d, $J = 8.5$ Hz, 2H), 6.96 (dd, $J = 6.8, 2.8$ Hz, 1H), 3.57 (s, 2H), 3.06 (s, 4H), 2.64 (s, 4H), 2.30 (s, 3H). ^{13}C NMR (126 MHz, $CDCl_3$) δ 169.57, 151.29, 149.71, 133.98, 130.12, 127.41, 124.49, 121.33, 118.58, 62.35, 53.18, 51.29, 21.14. IR (neat): 2942, 2830, 1747, 1577 cm^{-1} . HRMS (ESI-TOF) m/z : $[M+H]^+$ calcd for $(C_{19}H_{21}Cl_2N_2O_2^+)$: 379.0980. Found: 379.0984. m.p.: 119 – 120 $^{\circ}C$.



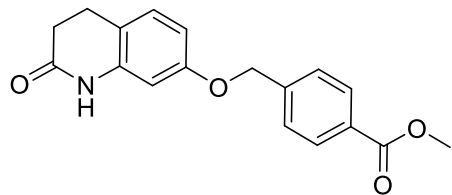
methyl 4-((4-phenylpiperazin-1-yl)methyl)benzoate (3-5). 1-phenylpiperazine (189 μL , 1.23 mmol) and K_2CO_3 (170 mg, 1.23 mmol) were dissolved in DMF (10 mL) at room temperature. To this solution, methyl-4-(bromomethyl)benzoate (281.76 mg, 1.23 mmol) was added with more DMF (5 mL). This mixture was then brought to reflux and allowed to stir for three hours. After three hours, the reaction was allowed to cool to room temperature and TLC (3:1 hexanes/ethyl acetate) was used to determine that the reaction had gone to completion. To the reaction mixture ethyl acetate (40 mL) was added and the solution was transferred to a separatory funnel. The reaction mixture was then washed four times with 10% LiBr solution to remove the DMF and water-soluble byproducts. Next, the remaining ethyl acetate solution was dried with Na_2SO_4 and concentrated under vacuum. The resulting crude product was then purified by flash column chromatography (silica, ethyl acetate/hexanes) affording **5** (pink/orange powder, 320.1 mg, 84%). ^1H NMR (500 MHz, CDCl_3) δ 8.02 (d, $J = 8.2$ Hz, 2H), 7.47 (d, $J = 7.9$ Hz, 2H), 7.27 – 7.24 (m, 2H), 6.93 (d, $J = 8.0$ Hz, 2H), 6.86 (t, $J = 7.3$ Hz, 1H), 3.91 (s, 3H), 3.65 (s, 2H), 3.23 (m, 4H), 2.65 (m, 4H). ^{13}C NMR (126 MHz, CDCl_3) δ 166.93, 151.12, 129.64, 129.07, 119.78, 116.10, 62.45, 53.03, 52.05, 48.93. IR (neat): 3090, 2950, 1717, 1598, 1273 cm^{-1} . HRMS (ESI-TOF) m/z : $[(\text{M}+\text{H})^+]$ calcd for ($\text{C}_{19}\text{H}_{23}\text{N}_2\text{O}_2^+$): 311.1760. Found: 311.1779. m.p.: 86 – 87 $^\circ\text{C}$.



methyl 4-((4-(2,3-dichlorophenyl)piperazin-1-yl)methyl)benzoate (3-6).

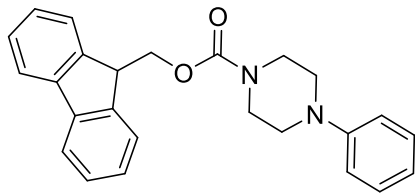
1-(2,3-dichlorophenyl)piperazine (200 mg, 0.747 mmol) and K_2CO_3 (103.2 mg, 0.747 mmol) were dissolved in DMF (10 mL) at room temperature. To this solution, methyl-4-(bromomethyl)benzoate (171.1 mg, 0.747 mmol) was added with more DMF (5 mL). This mixture was then brought to reflux and allowed to stir for three hours. After three hours, the reaction was allowed to cool to room temperature and TLC (3:1 hexanes/ethyl acetate) was used to determine that the reaction had gone to completion. To the reaction mixture ethyl acetate (40 mL) was added and the solution was transferred to a separatory funnel. The reaction mixture was then washed four times with 10% LiBr solution to remove the DMF and water-soluble byproducts. Next, the remaining ethyl acetate solution was dried with Na_2SO_4 and concentrated under vacuum. The resulting crude product was then purified by flash column chromatography (silica, ethyl acetate/hexanes) affording **6** (pink/orange powder, 190 mg, 67% yield).

1H NMR (500 MHz, $CDCl_3$) δ 8.03 (d, $J = 7.1$ Hz, 2H), 7.49 (m, 2H), 7.17 – 7.12 (m, 2H), 6.97 (m, 1H), 3.91 (s, 3H), 3.71 (s, 2H), 3.12 (m, 4H), 2.72 (m, 4H). ^{13}C NMR (126 MHz, $CDCl_3$) δ 166.88, 134.00, 129.73, 129.34, 127.47, 124.76, 118.66, 62.34, 53.10, 52.10, 50.87. IR (neat): 3095, 2967, 1712, 1577, 1270 cm^{-1} . HRMS (ESI-TOF) m/z : $[(M+H)^+]$ calcd for $(C_{19}H_{21}Cl_2N_2O_2^+)$: 379.0980. Found: 379.0985. m.p.: 92 – 93 $^{\circ}C$.



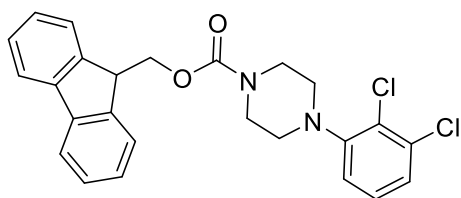
methyl 4-(((2-oxo-1,2,3,4-tetrahydroquinolin-7-yl)oxy)methyl)benzoate (3-7). To a solution of 7-hydroxy-3,4-dihydro-2(1H)-quinolinone (50 mg, 0.31 mmol) in DMF (10 mL) at 0°C NaH (8.9 mg, 0.372 mmol) was added. This mixture was stirred under nitrogen atmosphere for 15 minutes. At this point, methyl-4-(bromomethyl)benzoate (71 mg, 0.31 mmol) was quickly added to avoid H₂O contamination. The resulting solution was then allowed to warm to room temperature and left to stir for hours. Upon completion, the reaction was quenched with the addition of water (10 ml). To this ethyl acetate (40 mL) was add and the resulting solution was transferred to a separatory funnel and washed three times with 10% LiBr solution to remove DMF. The resulting organic solution was then dried with Na₂SO₄ and concentrated under vacuum. The resulting crude product was then purified by flash column chromatography (silica, ethyl acetate/hexanes) affording **7** (white powder, 59.1 mg, 61% yield).

¹H NMR (500 MHz, CDCl₃) δ 8.06 (d, *J* = 8.3 Hz, 2H), 7.67 (s, br., 1H), 7.49 (d, *J* = 8.3 Hz, 2H), 7.07 (d, *J* = 8.3 Hz, 1H), 6.59 (dd, *J* = 8.3, 2.5 Hz, 1H), 6.37 (d, *J* = 2.5 Hz, 1H), 5.10 (s, 2H), 4.12 (q, *J* = 7.2 Hz, 1H), 3.92 (s, 3H), 2.92 – 2.89 (m, 2H), 2.63 – 2.60 (m, 2H). ¹³C NMR (126 MHz, CDCl₃) δ 171.32, 141.89, 138.14, 129.91, 128.82, 126.91, 116.44, 108.81, 102.53, 69.49, 52.17, 31.00, 24.59. IR (neat): 3010, 2945, 1724, 1670, 1592 cm⁻¹. HRMS (ESI-TOF) *m/z*: [(M+H)⁺] calcd for (C₁₈H₁₈NO₄⁺): 312.1236. Found: 312.1237. m.p.: 176 – 177 °C.



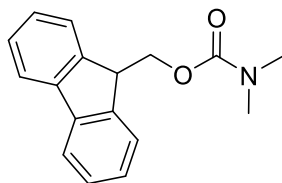
9H-fluoren-9-yl)methyl 4-phenylpiperazine-1-carboxylate (3-8). 1-phenylpiperazine (54 μ L, 0.352 mmol) and triethylamine (54 μ L, 0.387 mmol) were dissolved in anhydrous DCM (10 mL) at 0°C. To this solution Fmoc-Cl (100 mg, 0.387 mmol) was added with a spatula. The resulting solution was allowed to warm to room temperature and was stirred overnight. The resulting solution was washed with water three times and extracted with ethyl acetate (40 mL). The combined organic solution was then washed three times with brine solution and dried over Na_2SO_4 . The resulting crude product was purified by flash column chromatography (silica, ethyl acetate/hexanes) affording **8** (white powder, 94.2 mg, 70% yield).

^1H NMR (500 MHz, CDCl_3) δ 7.79 (d, $J = 7.5$ Hz, 2H), 7.60 (d, $J = 7.4$ Hz, 2H), 7.43 (t, $J = 7.5$ Hz, 2H), 7.35 (m, 4H), 6.95 (m, 3H), 4.49 (d, $J = 6.7$ Hz, 2H), 4.29 (t, $J = 6.7$ Hz, 1H), 3.63 (m, 4H), 3.12 (m, 4H). ^{13}C NMR (126 MHz, CDCl_3) δ 155.11, 151.13, 143.95, 141.33, 129.21, 127.70, 127.05, 124.93, 120.46, 119.99, 116.72, 67.28, 49.38, 47.35. IR (neat): 3052, 2904, 1681, 1597, 1218 cm^{-1} . HRMS (ESI-TOF) m/z : $[(\text{M}+\text{H})^+]$ calcd for ($\text{C}_{25}\text{H}_{25}\text{N}_2\text{O}_2^+$): 385.1916. Found: 385.1923. m.p.: 146 – 147 °C.



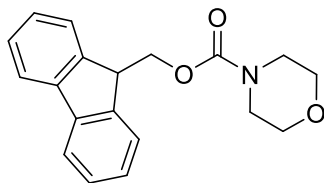
9H-fluoren-9-yl)methyl 4-(2,3-dichlorophenyl)piperazine-1-carboxylate (3-9). 1-(2,3-dichlorophenyl)piperazine (93.1 mg, 0.352 mmol) and triethylamine (54 μ L, 0.387 mmol) were dissolved in anhydrous DCM (10 mL) at 0°C. To this solution Fmoc-Cl (100 mg, 0.387 mmol)

was added with a spatula. The resulting solution was allowed to warm to room temperature and was stirred overnight. The resulting solution was washed with water three times and extracted with ethyl acetate (40 mL). The combined organic solution was then washed three time with brine solution and dried over Na₂SO₄. The resulting crude product was purified by flash column chromatography (silica, ethyl acetate/hexanes) affording **9** (white semi-solid, 78.8 mg, 49% yield). ¹H NMR (500 MHz, CDCl₃) δ 7.78 (d, *J* = 7.5 Hz, 2H), 7.60 (d, *J* = 7.5 Hz, 2H), 7.41 (t, *J* = 7.4 Hz, 2H), 7.33 (t, *J* = 7.4 Hz, 2H), 7.21 – 7.15 (m, 2H), 6.92 (dd, *J* = 7.7, 1.8 Hz, 1H), 4.50 (d, *J* = 6.7 Hz, 2H), 4.27 (t, *J* = 6.7 Hz, 1H), 3.66 – 3.63 (m, 4H), 2.98 – 2.94 (m, 4H). ¹³C NMR (126 MHz, CDCl₃) δ 155.20, 150.84, 143.95, 141.34, 134.15, 127.70, 127.51, 127.05, 125.09, 124.94, 120.00, 118.75, 67.27, 51.16, 47.37. IR (neat): 3065, 2918, 1698, 1577, 1204 cm⁻¹. HRMS (ESI-TOF) *m/z*: [(M+H)⁺] calcd for (C₂₅H₂₃Cl₂N₂O₂⁺): 453.1136. Found: 453.1142.



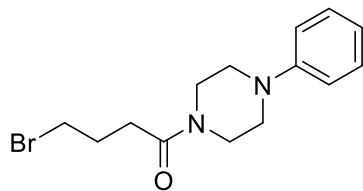
9H-fluoren-9-yl)methyl dimethylcarbamate (3-10). Dimethylamine (176 μL, 0.352 mmol) and triethylamine (54 μL, 0.387 mmol) were dissolved in anhydrous DCM (10 mL) at 0°C. To this solution Fmoc-Cl (100 mg, 0.387 mmol) was added with a spatula. The resulting solution was allowed to warm to room temperature and was stirred overnight. The resulting solution was washed with water three times and extracted with ethyl acetate (40 mL). The combined organic solution was then washed three time with brine solution and dried over Na₂SO₄. The resulting crude product was purified by flash column chromatography (silica, ethyl acetate/hexanes) affording **10** (94 mg, 99%).

^1H NMR (500 MHz, CDCl_3) δ 7.78 (d, $J = 7.6$ Hz, 2H), 7.62 (d, $J = 7.6$ Hz, 2H), 7.41 (t, $J = 7.4$ Hz, 2H), 7.32 (td, $J = 7.5, 1.1$ Hz, 2H), 4.40 (d, $J = 7.0$ Hz, 2H), 4.26 (t, $J = 7.0$ Hz, 1H), 2.95 (s, 6H). ^{13}C NMR (126 MHz, CDCl_3) δ 156.46, 144.12, 141.29, 127.61, 126.98, 125.00, 119.93, 67.35, 47.32, 36.48, 35.91. IR (neat): 3061, 2929, 2763, 1702, 1447 cm^{-1} . m.p.: 146 – 147 $^\circ\text{C}$. Mass spectroscopy data was not possible to identify.



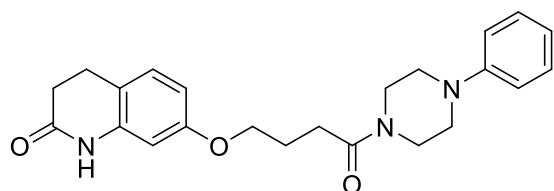
9H-fluoren-9-yl)methyl morpholine-4-carboxylate (3-11). Morpholine (30 μL , 0.352 mmol) and triethylamine (54 μL , 0.387 mmol) were dissolved in anhydrous DCM (10 mL) at 0°C . To this solution Fmoc-Cl (100 mg, 0.387 mmol) was added with a spatula. The resulting solution was allowed to warm to room temperature and was stirred overnight. The resulting solution was washed with water three times and extracted with ethyl acetate (40 mL). The combined organic solution was then washed three times with brine solution and dried over Na_2SO_4 . The resulting crude product was purified by flash column chromatography (silica, ethyl acetate/hexanes) affording **11** (96.9 mg, 89%).

^1H NMR (500 MHz, CDCl_3) δ 7.78 (d, $J = 7.5$ Hz, 2H), 7.58 (d, $J = 7.5$ Hz, 2H), 7.42 (t, $J = 7.5$ Hz, 2H), 7.34 (td, $J = 7.5, 1.0$ Hz, 2H), 4.48 (d, $J = 6.7$ Hz, 2H), 4.26 (t, $J = 6.7$ Hz, 1H), 3.64 – 3.60 (m, 4H), 3.47 – 3.43 (m, 4H). ^{13}C NMR (126 MHz, CDCl_3) δ 143.90, 141.33, 127.71, 127.05, 124.89, 119.99, 67.29, 47.33. IR (neat): 3038, 2963, 1684, 1421 cm^{-1} . m.p.: 110 – 111 $^\circ\text{C}$. Mass spectroscopy data was not possible to identify.



4-bromo-1-(4-phenylpiperazin-1-yl)butan-1-one (intermediate to compound 12). To a round bottom flask with a stir bar and molecular sieves was added 4-bromobutanoyl chloride (417 μL , 3.6 mmol) in dry THF (10 mL). This was then cooled to 0 $^{\circ}\text{C}$ and to it was slowly added a solution of 1-phenylpiperazine (458 μL , 3.0 mmol) and triethylamine (416 μL , 3.0 mmol) in dry THF (10 mL). This mixture was stirred at 0 $^{\circ}\text{C}$ and gradually allowed to warm to room temperature overnight. The reaction was then poured into DI H₂O (40 mL) and extracted with DCM (40 mL). The organic layers were then washed with brine solution, dried with Na₂SO₄ and concentrated under vacuum. The crude material was then purified by flash column chromatography (silica, ethyl acetate/hexanes) affording the intermediate to compound **12**, but there remained significant amounts of an unidentified contaminate. This prevented full characterization data and accurate yields from being reported, but the crude material was carried forward for the synthesis of compound **12**.

HRMS (ESI-TOF) m/z : [(M+H)⁺] calcd for (C₁₄H₂₀BrN₂O⁺): 311.0759. Found: 311.0766.



7-(4-oxo-4-(4-phenylpiperazin-1-yl)butoxy)-3,4-dihydroquinolin-2(1H)-one (3-12). To a round bottom flask with a stir bar was added 7-hydroxy-3,4-dihydroquinolin-2(1H)-one (50 mg, 0.31 mmol) in DMF (3 mL) and NaH (14.9 mg, 0.372 mmol). This mixture was allowed to stir under N₂ atmosphere for about 10 minutes and then to it was added 4-bromo-1-(4-phenylpiperazin-

1-yl)butan-1-one (115.8 mg, 0.372 mmol) in DMF (3 mL). The resulting mixture was stirred at room temperature overnight. To the reaction was then added ethyl acetate (40 mL) and the organics were washed with a 10% LiBr solution and then a brine solution to remove DMF. The organic layer was collected, dried with Na₂SO₄ and concentrated under vacuum. The crude material was then purified by flash column chromatography (silica, ethyl acetate/hexanes) affording **12** (9.5 mg, 8% yield).

¹H NMR (500 MHz, CDCl₃) δ 7.99 (s, br., 1H), 7.30 – 7.26 (m, 2H), 7.05 (d, *J* = 8.3 Hz, 1H), 6.93 – 6.89 (m, 3H), 6.54 (dd, *J* = 8.3, 2.4 Hz, 1H), 6.34 (m, 1H), 4.03 (t, *J* = 5.9 Hz, 2H), 3.79 (t, *J* = 5.1 Hz, 2H), 3.65 (t, *J* = 5.1 Hz, 2H), 3.15 (t, *J* = 5.2 Hz, 4H), 2.88 (t, *J* = 7.2 Hz, 2H), 2.59 (m, 4H), 2.19 – 2.10 (m, 2H). ¹³C NMR (126 MHz, CDCl₃) δ 170.75, 158.45, 150.89, 129.23, 128.72, 120.57, 116.63, 115.83, 108.54, 102.10, 67.13, 49.69, 49.44, 45.38, 41.54, 31.05, 29.28, 24.77, 24.54. IR (neat): 3239, 2963, 1683, 1623, 1592 cm⁻¹. HRMS (ESI-TOF) *m/z*: [(M+H)⁺] calcd for (C₂₃H₂₈N₃O₃⁺): 394.2131. Found: 394.2136. m.p. data was not obtainable due to insufficient amount of material remaining.

REFERENCES

- (1) Klaips, C. L.; Jayaraj, G.; Hartl, F. Pathways of cellular proteostasis in aging and disease. *The Journal of cell biology* **2018**, *217* (1), 51-63. DOI: 10.1083/jcb.201709072.
- (2) Powers, E. T.; Morimoto, R. I.; Dillin, A.; Kelly, J. W.; Balch, W. E. Biological and Chemical Approaches to Diseases of Proteostasis Deficiency. *Annual Review of Biochemistry* **2009**, *78* (1), 959-991. DOI: 10.1146/annurev.biochem.052308.114844.
- (3) Labbadia, J.; Morimoto, R. I. The biology of proteostasis in aging and disease. *Annual review of biochemistry* **2015**, *84*, 435-464. DOI: 10.1146/annurev-biochem-060614-033955.
- (4) Balch, W. E.; Morimoto, R. I.; Dillin, A.; Kelly, J. W. Adapting proteostasis for disease intervention. 2008; Vol. 319, pp 916-919.
- (5) Hartl, F. U. Cellular Homeostasis and Aging. *Annual Review of Biochemistry* **2016**, *85* (1), 1-4. DOI: 10.1146/annurev-biochem-011116-110806.
- (6) Deshmukh, F. K.; Yaffe, D.; Olshina, M. A.; Ben-Nissan, G.; Sharon, M. The Contribution of the 20S Proteasome to Proteostasis. *Biomolecules* **2019**, *9* (5), 190, Review. DOI: 10.3390/biom9050190.
- (7) Lehtonen, Š.; Sonninen, T. M.; Wojciechowski, S.; Goldsteins, G.; Koistinaho, J. Dysfunction of Cellular Proteostasis in Parkinson's Disease. *Frontiers in neuroscience* **2019**, *13* (10), 457. DOI: 10.3389/fnins.2019.00457.
- (8) Kurtishi, A.; Rosen, B.; Patil, K. S.; Alves, G. W.; G., M. S. Cellular Proteostasis in Neurodegeneration. *Molecular neurobiology* **2019**, *56* (5), 3676-3689. DOI: 10.1007/s12035-018-1334-z.
- (9) Hipp, M. S.; Kasturi, P.; Hartl, F. U. The proteostasis network and its decline in ageing. *Nature reviews. Molecular cell biology* **2019**, *20* (7), 421-435. DOI: 10.1038/s41580-019-0101-y.
- (10) McNaught, K. S. P.; Olanow, C. W.; Halliwell, B.; Isacson, O.; Jenner, P. Failure of the ubiquitin–proteasome system in Parkinson's disease. *Nature Reviews Neuroscience* **2001**, *2* (8), 589-594. DOI: 10.1038/35086067.
- (11) Saez, I.; Vilchez, D. The Mechanistic Links Between Proteasome Activity, Aging and Age-related Diseases. *Current genomics* **2014**, *15* (1), 38-51. DOI: 10.2174/138920291501140306113344.
- (12) Lam, Y. A.; Pickart, C. M.; Alban, A.; Landon, M.; Jamieson, C.; Ramage, R.; Mayer, R. J.; Layfield, R. Inhibition of the ubiquitin-proteasome system in Alzheimer's disease. *Proceedings of the National Academy of Sciences of the United States of America* **2000**, *97* (18), 9902-9906. DOI: 10.1073/pnas.170173897.

- (13) Ross, C. A.; Poirier, M. A. Protein aggregation and neurodegenerative disease. *Nature Medicine* **2004**, *10* (7), S10-S17. DOI: 10.1038/nm1066.
- (14) Soto, C. Unfolding the role of protein misfolding in neurodegenerative diseases. *Nature Reviews Neuroscience* **2003**, *4* (1), 49-60. DOI: 10.1038/nrn1007.
- (15) Keller, J. N.; Hanni, K. B.; Markesbery, W. R. Impaired Proteasome Function in Alzheimer's Disease. *Journal of Neurochemistry* **2001**, *75* (1), 436-439. DOI: 10.1046/j.1471-4159.2000.0750436.x.
- (16) Tofaris, G. K.; Layfield, R.; Spillantini, M. G. alpha-synuclein metabolism and aggregation is linked to ubiquitin-independent degradation by the proteasome. *FEBS letters* **2001**, *509* (1), 22-26. DOI: 10.1016/s0014-5793(01)03115-5.
- (17) Alafuzoff, I.; Hartikainen, P. Alpha-synucleinopathies. *Handbook of clinical neurology* **2017**, *145*, 339-353. DOI: 10.1016/B978-0-12-802395-2.00024-9.
- (18) Bengoa-Vergniory, N.; Roberts, R. F.; Wade-Martins, R.; Alegre-Abarrategui, J. Alpha-synuclein oligomers: a new hope. *Acta neuropathologica* **2017**, *134* (6), 819-838. DOI: 10.1007/s00401-017-1755-1.
- (19) Berrocal, R.; Vasquez, V.; Krs, S. R.; Gadad, B. S.; Ks, R. α -Synuclein Misfolding Versus Aggregation Relevance to Parkinson's Disease: Critical Assessment and Modeling. Humana Press Inc.: 2015; Vol. 51, pp 1417-1431.
- (20) Uversky, V. N.; Oldfield, C. J.; Dunker, A. K. Intrinsically Disordered Proteins in Human Diseases: Introducing the D ² Concept. *Annual Review of Biophysics* **2008**, *37* (1), 215-246. DOI: 10.1146/annurev.biophys.37.032807.125924.
- (21) Uversky, V. N. Intrinsically disordered proteins and their (disordered) proteomes in neurodegenerative disorders. *Frontiers in aging neuroscience* **2015**, *7*, 18-18. DOI: 10.3389/fnagi.2015.00018.
- (22) Choi, M. L.; Gandhi, S. Crucial role of protein oligomerization in the pathogenesis of Alzheimer's and Parkinson's diseases. *The FEBS Journal* **2018**, *285* (19), 3631-3644. DOI: 10.1111/febs.14587.
- (23) Levine, Z. A.; Larini, L.; LaPointe, N. E.; Feinstein, S. C.; Shea, J.-E. Regulation and aggregation of intrinsically disordered peptides. *Proceedings of the National Academy of Sciences of the United States of America* **2015**, *112* (9), 2758-2763. DOI: 10.1073/pnas.1418155112.
- (24) Korsak, M.; Kozyreva, T. Beta Amyloid Hallmarks: From Intrinsically Disordered Proteins to Alzheimer's Disease. Springer, Cham, 2015; pp 401-421.
- (25) Cheng, B.; Gong, H.; Xiao, H.; Petersen, R. B.; Zheng, L.; Huang, K. Inhibiting toxic aggregation of amyloidogenic proteins: a therapeutic strategy for protein misfolding diseases. *Biochimica et biophysica acta* **2013**, *1830* (10), 4860-4871. DOI: 10.1016/j.bbagen.2013.06.029.

- (26) Castillo-Carranza, D. L.; Guerrero-Muñoz, M. J.; Sengupta, U.; Gerson, J. E.; Kaye, R. α -Synuclein Oligomers Induce a Unique Toxic Tau Strain. *Biological Psychiatry* **2018**, *84* (7), 499-508. DOI: 10.1016/j.biopsych.2017.12.018.
- (27) Emmanouilidou, E.; Stefanis, L.; Vekrellis, K. Cell-produced alpha-synuclein oligomers are targeted to, and impair, the 26S proteasome. *Neurobiology of aging* **2010**, *31* (6), 953-968. DOI: 10.1016/j.neurobiolaging.2008.07.008.
- (28) Ben-Nissan, G.; Sharon, M. Regulating the 20S proteasome ubiquitin-independent degradation pathway. *Biomolecules* **2014**, *4* (3), 862-884. DOI: 10.3390/biom4030862.
- (29) Asher, G.; Reuven, N.; Shaul, Y. 20S proteasomes and protein degradation “by default”. *BioEssays* **2006**, *28* (8), 844-849. DOI: 10.1002/bies.20447.
- (30) Njomen, E.; Tepe, J. J. Regulation of Autophagic Flux by the 20S Proteasome. *Cell Chemical Biology* **2019**, *26* (9), 1283-1294.e1285. DOI: 10.1016/j.chembiol.2019.07.002.
- (31) Korovila, I.; Hugo, M.; Castro, J. P.; Weber, D.; Höhn, A.; Grune, T.; Jung, T. Proteostasis, oxidative stress and aging. *Redox biology* **2017**, *13*, 550-567. DOI: 10.1016/j.redox.2017.07.008.
- (32) Jung, T.; Grune, T. The proteasome and its role in the degradation of oxidized proteins. *IUBMB Life* **2008**, *60* (11), 743-752. DOI: 10.1002/iub.114.
- (33) Jung, T.; Höhn, A.; Grune, T. The proteasome and the degradation of oxidized proteins: Part II – protein oxidation and proteasomal degradation. *Redox Biology* **2014**, *2*, 99-104. DOI: 10.1016/J.REDOX.2013.12.008.
- (34) Jung, T.; Höhn, A.; Grune, T. The proteasome and the degradation of oxidized proteins: Part III—Redox regulation of the proteasomal system. *Redox Biology* **2014**, *2*, 388-394. DOI: 10.1016/J.REDOX.2013.12.029.
- (35) Chondrogianni, N.; Petropoulos, I.; Grimm, S.; Georgila, K.; Catalgol, B.; Friguet, B.; Grune, T.; Gonos, E. Protein damage, repair and proteolysis. *Molecular aspects of medicine* **2014**, *35*, 1-71. DOI: 10.1016/j.mam.2012.09.001.
- (36) Myers, N.; Olender, T.; Savidor, A.; Levin, Y.; Reuven, N.; Shaul, Y. The Disordered Landscape of the 20S Proteasome Substrates Reveals Tight Association with Phase Separated Granules. *PROTEOMICS* **2018**, *18* (21-22), 1800076. DOI: 10.1002/pmic.201800076.
- (37) Zondler, L.; Kostka, M.; Garidel, P.; Heinzlmann, U.; Hengerer, B.; Mayer, B.; Weishaupt, J. H.; Gillardon, F.; Danzer, K. M. Proteasome impairment by α -synuclein. *PloS one* **2017**, *12* (9), e0184040-e0184040. DOI: 10.1371/journal.pone.0184040.
- (38) Thibaut, T. A.; Anderson, R. T.; Smith, D. M. A common mechanism of proteasome impairment by neurodegenerative disease-associated oligomers. *Nature Communications* **2018**, *9* (1), 1097-1097. DOI: 10.1038/s41467-018-03509-0.

- (39) Smith, D. M. Could a Common Mechanism of Protein Degradation Impairment Underlie Many Neurodegenerative Diseases? *Journal of experimental neuroscience* **2018**, *12*, 1179069518794675-1179069518794675. DOI: 10.1177/1179069518794675.
- (40) Myeku, N.; Clelland, C. L.; Emrani, S.; Kukushkin, N. V.; Yu, W. H.; Goldberg, A. L.; Duff, K. E. Tau-driven 26S proteasome impairment and cognitive dysfunction can be prevented early in disease by activating cAMP-PKA signaling. *Nature Medicine* **2016**, *22* (1), 46-53. DOI: 10.1038/nm.4011.
- (41) Ruegsegger, C.; Saxena, S. Proteostasis impairment in ALS. *Brain research* **2016**, *1648*, 571-579. DOI: 10.1016/j.brainres.2016.03.032.
- (42) Njomen, E.; Tepe, J. J. Proteasome Activation as a New Therapeutic Approach to Target Proteotoxic Disorders. *Journal of Medicinal Chemistry* **2019**, *62* (14), 6469-6481. DOI: 10.1021/acs.jmedchem.9b00101.
- (43) Jones, C. L.; Tepe, J. J. Proteasome Activation to Combat Proteotoxicity. *Molecules* **2019**, *24* (15), 2841, Review. DOI: 10.3390/molecules24152841.
- (44) Coleman, R. A.; Trader, D. J. All About the Core: A Therapeutic Strategy to Prevent Protein Accumulation with Proteasome Core Particle Stimulators. *ACS Pharmacology & Translational Science* **2018**, *1* (2), 140-142. DOI: 10.1021/acsptsci.8b00042.
- (45) Opoku-Nsiah, K. A.; Gestwicki, J. E. Aim for the core: suitability of the ubiquitin-independent 20S proteasome as a drug target in neurodegeneration. Mosby Inc.: 2018; Vol. 198, pp 48-57.
- (46) Maresh, M. E.; Salazar-Chaparro, A. F.; Trader, D. J. Methods for the discovery of small molecules to monitor and perturb the activity of the human proteasome. *Future Medicinal Chemistry* **2020**, *13* (2), 99-116, review-article. DOI: 10.4155/fmc-2020-0288.
- (47) Zerfas, B. L.; Coleman, R. A.; Salazar-Chaparro, A. F.; Macatangay, N. J.; Trader, D. J. Fluorescent Probes with Unnatural Amino Acids to Monitor Proteasome Activity in Real-Time. *ACS Chemical Biology* **2020**, *15* (9), 2588– 2596, research-article. DOI: 10.1021/acscchembio.0c00634.
- (48) Coleman, R. A.; Trader, D. J. Methods to Discover and Evaluate Proteasome Small Molecule Stimulators. *Molecules* **2019**, *24* (12), 2341, Review. DOI: 10.3390/molecules24122341.
- (49) Fiolek, T.; Magyar, C.; Wall, T.; Davies, S.; Campbell, M.; Savich, C.; Tepe, J.; Mosey, R. Dihydroquinazolines enhance 20S proteasome activity and induce degradation of α -synuclein, an intrinsically disordered protein associated with neurodegeneration. *Bioorganic & Medicinal Chemistry Letters* **2021**, *36*, 127821. DOI: 10.1016/j.bmcl.2021.127821.
- (50) Njomen, E.; Osmulski, P. A.; Jones, C. L.; Gaczynska, M.; Tepe, J. J. Small Molecule Modulation of Proteasome Assembly. *Biochemistry* **2018**, *57* (28), 4214-4224. DOI: 10.1021/acs.biochem.8b00579.

- (51) Jones, C. L.; Njomen, E.; Sjögren, B.; Dexheimer, T. S.; Tepe, J. J. Small Molecule Enhancement of 20S Proteasome Activity Targets Intrinsically Disordered Proteins. *ACS Chemical Biology* **2017**, *12* (9), 2240-2247. DOI: 10.1021/acscchembio.7b00489.
- (52) Coleman, R. A.; Muli, C. S.; Zhao, Y.; Bhardwaj, A.; Newhouse, T. R.; Trader, D. J. Analysis of chain length, substitution patterns, and unsaturation of AM-404 derivatives as 20S proteasome stimulators. *Bioorganic & Medicinal Chemistry Letters* **2019**, *29* (3), 420-423. DOI: 10.1016/J.BMCL.2018.12.030.
- (53) Coleman, R. A.; Trader, D. J. Development and Application of a Sensitive Peptide Reporter to Discover 20S Proteasome Stimulators. *ACS Combinatorial Science* **2018**, *20* (5), 269-276. DOI: 10.1021/acscombsci.7b00193.
- (54) Trader, D. J.; Simanski, S.; Dickson, P.; Kodadek, T. Establishment of a suite of assays that support the discovery of proteasome stimulators. *Biochimica et Biophysica Acta (BBA) - General Subjects* **2017**, *1861* (4), 892-899. DOI: 10.1016/J.BBAGEN.2017.01.003.
- (55) Giżyńska, M.; Witkowska, J.; Karpowicz, P.; Rostankowski, R.; Chocron, E. S.; Pickering, A. M.; Osmulski, P.; Gaczynska, M.; Jankowska, E. Proline- and Arginine-Rich Peptides as Flexible Allosteric Modulators of Human Proteasome Activity. *Journal of Medicinal Chemistry* **2018**, *62* (1), 359-370, research-article. DOI: 10.1021/acs.jmedchem.8b01025.
- (56) Harder, B.; Blomquist, M.; Wang, J.; Kim, A.; Woodworth, G.; Winkles, J.; Loftus, J.; Tran, N. Developments in Blood-Brain Barrier Penetration and Drug Repurposing for Improved Treatment of Glioblastoma. *Frontiers in Oncology* **2018**, *8*. DOI: doi:10.3389/fonc.2018.00462.
- (57) Pushpakom, S.; Iorio, F.; Eyers, P. A.; Escott, K. J.; Hopper, S.; Wells, A.; Doig, A.; Guilliams, T.; Latimer, J.; McNamee, C.; et al. Drug repurposing: progress, challenges and recommendations. *Nature Reviews Drug Discovery* **2018**, *18* (1), 41-58, ReviewPaper. DOI: doi:10.1038/nrd.2018.168.
- (58) Fletcher, E.; Kaminski, T.; Williams, G.; Duty, S. Drug repurposing strategies of relevance for Parkinson's disease. *Pharmacology Research & Perspectives* **2021**, *9* (4), 841. DOI: 10.1002/prp2.841.
- (59) Katsiki, M.; Chondrogianni, N.; Chinou, I.; Rivett, A. J.; Gonos, E. S. The Olive Constituent Oleuropein Exhibits Proteasome Stimulatory Properties *In Vitro* and Confers Life Span Extension of Human Embryonic Fibroblasts. *Rejuvenation Research* **2007**, *10* (2), 157-172. DOI: 10.1089/rej.2006.0513.
- (60) Huang, L.; Ho, P.; Chen, C.-H. Activation and inhibition of the proteasome by betulinic acid and its derivatives. *FEBS Letters* **2007**, *581* (25), 4955-4959. DOI: 10.1016/j.febslet.2007.09.031.
- (61) Gaczynska, M.; Osmulski, P. A. Characterization of noncompetitive regulators of proteasome activity. Academic Press Inc.: 2005; Vol. 398, pp 425-438.

- (62) Boyd-Kimball, D.; Gonczy, K.; Lewis, B.; Mason, T.; Siliko, N.; Wolfe, J. Classics in Chemical Neuroscience: Chlorpromazine. *ACS chemical neuroscience* **2019**, *10* (1), 79-88. DOI: 10.1021/acscemneuro.8b00258.
- (63) McGavin, J. K.; Goa, K. L. Aripiprazole. *CNS Drugs* **2012**, *16* (11), 779-786, OriginalPaper. DOI: doi:10.2165/00023210-200216110-00008.
- (64) van Epen, J. H. Experience with fluspirilene (R 6218), a long-acting neuroleptic. *Psychiatria, neurologia, neurochirurgia* **1970**, *73* (4), 277-284.
- (65) Janssen, P. A.; Niemegeers, C. J.; Schellekens, K. H.; Lenaerts, F. M.; Verbruggen, F. J.; van Nueten, J. M.; Marsboom, R. H.; Hérin, V. V.; Schaper, W. K. The pharmacology of fluspirilene (R 6218), a potent, long-acting and injectable neuroleptic drug. *Arzneimittel-Forschung* **1970**, *20* (11), 1689-1698.
- (66) Bennett, M.; Bishop, J.; Leng, Y.; Chock, P.; Chase, T.; Mouradian, M. Degradation of α -Synuclein by Proteasome. *Journal of Biological Chemistry* **1999**, *274* (48), 33855-33858. DOI: 10.1074/jbc.274.48.33855.
- (67) Meng, L.; Mohan, R.; Kwok, B. H. B.; Elofsson, M.; Sin, N.; Crews, C. M. Epoxomicin, a potent and selective proteasome inhibitor, exhibits in vivo antiinflammatory activity. *PNAS* **1999**, *96* (18), 10403-10408, research-article. DOI: 10.1073/pnas.96.18.10403.
- (68) Mohammadi, A.; Khalili, B.; Tahavor, M. Novel push-pull heterocyclic azo disperse dyes containing piperazine moiety: Synthesis, spectral properties, antioxidant activity and dyeing performance on polyester fibers. *Spectrochimica Acta Part A: Molecular and Biomolecular Spectroscopy* **2015**, *150*, 799-805. DOI: 10.1016/J.SAA.2015.06.024.
- (69) Kisselev, A. F.; Akopian, T. N.; Castillo, V.; Goldberg, A. L. Proteasome active sites allosterically regulate each other, suggesting a cyclical bite-chew mechanism for protein breakdown. *Mol. Cell* **1999**, *4* (3), 395-402.
- (70) Homan, E. J.; Wikström, H. V.; Grol, C. J. Molecular modeling of the dopamine D2 and serotonin 5-HT(1A) receptor binding modes of the enantiomers of 5-OMe-BPAT. *Bioorganic and Medicinal Chemistry* **1999**, *7* (9), 1805-1820. DOI: 10.1016/S0968-0896(99)00134-0.
- (71) Chen, G.; Xia, H.; Cai, Y.; Ma, D.; Yuan, J.; Yuan, C. Synthesis and SAR study of diphenylbutylpiperidines as cell autophagy inducers. *Bioorg. Med. Chem. Lett.* **2011**, *21* (1), 234-239. DOI: 10.1016/j.bmcl.2010.11.029.
- (72) BIOVIA, Dassault Systèmes, Discovery Studio. *San Diego* 2020.
- (73) Longhena, F.; Spano, P.; Bellucci, A. Targeting of Disordered Proteins by Small Molecules in Neurodegenerative Diseases. *Handb Exp Pharmacol* **2017**. DOI: 10.1007/164_2017_60.
- (74) Boland, B.; Yu, W. H.; Corti, O.; Mollereau, B.; Henriques, A.; Bezard, E.; Pastores, G. M.; Rubinsztein, D. C.; Nixon, R. A.; Duchon, M. R.; et al. Promoting the clearance of neurotoxic

proteins in neurodegenerative disorders of ageing. *Nature Reviews Drug Discovery* **2018**, *17* (9), 660-688. DOI: 10.1038/nrd.2018.109.

(75) Ciechanover, A.; Kwon, Y. T. Degradation of misfolded proteins in neurodegenerative diseases: therapeutic targets and strategies. *Experimental & Molecular Medicine* **2015**, *47* (3), e147-e147. DOI: 10.1038/emm.2014.117.

(76) Deger, J. M.; Gerson, J. E.; Kaye, R. The interrelationship of proteasome impairment and oligomeric intermediates in neurodegeneration. *Aging cell* **2015**, *14* (5), 715-724. DOI: 10.1111/accel.12359.

(77) Gitler, A. D.; Dhillon, P.; Shorter, J. Neurodegenerative disease: Models, mechanisms, and a new hope. Company of Biologists Ltd: 2017; Vol. 10, pp 499-502.

(78) Pinotsi, D.; Michel, C. H.; Buell, A. K.; Laine, R. F.; Mahou, P.; Dobson, C. M.; Kaminski, C. F.; Kaminski Schierle, G. S. Nanoscopic insights into seeding mechanisms and toxicity of alpha-synuclein species in neurons. *Proc. Natl. Acad. Sci. U S A* **2016**, *113* (14), 3815-3819. DOI: 10.1073/pnas.1516546113.

(79) Danzer, K. M.; Haasen, D.; Karow, A. R.; Moussaud, S.; Habeck, M.; Giese, A.; Kretschmar, H.; Hengerer, B.; Kostka, M. Different species of alpha-synuclein oligomers induce calcium influx and seeding. *J Neurosci* **2007**, *27* (34), 9220-9232. DOI: 10.1523/JNEUROSCI.2617-07.2007.

(80) Winner, B.; Jappelli, R.; Maji, S. K.; Desplats, P. A.; Boyer, L.; Aigner, S.; Hetzer, C.; Loher, T.; Vilar, M.; Campioni, S.; et al. In vivo demonstration that alpha-synuclein oligomers are toxic. *Proc. Natl. Acad. Sci. U S A* **2011**, *108* (10), 4194-4199. DOI: 10.1073/pnas.1100976108.

(81) Wills, J.; Jones, J.; Haggerty, T.; Duka, V.; Joyce, J. N.; Sidhu, A. Elevated tauopathy and alpha-synuclein pathology in postmortem Parkinson's disease brains with and without dementia. *Experimental Neurology* **2010**, *225* (1), 210-218. DOI: 10.1016/j.expneurol.2010.06.017.

(82) Ibáñez, P.; Bonnet, A. M.; Débarges, B.; Lohmann, E.; Tison, F.; Agid, Y.; Dürr, A.; Brice, A.; Pollak, P. Causal relation between α -synuclein locus duplication as a cause of familial Parkinson's disease. *The Lancet* **2004**, *364* (9440), 1169-1171. DOI: 10.1016/S0140-6736(04)17104-3.

(83) Ingelsson, M. Alpha-Synuclein Oligomers-Neurotoxic Molecules in Parkinson's Disease and Other Lewy Body Disorders. *Frontiers in neuroscience* **2016**, *10*, 408-408. DOI: 10.3389/fnins.2016.00408.

Appendix:

Figure 3.12 ^1H and ^{13}C NMR spectra of compound 3-1

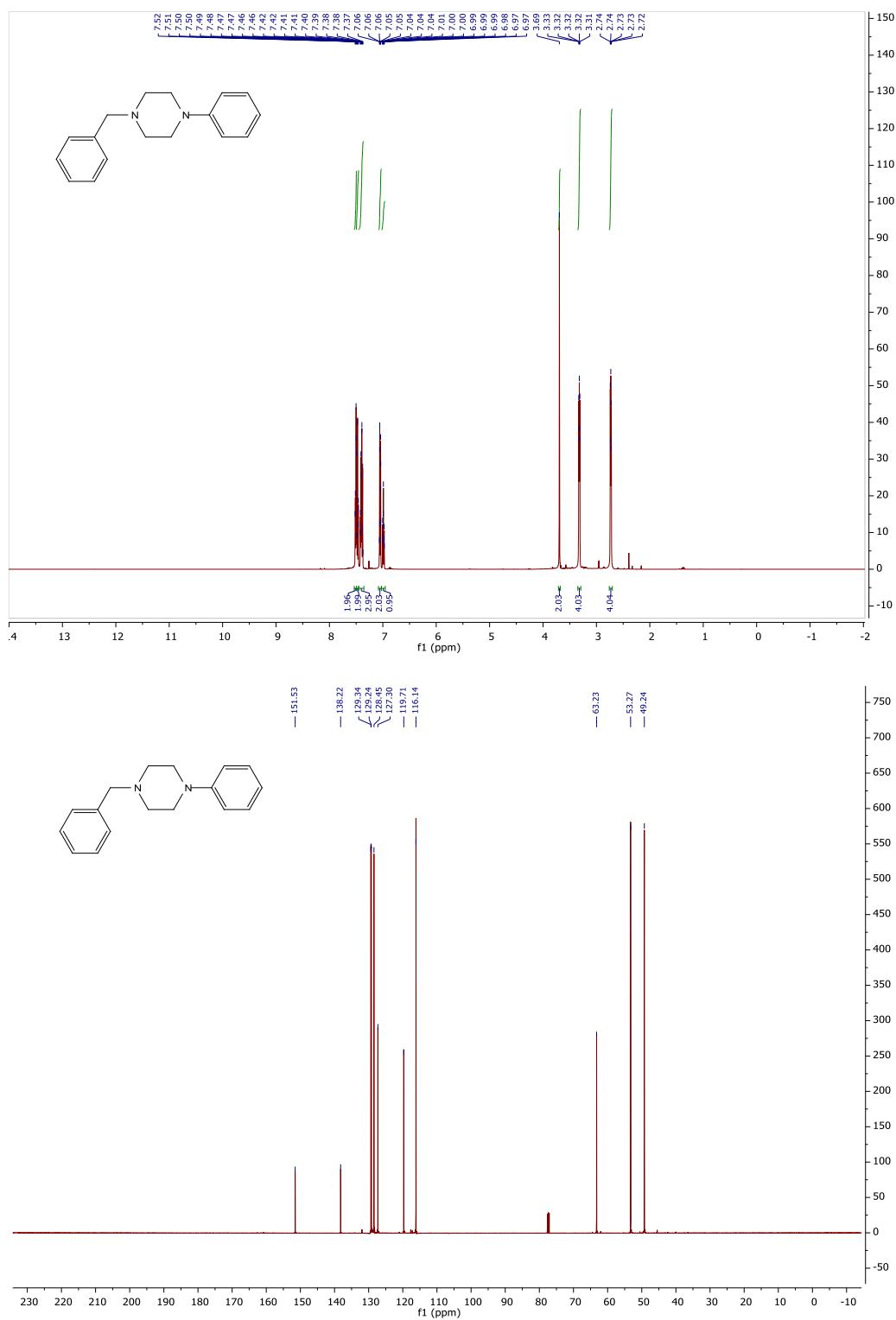


Figure 3.13 ^1H and ^{13}C NMR spectra of compound 3-2

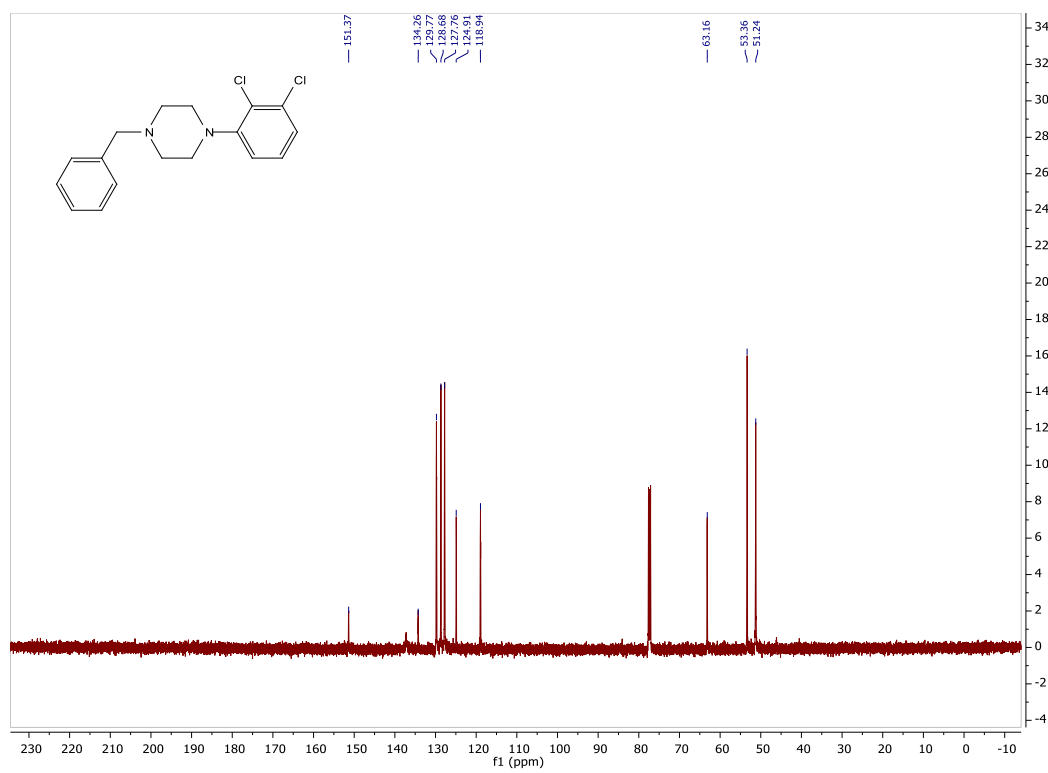
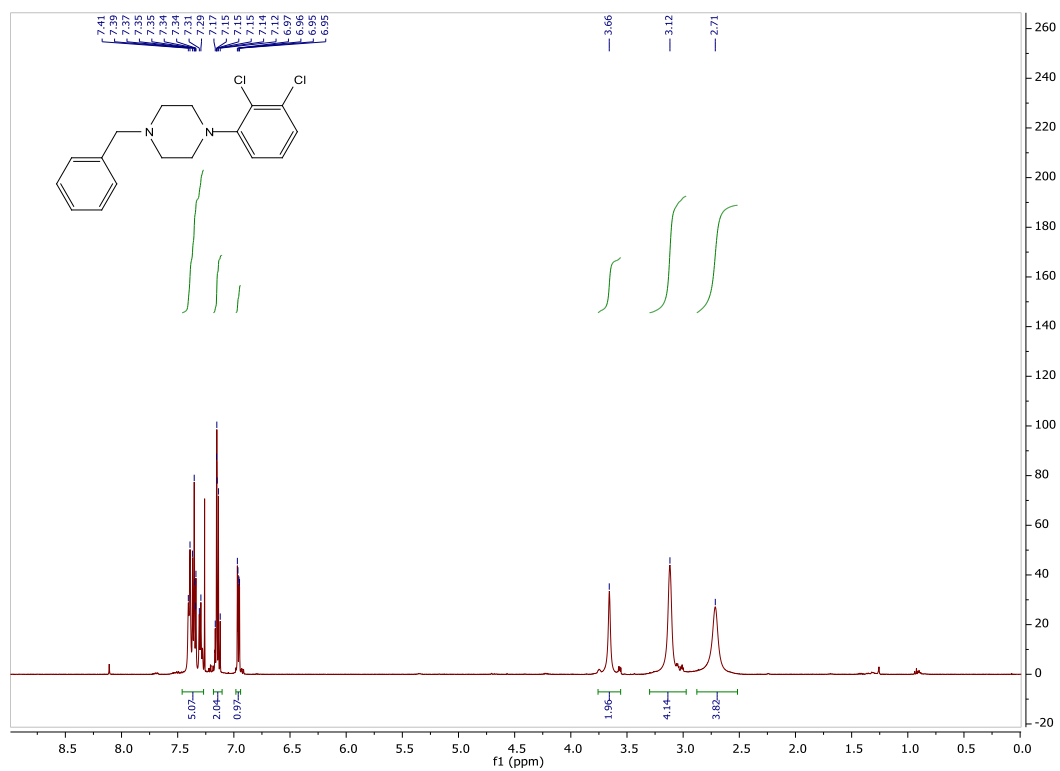


Figure 3.14 ^1H and ^{13}C NMR spectra of compound 3-3

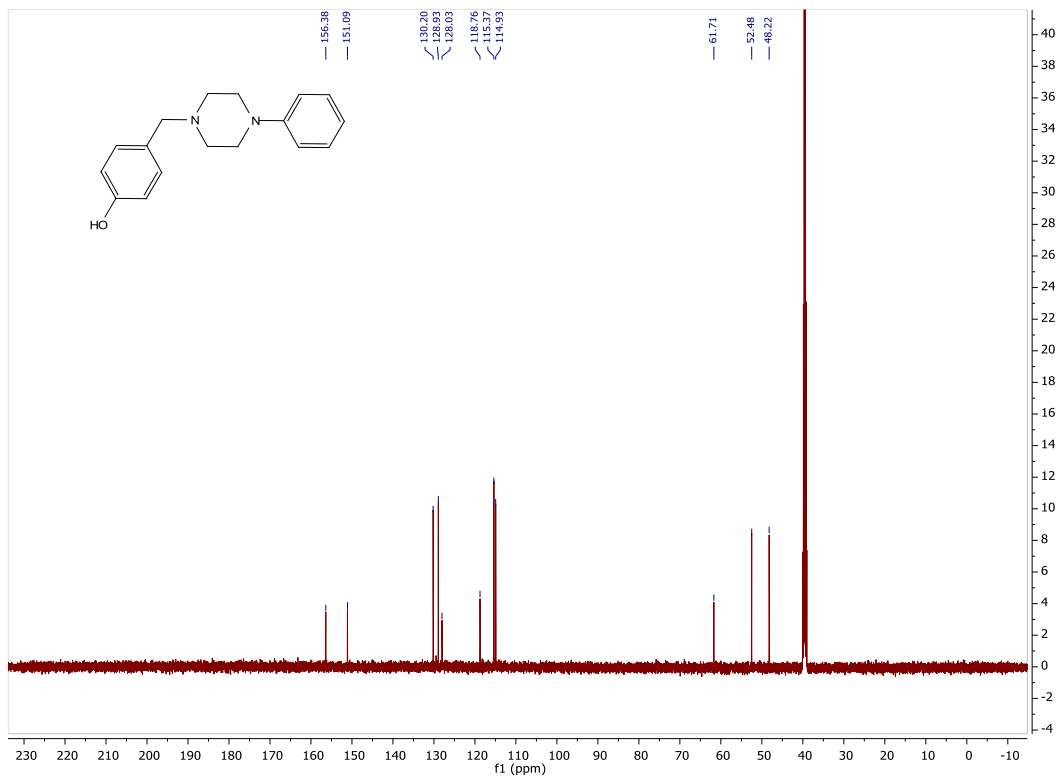
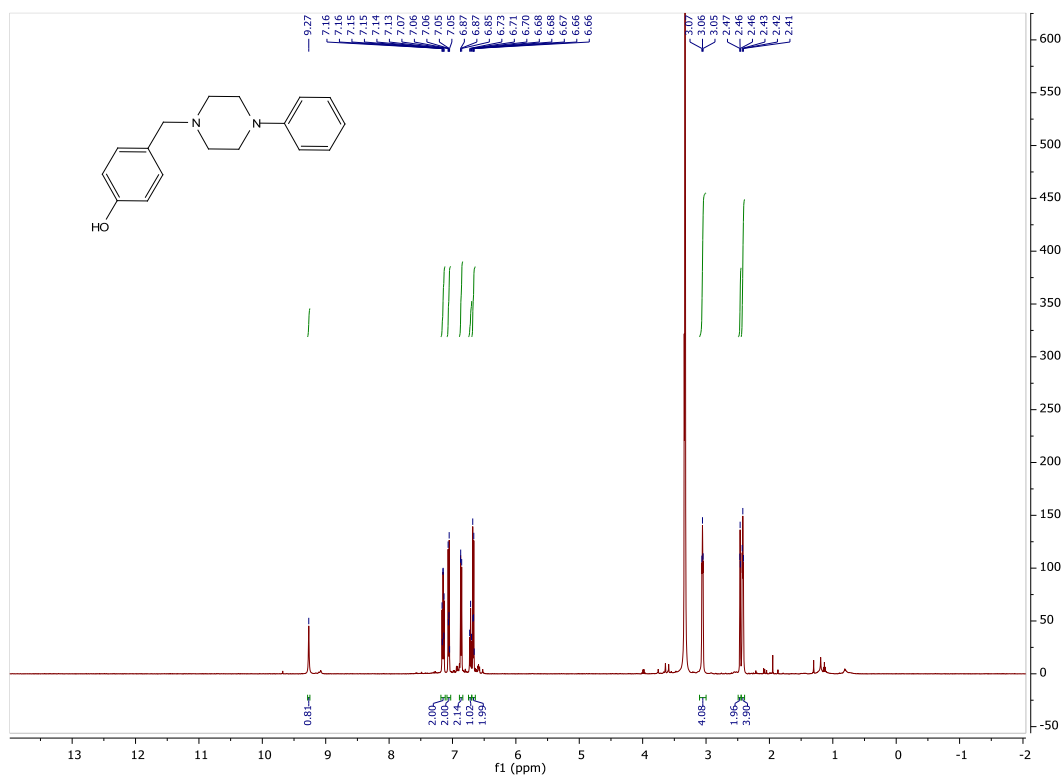


Figure 3.15 ^1H and ^{13}C NMR spectra of compound 3-4

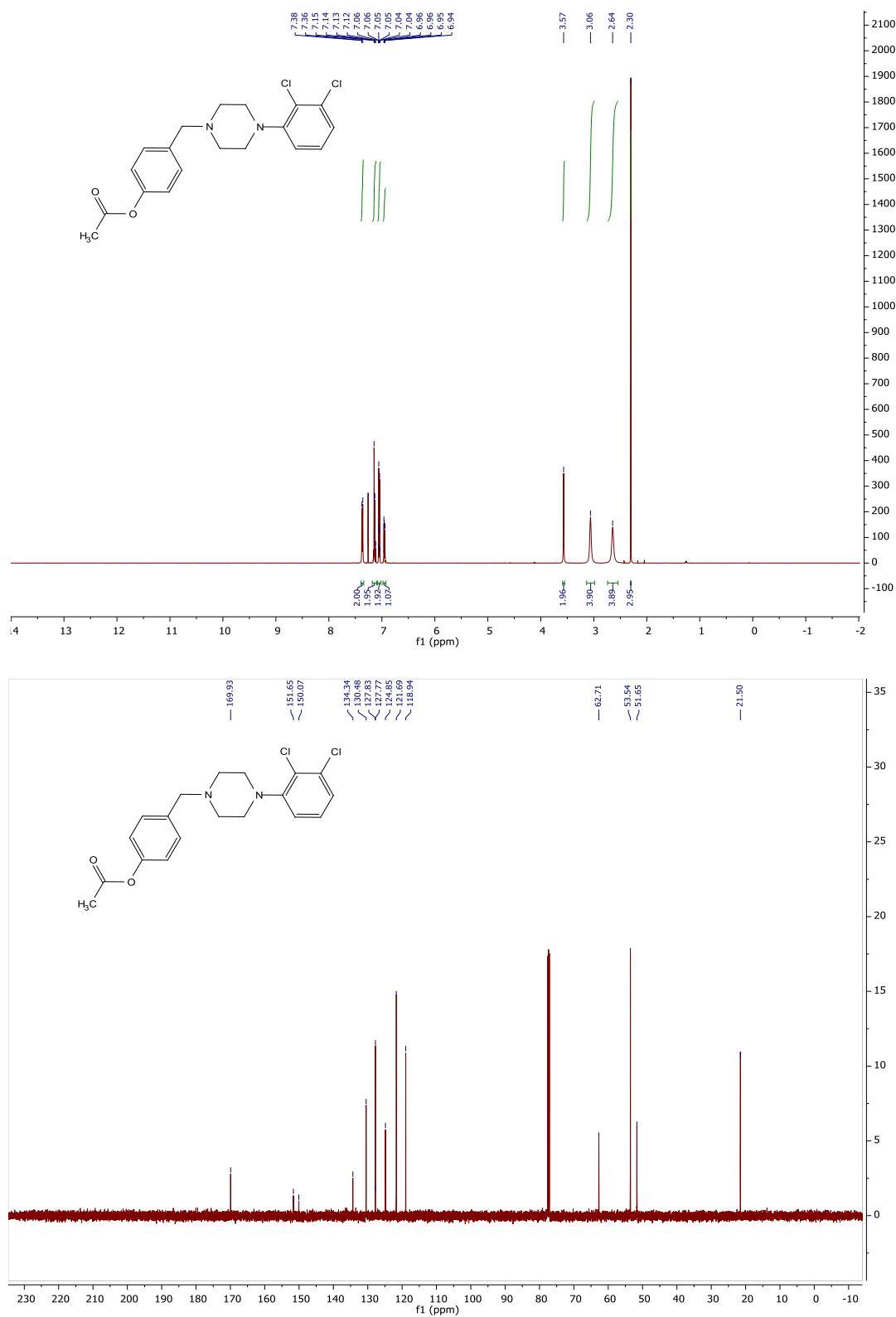


Figure 3.16 ^1H and ^{13}C NMR spectra of compound **3-5**

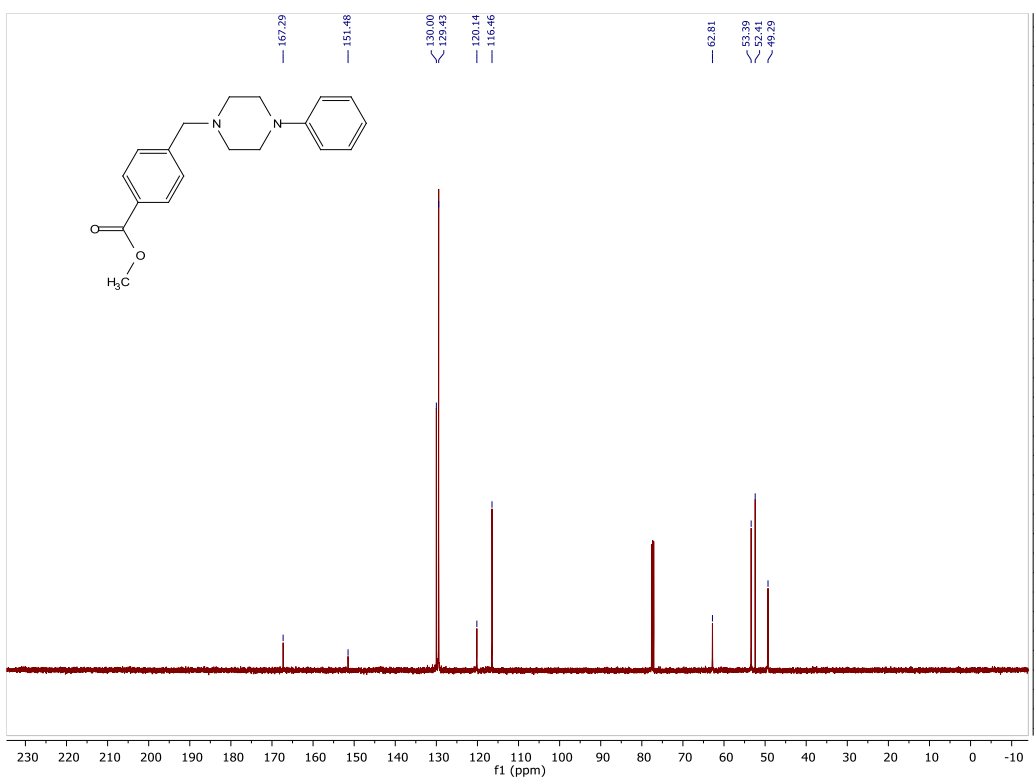
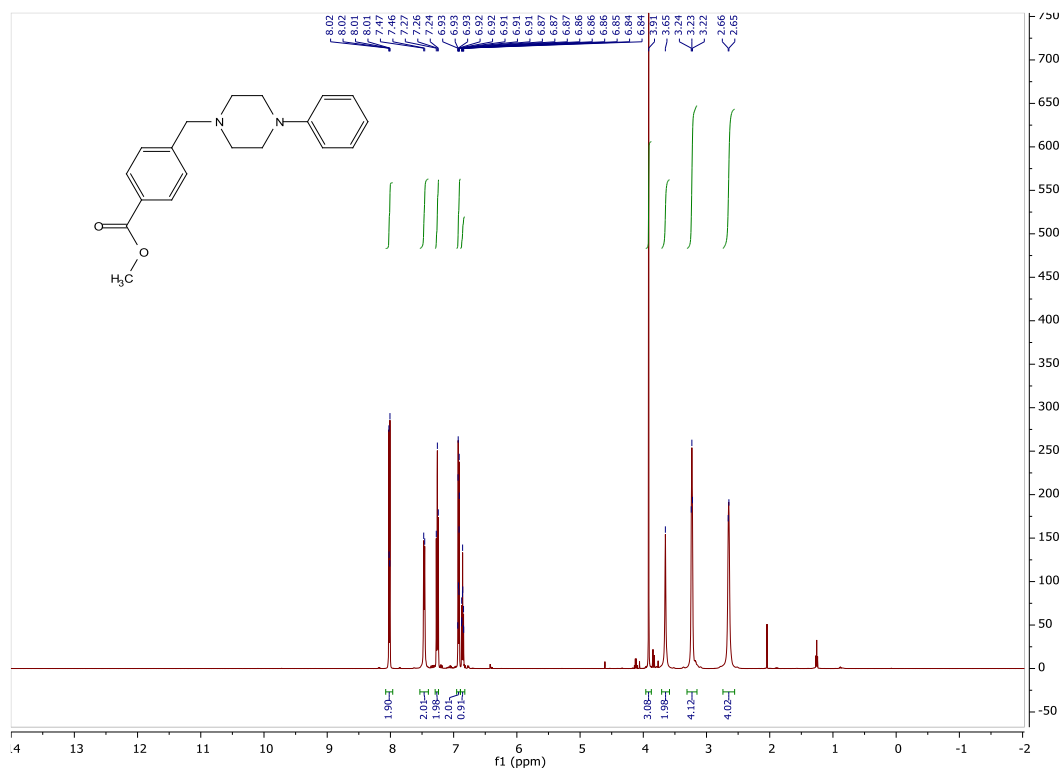


Figure 3.17 ^1H and ^{13}C NMR spectra of compound 3-6

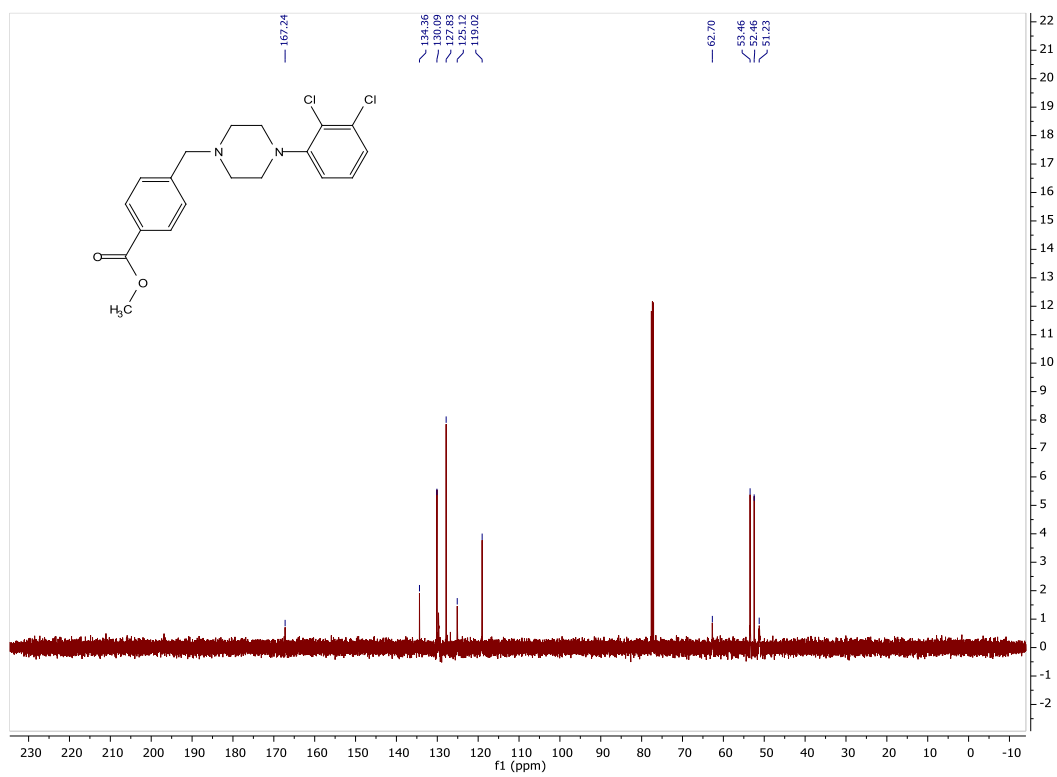
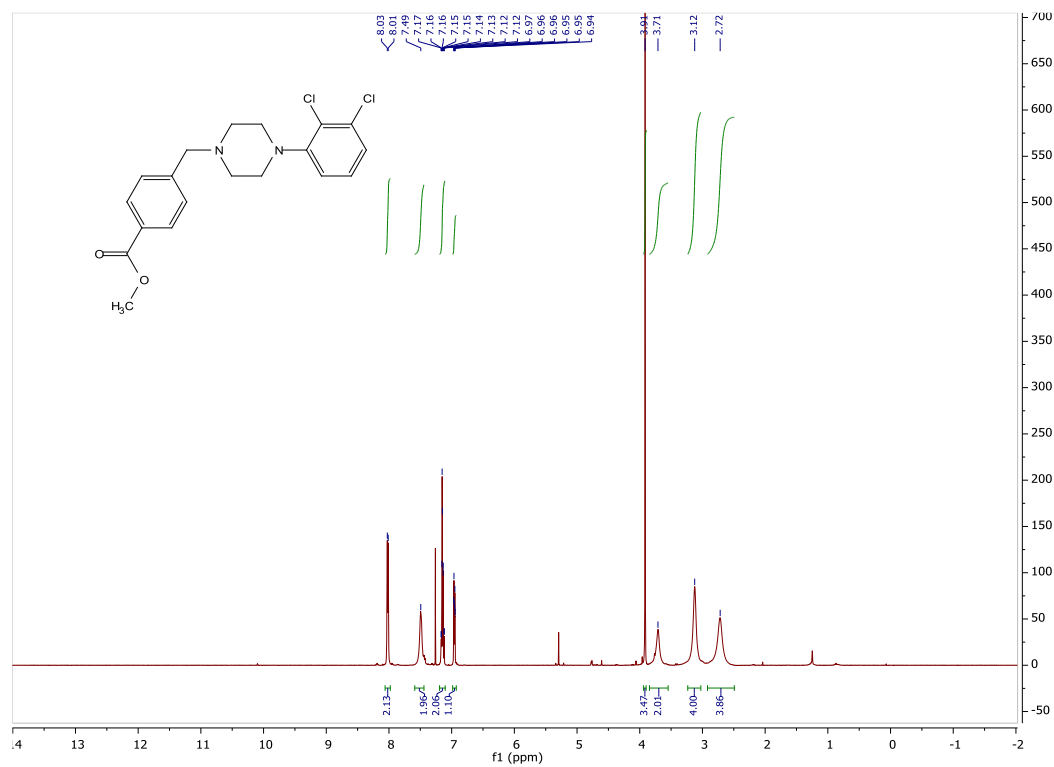


Figure 3.18 ^1H and ^{13}C NMR spectra of compound 3-7

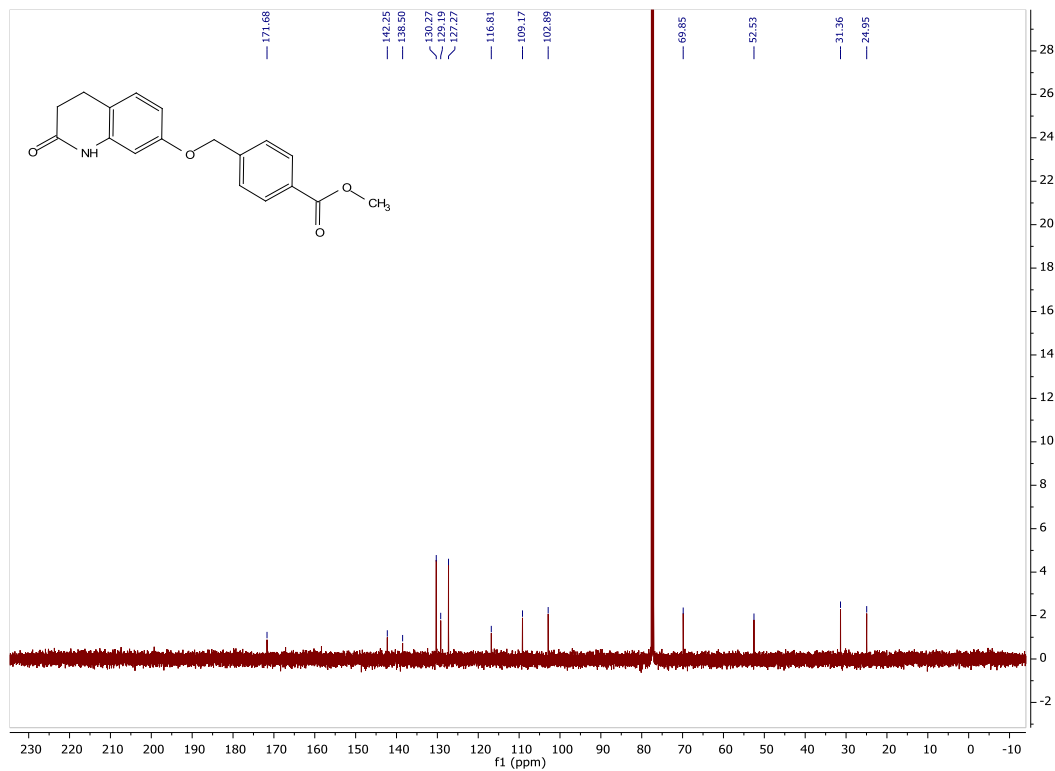
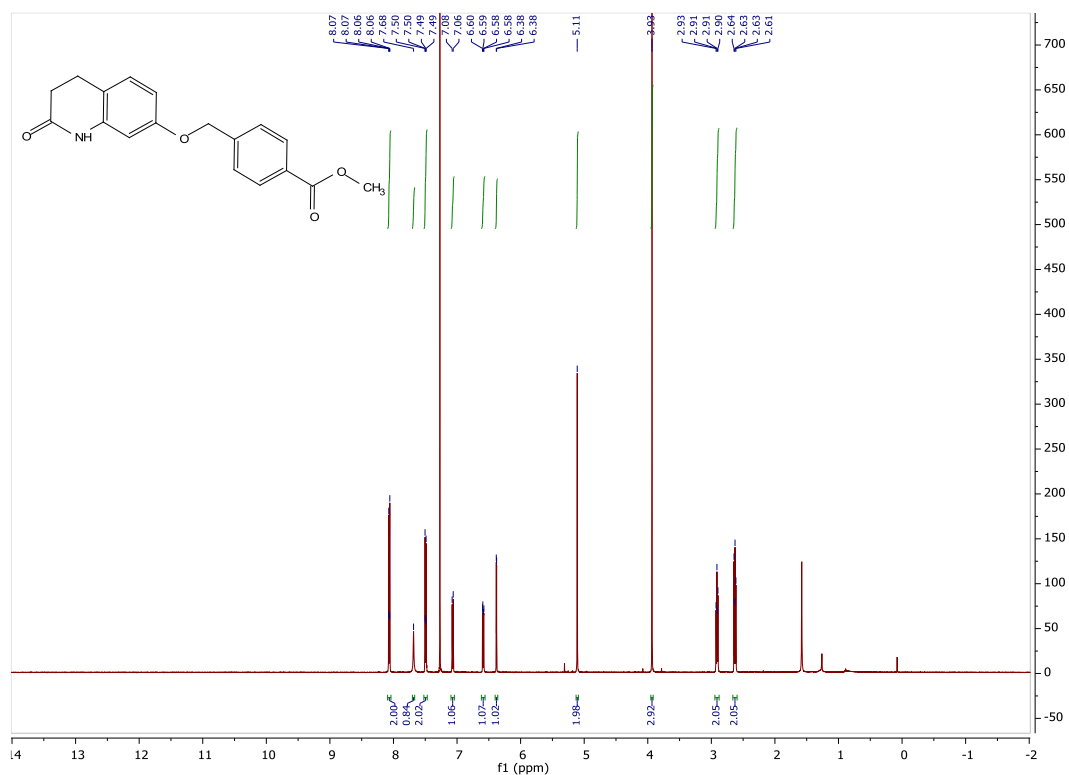


Figure 3.19 ^1H and ^{13}C NMR spectra of compound 3-8

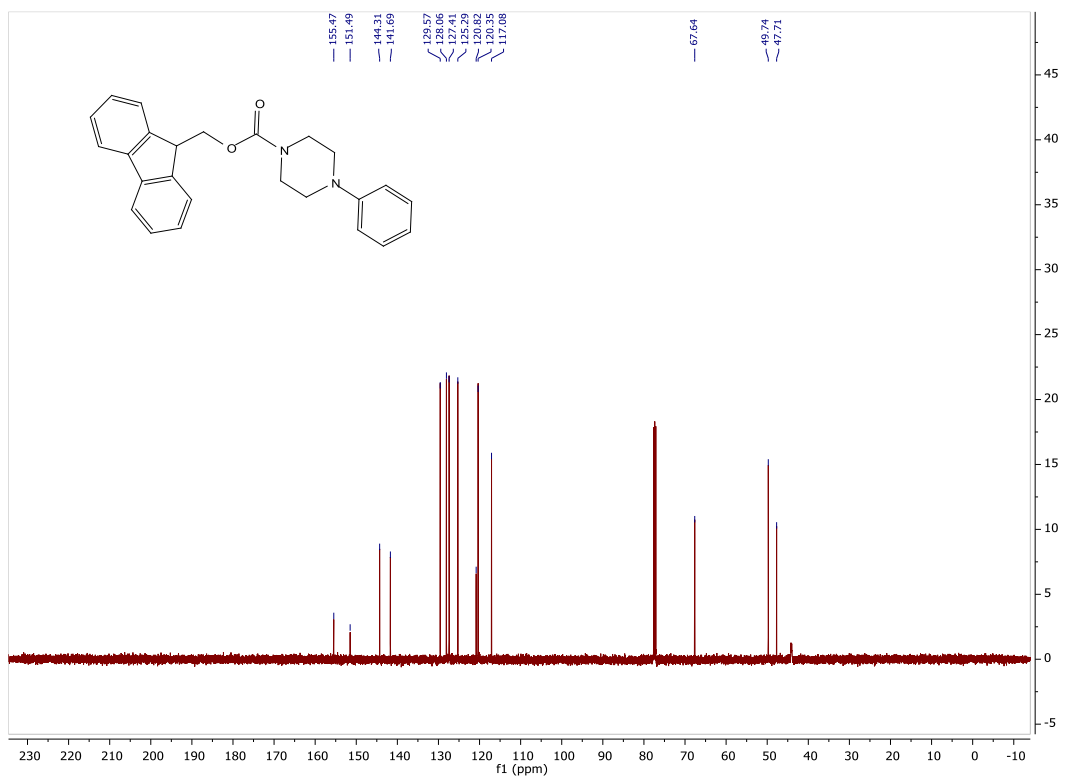
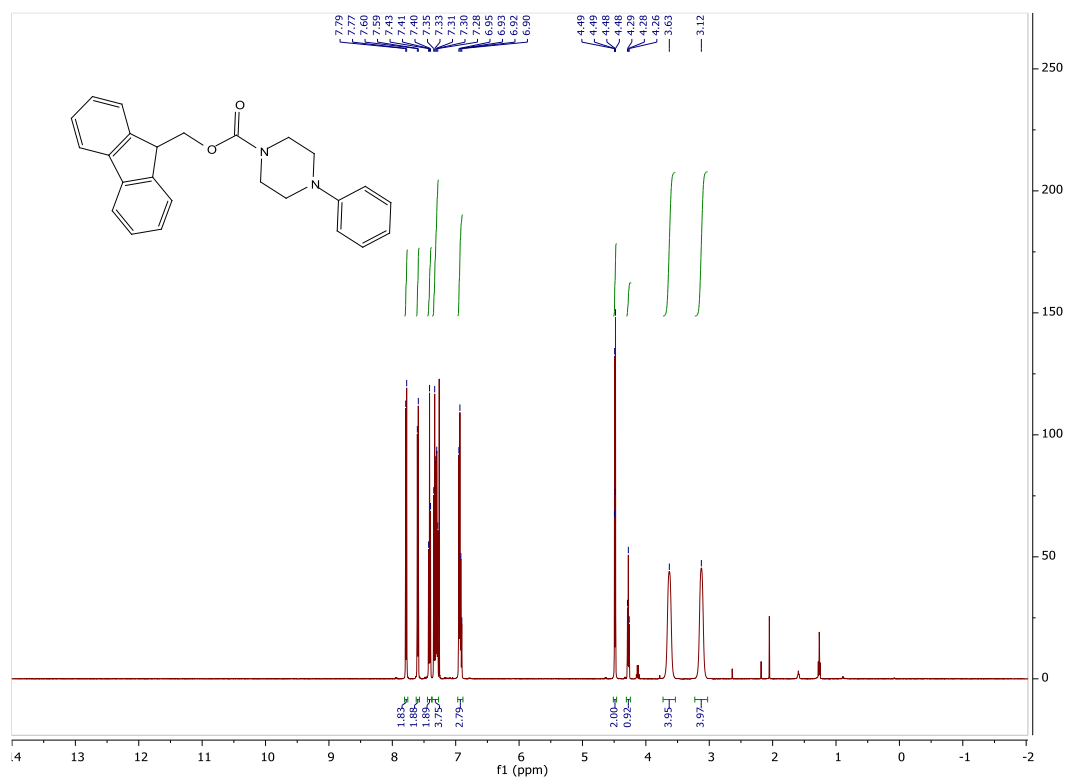


Figure 3.20 ^1H and ^{13}C NMR spectra of compound 3-9

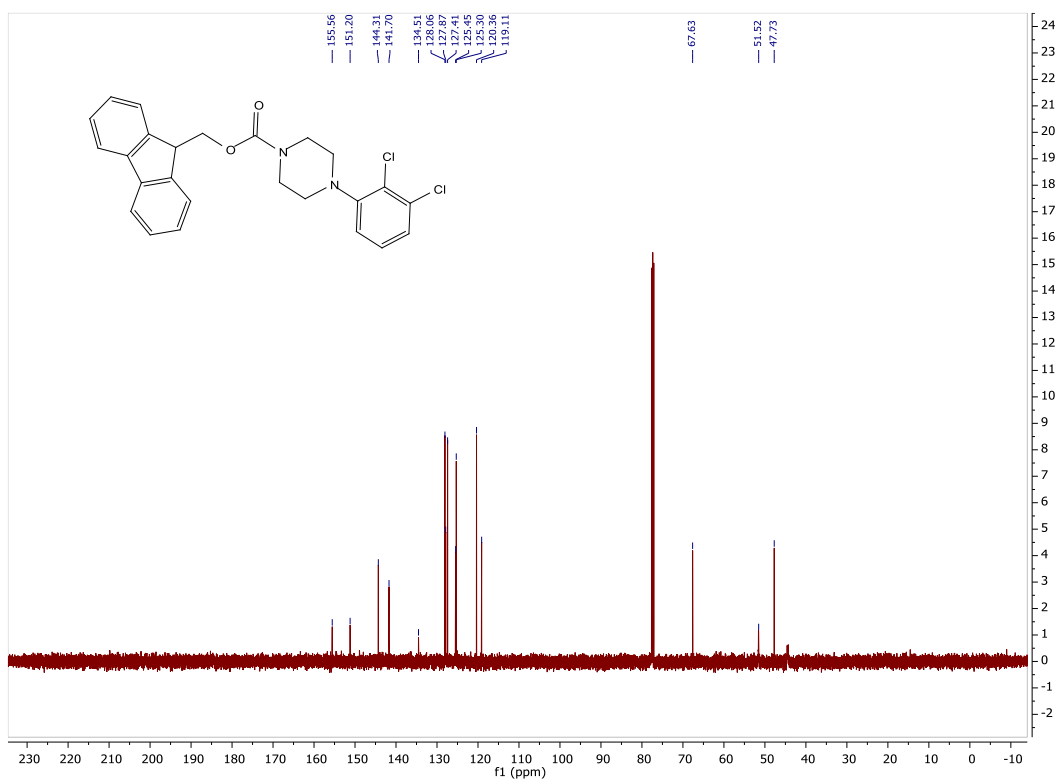
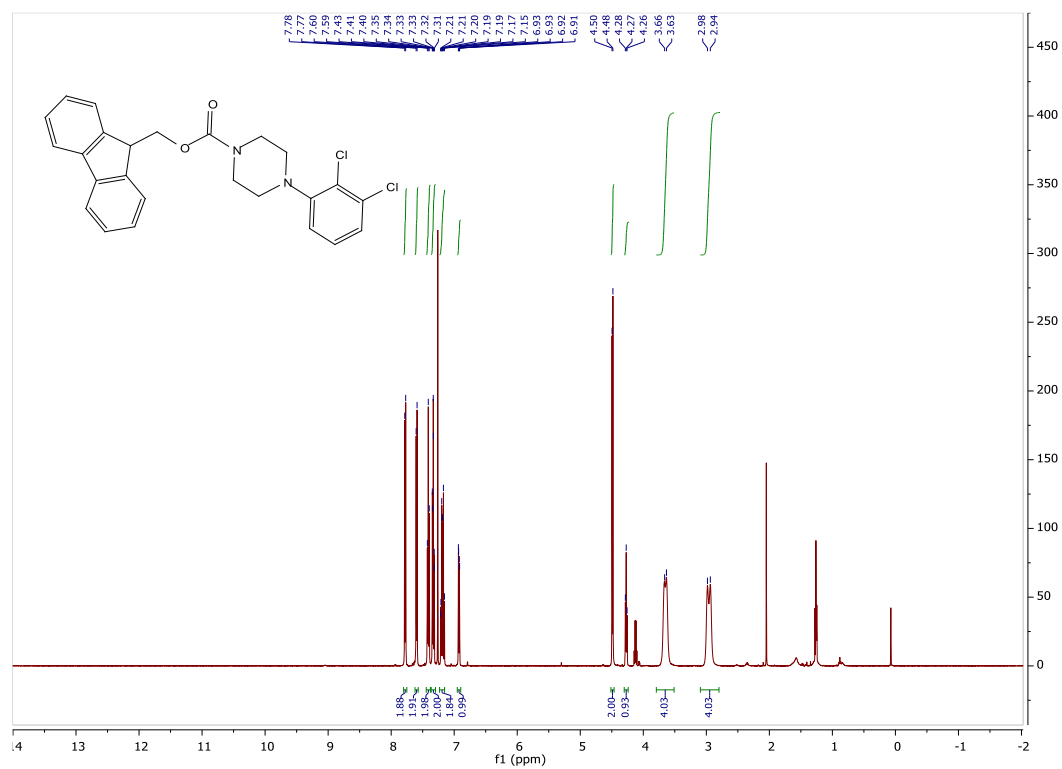


Figure 3.21 ^1H and ^{13}C NMR spectra of compound 3-10

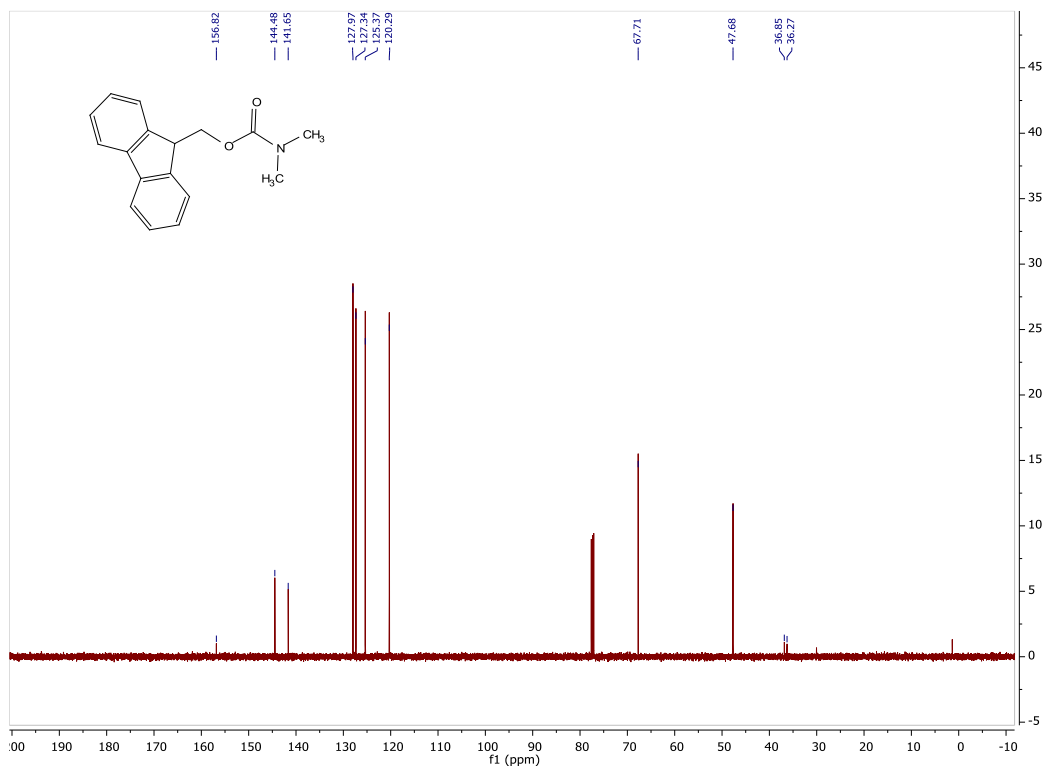
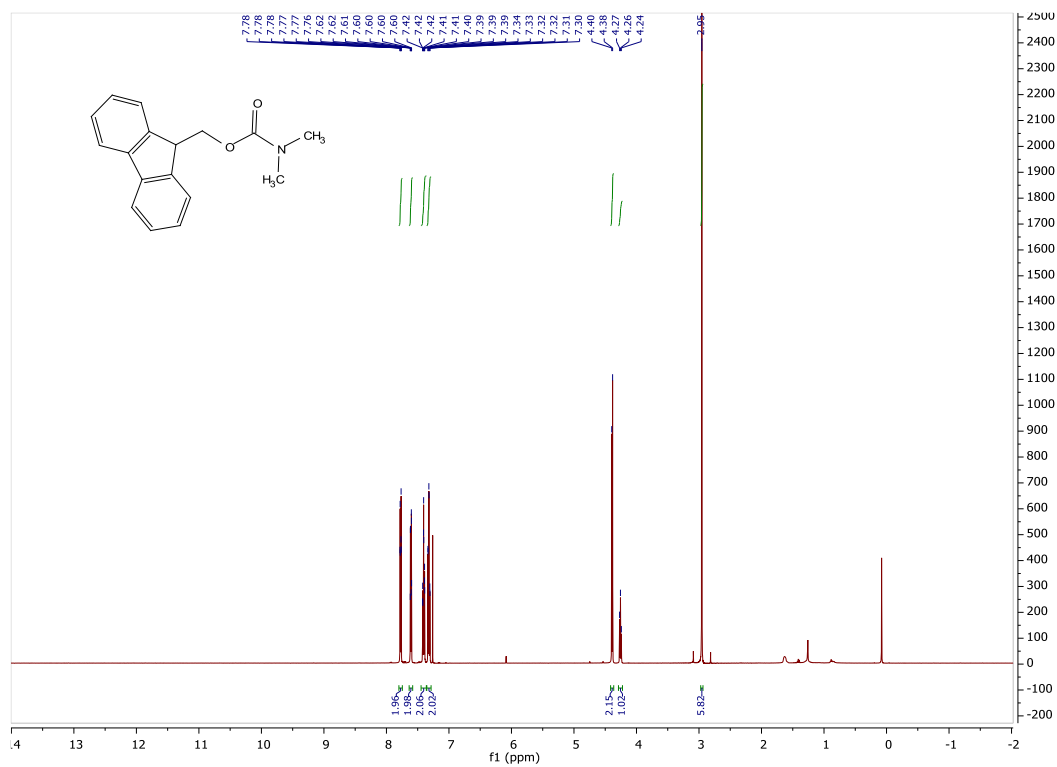


Figure 3.22 ¹H and ¹³C NMR spectra of compound 3-11

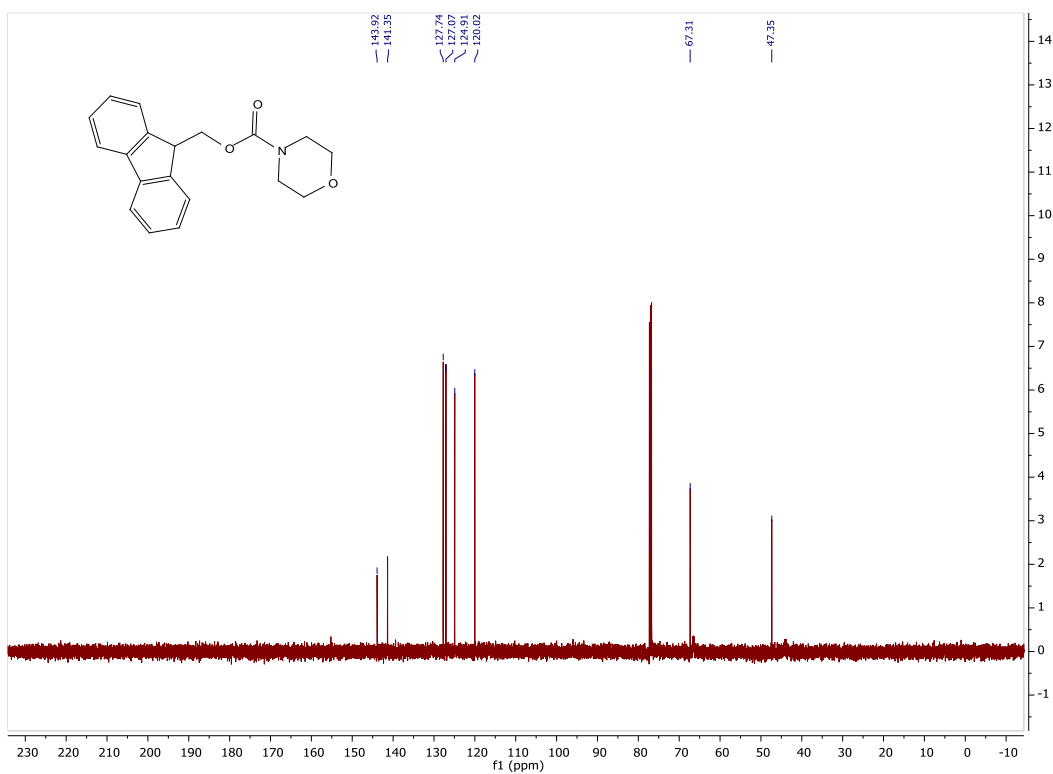
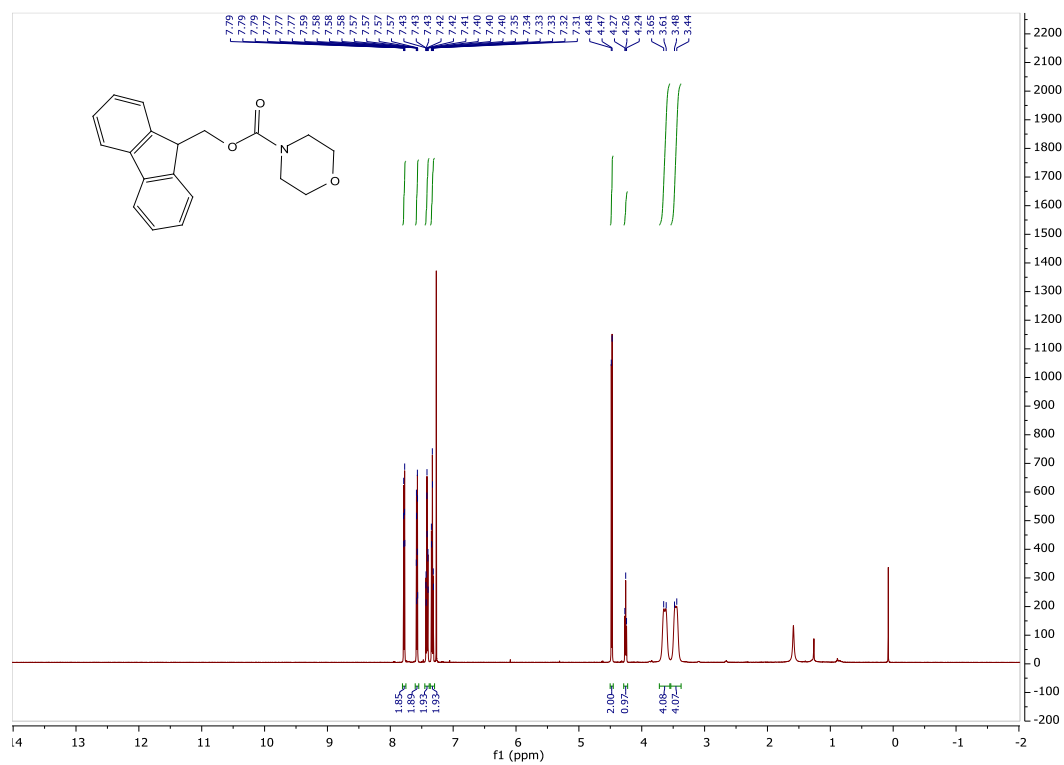
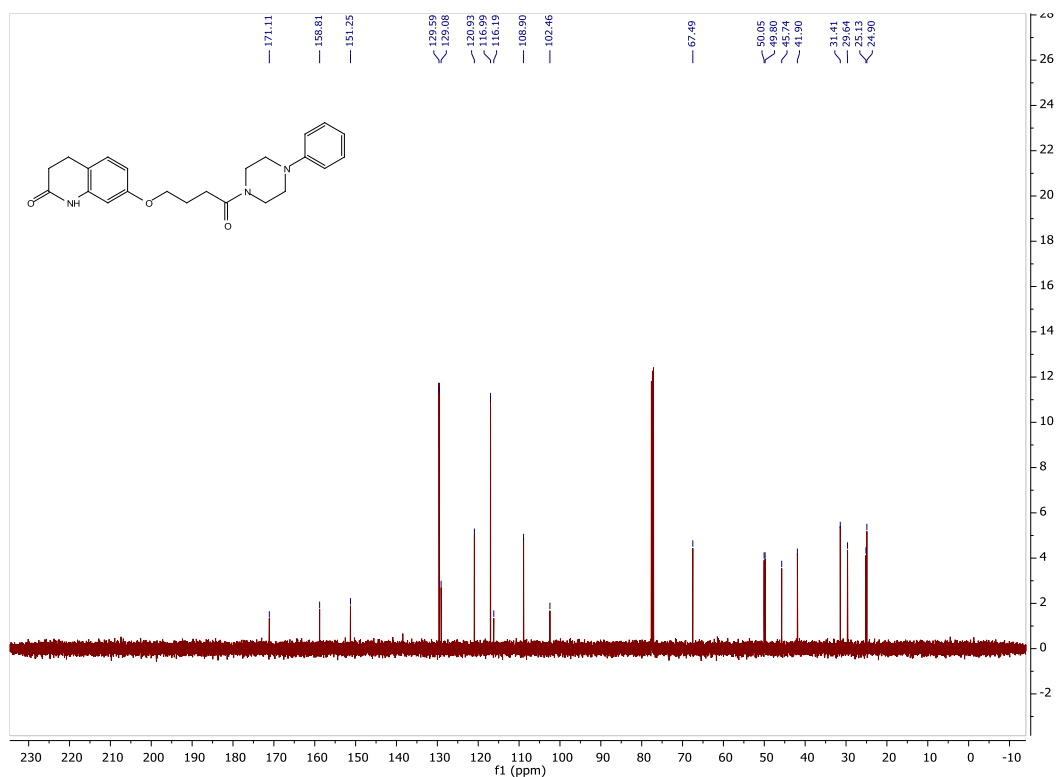
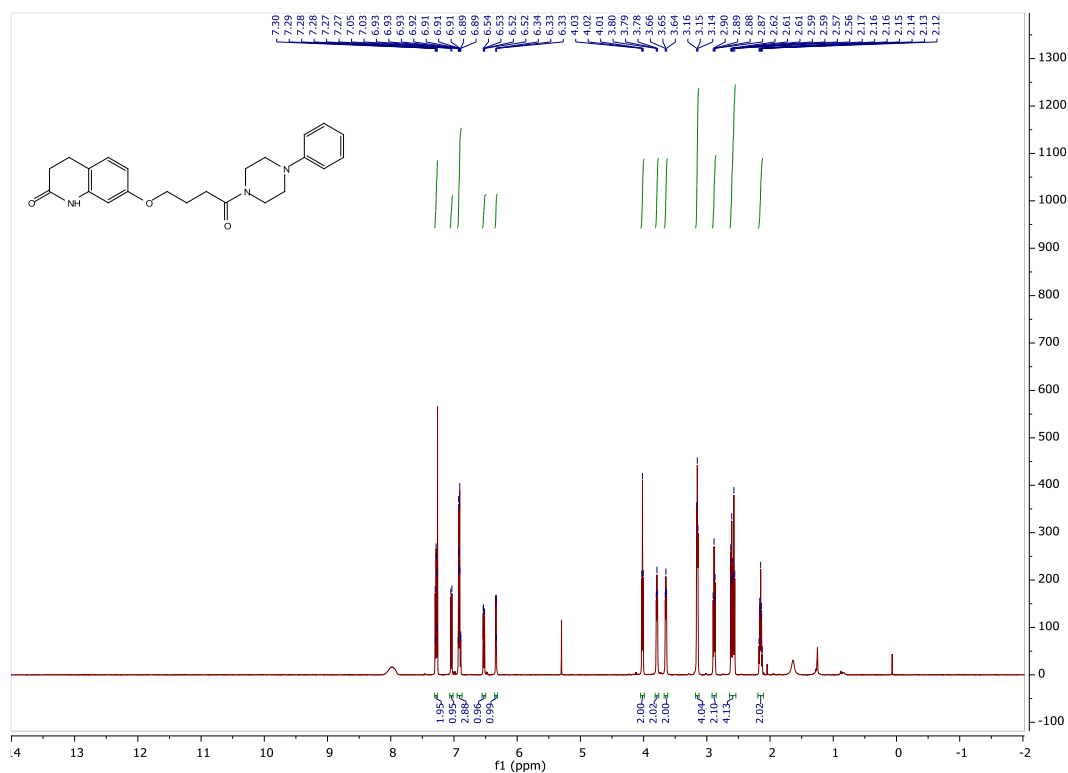


Figure 3.23 ¹H and ¹³C NMR spectra of compound 3-12



CHAPTER FOUR

Development of Neurodegenerative Disease Model Systems for Evaluating 20S Proteasome Activation as an Innovative Therapeutic Strategy

Reproduced in part with permission from **Fiolek J. Taylor**, Keel L. Katarina and Tepe J. Jetze. Fluspirilene Analogs Activate the 20S Proteasome and Overcome Proteasome Impairment by Intrinsically Disordered Protein Oligomers. *ACS Chem. Neurosci.* **2021**. Copyright 2021 American Chemical Society

4.1 Introduction

4.1.1 Background

The utility of small molecule activators of the 20S proteasome as biochemical tools for studying the proteasome is unquestionable, given the wide use of SDS for studying proteasome inhibition¹⁻³ and the proteasomes involvement in numerous essential biological pathways.⁴⁻¹¹ However, regarding their potential for use as therapeutics targeting neurodegenerative diseases, there remains much to be explored. Several recent studies have suggested this potential application of small molecule 20S proteasome activators and have begun to explore it in purified protein and cell-based systems.¹¹⁻¹⁸ These studies have made use of a variety of substrates, including IDPs that are associated with neurodegenerative disease pathogenesis, like α -synuclein and tau.^{11-13, 17} As a result, interest in this potential method for combating neurodegenerative diseases has grown, but several key questions remain unanswered regarding their potential in more disease relevant systems.

In neurodegenerative diseases, like Parkinson's disease and Alzheimer's disease, IDPs are known to exist in a variety of states of oligomerization and fibrilization. In fact, these various aggregate forms of IDPs are often considered hallmarks of the development of these diseases.¹⁹⁻³⁰ The mixture of IDP monomers, oligomers and large aggregates or fibrils seen in diseased systems represents a very different potential substrate and environment for the proteasome, when compared to purely monomeric IDPs. While the precise role that each form of these IDPs play within neurodegenerative disease pathogenesis is not fully understood, mounting evidence suggests that smaller oligomeric forms may represent the most toxic species, as opposed to the monomers, large aggregates, and fibrils.³¹⁻³⁷ Additionally, some forms of these IDP oligomers have been shown to directly inhibit the proteasome, which may contribute to their further accumulation, aggregation,

and disease progression.³⁸⁻⁴⁰ The complex nature of IDPs seen within neurodegenerative diseases necessitates that we address a couple of important questions regarding small molecule activation of the 20S proteasome. First, can small molecule activators of the 20S proteasome assist in maintaining its activity in the presence of inhibitory IDP oligomers? Secondly, can they effect the levels of accumulated IDP oligomers via 20S proteasome activation, or only the monomeric IDPs? Answering these questions, regarding the interplay of small molecule activators of the 20S proteasome and the various oligomeric forms of IDPs, is critical to better understand the potential of this therapeutic strategy.

In addition to the various forms of IDPs seen in neurodegenerative diseases, there are yet other compounding factors. For example, multiple cell types are affected during the progression of these diseases. In addition to neurons, there exist immune cells that are critical to healthy brain function and are sensitive to disruptions in brain homeostasis. The perturbation of this delicate system, as seen in neurodegenerative diseases, leads to the development of neuroinflammation.⁴¹⁻
⁴³ Neuroinflammation is deeply involved in the progression of neurodegenerative diseases, and while the extent to which it contributes to disease progression is not fully understood, it is widely thought to have a detrimental role.^{41, 44-47} Microglia, the primary native immune cells of the brain, are thought to be one of the key drivers of neuroinflammation in neurodegenerative disease pathogenesis.^{43, 48} IDPs that are released by degenerating neurons into the extracellular space can induce activation of microglia, leading to the secretion of pro-inflammatory signaling molecules, like cytokines, chemokines, and reactive oxygen species. The inflammation resulting from their release contributes to further neuron degeneration and death. This is thought to contribute to the initiation of a deleterious cycle of neuron degeneration, IDP release, and neuroinflammation, where each aspect further aggravates the others.^{41-43, 46, 49-52} Whether 20S proteasome activators

can break this cycle of increasing neuron degeneration and neuroinflammation is not yet known. Exploration of the effects of 20S activators on neurons, microglia and neuroinflammation will be necessary to fully understand their effects in diseased systems.

To address the questions posed above and push forward the development of small molecule activators of the 20S proteasome as therapeutics targeting neurodegenerative diseases, novel assays and disease models will need to be developed and implemented in their evaluation. Prior to the studies outlined here, there had been no published attempts at exploring the interplay between small molecule activators of the 20S proteasome and IDP oligomers that inhibit the proteasome.³⁸ Additionally, while some cell-based assays have been explored for validation of the activity of small molecule 20S proteasome activators, there remains a need for more neurodegenerative disease relevant models in which they can be evaluated.¹¹⁻¹⁸ Furthermore, what effect these 20S proteasome activators might have on neuroinflammation, seen in the development of these diseases, has yet to be explored.^{41, 44-47} Considering the complex nature of these diseases, involving numerous forms of IDPs and cell types, much work remains to be done to validate this proposed therapeutic strategy.

To this end, I sought to begin to address some of these questions surrounding the potential of small molecule activators of the 20S proteasome as a therapeutic strategy for treating neurodegenerative diseases, by developing novel assays and models to expand our experimental program. To begin this effort, I followed work done by the Smith group, that demonstrated IDP oligomer-mediated inhibition of the proteasome³⁸ and worked to explore the effects of 20S activators in similar systems. My hypothesis was that small molecule activators of the 20S proteasome can maintain 20S proteasome activity in the presence of inhibitory IDP oligomers, thus helping to reestablish proteostasis (**Fig. 4.1**). Additionally, I explored the effects of 20S

activators in a cell-based model of familial Parkinson's disease, making use of the A53T mutant form of α -synuclein.⁵³⁻⁵⁵ Finally, I wanted to ensure that the 20S activators are not going to have a detrimental effect on disease relevant cell types and begin to explore their effects on neuroinflammation. For this, I evaluated their effect on the viability of immortalized microglia and on IDP-induced release of the inflammatory cytokine TNF- α , by the same cells. I will also briefly outline efforts made towards the development of other tools and model systems for use in future studies by the Tepe lab, focused on furthering our ability to evaluate the potential of this therapeutic strategy.

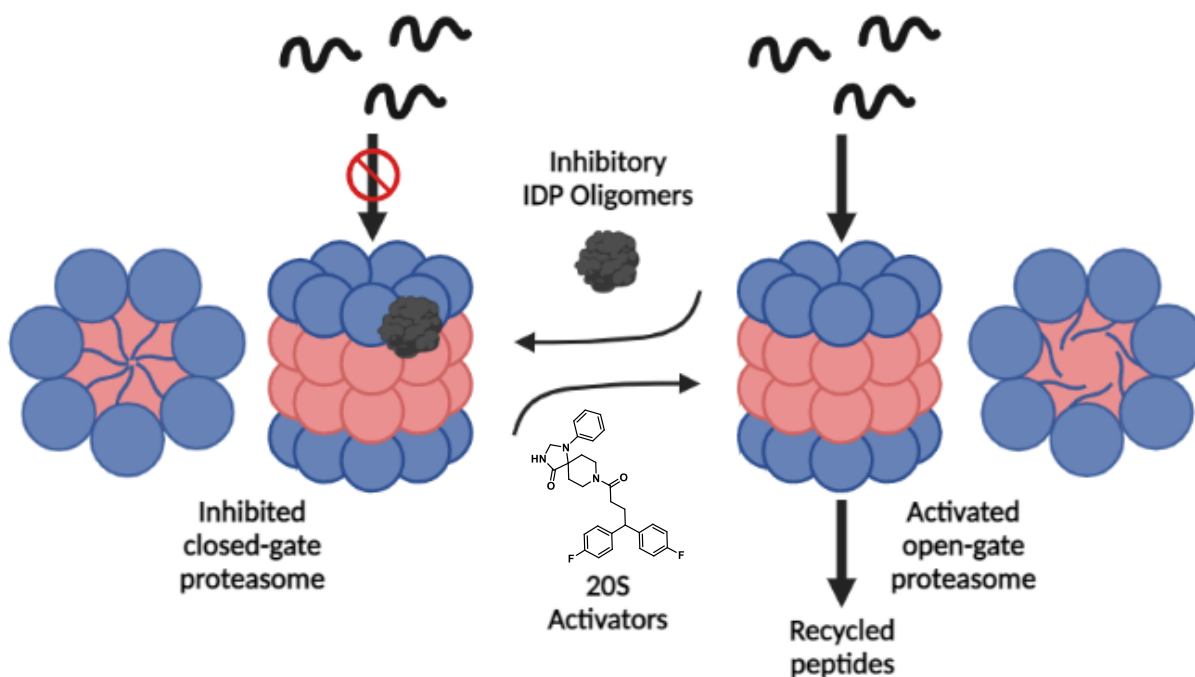


Figure 4.1: Cartoon of proposed inhibition of 20S activity by IDP oligomers³⁸ and activation via small molecule activators being developed by the Tepe lab.^{12, 13, 17, 56}

4.1.2 Objective

The goals of these studies were: (1) investigate the interplay between small molecule 20S proteasome activators and inhibitory IDP oligomers, (2) develop novel methods, tools, and cell-based models to further demonstrate the potential of small molecule 20S proteasome activation as an innovative therapeutic strategy targeting neurodegenerative diseases, (3) explore the effects of 20S proteasome activators on microglia and neuroinflammation induced by α -synuclein.

4.2 Results and Discussion

4.2.1 20S activators maintain activity in the presence of inhibitory α -synuclein oligomers

In neurodegenerative diseases, like Alzheimer's disease and Parkinson's disease, proteasome impairment is a major contributor to the accumulation of neurotoxic IDP oligomers.⁵⁷⁻

⁶⁸ In fact, it was recently shown that IDP oligomers associated with neurodegenerative diseases, such as α -synuclein, amyloid β , and Huntingtin protein, can directly inhibit the 20S proteasome.^{38,}

⁴⁰ This IDP oligomer-induced 20S proteasome impairment has the potential to contribute to further accumulation of the IDPs, thus promoting disease progression. I hypothesized that small molecule 20S proteasome activators can protect against IDP-mediated impairment of the 20S proteasome, and as a result may assist in reestablishing the clearing of IDPs. If IDP clearance by the proteasome can be reestablished and free IDP levels can be reduce, then proteostasis can begin to be reestablished as well.

To monitor the effects of small molecule 20S proteasome activators, like TCH-165, Fluspirilene and *N*-acylated Fluspirilene, on an IDP oligomer-impaired 20S proteasome I followed work published by the Smith group.³⁸ Briefly, purified 20S proteasome was incubated with the compounds and an aggregate mixture of α -synuclein (purchased from Novus Biologicals) was introduced prior to addition of a fluorogenic peptide substrate (CT-L). Consistent with their

findings,³⁸ it was found that the α -synuclein aggregate mixture significantly reduced 20S-mediated proteolysis of the fluorogenic peptide substrate (**Fig. 4.2**). Excitingly, it was also found that the 20S proteasome activators TCH-165, Fluspirilene and *N*-acylated Fluspirilene, were each able to maintain 20S proteasome activity in the presence of the mixed α -synuclein aggregates, in a concentration dependent manner (**Fig. 4.2**).

These findings were very exciting, because prior to this experiment no one had explored the interplay between inhibitory IDP oligomers and small molecule activators of the 20S proteasome. It was previously unknown whether small molecule activators of the 20S proteasome would have any effect on its activity in the presence of an inhibitory IDP species, such as these mixed α -synuclein aggregates. This represents a promising step towards validating the potential of this method, considering that in neurodegenerative disease afflicted systems there will likely be a variety of IDP species, including inhibitory oligomeric forms.^{19-30, 38-40} So, for 20S proteasome activators to have substantial effects on neurodegenerative disease progression, they must still affect 20S proteasome activity in such a system.

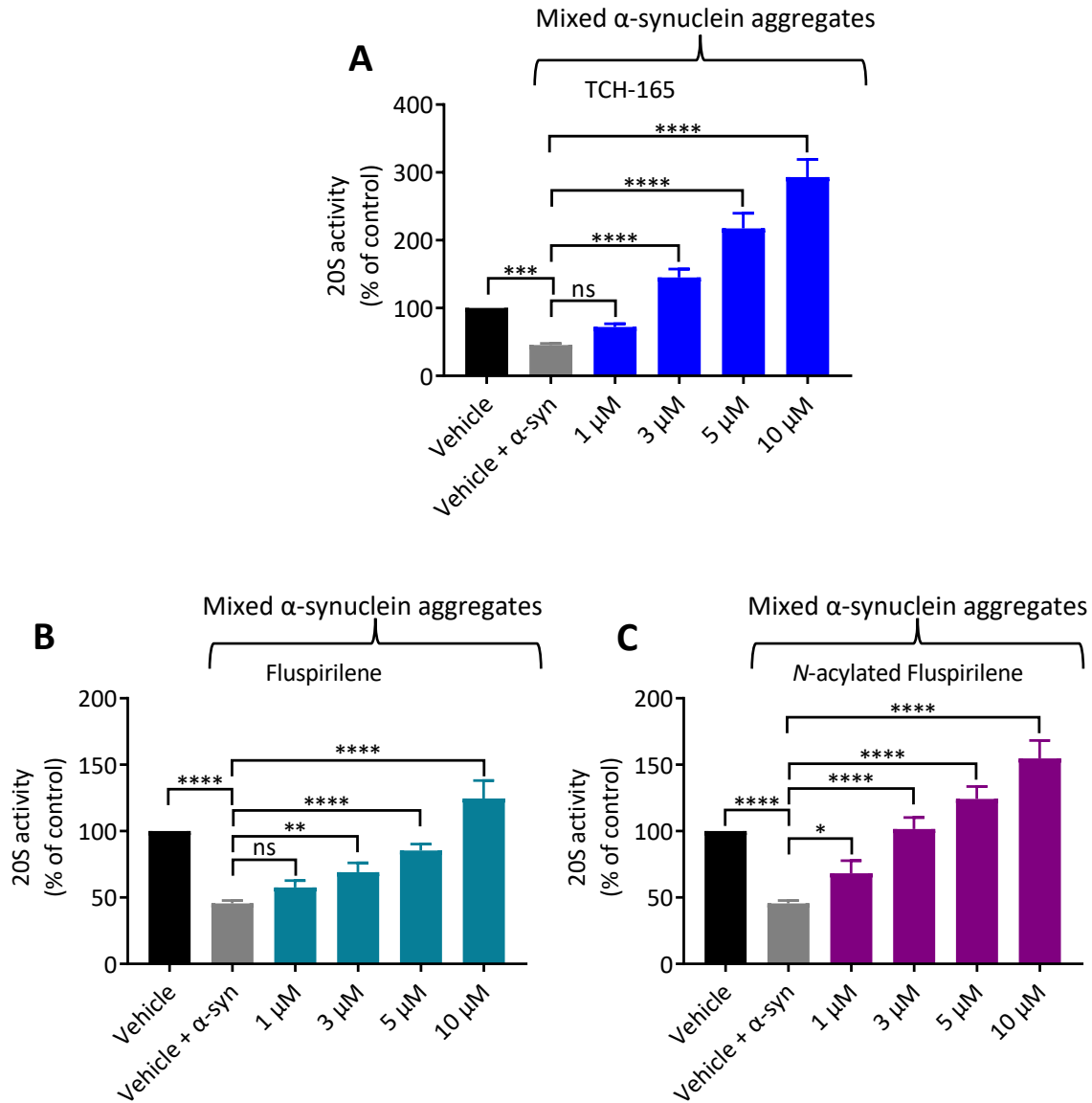


Figure 4.2: 20S proteasome activators maintain 20S activity in the presence of inhibitory α -synuclein oligomers. 20S proteasome-mediated degradation of a fluorogenic peptide substrate (CT-L) impaired by α -synuclein mixed aggregates in the presence of a concentration-gradient of (A) TCH-165, (B) Fluspirilene, or (C) N-acylated Fluspirilene. These data were collected in triplicate (n=3). Error bars denote standard deviation. One-way ANOVA statistical analysis was used to determine statistical significance. (ns=not significant, *p<0.05, **p<0.01, ***p<0.001, ****p<0.0001).

It should be noted that differences in level of activity were seen between TCH-165 and the Fluspirilene analogues tested here, especially at higher concentrations (**Fig. 4.2**). Several factors could contribute to these differences, including which inter-subunit pocket they interact with ($\alpha 1/2$ for TCH-165¹³ and $\alpha 2/3$ for the Fluspirilenes (**Chapter 3**)), interactions between the small molecules and the oligomers, their normal differences in activity levels, or some combination thereof. Studies being undertaken by other members of the Tepe lab may shed light on these differences in activity going forward, but that is beyond the scope of this work.

4.2.2 20S activators maintain 20S activity in the presence of inhibitory Abeta oligomers

Similar to what is seen in Parkinson's disease with α -synuclein accumulation and oligomerization, in Alzheimer's disease the IDP amyloid β is known to accumulate and aggregate.^{23, 29, 38, 69-72} This effect is thought to similarly contribute to disease progression, although the exact mechanisms are not fully understood, as with Parkinson's disease. As was mentioned above, Smith and co-workers were able to demonstrate that mixed amyloid β oligomers were also able to directly inhibit the activity of the proteasome *in vitro*.³⁸ While this inhibition across the different IDPs in their study seemed to be similar, it is possible that the exact interactions taking place could be varied. As a result, it is possible that the interplay between different inhibitory IDP oligomers and 20S proteasome activators could be varied. I hypothesized that the 20S proteasome activators TCH-165, Fluspirilene and *N*-acylated Fluspirilene could also maintain 20S proteasome activity in the presence of amyloid β mixed aggregates, like what was seen with α -synuclein. This would further support the hypothesis that small molecule 20S proteasome activation is a promising method by which to address the problem of IDP accumulation and aggregation in multiple neurodegenerative diseases that share similarities in terms of IDP accumulation and aggregation but differ in the IDP that is associated with their pathogenesis.

For this study, amyloid β mixed aggregates were generated following literature precedence.^{38, 73} Briefly, synthetic amyloid β (1–42) (purchased from Eurogentec) was dissolved in 100% hexafluoroisopropanol (HFIP) and incubated at 37 °C for 2 hours to remove any pre-existing aggregates. The HFIP was removed via lyophilization, and the resulting peptide films were stored at –80 °C until use. Aggregate mixtures were prepared by resuspending amyloid β films in DMSO, followed by addition of ultrapure H₂O and rapid addition of 2 M Tris-base at pH 7.6. The solution was then briefly vortexed and allowed to incubate at room temperature for 5 min. The amyloid β aggregate mixture was then diluted to the desired concentration and used immediately. Following generation of the mixed amyloid β aggregates, the same procedure that was used for generating the data seen in **Fig. 4.3** was followed, except the addition of α -synuclein mixed aggregates was replaced with the amyloid β aggregate mixture.

Consistent with the findings of Smith and co-workers³⁸ and my own findings with α -synuclein mixed aggregates (**Fig. 4.2**), the amyloid β aggregate mixture also inhibited the 20S proteasome's ability to degrade the fluorogenic peptide substrate (**Fig 4.3**). Additionally, as was found with α -synuclein, the 20S proteasome activators (TCH-165, Fluspirilene or *N*-acylated Fluspirilene) maintained 20S proteasome activity in the presence of the amyloid β aggregates, in a concentration-dependent manner. At the higher concentrations (3–10 μ M depending on the activator) each 20S activator was able to achieve levels of activity on par with or above that of the untreated 20S proteasome control, for both the α -synuclein and amyloid β treated 20S proteasomes (**Fig. 4.2 and Fig. 4.3**).

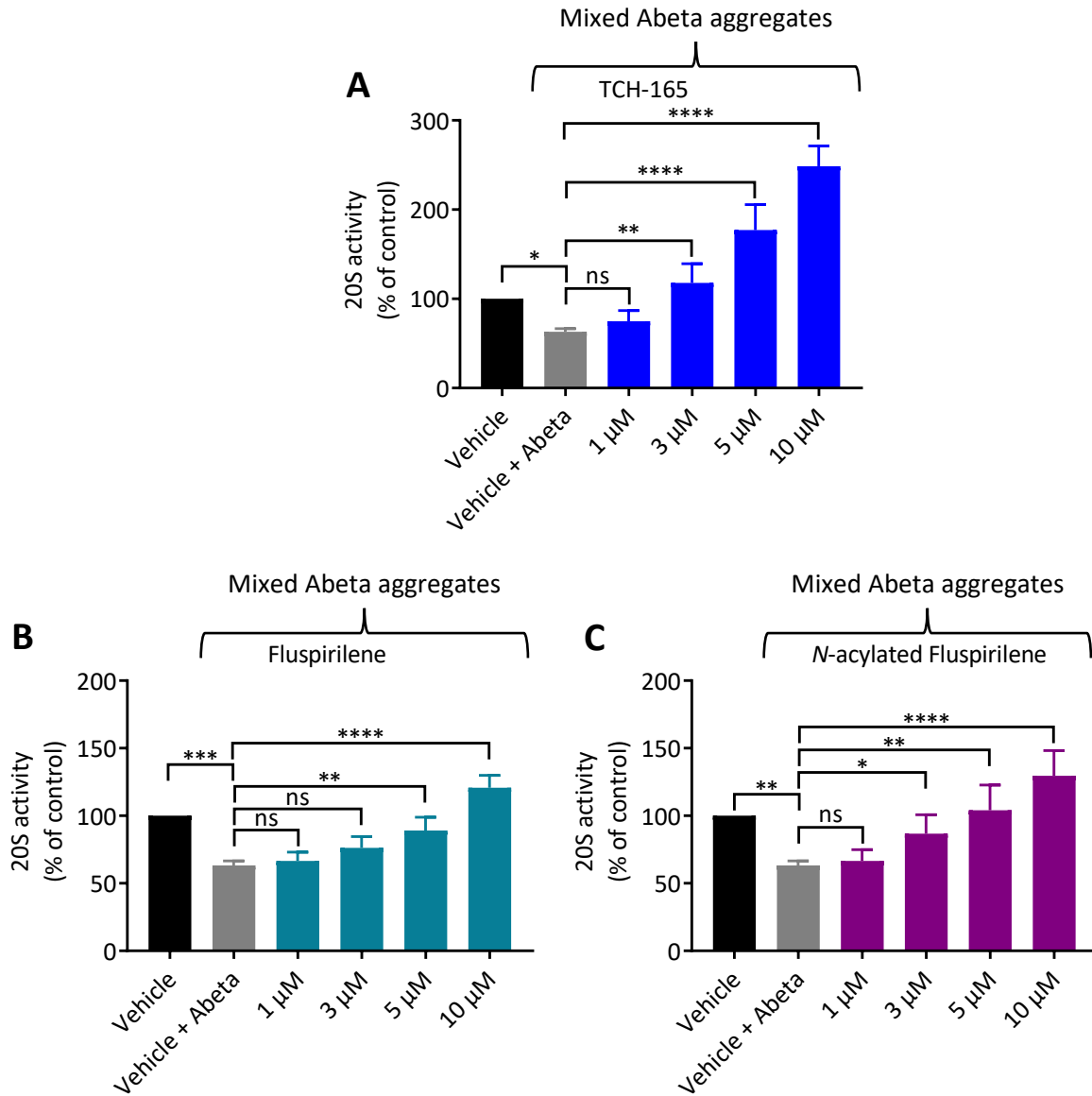


Figure 4.3: 20S proteasome activators maintain 20S activity in the presence of inhibitory amyloid β oligomers. 20S proteasome-mediated degradation of fluorogenic peptide substrate (CT-L) impaired by amyloid β mixed aggregates in the presence of a concentration-gradient of (A) TCH-165, (B) Fluspirilene, or (C) *N*-acylated Fluspirilene. These data were collected in triplicate ($n=3$). Error bars denote standard deviation. One-way ANOVA statistical analysis was used to determine statistical significance. (ns=not significant, $*p<0.05$, $**p<0.01$, $***p<0.001$, $****p<0.0001$).

The results obtained for both experiments were very encouraging and suggested that 20S proteasome activators have the potential to preserve 20S proteasome activity at or above normal levels in diseased systems where inhibitory IDP oligomers are present. These data represent the first examples of 20S proteasome small molecule activators being used in conjunction with IDP oligomers. To further investigate the interplay between 20S activators and oligomeric IDPs that can inhibit the 20S proteasome, I wanted to examine what effects the activated 20S proteasome was having on the IDPs themselves.

4.2.3 Fluspirilene analogues reduce monomeric and oligomeric α -synuclein *in vitro*

IDP oligomers, like those that inhibit the 20S proteasome,³⁸⁻⁴⁰ are thought to exist in a dynamic equilibrium with the monomeric form.^{25, 71, 74, 75} According to the studies by Smith and co-workers, the medium size oligomers (~50 kDa) were the species responsible for the proteasome inhibition, not the monomeric forms or larger aggregates.³⁸ I hypothesized that small molecule 20S activators can maintain its activity in the presence of these inhibitory species, enhance 20S-mediated degradation of monomeric α -synuclein, and shift the equilibrium towards formation of monomers, thus indirectly reducing the inhibitory medium sized oligomers.³⁸

This was explored by examining α -synuclein oligomer levels after an incubation of 24 hours with 20S proteasome, pretreated with either Fluspirilene, *N*-acylated Fluspirilene, or vehicle control (DMSO). The remaining α -synuclein monomers and oligomers were visualized using western blot, and the medium sized oligomers (as indicated within the green box, **Fig. 4.4A and B**) were quantified (**Fig. 4.4C and D**). It was found that the addition of Fluspirilene or *N*-acylated Fluspirilene led to a significant concentration-dependent reduction in remaining inhibitory α -synuclein oligomers, relative to the vehicle control (**Fig. 4.4C and D**). This is the first evidence that small molecule 20S proteasome activation can influence levels of oligomeric IDP.

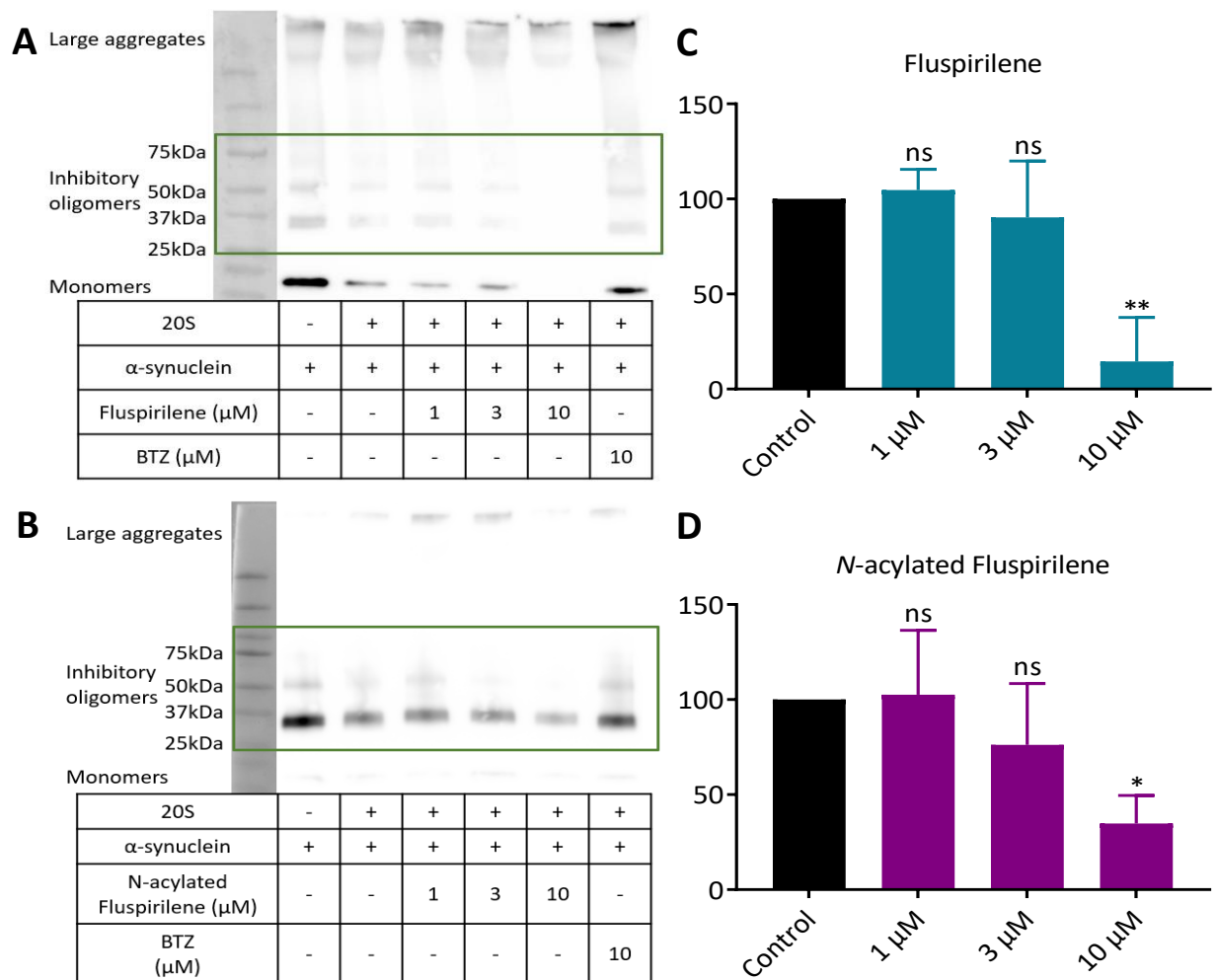


Figure 4.4: Fluspirilene and N-acylated Fluspirilene reduce monomeric and oligomeric α -synuclein *in vitro*. (A) Western blot analysis of 20S proteasome-mediated α -synuclein oligomer digestion with Fluspirilene (1, 3 or 10 μ M) and (C) quantification of remaining oligomeric α -synuclein. Densitometry of Fluspirilene α -synuclein oligomer digestions done using image J (n=3). (B) Western blot analysis of 20S proteasome-mediated α -synuclein oligomer digestion with N-acylated Fluspirilene (1, 3 or 10 μ M) and (D) quantification of remaining oligomeric α -synuclein. Densitometry of N-acylated Fluspirilene α -synuclein oligomer digestions done using image J (n=4). Error bars denote standard deviation. One-way ANOVA statistical analysis was used to determine statistical significance (ns=not significant, (*p<0.05, **p<0.01).

These studies (**Figs. 4.2 – 4.4**) demonstrate the potential of 20S activators to assist in reestablishing proteostasis in systems where inhibitory IDP oligomers are present, as seen in many neurodegenerative diseases, by maintaining 20S proteasome activity and reducing accumulated IDPs.³⁸⁻⁴⁰

4.2.4 20S activators reduce the accumulation of A53T-mutant α -synuclein in transfected HEK-293T cells

Next, I sought to develop a cellular model that could be employed to begin to evaluate 20S proteasome activators within a cell-based system and on a neurodegenerative disease relevant substrate. The A53T mutation of α -synuclein has been linked to some cases of early onset familial Parkinson's disease. This point mutation on α -synuclein leads to faster oligomerization than the wild-type protein and as a result more readily disrupts proteostasis in neurons.⁵³⁻⁵⁵ Because of its involvement with some cases of familial Parkinson's disease and the disordered nature of α -synuclein, cells expressing the A53T mutant form of α -synuclein could serve as a promising model for evaluating small molecule 20S proteasome activators.⁵³⁻⁵⁵

To this end, I transiently transfected a plasmid containing A53T α -synuclein into HEK-293T cells. Following transfection, the cells were incubated for 24 hours to allow for accumulation of the A53T α -synuclein to begin. Then, the cells were treated with DMSO (vehicle) or 20S proteasome activators (Fluspirilene or *N*-acylated Fluspirilene) for 8 hours. The cells were then lysed, and total protein concentration was normalized for each sample. The resulting cell lysates were subjected to SDS-PAGE, western blot and probed for A53T α -synuclein protein that had accumulated. To ensure that the observed effects were due to changes at the protein level, cycloheximide was added prior to treatment with 20S activators to block protein synthesis.

HEK-293T cells do not normally express easily detectable levels of α -synuclein, as can be seen when comparing the no plasmid control to the transfected vehicle control (**Fig. 4.5**). Excitingly, it was found that both Fluspirilene and *N*-acylated Fluspirilene effectively reduced the accumulation of A53T α -synuclein protein in these transfected HEK-293T cells in a concentration-dependent manner (**Fig. 4.5**). Importantly, the effect of the 20S proteasome activator *N*-acylated Fluspirilene was abrogated by blocking proteasome activity, with the proteasome inhibitor bortezomib (BTZ),⁷⁶ thereby implicating proteasome-mediated degradation as responsible for this reduced accumulation of A53T α -synuclein. These results demonstrated that Fluspirilene analogues can enhance the activity of cellular 20S proteasomes and reduce the accumulation of disease-causing IDPs, like A53T α -synuclein. Moreover, this cellular model of familial Parkinson's disease⁵³⁻⁵⁵ can be used to evaluate novel 20S proteasome activators and assist in their optimization for cell-based systems.

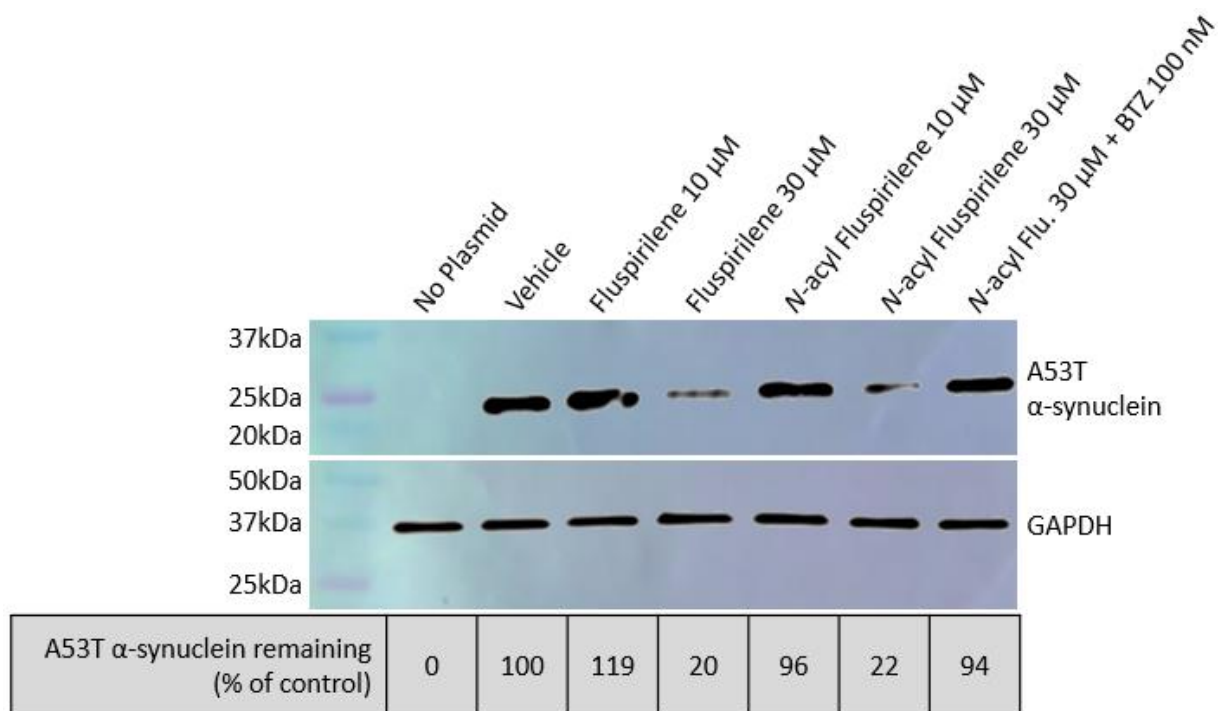


Figure 4.5: Fluspirilene and *N*-acylated Fluspirilene reduce the accumulation of A53T α -synuclein in transiently transfected HEK-293T cells in a concentration-dependent manner. Western blot analysis of remaining A53T α -synuclein in HEK-293T cell lysates following 8 h treatment with DMSO (vehicle), Fluspirilene (10 or 30 μ M), *N*-acylated Fluspirilene (10 or 30 μ M), or a combination of *N*-acylated Fluspirilene (30 μ M) and Bortezomib (100 nM). Densitometry of resulting bands was performed using image J. Lanes were normalized for loading differences using the housekeeping protein GAPDH. Quantifications shown as percent of vehicle.

This cell-based model system of familial Parkinson's disease continues to serve as a valuable tool for evaluating the effectiveness of various 20S proteasome activators in cells. However, improvements in terms of throughput, workflow and consistency could still be made to this model. For example, the development of a cell line that is stably transfected with an expression system that allows for switching or tuning of expression, such as a tetracycline or doxycycline-controlled system, could offer some of these improvements. Such a system would eliminate the

need to perform transient transfections prior to every experiment and allow for easier tuning of A53T α -synuclein levels prior to treatments, providing enhanced reproducibility and ease of optimization. The development of such a system is currently being explored by other members of the Tepe lab.

4.2.5 Treatment of primary mouse hippocampal neurons with pre-formed α -synuclein fibrils seeds accumulation of phosphorylated α -synuclein aggregates

To continue the investigation of 20S proteasome activation as a potential therapeutic strategy for neurodegenerative diseases, their efficacy will need to be explored in more relevant cell types, prior to movement into *in vivo* models. In an attempt to address this need, and to further explore the effects of 20S activators on accumulation of oligomeric IDPs, I sought to develop a cellular model using primary mouse hippocampal neurons. In this proposed model, I aimed to induce aggregation of endogenous α -synuclein by treating primary mouse hippocampal neurons with pre-formed α -synuclein aggregate seeds, following protocols similar to those reported in the literature.^{77, 78} These cells could then serve as a disease relevant model system to evaluate 20S proteasome activators for their ability to reduce α -synuclein aggregation caused by exogenous seeding, as is believed to occur in neurodegenerative disease pathogenesis.^{24, 27, 47, 77-79} This would also represent one of the most relevant models of neurodegenerative disease, in terms of cell type, that has been explored with small molecule 20S proteasome activators to date.

These studies were done in collaboration with Dr. Caryl Sortwell and her lab at MSU's Grand Rapids campus. The Sortwell lab obtained pre-formed α -synuclein fibrils from a collaborator and then assisted me through training on primary cell culture and processing of the pre-formed α -synuclein fibrils, via sonication, to generate the desired α -synuclein pre-formed fibril seeds. I was then able to employ these techniques myself using our own equipment and facilities.

Following this training, our collaboration continued, where I cultured the primary neurons and performed pre-formed fibril and 20S activator treatments. The Sortwell lab then confirmed proper pre-formed fibril seed formation, via AFM imaging, and imaged the final fixed neurons with a Lionheart fluorescent microscope. Unfortunately, after several rounds of optimization the progress of these studies was halted, due to the prohibitive costs associated with purchasing the neurons and other required supplies for their culturing and treatment. Prior to the cessation of these experiments, however, we were able to achieve seeding of endogenous α -synuclein that could be visualized via immunostaining for phosphorylated α -synuclein (**Fig. 4.6**). Additional optimization was deemed necessary to achieve better seeding efficiency and to reduce background signal. This need for further optimization at this stage, along with the likelihood of needing further optimization upon incorporation of 20S proteasome activator treatments, would have been quite costly, despite this successful preliminary experiment. It was for this reason that these studies were put on hold.

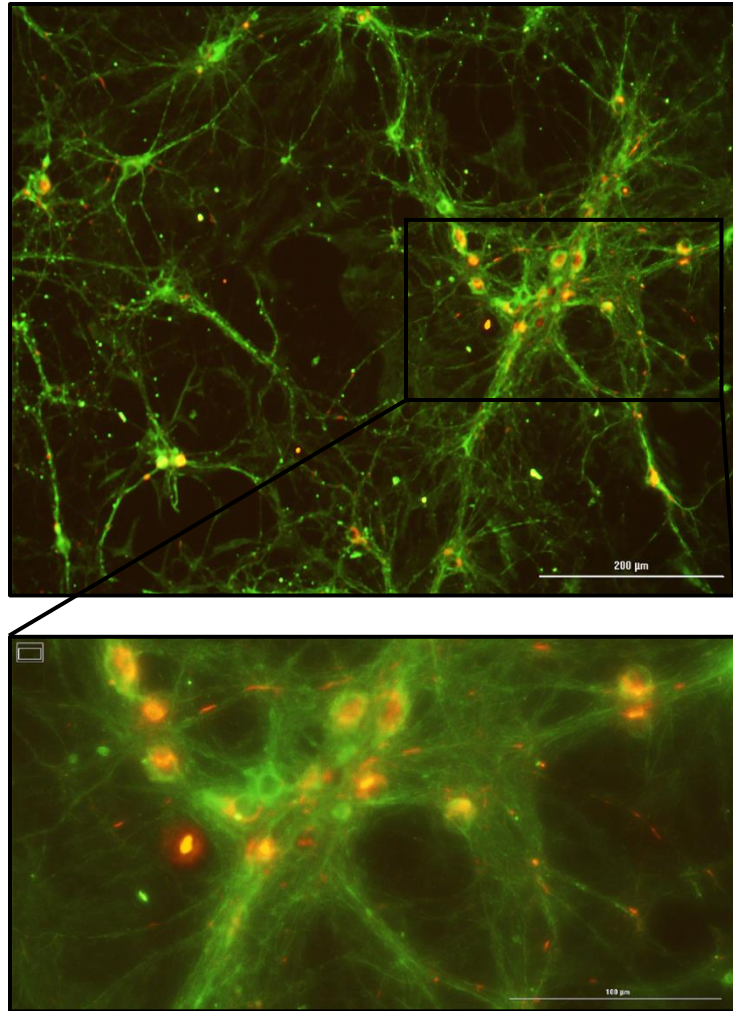


Figure 4.6: Seeding of primary mouse hippocampal neurons with pre-formed α -synuclein fibrils induced aggregation of endogenous α -synuclein. Fluorescence microscopy images of primary mouse hippocampal neurons following 14-day treatment with pre-formed α -synuclein fibril seeds. Cell bodies (green) were probed for tubulin using a primary IgM mouse antibody for 5H1 and a GFP-conjugated (488) secondary goat anti-mouse IgM antibody. Phosphorylated α -synuclein (red) was probed with a primary IgG2a mouse antibody, followed by an RFP-conjugated (594 nm) secondary goat anti-mouse IgG2a antibody. The bottom image is zoomed in portion of the top image displaying an area with high levels of phosphorylated α -synuclein aggregation.

I later planned an alternative method, but its development has not yet begun. This alternative method would make use of an immortalized mouse hippocampal neuron cell line (HT-22 cells), in place of the primary neurons, but retain the same α -synuclein seeding strategy. These neurons can be grown and passaged, unlike primary neurons, under normal mammalian cell culture conditions and are much less sensitive to perturbations. These cells would allow for much more cost efficient and rapid optimization of a similar model, if this cell line is amendable to seeding with α -synuclein pre-formed fibril seeds, like the primary neurons. In the next section, I will discuss the synthesis and testing of a fluorescent probe for IDP aggregation that could be used in conjunction with this proposed HT-22 cellular model to further simplify the workflow and allow for live-cell labeling.

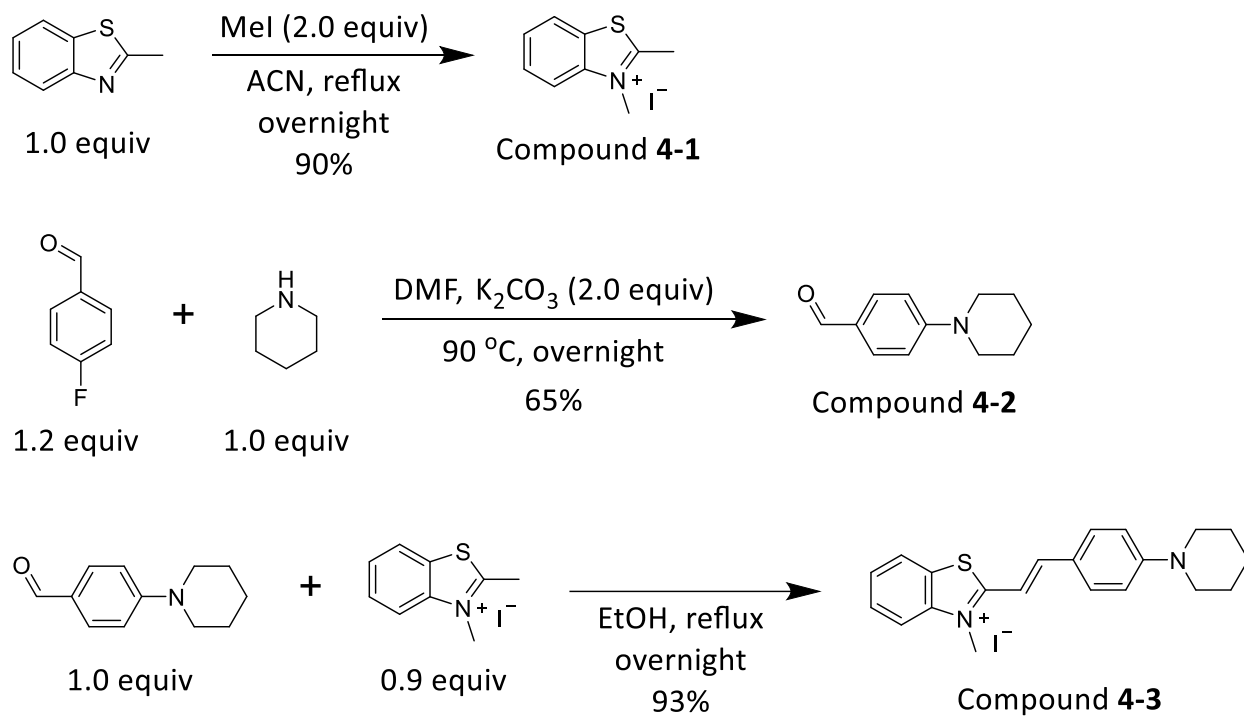
4.2.6 Synthesis and testing of a fluorescent probe for monitoring IDP aggregation

Cell-based models of IDP aggregation and neurodegeneration can be challenging and expensive to develop (see discussion above). As such, any tools that can simplify the workflow and provide greater experimental flexibility can provide substantial benefits. While working on the development of the primary neuron α -synuclein aggregation model above, I undertook the synthesis (**Scheme 4.1**) and testing (**Fig. 4.7**) of a fluorescent probe (compound **4.3**) that had been reported in the literature.⁸⁰ This probe was developed to provide a simple method to monitor IDP aggregation in living cellular models of neurodegenerative disease. Compound **4-3** functions as a molecular rotor-like dye, which following excitation can dissipate energy through nonradiative pathways, because of its free intramolecular rotation around the vinyl linkage in non-rigid environments. Upon binding to IDP aggregates however, this rotation is restricted and relaxation back to the ground-state occurs through fluorescence ($\lambda_{em} = 605$ nm), much like what is seen with thioflavin T and other amyloid fibril dyes.⁸⁰⁻⁸⁴ This probe was designed to improve on the cell

permeability of thioflavin T and to reduce background fluorescence, which makes this probe more ideal than the commercially available thioflavin T for our purposes.⁸⁰ Such a probe would provide a simpler method to probe for IDP aggregation, relative to immunostaining, and allow for monitoring this aggregation in living cells without the need for fixation. This could allow for live-cell imaging, time-lapse studies, and a simplified and less expensive workflow. Since this probe is not commercially available, the synthesis was undertaken to obtain the probe following the published route (**Scheme 4.1**).⁸⁰ Our lab had the 2-methylbenzothiazole intermediate on hand, so 3 steps were needed to form the final product.

Briefly, compound **4-1** was synthesized by refluxing 2-methylbenzothiazole and methyl iodide in acetonitrile (ACN) overnight. Subsequent cooling of the reaction mixture, filtering and washing with ethyl acetate yielded 90% of pure compound **4-1**. Compound **4-2** was synthesized by dissolving piperidine and 4-fluorobenzaldehyde in DMF with potassium carbonate and heating to 90 °C overnight. The resulting mixture was then cooled to room temperature and added dropwise to ice water. The product was then extracted using DCM and dried to yield pure compound **4-2** in 65% yield. Compound **4-3** was synthesized by dissolving compounds **4-1** and **4-2** in EtOH and refluxing while stirring overnight. The reaction was then cooled to room temperature, filtered and the solid was rinsed 3 times with ethyl acetate. Pure compound **4-3** was obtained directly as a dark red powder in 93% yield.

Scheme 4.1: Synthesis of a fluorescent probe for monitoring IDP oligomerization and fibrilization, following work by Shvadchak et al.⁸⁰



Following the synthesis of compound **4-3**, it was tested for its ability to preferentially detect α -synuclein oligomers over their monomeric form, seen as an increase in fluorescence intensity ($\lambda_{\text{exc}} = 570 \text{ nm}$, $\lambda_{\text{em}} = 605 \text{ nm}$). This was done by briefly incubating pure monomeric α -synuclein or the α -synuclein oligomeric mixture that was used previously (**Fig. 4.2** and **Fig. 4.4**) with compound **4-3**. Fluorescence was then measured using our SpectraMax plate reader ($\lambda_{\text{exc}} = 570 \text{ nm}$, $\lambda_{\text{em}} = 605 \text{ nm}$), following a similar protocol to what was used in the initial report of this probe.⁸⁰ It was found that incubation of the probe with the α -synuclein oligomeric mixtures resulted in a large (~300-fold) increase in fluorescence intensity, relative to that of the probe alone or with monomeric α -synuclein (**Fig. 4.7**).

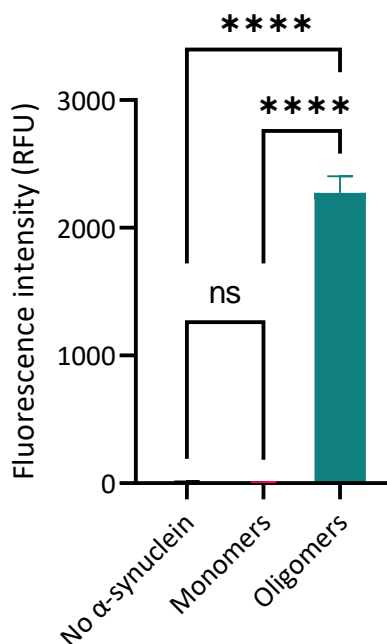


Figure 4.7: Compound 4-3 shows increased fluorescence in the presence of oligomeric α -synuclein. Brief incubation (15 mins) of compound 4-3 (4 μ M) in PBS buffer with either monomeric α -synuclein (10 μ M) or the mixed aggregates of α -synuclein (10 μ M), followed by reading on our SpectraMax plate reader ($\lambda_{exc} = 570$ nm, $\lambda_{em} = 605$ nm). These data were collected in triplicate (n=3). Error bars denote standard deviations. One-way ANOVA statistical analysis was used to determine statistical significance (ns=not significant, ****p<0.001).

Compound 4-3 will be used to help develop cell-based models of IDP aggregation for the testing of 20S proteasome activators going forward. It should provide a more simplified workflow and lower cost option, relative to immunostaining, and will allow for live-cell imaging using confocal microscopy, further diversifying our toolset for evaluating this potential therapeutic strategy. It is planned to be used in conjunction with the immortalized mouse hippocampal neurons, discussed above, to allow for live-cell imaging and quantitative evaluation of pre-formed fibril seed-induced aggregation of endogenous α -synuclein. Additionally, it is serving as a valuable

tool for use in other cell-based models currently being worked on by other members of the Tepe lab.

4.2.7 Fluspirilene analogues and TCH-165 are well tolerated by microglia

The involvement of neuroinflammation in the pathogenesis of neurodegenerative diseases has been an area of increasing interest, as more ties between the two are identified. Numerous studies have shown that neuroinflammation appears to play a critical role in disease progression. However, it is still unclear at what stage in disease development it begins to contribute or to what degree it is responsible for the continued neuron degeneration.^{41, 44-47} The initiation of neuroinflammation seen in neurodegenerative diseases appears to be due, at least in part, to the release of accumulated IDPs, like α -synuclein in Parkinson's disease, by degenerating neurons into the extracellular space. These IDPs released by degenerating neurons are not normally present in the extracellular space within the brain. As such, the primary native immune cells of the brain, microglia, detect these abnormal proteins, through their binding to multiple potential receptors on the cell surface (TLR2, TLR4, FC γ R, and CD36), and become activated.^{41-43, 46, 49-52} These activated microglia undergo a phenotype switch to their activated form, much like what is seen with macrophages when they detect pathogens and switch to their M1 (pro-inflammatory) phenotype. As a result, the activated microglia begin to secrete inflammatory signaling molecules, including cytokines, chemokines, and reactive oxygen species.^{41, 43, 48, 85} These pro-inflammatory signaling molecules have been shown to contribute to further neuron degeneration. These events are believed to culminate in the initiation of a deleterious cycle of increasing neuron degeneration, IDP release, microglia activation, and neuroinflammation.^{41-43, 46, 49-52}

I hypothesized that 20S proteasome activators can help to disrupt this cycle of degeneration by enhancing the degradation of the IDPs that are activating the microglia. This could take place

at the level of the neurons that are producing and releasing the IDPs, but I also wanted to explore whether they could have an effect at the level of the microglia and their activation. To explore this, I set out to develop a cell-based model of neuroinflammation caused by IDPs. For this, I cultured immortalized mouse microglial (IMG) cells and then treated them with 20S proteasome activators, TCH-165 or *N*-acylated Fluspirilene, followed by addition of A53T α -synuclein directly into the media. Following a 24-hour incubation together with the A53T α -synuclein, an MTS assay was performed on the microglial cells to monitor viability and a TNF- α ELISA was performed on media taken from the cells. TNF- α is a cytokine that is commonly associated with inflammatory responses triggered by immune cells and has been implicated in neuroinflammation development.^{41, 42, 49} TNF- α is secreted by microglial cells following their activation, so by monitoring the levels of TNF- α in the media with an ELISA, I could monitor the degree of microglia activation seen in each treatment.^{41, 42, 49}

Following treatment of the IMG cells with 20S activators and A53T α -synuclein, it was found that both TCH-165 and *N*-acylated Fluspirilene were well tolerated by the microglia, showing no significant decrease in viability up to 5 μ M for TCH-165 and upwards of 10 μ M for *N*-acylated Fluspirilene (**Fig. 4.8**). This result was very important, because if 20S proteasome activators show significant deleterious effects on microglial viability it could lead to more inflammatory signaling and further disruption of brain homeostasis.

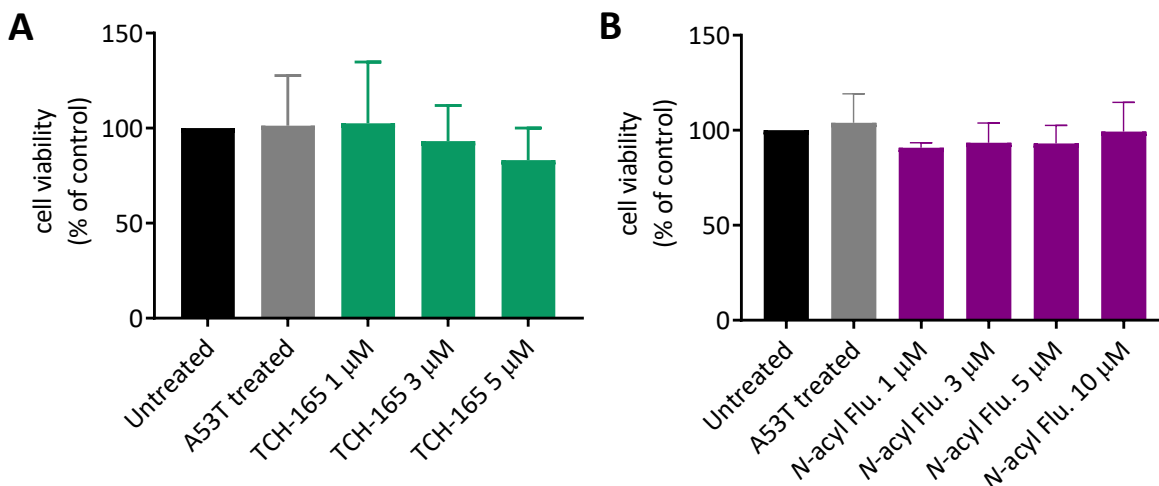


Figure 4.8: TCH-165 and *N*-acylated Fluspirilene are well tolerated by microglia. MTS assay monitoring cell viability of immortalized mouse microglia treated with A53T α -synuclein and either DMSO (A53T treated), (A) TCH-165 at various concentrations or (B) *N*-acylated Fluspirilene at various concentrations. These data were collected in triplicate (n=3). Error bars denote standard deviations. One-way ANOVA statistical analysis was used to determine statistical significance. No statistically significant differences between treatments were found.

4.2.8 20S activators reduce the release of the pro-inflammatory cytokine TNF- α by immortalized microglia activated with A53T α -synuclein

Alongside the MTS assay being performed on the treated microglia cells, a TNF- α ELISA was performed on the media removed from the cultures. This was done to monitor TNF- α release associated with microglia activation.^{41, 42, 49} As anticipated, the addition of A53T α -synuclein to the microglia cultures induced increased release of TNF- α into the media, as detected by the ELISA (Fig. 4.9), corresponding to an increase in activated microglia. This was consistent with previous literature precedence and the consensus in the field surrounding IDP-induced neuroinflammation as a contributing factor to neurodegenerative disease pathogenesis.^{42, 43, 49, 51} Excitingly, it was also found that treatment with TCH-165 or *N*-acylated Fluspirilene resulted in

concentration-dependent reductions in the A53T α -synuclein-induced TNF- α release by these microglia (**Fig. 4.9**). Both, TCH-165 and *N*-acylated Fluspirilene were able to reduce the levels of TNF- α release back down to near what was seen in the media of untreated microglia, despite the addition of the activating IDP. These results suggest that 20S proteasome activators have the potential to help to not only reduce accumulating IDPs associated with neurodegenerative disease (**Fig 4.4** and **Fig. 4.5**), but also to help combat their pro-inflammatory effects on microglial cells that are believed to contribute to the progression of these diseases (**Fig. 4.9**).

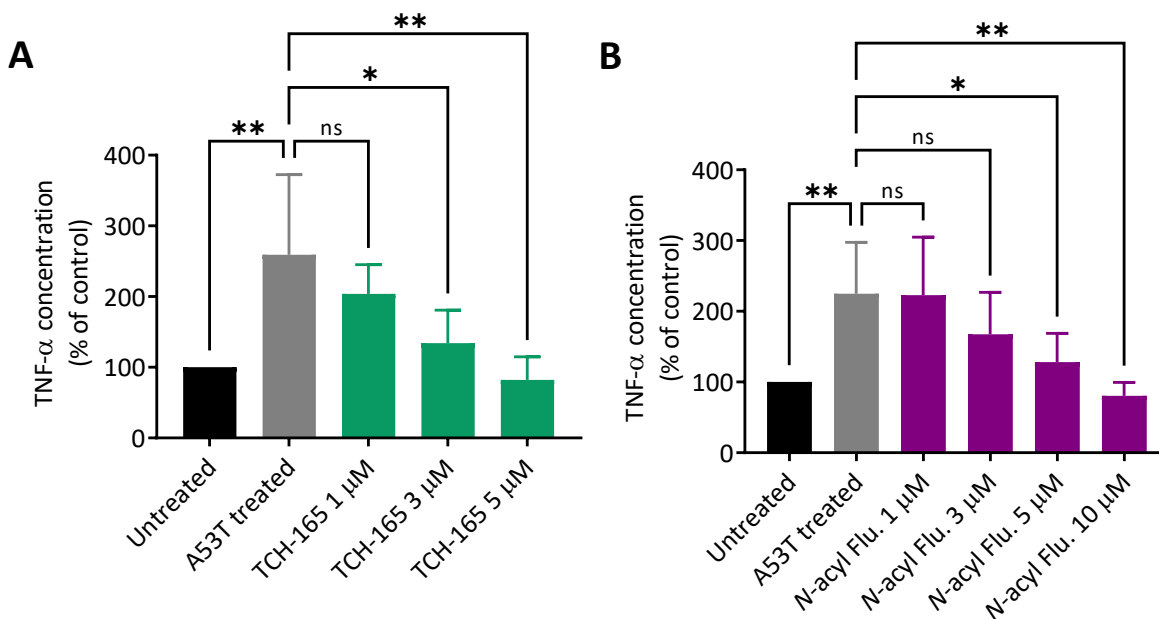


Figure 4.9: TCH-165 and *N*-acylated Fluspirilene reduce the release of TNF- α by microglia activated with A53T α -synuclein. Sandwich ELISA of TNF- α secreted into the media by IMG cell cultures treated with A53T α -synuclein and either DMSO (A53T treated), **(A)** TCH-165 at various concentrations (1, 3 or 5 μ M) or **(B)** *N*-acylated Fluspirilene at various concentrations (1, 3, 5 or 10 μ M). These data were collected in triplicate (n=3). Error bars denote standard deviations. One-way ANOVA statistical analysis was used to determine statistical significance (ns=not significant, *p<0.05, **p<0.01).

While these results were very exciting and suggested that 20S activators have the potential to address multiple factors related to neurodegenerative disease pathogenesis (i.e., IDP accumulation (**Fig. 4.5**), oligomer-induced proteasome inhibition (**Fig. 4.2–4.4**), and neuroinflammation (**Fig. 4.9**)), the exact mechanism by which this reduction of TNF- α release is occurring is not made clear by the results of this experiment. While the hypothesis was that 20S activators could enhance the degradation of the activating IDPs to lead to a reduction in inflammatory signaling, this experiment cannot directly show that IDP reduction is what led to TNF- α release being reduced. Several methods could be used to explore the mechanism. For example, the addition of a proteasome inhibitor could block this effect if it were indeed occurring, but proteasome inhibitors are generally toxic to cells.⁶ Using western blotting or an ELISA to look at the amounts of remaining α -synuclein is a strategy that could be employed to explore whether it is being degraded at an enhanced rate, but whether this should be done on extracellular α -synuclein, α -synuclein that has entered the microglia, or both is not clear. The exact mechanism for α -synuclein induced microglia activation is not fully understood, so which fractions should be analyzed is also unclear. Additionally, there is mounting evidence for the presence of extracellular proteasomes,^{86, 87} so it is possible that degradation may take place outside, as well as inside of these cells, further complicating the matter.

To begin to shed light on the mechanism by which these 20S activators were able to reduce TNF- α release, I chose to explore whether this effect of 20S activators was dependent on activation via an IDP, like A53T α -synuclein. To do this, lipopolysaccharide (LPS) was used to activate the microglia in place of the A53T α -synuclein. LPS is commonly used to induce inflammatory responses in cell culture because it is readily identified by immune cells as foreign, due to its presence being indicative of bacterial infection when present in the body.^{48, 49, 85, 88} As expected,

LPS induces a large increase in TNF- α release by the microglia, making use of the same ELISA for TNF- α detection and quantification (**Fig. 4.10**). Interestingly, it was found that the 20S proteasome activators TCH-165 and *N*-acylated Fluspirilene were also able to reduce the amount LPS-induced TNF- α release in this assay (**Fig. 4.10**), like what was seen with A53T α -synuclein (**Fig. 4.9**). This suggests that the initial hypothesis, that 20S activators could reduce the release of TNF- α caused by A53T α -synuclein by enhancing the degradation of the A53T α -synuclein, should be rejected. In fact, these results suggest that the reduction in TNF- α release seen in these assays may represent a broader anti-inflammatory effect caused by these 20S proteasome activators, independent of activation via extracellular IDPs.

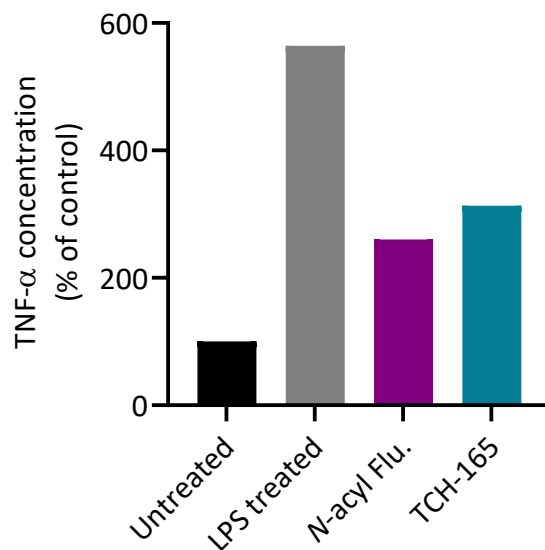


Figure 4.10: TCH-165 and *N*-acylated Fluspirilene reduce the release of TNF- α by microglia activated with LPS. TNF- α ELISA of the media from immortalized mouse microglia cultures treated with LPS and either DMSO (LPS treated), TCH-165 (5 μ M) or *N*-acylated Fluspirilene (10 μ M).

While these results complicate the mechanistic study, this potential anti-inflammatory effect could still prove to be beneficial in the case of neurodegenerative disease treatment, where

both IDP accumulation and neuroinflammation are thought to contribute to disease progression.^{41-43, 46, 49-52} Further studies are required to elucidate the mechanism through which 20S proteasome activators, such as TCH-165 and *N*-acylated Fluspirilene, can reduce TNF- α release by microglia following their activation with pro-inflammatory stimuli.

4.3 Conclusions

In summary, several novel methods were developed herein to further evaluate 20S proteasome activators as a therapeutic method for the treatment of neurodegenerative diseases. These studies focused on providing disease relevant models to evaluate 20S activators and answering crucial questions regarding the implications of 20S activation in neurodegenerative disease model systems. It was found that TCH-165 and the Fluspirilene analogues could maintain 20S proteasome activity in the presence of inhibitory IDP oligomers and can begin to reduce monomeric and oligomeric forms of α -synuclein *in vitro*. These findings support the hypothesis that 20S proteasome activators can reestablish proteostasis in neurodegenerative disease systems, where IDP accumulation and inhibitory IDP oligomers contribute to the disruption of proteostasis.

19-30, 38-40

Additional cell-based models of Parkinson's disease were explored, focusing on differing aspects of the disease. First, HEK-293T cells transfected with A53T α -synuclein served as a model of early onset familial Parkinson's disease.⁵³⁻⁵⁵ This model has allowed for evaluation of the ability of 20S proteasome activators to reduce accumulation of a disease relevant substrate in live cells.

To further the studies focused on IDP oligomers, I began to develop a cellular model of IDP aggregation, using primary mouse hippocampal neurons treated with pre-formed α -synuclein fibril seeds.^{77, 78} While the development of this method did not reach completion, due to cost constraints, the preliminary results suggest that this seeding was successful in inducing aggregation of

endogenous α -synuclein. The development of a closely related model, using immortalized mouse hippocampal neurons, was planned to achieve the same goal of exploring the effects of 20S activators on cellular IDP aggregation. In conjunction with the fluorescent probe (compound **4-3**) synthesized herein, this model could be developed in a more cost-effective way, with a simplified workflow and allow for analysis in living neurons.⁸⁰

To explore the effects of small molecule 20S activators on the development of neuroinflammation associated with Parkinson's disease,^{42, 43, 49, 51} immortalized mouse microglial cells were treated with 20S activators and A53T α -synuclein. Treatment with A53T α -synuclein induced increased secretion of the inflammatory cytokine TNF- α . This effect was prevented by addition of small molecule 20S proteasome activators, in a concentration-dependent manner. A similar effect was seen when LPS was used in place of A53T α -synuclein to activate the microglia, which suggests that this anti-inflammatory effect is not specific to activation by IDPs. As a result, the hypothesis that small molecule 20S proteasome activators could reduce the activation of microglia by reducing the activating IDPs was rejected. However, despite this effect not being IDP specific, it could still prove to be beneficial to the treatment of neurodegenerative diseases where neuroinflammation is believed to contribute to disease pathogenesis.^{41, 44-47} Further studies are required to elucidate the exact mechanism by which 20S activators reduce TNF- α release in this model system.

1. 20S activators were found to be able to preserve 20S proteasome activity in the presence of inhibitory IDP oligomers and reduce monomeric and oligomeric forms of α -synuclein in those systems.
2. Novel methods and tools were developed to enable evaluation of 20S activators effects on inhibition of the 20S by IDP oligomers, direct effects on IDP oligomers, cellular

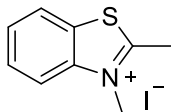
accumulation of A53T α -synuclein and neuroinflammation caused by A53T α -synuclein. The tools, general protocol and initial attempts at development of a model to allow for monitoring of α -synuclein aggregation in live neurons was also explored herein.

3. 20S proteasome activators can reduce A53T α -synuclein-induced release of TNF- α by microglia, however this effect is not specific to activation of microglia by IDPs. Additional studies are needed to elucidate the mechanism of reduced TNF- α release.

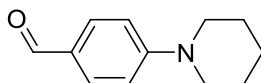
4.4 Experimental

General information

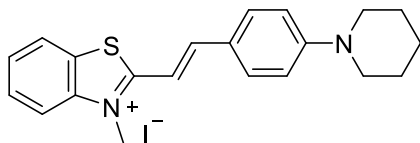
Reactions were carried out under a nitrogen atmosphere in flame-dried glassware. Solvents and reagents were purchased from commercial suppliers and used without further purification. Magnetic stirring was used for all reactions. Yields refer to chromatographically and spectroscopically pure compounds unless otherwise noted. Infrared spectra were recorded on a Jasco Series 6600 FTIR spectrometer. ^1H and ^{13}C NMR spectra were recorded on a Varian Unity Plus-500 spectrometer. Chemical shifts are reported relative to the residue peaks of the solvent (CDCl_3 : 7.26 ppm for ^1H and 77.0 ppm for ^{13}C) (CD_3OD : 3.31 ppm for ^1H and 47.6 ppm for ^{13}C) ($\text{DMSO-}d_6$: 2.50 ppm for ^1H and 39.5 ppm for ^{13}C). The following abbreviations are used to denote the multiplicities: s = singlet, d = doublet, and m = multiplet. HRMS were obtained at the Mass Spectrometry Facility of Michigan State University with a Micromass Q-ToF Ultima API LC-MS/MS mass spectrometer. Column chromatography was performed using a Teledyne ISCO CombiFlash® NextGen system with prepacked columns (RediSep® Normal-phase silica, 20-40 microns). TLCs were performed on pre-coated 0.25 mm thick silica gel 60 F254 plates and visualized using UV light and iodine staining.



Compound 4-1: 2-Methylbenzothiazole (1.0 eq) and methyl iodide (2.0 eq) were dissolved in dry acetonitrile (3.6 mL) and refluxed overnight. The reaction mixture was then cooled to room temperature and the product was collected by filtration. The product was then washed with ethyl acetate three times to yield pure product. Purple solid (2.70 g, 90%). ^1H NMR (500 MHz, CD_3OD) δ 8.32 (d, $J = 8.2$ Hz, 1H), 8.24 (d, $J = 8.5$ Hz, 1H), 7.94 – 7.90 (m, 1H), 7.84 – 7.80 (m, 1H), 4.30 (s, 3H), 3.22 (s, 3H). ^{13}C NMR (126 MHz, CD_3OD) δ 176.85, 142.01, 129.51, 128.90, 128.30, 123.77, 116.38, 35.67, 16.20. IR: 3056, 2965 cm^{-1} . HRMS (ESI-TOF) m/z : $[(\text{M}-\text{I})^+]$ calcd for ($\text{C}_9\text{H}_{10}\text{NS}^+$) 164.0534; Found 164.0538. Melting point: >200 $^\circ\text{C}$. Reported 258 $^\circ\text{C}$.⁸⁰



Compound 4-2: A mixture of piperidine (1.0 eq.), 4-fluorobenzaldehyde (1.2 eq.) and potassium carbonate (2 eq.) in 4 mL of DMF was heated to 90 $^\circ\text{C}$ overnight. The mixture was then cooled to room temperature, added dropwise to ice water, and extracted with DCM to yield pure product. Brown solid (40.3 mg, 21%). ^1H NMR (500 MHz, CDCl_3) δ 9.71 (s, 1H), 7.70 (d, $J = 8.9$ Hz, 2H), 6.86 (d, $J = 8.5$ Hz, 2H), 3.37 (m, 4H), 1.63 (m, 6H). ^{13}C NMR (126 MHz, CDCl_3) δ 190.22, 154.94, 131.92, 113.36, 48.46, 25.21, 24.23. IR: 3002, 2947, 1662 cm^{-1} . HRMS (ESI-TOF) m/z : $[(\text{M}+\text{H})^+]$ calcd for ($\text{C}_{12}\text{H}_{16}\text{NO}^+$) 190.1232; Found 190.1233. Melting point: 56-58 $^\circ\text{C}$.



Compound 4-3: Compounds **4-1** (0.91 eq.) and **4-2** (1.0 eq.) were dissolved in 20mL (5mL/mmol) of EtOH and refluxed while stirring overnight. The reaction was then cooled to room temperature,

filtered and the solid product was rinsed 3 times with ethyl acetate. Pure compound **3** was obtained directly as a violet powder (1.63 g, 93%). ^1H NMR (500 MHz, $\text{DMSO-}d_6$) δ 8.32 (d, $J = 7.4$ Hz, 1H), 8.11 (d, $J = 7.5$ Hz, 1H), 8.07 (d, $J = 15.0$ Hz, 1H), 7.90 (d, $J = 7.2$ Hz, 2H), 7.79 (m, 1H), 7.70 – 7.64 (m, 2H), 7.06 (d, $J = 7.0$ Hz, 2H), 4.24 (s, 3H), 3.50 (m, 4H), 1.60 (m, 6H). ^{13}C NMR (126 MHz, $\text{DMSO-}d_6$) δ 171.42, 153.57, 149.66, 141.96, 132.88, 128.90, 127.52, 126.88, 123.84, 122.25, 116.02, 113.45, 106.92, 47.54, 35.64, 25.10, 23.94. IR (neat): 3043, 2926, 1563, 1241 cm^{-1} . HRMS (ESI-TOF) m/z : $[(\text{M-I})^+]$ calcd for $(\text{C}_{21}\text{H}_{23}\text{N}_2\text{S}^+)$ 335.1576; Found 335.1621. Melting point: >200 $^\circ\text{C}$. Reported 252 $^\circ\text{C}$.⁸⁰

REFERENCES

- (1) Dahlmann, B.; Rutschmann, M.; Kuehn, L.; Reinauer, H. Activation of the multicatalytic proteinase from rat skeletal muscle by fatty acids or sodium dodecyl sulphate. *Biochemical Journal* **1985**, *228* (1), 171-177. DOI: 10.1042/bj2280171.
- (2) Tanaka, K.; Yoshimura, T.; Ichihara, A. Role of substrate in reversible activation of proteasomes (multi-protease complexes) by sodium dodecyl sulfate. *Journal of biochemistry* **1989**, *106* (3), 495-500.
- (3) Azevedo, L. M.; Lansdell, T. A.; Ludwig, J. R.; Mosey, R. A.; Woloch, D. K.; Cogan, D. P.; Patten, G. P.; Kuszpit, M. R.; Fisk, J. S.; Tepe, J. J. Inhibition of the Human Proteasome by Imidazoline Scaffolds. *Journal of Medicinal Chemistry* **2013**, *56* (14), 5974-5978. DOI: 10.1021/jm400235r.
- (4) Voges, D.; Zwickl, P.; Baumeister, W. The 26S Proteasome: A Molecular Machine Designed for Controlled Proteolysis. *Annual Review of Biochemistry* **1999**, *68*, 1015-1068, review-article. DOI: 10.1146/annurev.biochem.68.1.1015.
- (5) McNaught, K. S. P.; Olanow, C. W.; Halliwell, B.; Isacson, O.; Jenner, P. Failure of the ubiquitin-proteasome system in Parkinson's disease. *Nature Reviews Neuroscience* **2001**, *2* (8), 589-594. DOI: 10.1038/35086067.
- (6) Voorhees, P.; Dees, E.; O'Neil, B.; Orlowski, R. The proteasome as a target for cancer therapy. *Clinical cancer research* **2003**, *9* (17), 6316-6325.
- (7) Ostrowska, H. The ubiquitin-proteasome system: a novel target for anticancer and anti-inflammatory drug research. *Cellular & Molecular Biology Letters* **2008**, *13* (3), 353-365. DOI: 10.2478/s11658-008-0008-7.
- (8) Calamini, B.; Morimoto, R. Protein homeostasis as a therapeutic target for diseases of protein conformation. *Current Topics in Medicinal Chemistry* **2012**, *12* (22), 2623-2640. DOI: 10.2174/1568026611212220014.
- (9) Huang, X.; Dixit, V. M. Drugging the undruggables: exploring the ubiquitin system for drug development. *Cell Research* **2016**, *26* (4), 484-498, ReviewPaper. DOI: doi:10.1038/cr.2016.31.
- (10) Tundo, G.; Sbardella, D.; Santoro, A.; Coletta, A.; Oddone, F.; Grasso, G.; Milardi, D.; Lacal, P.; Marini, S.; Purrello, R.; et al. The proteasome as a druggable target with multiple therapeutic potentialities: Cutting and non-cutting edges. *Pharmacology & therapeutics* **2020**, *213*, 107579. DOI: 10.1016/j.pharmthera.2020.107579.
- (11) Njomen, E.; Tepe, J. J. Proteasome Activation as a New Therapeutic Approach to Target Proteotoxic Disorders. *Journal of Medicinal Chemistry* **2019**, *62* (14), 6469-6481. DOI: 10.1021/acs.jmedchem.9b00101.

- (12) Jones, C. L.; Njomen, E.; Sjögren, B.; Dexheimer, T. S.; Tepe, J. J. Small Molecule Enhancement of 20S Proteasome Activity Targets Intrinsically Disordered Proteins. *ACS Chemical Biology* **2017**, *12* (9), 2240-2247. DOI: 10.1021/acscchembio.7b00489.
- (13) Njomen, E.; Osmulski, P. A.; Jones, C. L.; Gaczynska, M.; Tepe, J. J. Small Molecule Modulation of Proteasome Assembly. *Biochemistry* **2018**, *57* (28), 4214-4224. DOI: 10.1021/acs.biochem.8b00579.
- (14) Njomen, E.; Tepe, J. J. Regulation of Autophagic Flux by the 20S Proteasome. *Cell Chemical Biology* **2019**, *26* (9), 1283-1294.e1285. DOI: 10.1016/j.chembiol.2019.07.002.
- (15) Trader, D. J.; Simanski, S.; Dickson, P.; Kodadek, T. Establishment of a suite of assays that support the discovery of proteasome stimulators. *Biochimica et Biophysica Acta (BBA) - General Subjects* **2017**, *1861* (4), 892-899. DOI: 10.1016/J.BBAGEN.2017.01.003.
- (16) Coleman, R. A.; Trader, D. J. Methods to Discover and Evaluate Proteasome Small Molecule Stimulators. *Molecules* **2019**, *24* (12), 2341, Review. DOI: 10.3390/molecules24122341.
- (17) Fiolek, T.; Magyar, C.; Wall, T.; Davies, S.; Campbell, M.; Savich, C.; Tepe, J.; Mosey, R. Dihydroquinazolines enhance 20S proteasome activity and induce degradation of α -synuclein, an intrinsically disordered protein associated with neurodegeneration. *Bioorganic & Medicinal Chemistry Letters* **2021**, *36*, 127821. DOI: 10.1016/j.bmcl.2021.127821.
- (18) Jones, C. L.; Tepe, J. J. Proteasome Activation to Combat Proteotoxicity. *Molecules* **2019**, *24* (15), 2841, Review. DOI: 10.3390/molecules24152841.
- (19) Alam, P.; Bousset, L.; Melki, R.; Otzen, D. E. α -synuclein oligomers and fibrils: a spectrum of species, a spectrum of toxicities. *Journal of neurochemistry* **2019**, *150* (5). DOI: 10.1111/jnc.14808.
- (20) Bengoa-Vergniory, N.; Roberts, R. F.; Wade-Martins, R.; Alegre-Abarrategui, J. Alpha-synuclein oligomers: a new hope. *Acta neuropathologica* **2017**, *134* (6), 819-838. DOI: 10.1007/s00401-017-1755-1.
- (21) Cárdenas-Aguayo, M. d. C.; Gómez-Virgilio, L.; DeRosa, S.; Meraz-Ríos, M. A. The Role of Tau Oligomers in the Onset of Alzheimer's Disease Neuropathology. *ACS Chemical Neuroscience* **2014**, *5* (12), 1178-1191. DOI: 10.1021/cn500148z.
- (22) Castillo-Carranza, D. L.; Guerrero-Muñoz, M. J.; Sengupta, U.; Gerson, J. E.; Kaye, R. α -Synuclein Oligomers Induce a Unique Toxic Tau Strain. *Biological Psychiatry* **2018**, *84* (7), 499-508. DOI: 10.1016/j.biopsych.2017.12.018.
- (23) Cheng, B.; Gong, H.; Xiao, H.; Petersen, R. B.; Zheng, L.; Huang, K. Inhibiting toxic aggregation of amyloidogenic proteins: a therapeutic strategy for protein misfolding diseases. *Biochimica et biophysica acta* **2013**, *1830* (10), 4860-4871. DOI: 10.1016/j.bbagen.2013.06.029.

- (24) Choi, M. L.; Gandhi, S. Crucial role of protein oligomerization in the pathogenesis of Alzheimer's and Parkinson's diseases. *The FEBS Journal* **2018**, *285* (19), 3631-3644. DOI: 10.1111/febs.14587.
- (25) Cremades, N.; Cohen, S. I. A.; Deas, E.; Abramov, A. Y.; Chen, A. Y.; Orte, A.; Sandal, M.; Clarke, R. W.; Dunne, P.; Aprile, F. A.; et al. Direct observation of the interconversion of normal and toxic forms of α -synuclein. *Cell* **2012**, *149* (5), 1048-1059. DOI: 10.1016/j.cell.2012.03.037.
- (26) Deger, J. M.; Gerson, J. E.; Kaye, R. The interrelationship of proteasome impairment and oligomeric intermediates in neurodegeneration. *Aging cell* **2015**, *14* (5), 715-724. DOI: 10.1111/acel.12359.
- (27) Danzer, K. M.; Haasen, D.; Karow, A. R.; Moussaud, S.; Habeck, M.; Giese, A.; Kretschmar, H.; Hengerer, B.; Kostka, M. Different Species of α -Synuclein Oligomers Induce Calcium Influx and Seeding. *Journal of Neuroscience* **2007**, *27* (34), 9220-9232. DOI: 10.1523/JNEUROSCI.2617-07.2007.
- (28) Ingelsson, M. Alpha-Synuclein Oligomers-Neurotoxic Molecules in Parkinson's Disease and Other Lewy Body Disorders. *Frontiers in neuroscience* **2016**, *10*, 408-408. DOI: 10.3389/fnins.2016.00408.
- (29) Sengupta, U.; Nilson, A. N.; Kaye, R. The Role of Amyloid- β Oligomers in Toxicity, Propagation, and Immunotherapy. Elsevier B.V.: 2016; Vol. 6, pp 42-49.
- (30) Levine, Z. A.; Larini, L.; LaPointe, N. E.; Feinstein, S. C.; Shea, J.-E. Regulation and aggregation of intrinsically disordered peptides. *Proceedings of the National Academy of Sciences of the United States of America* **2015**, *112* (9), 2758-2763. DOI: 10.1073/pnas.1418155112.
- (31) Kaye, R.; Dettmer, U.; Lesné, S. E. Soluble endogenous oligomeric α -synuclein species in neurodegenerative diseases: Expression, spreading, and cross-talk. *Journal of Parkinson's disease* **2020**, *10* (3), 791-818. DOI: 10.3233/JPD-201965.
- (32) Haass, C.; Selkoe, D. J. Soluble protein oligomers in neurodegeneration: lessons from the Alzheimer's amyloid beta-peptide. *Nature reviews. Molecular cell biology* **2007**, *8* (2), 101-112. DOI: 10.1038/nrm2101.
- (33) Brettschneider, J.; Del Tredici, K.; Lee, V. M.; Trojanowski, J. Q. Spreading of pathology in neurodegenerative diseases: a focus on human studies. *Nature reviews. Neuroscience* **2015**, *16* (2), 109-120. DOI: 10.1038/nrn3887.
- (34) Rubinsztein, D. C. The roles of intracellular protein-degradation pathways in neurodegeneration. *Nature* **2006**, *443* (7113), 780-786. DOI: 10.1038/nature05291.
- (35) Selkoe, D. J. Folding proteins in fatal ways. *Nature* **2023**, *426* (6968), 900-904, ReviewPaper. DOI: doi:10.1038/nature02264.

- (36) Selkoe, D. J.; Hardy, J. The amyloid hypothesis of Alzheimer's disease at 25 years. *EMBO molecular medicine* **2016**, *8* (6), 595-608. DOI: 10.15252/emmm.201606210.
- (37) Chabrier, M. A.; Blurton-Jones, M.; Agazaryan, A. A.; Nerhus, J. L.; Martinez-Coria, H.; LaFerla, F. M. Soluble $\alpha\beta$ promotes wild-type tau pathology in vivo. *The Journal of neuroscience : the official journal of the Society for Neuroscience* **2012**, *32* (48), 17345-17350. DOI: 10.1523/JNEUROSCI.0172-12.2012.
- (38) Thibautaud, T. A.; Anderson, R. T.; Smith, D. M. A common mechanism of proteasome impairment by neurodegenerative disease-associated oligomers. *Nature Communications* **2018**, *9* (1), 1097-1097. DOI: 10.1038/s41467-018-03509-0.
- (39) Zondler, L.; Kostka, M.; Garidel, P.; Heinzlmann, U.; Hengerer, B.; Mayer, B.; Weishaupt, J. H.; Gillardon, F.; Danzer, K. M. Proteasome impairment by α -synuclein. *PLOS ONE* **2017**, *12* (9), e0184040-e0184040. DOI: 10.1371/journal.pone.0184040.
- (40) Smith, D. M. Could a Common Mechanism of Protein Degradation Impairment Underlie Many Neurodegenerative Diseases? *Journal of experimental neuroscience* **2018**, *12*, 1179069518794675-1179069518794675. DOI: 10.1177/1179069518794675.
- (41) Yang, Q.; Zhou, J. Neuroinflammation in the central nervous system: Symphony of glial cells. *Glia* **2019**, *67* (6), 1017-1035. DOI: 10.1002/glia.23571.
- (42) Su, X.; Maguire-Zeiss, K.; Giuliano, R.; Prifti, L.; Venkatesh, K.; Federoff, H. Synuclein activates microglia in a model of Parkinson's disease. *Neurobiology of Aging* **2007**, *29* (11), 1690-1701. DOI: 10.1016/j.neurobiolaging.2007.04.006.
- (43) Song, N.; Chen, L.; Xie, J. Alpha-Synuclein Handling by Microglia: Activating, Combating, and Worsening. *Neuroscience Bulletin* **2021**, *37* (5), 751-753, OriginalPaper. DOI: doi:10.1007/s12264-021-00651-6.
- (44) Cao, S.; Standaert, D.; Harms, A. The gamma chain subunit of Fc receptors is required for alpha-synuclein-induced pro-inflammatory signaling in microglia. *Journal of neuroinflammation* **2012**, *9*, 259. DOI: 10.1186/1742-2094-9-259.
- (45) Nilson, A. N.; English, K. C.; Gerson, J. E.; Barton Whittle, T.; Nicolas Crain, C.; Xue, J.; Sengupta, U.; Castillo-Carranza, D. L.; Zhang, W.; Gupta, P.; et al. Tau Oligomers Associate with Inflammation in the Brain and Retina of Tauopathy Mice and in Neurodegenerative Diseases. *Journal of Alzheimer's disease : JAD* **2017**, *55* (3), 1083-1099. DOI: 10.3233/JAD-160912.
- (46) Tu, H.; Yuan, B.; Hou, X.; Zhang, X.; Pei, C.; Ma, Y.; Yang, Y.; Fan, Y.; Qin, Z.; Liu, C.; et al. α -synuclein suppresses microglial autophagy and promotes neurodegeneration in a mouse model of Parkinson's disease. *Aging cell* **2021**, *20* (12), e13522. DOI: 10.1111/accel.13522.
- (47) Garcia, P.; Jürgens-Wemheuer, W.; Huarte, O.; Michelucci, A.; Masuch, A.; Brioschi, S.; Weihofen, A.; Koncina, E.; Coowar, D.; Heurtaux, T.; et al. Neurodegeneration and neuroinflammation are linked, but independent of alpha-synuclein inclusions, in a

seeding/spreading mouse model of Parkinson's disease. *Glia* **2022**, *70* (5), 935-960. DOI: 10.1002/glia.24149.

(48) Aloisi, F. Immune function of microglia. *Glia* **2001**, *36* (2), 165-179. DOI: 10.1002/glia.1106.

(49) Hoenen, C.; Gustin, A.; Birck, C.; Kirchmeyer, M.; Beaume, N.; Felten, P.; Grandbarbe, L.; Heuschling, P.; Heurtaux, T. Alpha-Synuclein Proteins Promote Pro-Inflammatory Cascades in Microglia: Stronger Effects of the A53T Mutant. *PLoS one* **2016**, *11* (9), e0162717. DOI: 10.1371/journal.pone.0162717.

(50) Raffaele, S.; Lombardi, M.; Verderio, C.; Fumagalli, M. TNF Production and Release from Microglia via Extracellular Vesicles: Impact on Brain Functions. *Cells* **2020**, *9* (10), 2145. DOI: 10.3390/cells9102145.

(51) Wood, H. α -Synuclein-activated microglia are implicated in PD pathogenesis. *Nature Reviews Neurology* **2022**, *18* (4), 188-188, BriefCommunication. DOI: doi:10.1038/s41582-022-00631-y.

(52) Xia, Y.; Zhang, G.; Kou, L.; Yin, S.; Han, C.; Hu, J.; Wan, F.; Sun, Y.; Wu, J.; Li, Y.; et al. Reactive microglia enhance the transmission of exosomal α -synuclein via toll-like receptor 2. *Brain : a journal of neurology* **2021**, *144* (7), 2024-2037. DOI: 10.1093/brain/awab122.

(53) Conway, K. A.; Harper, J. D.; Lansbury, P. T. Accelerated in vitro fibril formation by a mutant α -synuclein linked to early-onset Parkinson disease. *Nature Medicine* **1998**, *4* (11), 1318-1320. DOI: 10.1038/3311.

(54) Wills, J.; Credle, J.; Haggerty, T.; Lee, J.-H.; Oaks, A. W.; Sidhu, A. Tauopathic changes in the striatum of A53T α -synuclein mutant mouse model of Parkinson's disease. *PLoS one* **2011**, *6* (3), e17953-e17953. DOI: 10.1371/journal.pone.0017953.

(55) Smith, W. W.; Jiang, H.; Pei, Z.; Tanaka, Y.; Morita, H.; Sawa, A.; Dawson, V. L.; Dawson, T. M.; Ross, C. A. Endoplasmic reticulum stress and mitochondrial cell death pathways mediate A53T mutant alpha-synuclein-induced toxicity. *Human Molecular Genetics* **2005**, *14* (24), 3801-3811. DOI: 10.1093/hmg/ddi396.

(56) Fiolek, T. J.; Keel, K. L.; Tepe, J. J. Fluspirilene Analogs Activate the 20S Proteasome and Overcome Proteasome Impairment by Intrinsically Disordered Protein Oligomers. *ACS Chemical Neuroscience* **2021**, *12* (8), 1438-1448. DOI: 10.1021/acscchemneuro.1c00099.

(57) Cecarini, V.; Bonfili, L.; Amici, M.; Angeletti, M.; Keller, J.; Eleuteri, A. Amyloid peptides in different assembly states and related effects on isolated and cellular proteasomes. *Brain research* **2008**, *1209*, 8-18. DOI: 10.1016/j.brainres.2008.03.003.

(58) Díaz-Hernández, M.; Valera, A.; Morán, M.; Gómez-Ramos, P.; Alvarez-Castelao, B.; Castaño, J.; Hernández, F.; Lucas, J. Inhibition of 26S proteasome activity by huntingtin filaments but not inclusion bodies isolated from mouse and human brain. *Journal of neurochemistry* **2006**, *98* (5), 1585-1596. DOI: 10.1111/j.1471-4159.2006.03968.x.

- (59) Gregori, L.; Fuchs, C.; Figueiredo-Pereira, M.; Van Nostrand, W.; Goldgaber, D. Amyloid beta-protein inhibits ubiquitin-dependent protein degradation in vitro. *The Journal of Biological Chemistry* **1995**, *270* (34), 19702-19708. DOI: 10.1074/jbc.270.34.19702.
- (60) Lindersson, E.; Beedholm, R.; Højrup, P.; Moos, T.; Gai, W.; Hendil, K. B.; Jensen, P. H. Proteasomal inhibition by alpha-synuclein filaments and oligomers. *The Journal of biological chemistry* **2004**, *279* (13), 12924-12934. DOI: 10.1074/jbc.M306390200.
- (61) Bence, N.; Sampat, R.; Kopito, R. Impairment of the ubiquitin-proteasome system by protein aggregation. *Science (New York, N.Y.)* **2001**, *292* (5521). DOI: 10.1126/science.292.5521.1552.
- (62) Oh, S.; Hong, H.; Hwang, E.; Sim, H.; Lee, W.; Shin, S.; Mook-Jung, I. Amyloid peptide attenuates the proteasome activity in neuronal cells. *Mechanisms of ageing and development* **2005**, *126* (12), 1292-1299. DOI: 10.1016/j.mad.2005.07.006.
- (63) Tanaka, K.; Matsuda, N. Proteostasis and neurodegeneration: the roles of proteasomal degradation and autophagy. *Biochimica et biophysica acta* **2014**, *1843* (1), 197-204. DOI: 10.1016/j.bbamcr.2013.03.012.
- (64) Tanaka, Y.; Engelender, S.; Igarashi, S.; Rao, R. K.; Wanner, T.; Tanzi, R. E.; Sawa, A.; L. Dawson, V.; Dawson, T. M.; Ross, C. A. Inducible expression of mutant alpha-synuclein decreases proteasome activity and increases sensitivity to mitochondria-dependent apoptosis. *Human Molecular Genetics* **2001**, *10* (9), 919-926. DOI: 10.1093/hmg/10.9.919.
- (65) Tseng, B. P.; Green, K. N.; Chan, J. L.; Blurton-Jones, M.; LaFerla, F. M. Abeta inhibits the proteasome and enhances amyloid and tau accumulation. *Neurobiology of aging* **2008**, *29* (11), 1607-1618. DOI: 10.1016/j.neurobiolaging.2007.04.014.
- (66) Emmanouilidou, E.; Stefanis, L.; Vekrellis, K. Cell-produced alpha-synuclein oligomers are targeted to, and impair, the 26S proteasome. *Neurobiology of aging* **2010**, *31* (6), 953-968. DOI: 10.1016/j.neurobiolaging.2008.07.008.
- (67) Kristiansen, M.; Deriziotis, P.; Dimcheff, D. E.; Jackson, G. S.; Ovaa, H.; Naumann, H.; Clarke, A. R.; van Leeuwen, F. W. B.; Menéndez-Benito, V.; Dantuma, N. P.; et al. Disease-associated prion protein oligomers inhibit the 26S proteasome. *Molecular cell* **2007**, *26* (2), 175-188. DOI: 10.1016/j.molcel.2007.04.001.
- (68) Deriziotis, P.; Tabrizi, S. Prions and the proteasome. *Biochimica et biophysica acta* **2008**, *1782* (12), 713-722. DOI: 10.1016/j.bbadis.2008.06.011.
- (69) Hampel, H.; Hardy, J.; Blennow, K.; Chen, C.; Perry, G.; Kim, S. H.; Villemagne, V. L.; Aisen, P.; Vendruscolo, M.; Iwatsubo, T.; et al. The Amyloid- β Pathway in Alzheimer's Disease. *Molecular Psychiatry* **2021**, *26* (10), 5481-5503, ReviewPaper. DOI: doi:10.1038/s41380-021-01249-0.
- (70) Ono, K. Alzheimer's disease as oligomeropathy. *Neurochemistry international* **2018**, *119*, 57-70. DOI: 10.1016/j.neuint.2017.08.010.

- (71) Michaels, T. C. T.; Šarić, A.; Curk, S.; Bernfur, K.; Arosio, P.; Meisl, G.; Dear, A. J.; Cohen, S. I. A.; Dobson, C. M.; Vendruscolo, M.; et al. Dynamics of oligomer populations formed during the aggregation of Alzheimer's A β 42 peptide. *Nature Chemistry* **2020**, *12* (5), 445-451, OriginalPaper. DOI: doi:10.1038/s41557-020-0452-1.
- (72) Korsak, M.; Kozyreva, T. Beta Amyloid Hallmarks: From Intrinsically Disordered Proteins to Alzheimer's Disease. Springer, Cham, 2015; pp 401-421.
- (73) Jan, A.; Hartley, D. M.; Lashuel, H. A. Preparation and characterization of toxic Abeta aggregates for structural and functional studies in Alzheimer's disease research. *Nature protocols* **2010**, *5* (6), 1186-1209. DOI: 10.1038/nprot.2010.72.
- (74) Carulla, N.; Caddy, G. L.; Hall, D. R.; Zurdo, J.; Gairí, M.; Feliz, M.; Giralt, E.; Robinson, C. V.; Dobson, C. M. Molecular recycling within amyloid fibrils. *Nature* **2023**, *436* (7050), 554-558, OriginalPaper. DOI: doi:10.1038/nature03986.
- (75) Gruning, C.; Klinker, S.; Wolff, M.; Schneider, M.; Toksoz, K.; Klein, A.; Nagel-Steger, L.; Willbold, D.; Hoyer, W. The Off-rate of Monomers Dissociating from Amyloid- β Protofibrils. *Journal of Biological Chemistry* **2013**, *288* (52), 37104-37111. DOI: 10.1074/jbc.M113.513432.
- (76) Kane, R.; Bross, P.; Farrell, A.; Pazdur, R. Velcade®: U.S. FDA Approval for the Treatment of Multiple Myeloma Progressing on Prior Therapy. *The Oncologist* **2003**, *8* (6), 508-513. DOI: 10.1634/theoncologist.8-6-508.
- (77) Volpicelli-Daley, L. A.; Luk, K. C.; Patel, T. P.; Tanik, S. A.; Riddle, D. M.; Stieber, A.; Meaney, D. F.; Trojanowski, J. Q.; Lee, V. M. Y. Exogenous α -synuclein fibrils induce Lewy body pathology leading to synaptic dysfunction and neuron death. *Neuron* **2011**, *72* (1), 57-71. DOI: 10.1016/j.neuron.2011.08.033.
- (78) Tanik, S.; Schultheiss, C.; Volpicelli-Daley, L.; Brunden, K.; Lee, V. Lewy body-like α -synuclein aggregates resist degradation and impair macroautophagy. *The Journal of biological chemistry* **2013**, *288* (21), 15194-15210. DOI: 10.1074/jbc.M113.457408.
- (79) Pinotsi, D.; Michel, C. H.; Buell, A. K.; Laine, R. F.; Mahou, P.; Dobson, C. M.; Kaminski, C. F.; Kaminski Schierle, G. S. Nanoscopic insights into seeding mechanisms and toxicity of α -synuclein species in neurons. *Proceedings of the National Academy of Sciences* **2016**, *113* (14), 3815-3819. DOI: 10.1073/pnas.1516546113.
- (80) Pankaj Gaur, M. G., Andrii Kurochka, Subrata Ghosh, Dmytro A. Yushchenko, and Volodymyr V. Shvadchak. Fluorescent Probe for Selective Imaging of α -Synuclein Fibrils in Living Cells. **2021**, *12*, 1293-1298.
- (81) Haidekker, M. A.; Theodorakis, E. A. Environment-sensitive behavior of fluorescent molecular rotors. *Journal of Biological Engineering* **2010**, *4* (1), 1-14, ReviewPaper. DOI: doi:10.1186/1754-1611-4-11.
- (82) Kitts, C.; Beke-Somfai, T.; Nordén, B. Michler's hydrol blue: a sensitive probe for amyloid fibril detection. *Biochemistry* **2011**, *50* (17), 3451-3461. DOI: 10.1021/bi102016p.

- (83) Wördehoff, M. M.; Hoyer, W. α -Synuclein Aggregation Monitored by Thioflavin T Fluorescence Assay. *Bio-protocol* **2018**, *8* (14). DOI: 10.21769/BioProtoc.2941.
- (84) Sulatskaya, A. I.; Rodina, N. P.; Sulatsky, M. I.; Povarova, O. I.; Antifeeva, I. A.; Kuznetsova, I. M.; Turoverov, K. K. Investigation of α -Synuclein Amyloid Fibrils Using the Fluorescent Probe Thioflavin T. *International journal of molecular sciences* **2018**, *19* (9). DOI: 10.3390/ijms19092486.
- (85) Orihuela, R.; McPherson, C.; Harry, G. Microglial M1/M2 polarization and metabolic states. *British Journal of Pharmacology* **2015**, *173* (4), 649-665. DOI: 10.1111/bph.13139.
- (86) Choi, W. H.; Kim, S.; Park, S.; Lee, M. J. Concept and application of circulating proteasomes. *Experimental & Molecular Medicine* **2021**, *53* (10), 1539-1546, ReviewPaper. DOI: doi:10.1038/s12276-021-00692-x.
- (87) Ben-Nissan, G.; Katzir, N.; Füzesi-Levi, M. G.; Sharon, M. Biology of the Extracellular Proteasome. *Biomolecules* **2022**, *12* (5), 619, Review. DOI: 10.3390/biom12050619.
- (88) Ye, X.; Zhu, M.; Che, X.; Wang, H.; Liang, X.; Wu, C.; Xue, X.; Yang, J. Lipopolysaccharide induces neuroinflammation in microglia by activating the MTOR pathway and downregulating Vps34 to inhibit autophagosome formation. *Journal of neuroinflammation* **2020**, *17* (1), 18. DOI: 10.1186/s12974-019-1644-8.

APPENDIX

Figure 4.10 ^1H and ^{13}C NMR spectra of compound **4-1**

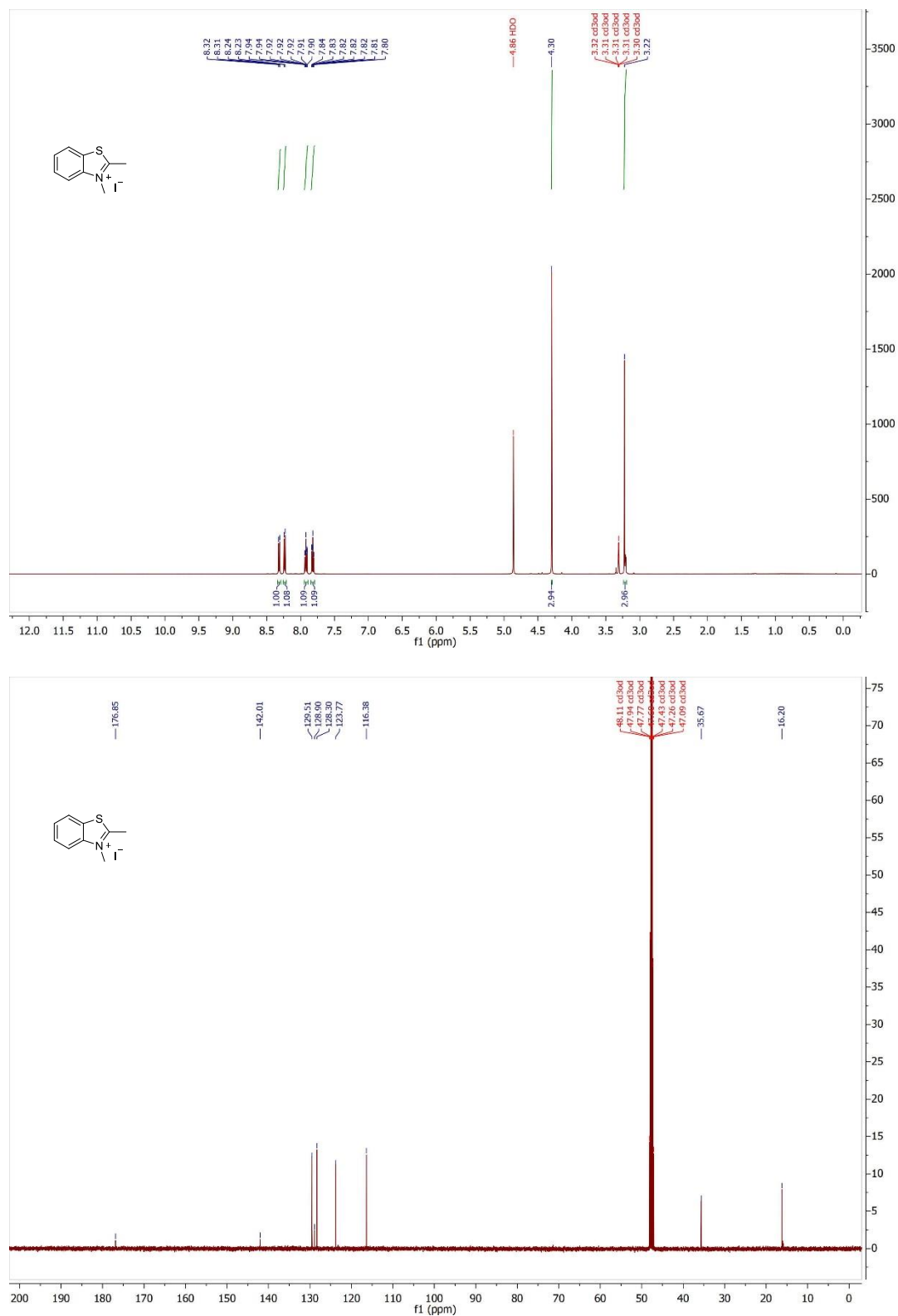


Figure 4.11 ^1H and ^{13}C NMR spectra of compound 4-2

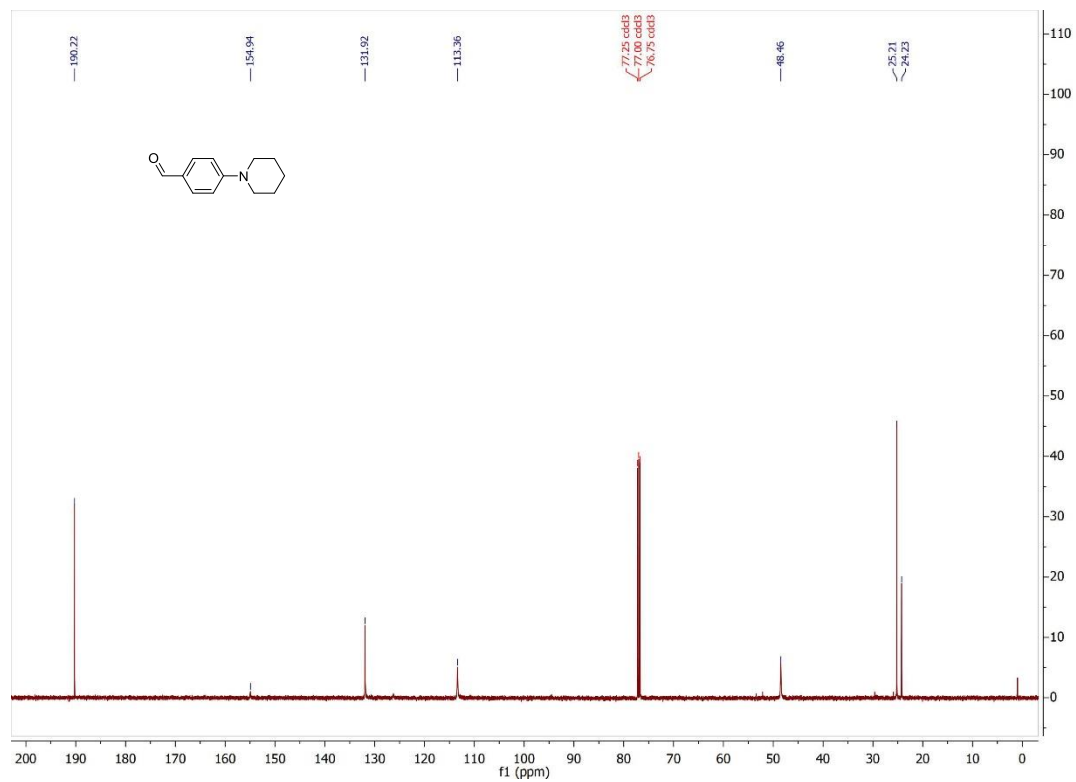
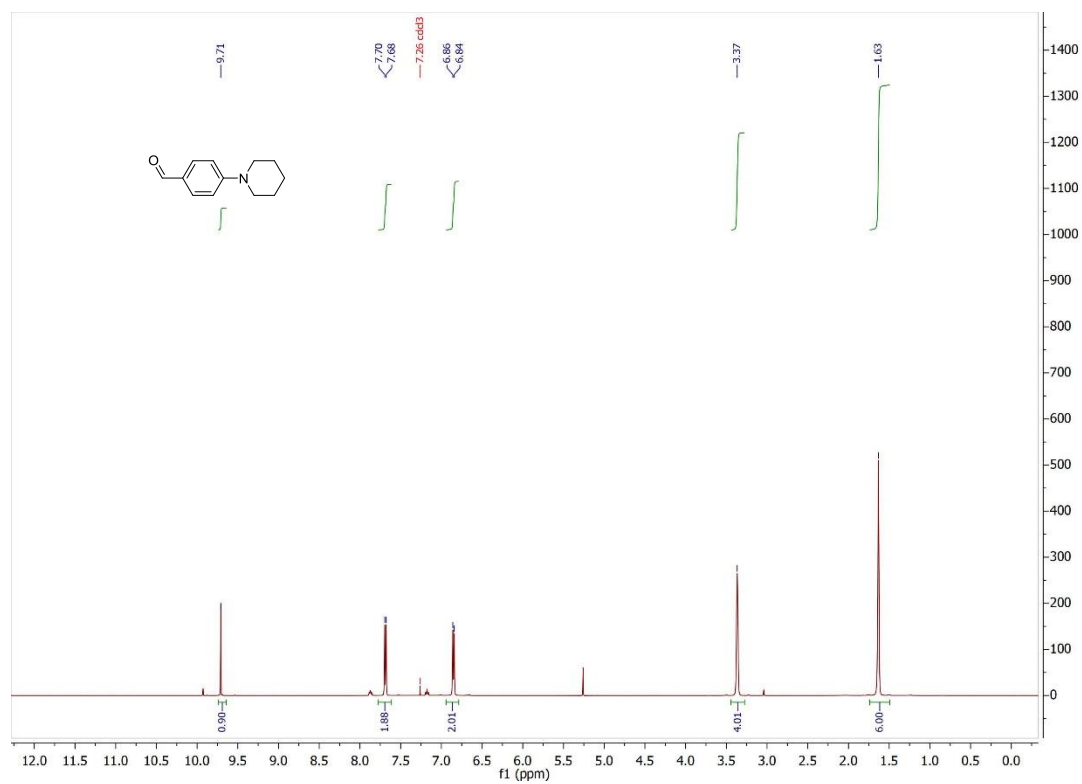
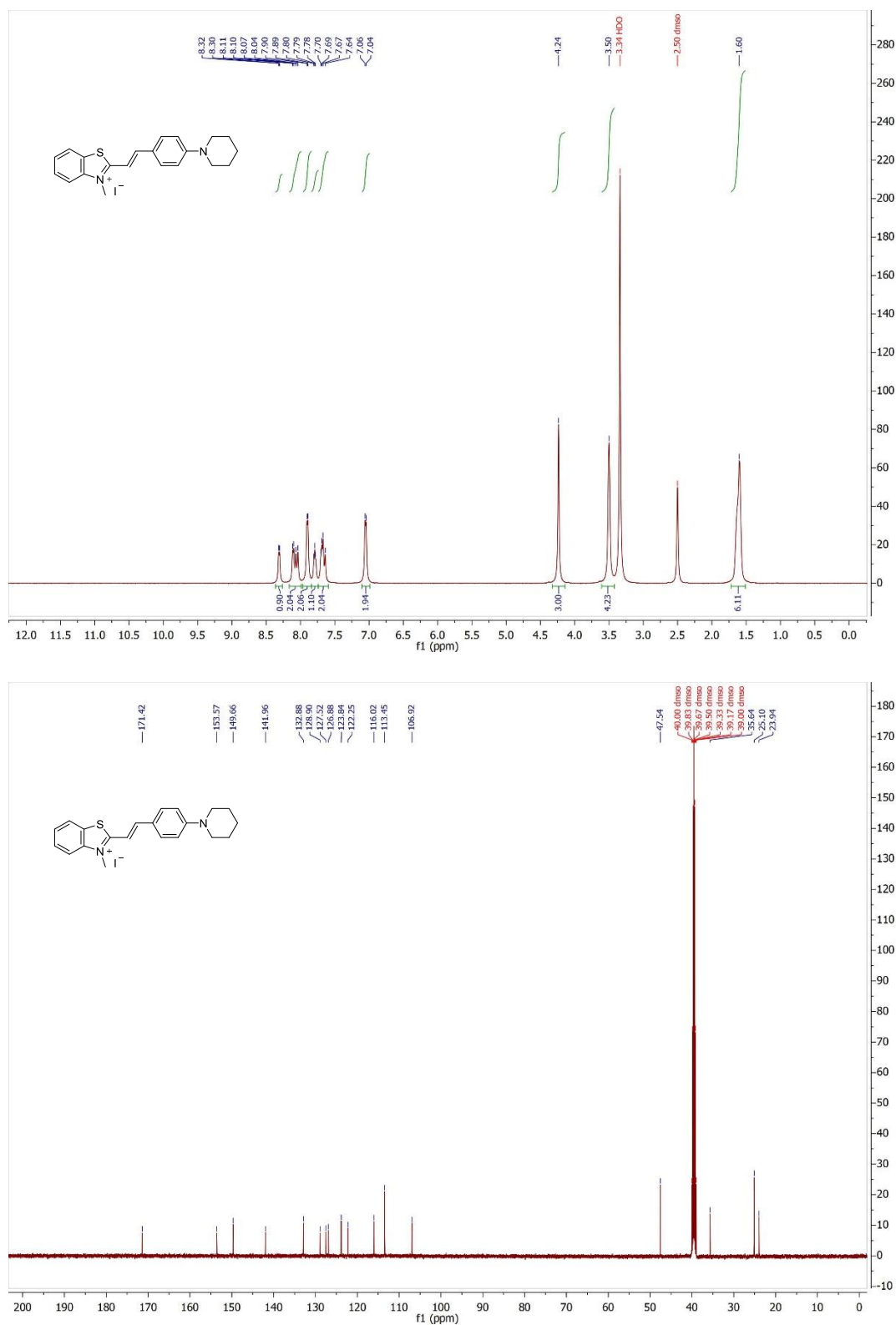


Figure 4.12 ^1H and ^{13}C NMR spectra of compound 4-3



CHAPTER FIVE

Conclusions and Future Directions

5.1 Conclusions and Future Directions

The UPS has long been envisioned as a promising therapeutic target due to its involvement in numerous critical biological pathways.¹⁻¹⁰ The success of inhibitors of the proteasome in the treatment of some cancers validated it as a therapeutic target.¹¹ In recent years, the importance of the lone 20S form of the proteasome as a player in the maintenance of proteostasis has come to light.¹² As a result, there has been a surge in interest in targeting the 20S form of the proteasome for treatment of a variety of diseases.^{7, 13-26} One area of particular interest is that of neurodegenerative disease treatment, considering the lack of disease modifying treatments and the devastation that is wrought on the lives of patients and their loved ones by these diseases.

My PhD studies have focused on furthering the development of small molecule 20S proteasome activators as an innovative therapeutic strategy aimed at treating neurodegenerative diseases. This was done by first identifying novel small molecule scaffolds that enhance 20S proteasome-mediated proteolysis, evaluating their activities, ensuring that this activity is translatable to disease relevant IDP substrates and initiating SAR studies focused on developing potent analogues.^{22, 23} With these novel activators in hand, I sought to further explore the potential of this proposed therapeutic strategy on more disease relevant substrates and in more disease relevant systems.²³ The result is an expanded toolbox of activators and methods with which they can be evaluated for their potential to effect neurodegenerative disease pathogenesis.

I was the first to explore the interplay between IDP oligomers seen in neurodegenerative diseases and small molecule 20S proteasome activators. Through these studies I found that small molecule 20S proteasome activators can maintain 20S proteasome activity in the presence of inhibitory IDP oligomers and reduce them *in vitro*.²³ These studies were the foundation for several ongoing studies in the Tepe lab aimed at further exploring this interplay, expanding to other disease

related IDPs and developing more disease relevant model systems for furthering small molecule 20S proteasome activation as a therapeutic strategy. Of particular interest is the development of a neuronal cell-based model for IDP accumulation and aggregation, as was initiated with the primary mouse hippocampal neuron studies outlined above. Substitution of this cell line with the immortalized hippocampal cells (HT-22 cell line) mentioned above could allow for a much more efficient, in terms of time and cost, means to develop this model system to explore the effects of small molecule 20S proteasome activators in a neuron model of IDP aggregation. These cells could also serve in the development of a model for IDP accumulation through stable transfection with an IDP, such as A53T α -synuclein. If toxicity proves to be a limiting factor here, an inducible expression system, like a Tet-on/off system, may permit for more controlled expression and accumulation.

I also demonstrated that small molecule 20S proteasome activators can reduce the release of the pro-inflammatory cytokine TNF- α by microglia that have been activated by the familial Parkinson's disease related IDP A53T α -synuclein. Chronic neuroinflammation is one of the hallmarks of neurodegenerative diseases, like Parkinson's disease, and is believed to be partially a result of activation of microglia by IDPs, as seen in these studies.²⁷⁻³² So, reduction of this pro-inflammatory signaling could show promise for development of therapeutics for these diseases. The reduction of TNF- α release seen in these studies was not specific to microglial activation with IDPs, but also those activated with LPS,³³ suggesting the possibility of a more general anti-inflammatory response caused by small molecule 20S proteasome activators in this system. While this lacks the specificity that was hypothesized, it may still serve as a promising secondary function during development of neurodegenerative disease therapeutics, where both inflammation and IDP accumulation, aggregation and toxicity play a role.³⁴⁻⁴⁰ Further studies are needed to elucidate the

mechanism associated with this reduction in TNF- α release by activated microglia. Some potential avenues to explore this mechanism include monitoring intracellular levels and release of other inflammatory signaling molecules as well as changes in vesicle trafficking. Proteomic and genomic analyses in these cells may also provide insight into how small molecule 20S proteasome activation might be affecting TNF- α release in this system. Going forward with these studies on neuroinflammation induced by IDP release, co-culture experiments with microglia and neuronal cells could serve as promising cell-based models of neurodegenerative disease for further evaluation of the effects of small molecule 20S proteasome activation. If a stably transfected neuronal model for IDP accumulation or aggregation can be developed, a cellular model demonstrating how IDPs can lead to the development of neuroinflammation could be conceived. Alternatively, activation of microglia through direct addition of IDPs could be used to develop a model in which the deleterious effects of neuroinflammation on neurons can be explored and potentially prevented with the addition of small molecule 20S proteasome activators.

REFERENCES

- (1) Voges, D.; Zwickl, P.; Baumeister, W. The 26S Proteasome: A Molecular Machine Designed for Controlled Proteolysis. *Annual Review of Biochemistry* **1999**, *68*, 1015-1068, review-article. DOI: 10.1146/annurev.biochem.68.1.1015.
- (2) McNaught, K. S. P.; Olanow, C. W.; Halliwell, B.; Isacson, O.; Jenner, P. Failure of the ubiquitin–proteasome system in Parkinson's disease. *Nature Reviews Neuroscience* **2001**, *2* (8), 589-594. DOI: 10.1038/35086067.
- (3) Voorhees, P.; Dees, E.; O'Neil, B.; Orlowski, R. The proteasome as a target for cancer therapy. *Clinical cancer research* **2003**, *9* (17), 6316-6325.
- (4) Ostrowska, H. The ubiquitin-proteasome system: a novel target for anticancer and anti-inflammatory drug research. *Cellular & Molecular Biology Letters* **2008**, *13* (3), 353-365. DOI: 10.2478/s11658-008-0008-7.
- (5) Calamini, B.; Morimoto, R. Protein homeostasis as a therapeutic target for diseases of protein conformation. *Current Topics in Medicinal Chemistry* **2012**, *12* (22), 2623-2640. DOI: 10.2174/1568026611212220014.
- (6) Huang, X.; Dixit, V. M. Drugging the undruggables: exploring the ubiquitin system for drug development. *Cell Research* **2016**, *26* (4), 484-498, ReviewPaper. DOI: doi:10.1038/cr.2016.31.
- (7) Njomen, E.; Tepe, J. J. Proteasome Activation as a New Therapeutic Approach to Target Proteotoxic Disorders. *Journal of Medicinal Chemistry* **2019**, *62* (14), 6469-6481. DOI: 10.1021/acs.jmedchem.9b00101.
- (8) Tundo, G.; Sbardella, D.; Santoro, A.; Coletta, A.; Oddone, F.; Grasso, G.; Milardi, D.; Lacal, P.; Marini, S.; Purrello, R.; et al. The proteasome as a druggable target with multiple therapeutic potentialities: Cutting and non-cutting edges. *Pharmacology & therapeutics* **2020**, *213*, 107579. DOI: 10.1016/j.pharmthera.2020.107579.
- (9) Thibaudeau, T. A.; Smith, D. M. A Practical Review of Proteasome Pharmacology. *Pharmacological reviews* **2019**, *71* (2), 170-197. DOI: 10.1124/pr.117.015370.
- (10) Shang, F.; Taylor, A. Ubiquitin-proteasome pathway and cellular responses to oxidative stress. *Free radical biology & medicine* **2011**, *51* (1), 5-16. DOI: 10.1016/j.freeradbiomed.2011.03.031.
- (11) Kane, R.; Bross, P.; Farrell, A.; Pazdur, R. Velcade®: U.S. FDA Approval for the Treatment of Multiple Myeloma Progressing on Prior Therapy. *The Oncologist* **2003**, *8* (6), 508-513. DOI: 10.1634/theoncologist.8-6-508.
- (12) Deshmukh, F. K.; Yaffe, D.; Olshina, M. A.; Ben-Nissan, G.; Sharon, M. The Contribution of the 20S Proteasome to Proteostasis. *Biomolecules* **2019**, *9* (5), 190, Review. DOI: 10.3390/biom9050190.

- (13) Jones, C. L.; Njomen, E.; Sjögren, B.; Dexheimer, T. S.; Tepe, J. J. Small Molecule Enhancement of 20S Proteasome Activity Targets Intrinsically Disordered Proteins. *ACS Chemical Biology* **2017**, *12* (9), 2240-2247. DOI: 10.1021/acscchembio.7b00489.
- (14) Trader, D. J.; Simanski, S.; Dickson, P.; Kodadek, T. Establishment of a suite of assays that support the discovery of proteasome stimulators. *Biochimica et Biophysica Acta (BBA) - General Subjects* **2017**, *1861* (4), 892-899. DOI: 10.1016/J.BBAGEN.2017.01.003.
- (15) Coleman, R. A.; Trader, D. J. Development and Application of a Sensitive Peptide Reporter to Discover 20S Proteasome Stimulators. *ACS Combinatorial Science* **2018**, *20* (5), 269-276. DOI: 10.1021/acscombsci.7b00193.
- (16) Njomen, E.; Osmulski, P. A.; Jones, C. L.; Gaczynska, M.; Tepe, J. J. Small Molecule Modulation of Proteasome Assembly. *Biochemistry* **2018**, *57* (28), 4214-4224. DOI: 10.1021/acs.biochem.8b00579.
- (17) Giżyńska, M.; Witkowska, J.; Karpowicz, P.; Rostankowski, R.; Chocron, E. S.; Pickering, A. M.; Osmulski, P.; Gaczynska, M.; Jankowska, E. Proline- and Arginine-Rich Peptides as Flexible Allosteric Modulators of Human Proteasome Activity. *Journal of Medicinal Chemistry* **2018**, *62* (1), 359-370, research-article. DOI: 10.1021/acs.jmedchem.8b01025.
- (18) Opoku-Nsiah, K. A.; Gestwicki, J. E. Aim for the core: suitability of the ubiquitin-independent 20S proteasome as a drug target in neurodegeneration. Mosby Inc.: 2018; Vol. 198, pp 48-57.
- (19) Coleman, R. A.; Muli, C. S.; Zhao, Y.; Bhardwaj, A.; Newhouse, T. R.; Trader, D. J. Analysis of chain length, substitution patterns, and unsaturation of AM-404 derivatives as 20S proteasome stimulators. *Bioorganic & Medicinal Chemistry Letters* **2019**, *29* (3), 420-423. DOI: 10.1016/J.BMCL.2018.12.030.
- (20) Njomen, E.; Tepe, J. J. Regulation of Autophagic Flux by the 20S Proteasome. *Cell Chemical Biology* **2019**, *26* (9), 1283-1294.e1285. DOI: 10.1016/j.chembiol.2019.07.002.
- (21) Coleman, R. A.; Trader, D. J. Methods to Discover and Evaluate Proteasome Small Molecule Stimulators. *Molecules* **2019**, *24* (12), 2341, Review. DOI: 10.3390/molecules24122341.
- (22) Fiolek, T.; Magyar, C.; Wall, T.; Davies, S.; Campbell, M.; Savich, C.; Tepe, J.; Mosey, R. Dihydroquinazolines enhance 20S proteasome activity and induce degradation of α -synuclein, an intrinsically disordered protein associated with neurodegeneration. *Bioorganic & Medicinal Chemistry Letters* **2021**, *36*, 127821. DOI: 10.1016/j.bmcl.2021.127821.
- (23) Fiolek, T. J.; Keel, K. L.; Tepe, J. J. Fluspirilene Analogs Activate the 20S Proteasome and Overcome Proteasome Impairment by Intrinsically Disordered Protein Oligomers. *ACS Chemical Neuroscience* **2021**, *12* (8), 1438-1448. DOI: 10.1021/acscemneuro.1c00099.
- (24) Ben-Nissan, G.; Katzir, N.; Füzesi-Levi, M. G.; Sharon, M. Biology of the Extracellular Proteasome. *Biomolecules* **2022**, *12* (5), 619, Review. DOI: 10.3390/biom12050619.

- (25) Jones, C. L.; Tepe, J. J. Proteasome Activation to Combat Proteotoxicity. *Molecules* **2019**, *24* (15), 2841, Review. DOI: 10.3390/molecules24152841.
- (26) George, D.; Tepe, J. Advances in Proteasome Enhancement by Small Molecules. *Biomolecules* **2021**, *11* (12), 1789. DOI: 10.3390/biom11121789.
- (27) Heneka, M.; Carson, M.; El Khoury, J.; Landreth, G.; Brosseron, F.; Feinstein, D.; Jacobs, A.; Wyss-Coray, T.; Vitorica, J.; Ransohoff, R.; et al. Neuroinflammation in Alzheimer's disease. *The Lancet. Neurology* **2015**, *14* (4), 388-405. DOI: 10.1016/S1474-4422(15)70016-5.
- (28) Calsolaro, V.; Edison, P. Neuroinflammation in Alzheimer's disease: Current evidence and future directions. *Alzheimer's & dementia : the journal of the Alzheimer's Association* **2016**, *12* (6), 719-732. DOI: 10.1016/j.jalz.2016.02.010.
- (29) Liu, J.; Wang, F. Role of Neuroinflammation in Amyotrophic Lateral Sclerosis: Cellular Mechanisms and Therapeutic Implications. *Frontiers in immunology* **2017**, *8*, 1005. DOI: 10.3389/fimmu.2017.01005.
- (30) Yang, Q.; Zhou, J. Neuroinflammation in the central nervous system: Symphony of glial cells. *Glia* **2019**, *67* (6), 1017-1035. DOI: 10.1002/glia.23571.
- (31) Tu, H.; Yuan, B.; Hou, X.; Zhang, X.; Pei, C.; Ma, Y.; Yang, Y.; Fan, Y.; Qin, Z.; Liu, C.; et al. α -synuclein suppresses microglial autophagy and promotes neurodegeneration in a mouse model of Parkinson's disease. *Aging cell* **2021**, *20* (12), e13522. DOI: 10.1111/accel.13522.
- (32) Hoenen, C.; Gustin, A.; Birck, C.; Kirchmeyer, M.; Beaume, N.; Felten, P.; Grandbarbe, L.; Heuschling, P.; Heurtaux, T. Alpha-Synuclein Proteins Promote Pro-Inflammatory Cascades in Microglia: Stronger Effects of the A53T Mutant. *PloS one* **2016**, *11* (9), e0162717. DOI: 10.1371/journal.pone.0162717.
- (33) Ye, X.; Zhu, M.; Che, X.; Wang, H.; Liang, X.; Wu, C.; Xue, X.; Yang, J. Lipopolysaccharide induces neuroinflammation in microglia by activating the MTOR pathway and downregulating Vps34 to inhibit autophagosome formation. *Journal of neuroinflammation* **2020**, *17* (1), 18. DOI: 10.1186/s12974-019-1644-8.
- (34) Uversky, V. N.; Oldfield, C. J.; Midic, U.; Xie, H.; Xue, B.; Vucetic, S.; Iakoucheva, L. M.; Obradovic, Z.; Dunker, A. K. Unfoldomics of human diseases: linking protein intrinsic disorder with diseases. *BMC genomics* **2009**, *10 Suppl 1* (Suppl 1), S7-S7. DOI: 10.1186/1471-2164-10-S1-S7.
- (35) Uversky, V. Intrinsically disordered proteins and their (disordered) proteomes in neurodegenerative disorders. *Frontiers in Aging Neuroscience* **2015**, *7*. DOI: 10.3389/fnagi.2015.00018.
- (36) Smith, D. M. Could a Common Mechanism of Protein Degradation Impairment Underlie Many Neurodegenerative Diseases? *Journal of experimental neuroscience* **2018**, *12*, 1179069518794675-1179069518794675. DOI: 10.1177/1179069518794675.

(37) Thibaut, T. A.; Anderson, R. T.; Smith, D. M. A common mechanism of proteasome impairment by neurodegenerative disease-associated oligomers. *Nature Communications* **2018**, *9* (1), 1097-1097. DOI: 10.1038/s41467-018-03509-0.

(38) Ross, C. A.; Poirier, M. A. Protein aggregation and neurodegenerative disease. *Nature Medicine* **2004**, *10* (7), S10-S17. DOI: 10.1038/nm1066.

(39) Gammon, K. Neurodegenerative disease: brain windfall. *Nature* **2014**, *515* (7526), 299-300. DOI: 10.1038/nj7526-299a.

(40) Onyango, I.; Jauregui, G.; Čarná, M.; Bennett, J.; Stokin, G. Neuroinflammation in Alzheimer's Disease. *Biomedicines* **2021**, *9* (5), 524. DOI: 10.3390/biomedicines9050524.

CHAPTER SIX
Materials and Methods

6.1 Materials

6.1.1 Key resource tables

Table 6.1: Antibodies

Reagent or Resources	Source	Catalogue number
GAPDH (14C10) Rabbit mAb HRP-linked	Cell Signaling Technology	3683S
α -synuclein (Syn204) mouse monoclonal antibody	Cell Signaling Technology	2647S
Recombinant anti-alpha-synuclein antibody [MJFR1] Rabbit	Abcam	ab138501
Goat anti-Rabbit IgG HRP-linked	Cell Signaling Technology	7074S
Horse anti-Mouse IgG HRP-linked	Cell Signaling Technology	7076S
Goat anti-Mouse IgG2a Alexa Fluor™ 594	Thermofisher Scientific	A-21135
Goat anti-Mouse IgM Alexa Fluor™ 488	Thermofisher Scientific	A-21042

Table 6.2: Peptides and recombinant proteins

Reagent or Resources	Source	Catalogue number
Human 20S proteasome	BostonBiochem	E-360
Human 20S proteasome	Enzo Life Sciences	BML-PW8720-0050
19S Proteasome	BostonBiochem	E-366
Recombinant WT human α -synuclein	Abcam	ab51189
Recombinant human GAPDH protein	Abcam	ab77109
N-Succinyl-Leu-Leu-Val-Tyr-7-amido-4-methylcoumarin (Suc-LLVY-AMC)	BostonBiochem	S-280
Z-Leu-Leu-Glu-7-amido-4-methylcoumarin (Z-LLE-AMC)	BostonBiochem	S-230
Boc-Leu-Arg-Arg-7-amido-4-methylcoumarin (Boc-LRR-AMC)	BostonBiochem	S-300
Recombinant Human α -synuclein Protein	Novus Biologicals	NBC1-18331
Recombinant Human GAPDH Protein	Novus Biologicals	NBC1-18528
Recombinant Human α -synuclein Active Pre-formed Fibrils (type 1) Protein	Novus Biologicals	NBP2-54789-100ug
Human α -synuclein, A53T	Kerafast Inc.	EGP013
Beta-Amyloid (1-42), Human	Eurogentec	AS-20276

Table 1.3: Cell lines, cell culture and transfection reagents

Reagent or Resources	Source	Catalogue number
Immortalized mouse microglia (IMG) cells	Sigma Aldrich	SCC134
HEK-293T	ATCC	CRL-3216
Primary Mouse Hippocampal Neurons	Gibco	A15587
Neurobasal Plus Medium	Gibco	A3582901
DMEM medium	Gibco	11995-065
0.25% Trypsin-EDTA (1x)	Gibco	25200-056
Fetal Bovine Serum	Gibco	16000044
Penicillin-Streptomycin	Gibco	15140-122
GlutaMAX (100x)	Gibco	35050-061
B-27 Supplement (50x)	Gibco	17504-044
Amphotericin B	Gibco	15290018
Gentamicin	Gibco	15750-060
X-tremeGENE HP DNA Transfection Reagent	Sigma Aldrich	06366236001
Dulbecco's Phosphate Buffered Saline	Sigma Aldrich	D8537-500ML

Table 6.4: Oligonucleotides and recombinant DNA

Reagent or Resources	Source	Catalogue number
pHM6-alphasynuclein-A53T	Addgene	40825

Table 6.5: Bacterial strains

Reagent or Resources	Source	Catalogue number
DH5 α Chemically Competent <i>E. coli</i>	ThermoFisher Scientific	18265017

Table 6.6: Commercial assay kits

Reagent or Resources	Source	Catalogue number
Pierce BCA Protein Assay Kit	Thermofisher Scientific	23225
Pierce Silver Stain Kit	Thermofisher Scientific	24612
CellTiter 96 Aqueous One Solution Cell Proliferation Assay	Promega	G3580
Mouse TNF- α ELISA kit	Invitrogen	BMS607-3
Plasmid Maxi kit	QIAGEN	12163

Table 6.7: Other chemicals and reagents

Reagent or Resources	Source	Catalogue number
TCH-165	Tepe lab	NA
Fluspirilene	Tepe lab	NA
N-acylated Fluspirilene	Tepe lab	NA
Other Fluspirilene analogues	Tepe lab	NA
Aripiprazole	Cayman Chemical	19989
Dihydroquinazoline analogues	Mosey lab	NA
Bortezomib	Cayman Chemical	10008822
Epoxomicin	Cayman Chemical	10007806
Cycloheximide	Cell Signaling Technology	2112
LB Broth	Sigma-Aldrich	L7275
cOmplete Mini, EDTA-free protease inhibitor cocktail tablets	Sigma Aldrich	11836170001
Adenosine 5'-triphosphate magnesium salt	Sigma Aldrich	A9187
Pierce RIPA buffer	Thermofisher Scientific	89901
Mini-PROTEAN® TGX™ Precast Gels	Bio-Rad	4561094
Immun-Blot® PVDF Membrane	Bio-Rad	1620177
Clarity™ Western ECL Substrate	Bio-Rad	1705060
Radiance Plus HRP Substrate	Azure Biosystems	AC2103
InstantBlue™ Coomassie stain	Expedeon	ISB1L
Blocking-grade Blocker (non-fat dry milk)	Bio-Rad	1706404

6.2 Methods

6.2.1 Cell culture

General cell culture: Human embryonic kidney cells (HEK-293T) or immortalized mouse microglial cells (IMG) were maintained in Dulbecco's modified Eagle's medium (DMEM) supplemented with 10% fetal bovine serum and 100 units/mL penicillin/streptomycin, at 37 °C with 5% CO₂.

6.2.2 Primary neuron cell culture

Plating media: Neurobasal Plus media supplemented with 10% FBS, 2% B-27 supplement, 1% GlutaMAX supplement, 1% Amphotericin B and 50 µg/mL of Gentamicin was

used for initial plating at the manufacturers recommended density and for the first 4 days of culturing the cells.

Culturing media: Beginning on day 4 after plating, plating media was exchanged for Neurobasal Plus media supplemented with 2% B-27 supplement, 1% GlutaMAX supplement, 1% Amphotericin B and 50 µg/mL of Gentamicin, without FBS, and was used to maintain the cells for the remainder of the culture time.

Plating and culturing procedures: From liquid nitrogen, the cells were rapidly thawed in a 37 °C water bath until a small ice crystal remained. The vial was then transferred to the cell culture hood and disinfected with 70% ethanol. Prior to every liquid transfer step with cells, all pipette tips and tubes must be pre-rinsed with media to prevent cells from adhering to the surfaces and to maximize viable cell count. The cells were then gently transferred with a pipette to a pre-rinsed 50 mL conical tube. Next, the cryo-preservation tube that the cells came from was washed using 1 mL of the plating media and this media was added dropwise while gently swirling the cells. To this was then added dropwise 2 mL of additional plating media. The cells were gently mixed with a pipette without creating any air bubbles. The cells were counted using 0.4% trypan blue and a hemocytometer. 1.7×10^4 cells were plated per well in a poly-D-lysine-coated 96-well plate. The cells were then diluted to 200 µL with the plating media and transferred to an incubator at 37 °C with humidified atmosphere of 5% CO₂ in air. After 24 h, half of the media was aspirated and replaced with fresh plating media. After 3 more days (72 h), 3/4 of the media was aspirated off and replaced with culture media (no FBS). This was done every 3 days for general culture or every 7 days for experiments with two treatments over 14 days. All media exchanges on primary mouse hippocampal neurons were done one well at a time to minimize any time exposed to air.

Pre-formed α -synuclein fibril seed preparation: Pre-formed α -synuclein fibrils, obtained from our collaborated Dr. Sortwell, (2 mg/mL) were sonicated with a micro probe tip sonicator with 60 pulses at 10% power (total of 30 s, 0.5 s on, 0.5 s off). Following sonication, pre-formed fibril seeds were diluted in culturing media to the desired final concentration (0.001 mg/mL) and immediately used for treatment of primary mouse hippocampal neurons.

Seeding of primary mouse hippocampal neurons with α -synuclein pre-formed fibrils: Following the initial plating procedure outlined above, on day 4 ~80% of the plating media was removed from primary mouse hippocampal cultures and was replaced with fresh culturing media containing desired final concentration of pre-formed α -synuclein fibril seeds. The cells were returned to the incubator for 7 days, after which 50% of the media was exchanged for fresh culturing media, without any pre-formed α -synuclein fibril seeds. When compound treatments were attempted (data not shown), treatments were done shortly following initial treatment with pre-formed α -synuclein fibril seeds and again 7 days later, for a total of 2 treatments. However, these experiments did not yield conclusive results due to suboptimal cell growth and seeding efficiencies. Following the 14-day incubation with pre-formed α -synuclein fibril seeds, all media was gently removed from neuron cultures and the cells were washed with warm TBS buffer 1x, fixed with 4% paraformaldehyde in TBS for 30 min at RT, and washed 2x with TBS buffer again. Cells could then be stored at 4 °C. Immunostaining and confocal immunofluorescence of resulting fixed primary mouse hippocampal neurons was performed by Dr. Caryl Sortwell and her lab.

6.2.3 Transient transfection of A53T α -synuclein plasmid into HEK-293T cells

HEK-293T cells were grown using the methods stated above to ~50-70% confluency in 60 mm plates. DNA (5 μ g of A53T α -synuclein plasmid) was mixed with 0.5 mL of serum free-DMEM medium. X-tremeGENE transfection reagent (10 μ L) was briefly vortexed, added to the

plasmid solution and then this mixture was incubated for 20 min at RT. The mixture was then added dropwise with swirling to the HEK-293T cells and allowed to incubate for 4 h at 37°C, 5% CO₂, in a tissue culture incubator. The transfection medium was replaced with fresh culture medium and cultured for a further 24 h.

6.2.4 Proteasome-mediated degradation of A53T α -synuclein in HEK-293T cells

HEK-293T cells were transfected as described above. The cells were then treated with 50 μ g/mL of cycloheximide, in combination with either vehicle (DMSO), Fluspirilene (10 or 30 μ M), N-acylated Fluspirilene (10 or 30 μ M), Bortezomib (100 nM), or a combination thereof for 8 h. The cells were then lysed, and the resulting cellular extracts were immunoblotted to monitor A53T α -synuclein levels.

6.2.5 Immunoblot

Transfected HEK-293T cells at 70-80% confluency were treated with test compounds at the reported concentrations and time as indicated in figure legends. Samples meant for immunoblot only were washed 2x with warm DPBS buffer and scrapped with chilled RIPA buffer supplemented with protease inhibitor cocktail. Samples were incubated at 0 °C for 15 min, centrifuged at ~14,000 g and the supernatant assayed for total protein content with bicinchoninic acid (BCA) assay. Normalized and boiled samples were resolved on 4-20% Tris-glycine gels, resolved via SDS-PAGE and blotted onto PVDF membranes. Membranes were blocked in 5% non-fat milk in TBST buffer for 60 min at RT. Membranes were then incubated with primary antibody in 5% non-fat milk TBST buffer, overnight at 4°C. Membranes were then washed 5x for 5 min each with TBST buffer and incubated in secondary antibody at RT for 60 min. Membranes were washed again as above and developed with ECL clarity or Azure Biosystems Radiance Plus

reagent. Images were captured with an Azure Biosystems 300Q Imager. All primary antibodies were used at a dilution of 1:1000.

6.2.6 Immortalized mouse microglia TNF- α and viability experiments

Culture and treatment procedure: IMG cells were plated in 96-well cell culture plates at a density of 10,000 cells per well. The cells were cultured under normal culture conditions for 24 h and then media was exchanged for fresh media (90 μ L). Compounds were first dissolved in DMSO at 1,000x the final desired concentration, and then further diluted to 10x the final desired concentration in media. To each well was then added DMSO, TCH-165 or N-acylated Fluspirilene (10 μ L) at various concentrations (see Figure legends for details). Each treatment was done on six different wells, so that three wells could be utilized for cell viability assessments and the media of the other three wells could be used to measure TNF- α release. This prevented loss of any cells when removing media influencing cell viability measurements. The cells were further incubated for 1 h under normal culture conditions, and then A53T α -synuclein was added to a final concentration of 10 μ M. The cells were then returned to the incubator for 24 h.

Cell viability assay: At the end of the treatments described above, to the cells was added 100 μ L of fresh media (totaling 200 μ L of media) and CellTiter 96 Aqueous One Solution Cell Proliferation Assay solution (20 μ L). The cells were then incubated for 1–4 h at 37 °C with 5% CO₂, while monitoring for color change. The assay plate was then allowed to equilibrate for 15 min at RT, gently agitated to ensure even distribution of color and absorbance readings were taken on a SpectraMax M5e Spectrometer. Data are presented as a percentage of the vehicle control for each experimental condition, after background subtraction.

TNF- α ELISA: At the end of the treatments described above, the media from the cells and from blank wells was removed and subjected to a TNF- α ELISA. This was done using a Mouse

TNF- α ELISA kit purchased from Invitrogen, following their recommended protocol and using their provided standards. Absorbance readings were taken on a SpectraMax M5e Spectrometer. A standard curve was generated from the provided standards and resulting absorbance readings using the GraphPad Prism 7 software. Using this standard curve, concentrations for the various treatments were determined from their absorbance readings. Data is represented as a percentage of the TNF- α concentration relative to the untreated IMG cell control.

6.2.7 Molecular docking studies.

Docking was performed using PyRx's Vina Wizard program, supported through computational resources and services provided by the Institute for Cyber-Enabled Research at Michigan State University. The macromolecule for these docking studies was defined using a crystal structure of the closed gate human 20S proteasome, obtained from the PDB database (PDB ID: 4R3O). Small molecule ligands were generated in Perkin Elmer's Chem3D. These small molecule ligands were minimized using the MM2 force field, converted into PDB files and uploaded to PyRx. Vina was run on a maximized grid of the h20S proteasome (grid box $153.2 \times 138.0 \times 189.4$ Å) to allow for unbiased docking on the entire human 20S proteasome. Docking was performed on each ligand three times with exhaustiveness set to 1000. The top nine reported docking states were analyzed using Schrödinger's PyMOL Molecular Graphics System. In the case of the Fluspirilene analogues, BIOVIA Discovery Studio 2020 was used to further analyze the docking models using the receptor-ligand interactions function. This allowed for exploration of how the human 20S proteasome (receptor) was predicted to interact with the Fluspirilene analogues at each of the 9 top docking states.

6.2.8 Fluorogenic peptide degradation 20S proteasome activity assay.

Activity assays were carried out in a 100 μ L reaction volume. Different concentrations (1–80 μ M) of test compounds in DMSO were added (1 μ L) to a black flat/clear bottom 96-well plate containing 1 nM of human constitutive 20S proteasome, in assay buffer (50 mM Tris-HCl at pH 7.8, 100 mM NaCl) and allowed to incubate for 15 min at 37 $^{\circ}$ C. Fluorogenic substrates were then added and the enzymatic activity measured at 37 $^{\circ}$ C on a SpectraMax M5e spectrometer by measuring the change in fluorescence unit per min for 1 h at 380/460 nm. Medium-throughput screening (MTPS) was carried out in 384-well plates as described above, with the following exceptions. Three concentrations of compounds (3, 10 and 30 μ M; 150 nL of 200x stocks in DMSO) were dispensed into a black flat bottom 384-well plate containing 25 μ L 20S proteasome in assay buffer, followed by 5 μ L of 6x substrate working solution (Suc-LLVY-AMC diluted in assay buffer), using automated liquid dispensers. Enzymatic activity was measured at 37 $^{\circ}$ C on a BioTek plate reader by measuring change in fluorescence unit per min for 1 h at 380/460 nm. The fluorescence units for the vehicle control were set as 100%, and the ratio of drug-treated sample relative to that of vehicle control was used to calculate the fold change in enzymatic activity. The fluorogenic substrates used were one of the following: Suc-LLVY-AMC (CT-L activity, 20 μ M), Z-LLE-AMC (Casp-L activity, 20 μ M), Boc-LRR-AMC (T-L activity, 40 μ M) or a combination of the three substrates (each at 6.67 μ M). Magnesium chloride (5 mM) and ATP (2.5 mM) were included in assays containing 26S proteasome.

6.2.9 In vitro purified α -synuclein degradation assay

Digestion of α -synuclein was carried out in a 50 μ L reaction volume made of 50 mM Tris at pH 7.8; 0.33 μ M purified α -synuclein and 6.7 nM purified human 20S proteasome. Briefly, 20S proteasome was diluted to 7.58 nM in the reaction buffer. Test compounds or vehicle (1 μ L of 50 \times

stock or DMSO, see Figures for treatment details) were added to 44 μL of 7.58 nM 20S and incubated at 37 °C for 20 min. 5 μL of 3.3 μM α -synuclein substrate was then added to the reaction mixture and incubated at 37 °C for 4 h. The reactions were quenched with concentrated sodium dodecyl sulfate (SDS) loading buffer. After boiling for 10 min, samples were resolved on a 4–20% Tris-glycine SDS-PAGE gel. The gels were then stained using InstantBlue Coomassie based staining solution or Pierce Silver Stain Kit and the manufacturers recommended procedures.

6.2.10 Amyloid beta aggregate preparation.

Synthetic amyloid beta was purchased from Eurogentec. To remove preexisting aggregates, synthetic amyloid beta peptide was dissolved in 100% HFIP and incubated at °C for 2 h. The HFIP was removed, and the remaining peptide films were stored at –80 °C until use. Aggregates were prepared by resuspending amyloid beta films with DMSO (50 μL per 1 mg of peptide), followed by addition of ultrapure H₂O (800 μL) and rapid addition of 2 M Tris-base (10 μL) at pH 7.6. The solution was then vortexed for 5 seconds and allowed to incubate at room temperature for 5 min. The Amyloid beta mixture was then diluted to the desired concentration and used immediately.

6.2.11 IDP oligomer inhibition in fluorogenic peptide degradation assay

Assays were carried out in a 100 μL reaction volume. Different concentrations (1–10 μM) of test compounds were added to a black flat/clear bottom 96-well plate containing 1 nM of human constitutive 20S proteasome, in 50 mM Tris-HCl at pH 7.8 and allowed to incubate for 15 min at 37 °C. Then, 1 μL of α -synuclein or amyloid beta oligomer mixture was added to each sample to a final concentration of 500 nM for α -synuclein and 2.5 μM for amyloid beta. This mixture was then allowed to incubate again for 15 min at 37 °C. Next, 10 μL of CT-L fluorogenic substrate was added to a final concentration of 20 μM . The enzymatic activity was measured at 37 °C on a

SpectraMax M5e spectrometer by measuring the change in fluorescence unit per min for 1 h at 380–460 nm. The fluorescence units for the vehicle control were set to 100%, and the ratio of drug-treated or just oligomer-treated samples to the vehicle control was used to calculate the relative enzymatic activity.

6.2.12 Proteasome-mediated degradation of α -synuclein oligomeric mixture

Digestion of α -synuclein oligomer mixture was carried out in a 50 μ L reaction volume made of 50 mM Tris at pH 7.8; 0.33 μ M α -synuclein oligomer mixture and 6.7 nM purified human 20S proteasome. Briefly, 20S proteasome was diluted to 7.58 nM in the reaction buffer. Fluspirilene, N-acylated Fluspirilene or vehicle (1 μ L of 50x stock or DMSO) were added to 44 μ L of 7.58 nM 20S and incubated at 37 °C for 20 min. The substrate (5 μ L of 3.3 μ M synuclein oligomer mixture) was then added to the reaction mixture and incubated at 37 °C for 24 h. The reactions were then quenched with concentrated SDS loading buffer. Samples were resolved on a 4–20% Tris-glycine SDS-PAGE and immunoblotted with mouse monoclonal anti α -synuclein IgG (1:2000) and anti-mouse HRP-linked IgG (1:2000). Blots were developed with ECL western reagent and imaged with an Azure Biosystems 300Q imager.

6.2.13 Plasmid preparation

Bacterial culture: *E. coli* were grown at 37 °C in LB supplemented ampicillin (25 μ g/mL).

Plasmid purification: A53T α -synuclein plasmid was purified and prepared from *E. coli* that had been transformed with the plasmid previously. Purification was done using a plasmid maxi prep kit obtained from Qiagen and was performed following their provided protocol. Resulting plasmid was diluted to ~1 μ g/ μ L in the provided TE buffer for use in transfections.

6.2.14 Quantification and statistical analysis

Data are presented as mean \pm standard deviation (SD). For each figure, the number of replicates is indicated in the figure legends. Statistical analysis was only performed on experiments with three or more n (biological replicates for cellular experiments or individual experiments for biochemical assays). Western blot quantifications were performed with ImageJ software. Statistical analysis was performed with GraphPad Prism 7 software. One-way ANOVA analysis with post Šidák correction test was used for multiple comparisons of means. Effect was considered significant for * $p < 0.05$, ** $p < 0.01$, *** $p < 0.001$, **** $p < 0.0001$.

Confocal immunofluorescence (By Dr. Caryl Sortwell)